PERIODO DE EJECUCIÓN: 2020-2023

DISEÑO Y OPERACIÓN INTELIGENTE ANTE AMENAZAS DE INTERRUPCIÓN DEL SUMINISTRO DE SISTEMAS DE TRANSPORTE DE ELECTRICIDAD CON ALTA PENETRACIÓN DE ENERGÍAS RENOVABLES

UNIVERSIDAD DE ZARAGOZA

Investigador principal 1.
Dr. José María Yusta Loyo
Investigador principal 2.
Dr. José Antonio Domínguez Navarro

Proyecto financiado por:
Ministerio de Ciencia e Innovación,
MCIN/AEI/ 501100011033/10.13039
Referencia: PID104711-2019RB-I00

MINISTERIO DE CIENCIA E INNOVACIÓN

AGENCIA ESTATAL DE INVESTIGACIÓN

PROYECTO RED4CRIT

ÍNDICE

04 Resumen del proyecto

05 Contexto y problema abordado

06 Propuesta de investigación

07 Desarrollo de actividades

19 Conclusiones

20 Difusión de los resultados

RESUMEN DEL PROYECTO

La finalidad principal de este proyecto de investigación es la evaluación conjunta de la fiabilidad, robustez y restauración de sistemas de transporte y distribución de electricidad con elevada penetración de energías renovables ante amenazas de interrupción del suministro eléctrico. Las fuentes renovables son esenciales para el actual proceso de descarbonización de los sistemas eléctricos en la mayoría de los países. Debido a su naturaleza estocástica y variable, estos recursos podrían exponer a una red eléctrica a cortes de energía inesperados. En este contexto, los estudios de seguridad son vitales para el funcionamiento seguro y cotidiano de la infraestructura.

El presente proyecto ha permitido avanzar en los siguientes aspectos en este campo de investigación:

- Se han seleccionado indicadores para los procesos de cálculo de fiabilidad, robustez y restauración de los sistemas eléctricos, y se han aplicado a casos de redes de prueba.
- Para el análisis de fiabilidad se ha utilizado el método Monte Carlo secuencial debido a su flexibilidad, precisión y capacidad.
- Para evaluar la robustez de las infraestructuras eléctricas, se ha desarrollado un modelo de desintegración basado en fallos en cascada considerando las características operativas de las líneas eléctricas mediante flujos de carga en DC.
- En cuanto a la restauración, se ha aplicado una técnica de optimización matemática mixta-entera para obtener la programación óptima de operaciones para recuperar las cargas y conectividad del sistema eléctrico tras un fallo en cascada.
- El análisis conjunto de los tres conceptos propuestos en esta investigación puede convertirse en un criterio muy útil para caracterizar diferentes topologías y mejorar la seguridad del suministro eléctrico.
- Se han analizado los efectos de las interconexiones en la resiliencia de los sistemas eléctricos acoplados, mediante el desarrollo de una metodología multicriterio que permite evaluar y priorizar proyectos de interconexión eléctrica transfronteriza considerando criterios técnicos, económicos, ambientales y sociales. Se ha aplicado al estudio de los nuevos proyectos de interconexión eléctrica España-Francia.
- Las conclusiones del proyecto ponen de relieve la importancia de la evaluación integrada de la fiabilidad, robustez y restauración para establecer sus características y relaciones entre ellos. Este enfoque puede tener un impacto significativo en el rendimiento y la calidad de una red eléctrica, mejorar la satisfacción de los consumidores y ayudar a los gestores de redes en el proceso de la toma de decisiones para conseguir una mejor planificación de las infraestructuras eléctricas.

CONTEXTO Y PROBLEMA ABRORDADO

Los sistemas eléctricos son fundamentales para el funcionamiento cotidiano de cualquier sociedad moderna. Estas infraestructuras son complejas y propensas a fallos y amenazas que pueden ocasionar graves interrupciones en los servicios que prestan a la sociedad (actividades económicas, salud pública, etc.). Por esta razón, todos los países anhelan disponer de un sistema fiable y seguro que garantice el suministro eléctrico ante cualquier situación.

En un entorno geopolítico cada vez más complejo y de lucha contra el cambio climático, la Unión Europea (UE) ha promovido, en los últimos años, una ambiciosa política energética para alcanzar un equilibrio entre el desarrollo sostenible, la competitividad y la seguridad del suministro eléctrico. En este contexto, las interconexiones eléctricas juegan un papel fundamental para llevar a cabo la transición energética, por lo que su refuerzo son una prioridad para los próximos años en el desarrollo de la red de transporte. Estas presentan numerosos beneficios económicos y técnicos para los países interconectados, tales como una mayor integración e intercambio de energía renovable, mayor competencia de precios entre los sistemas eléctricos vecinos, la reducción de la dependencia de importación de combustibles fósiles, la mejora en la seguridad y fiabilidad del sistema, además de aumentar las posibilidades de compartir reservas de regulación.

En definitiva, las redes eléctricas son garantes de la prosperidad económica de la sociedad, pero no son descartables fallos en cascada debido a fenómenos naturales, acciones maliciosas, envejecimiento de activos, etc. Una evaluación adecuada es importante para reducir la probabilidad de ocurrencia de estos posibles sucesos: minimizar estas amenazas plantea grandes retos de análisis que han constituido la base de este proyecto de investigación.

PROPUESTA DE INVESTIGACIÓN

El objetivo general del proyecto es el diseño y operación inteligente ante amenazas de interrupción del suministro de sistemas de transporte de electricidad con alta penetración de energías renovables. Para abordar este objetivo general, se han planteado cuatro objetivos específicos.

1

OBJETIVO 1

Desarrollar una metodología computacionalmente eficiente para evaluar la fiabilidad y la robustez de la red de transporte y distribución de electricidad con elevada penetración de renovables ante contingencias ciberfísicas con distinta probabilidad de ocurrencia e impacto.

2

OBJETIVO 2

Investigar la aplicación de técnicas matemáticas de inteligencia artificial al problema de restauración óptima del suministro eléctrico después de un fallo generalizado en redes eléctricas con elevada penetración de renovables.

3

OBJETIVO 3

Categorizar los posibles diseños de la topología de las redes eléctricas según su resiliencia, integrando los indicadores de fiabilidad, robustez y restauración en una única herramienta de análisis multicriterio (MCDM).

4

OBJETIVO 4

Evaluar la seguridad de las interconexiones transfronterizas en la red europea de transporte de electricidad, evaluando particularmente los nuevos proyectos de interconexión España-Francia financiados por la Unión Europea bajo el programa de infraestructuras claves PCI (Projects of Common Interest).

Desarrollo de

ACTIVIDADES

ACTIVIDAD 1

Metodología evaluación fiabilidad y robustez sistemas eléctricos con renovables ante contingencias ciberfísicas de probabilidad e impacto variables.

ACTIVIDAD 2

Metodología IA para restauración óptima del suministro eléctrico tras fallos en sistemas con renovables. Incluye reconfiguración y categorización de la resiliencia de la red.

ACTIVIDAD 3

Metodología integra indicadores de fiabilidad, robustez y restauración en sistemas eléctricos con renovables ante contingencias ciberfísicas. Proporciona herramienta MCDM para diseño de topologías de red seguras.

ACTIVIDAD 4

Aplicación de la metodología MCDM al estudio de seguridad en interconexiones transfronterizas de la red eléctrica europea. Enfoque en proyectos de interconexión España-Francia financiados por la UE en el programa PCI.

DESARROLLO DE ACTIVIDADES

ACTIVIDAD 1

En los últimos años, los sistemas de energía eléctrica se han vuelto cada vez más interconectados, complejos e interdependientes. Además, la integración creciente de generación de energía renovable en las redes eléctricas existentes, ha obligado a los operadores de red a vigilar más estrechamente los niveles de seguridad de la infraestructura eléctrica para responder ante posibles contingencias. Para medir el desempeño de la infraestructura eléctrica se utilizan los parámetros de la fiabilidad y la robustez. La fiabilidad está relacionada con la continuidad de las operaciones en caso de fallo de uno o dos activos de la infraestructura, mientras que la robustez está asociada con el funcionamiento de la red eléctrica frente a la pérdida de múltiples activos. El efecto de la alta penetración de las energías renovables sobre la fiabilidad y robustez de los sistemas eléctricos interconectados abre un nuevo campo de investigación, que requiere la necesidad de proponer marcos metodológicos integrados para estudiar diferentes atributos interrelacionados de ambos conceptos.

La primera actividad propuesta en esta investigación ha tenido como objetivo el desarrollo de una metodología para evaluar la fiabilidad y robustez conjuntamente de las redes integradas con fuentes de generación renovable. Las etapas principales que componen este procedimiento son las siguientes.

Análisis de fiabilidad

Primero, se realizó el análisis de fiabilidad mediante la aplicación de la técnica de cálculo de Monte Carlo secuencial. Este método es una técnica precisa para simular el proceso cronológico real de la red, estudiar el comportamiento aleatorio del sistema y medir diferentes indicadores de fiabilidad de la infraestructura eléctrica. Está basado en la utilización de información estadística sobre las tasas de fallo y tiempos de recuperación de los componentes de la red. No obstante, requiere bastante esfuerzo computacional.

Análisis de robustez

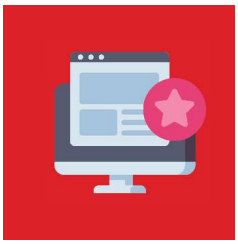

Posteriormente, se llevó a cabo el análisis de robustez a través de un procedimiento de desintegración en cascada de la red eléctrica, que consiste en la eliminación aleatoria e iterativa de cada uno de los buses de los sistemas interconectados. Se seleccionaron los indicadores a considerar en el proceso de cálculo de robustez de la red eléctrica. En cada fase de descomposición del sistema, se calculan los flujos de potencia óptimos en corriente continua, se mide el índice de carga desconectada (DL) para evaluar la funcionalidad del sistema durante eventos de contingencia, y se cuantifica también el índice de área de daño (DA) para analizar con precisión las curvas de comportamiento de la total desintegración de la infraestructura.

Validación de la metodología

Para validar la metodología desarrollada, los procedimientos planteados se han aplicado secuencialmente en seis casos de estudio con diferentes porcentajes de generación y grados de acoplamiento basadas en las redes de prueba IEEE RTS-96 e IEEE RTS-GMLC (red modificada de NREL con generadores renovables).

Los principales resultados obtenidos de esta actividad se publicaron en un artículo científico en la revista Reliability Engineering & System Safety, indexada Q1 en el ranking JCR.

- "**The effects of the high penetration of renewable energies on the reliability and vulnerability of interconnected electric power systems**", Reliability Engineering & System Safety, Vol. 215, 2021, 107881, ISSN 0951-8320, https://doi.org/10.1016/j.ress.2021.107881

El desarrollo de esta actividad ha permitido comprobar que las fuentes renovables tienen un mayor impacto en la fiabilidad del sistema, mientras que las líneas de interconexión permiten mejorar la distribución de energía entre las redes acopladas, pero al mismo tiempo son activos críticos propensos a propagar perturbaciones de un sistema a otro. Por tanto, la mejor solución es aumentar la capacidad de interconexión para diseñar sistemas fiables y robustos y responder a contingencias n-1 y n-k, respectivamente.

DESARROLLO DE ACTIVIDADES

ACTIVIDAD 2

Proponer, desarrollar y validar una metodología de restauración óptima del suministro eléctrico después de un fallo generalizado en sistemas eléctricos con elevada penetración de renovables, utilizando técnicas matemáticas de inteligencia artificial. Esta metodología servirá tanto como herramienta para la reconfiguración óptima del sistema después de un fallo en cascada como para categorizar la topología de la red según su resiliencia.

La restauración de un sistema de potencia depende tanto de su robustez como de la velocidad de recuperación de la carga. Una infraestructura eléctrica puede operar en condiciones estables hasta que falle un activo, lo que podría desencadenar efectos adversos y degradar una parte importante de la red. En esta última condición, los operadores ejecutan acciones iterativas para recuperar la demanda de energía eléctrica. La Figura 1 representa el comportamiento del sistema eléctrico cuando se produce algún fallo o desastre natural.

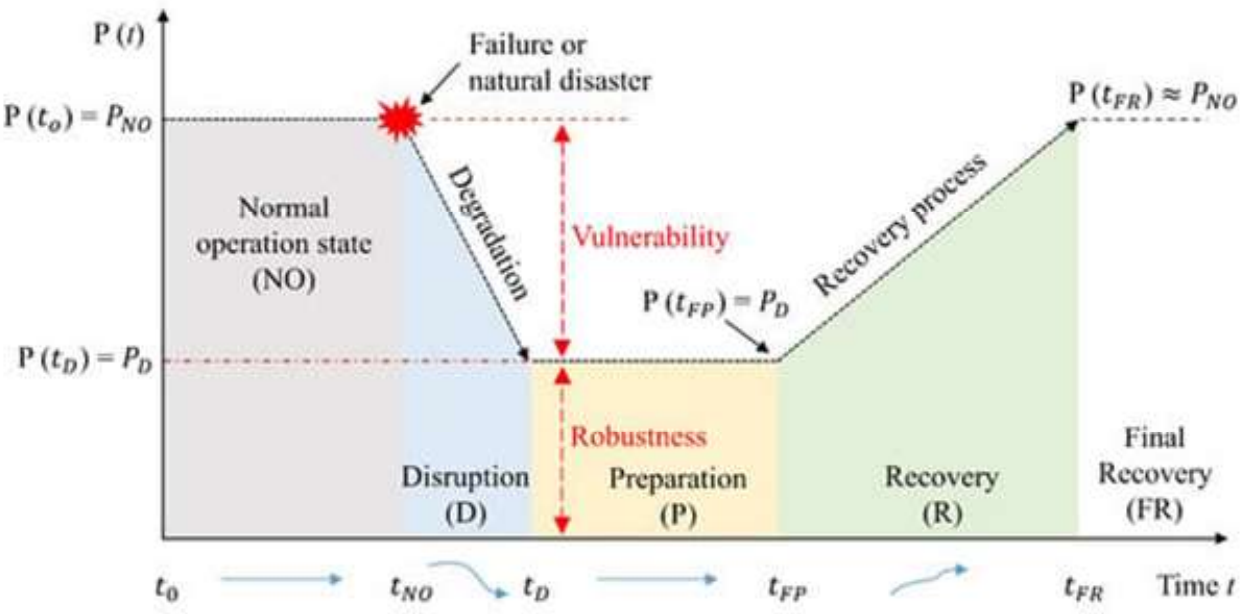

Figura 1. Comportamiento de un sistema eléctrico durante fallos y desastres naturales.

El objetivo de la segunda actividad propuesta en este proyecto de investigación es el desarrollo de una metodología para evaluar conjuntamente la robustez y resiliencia, y así estudiar en detalle

el impacto de las perturbaciones en los sistemas de potencia. Este análisis puede mejorar el rendimiento estructural de la red, la planificación del sistema, la fiabilidad e incluso la seguridad del suministro eléctrico.
La primera parte del desarrollo de esta actividad se ha centrado en la investigación de los distintos tipos de técnicas matemáticas de optimización combinatoria, programación dinámica, entre otras, para la planificación óptima multietapa de las acciones de restauración del suministro después de una contingencia severa en la red eléctrica con resultado de interrupción total o parcial de la demanda eléctrica.

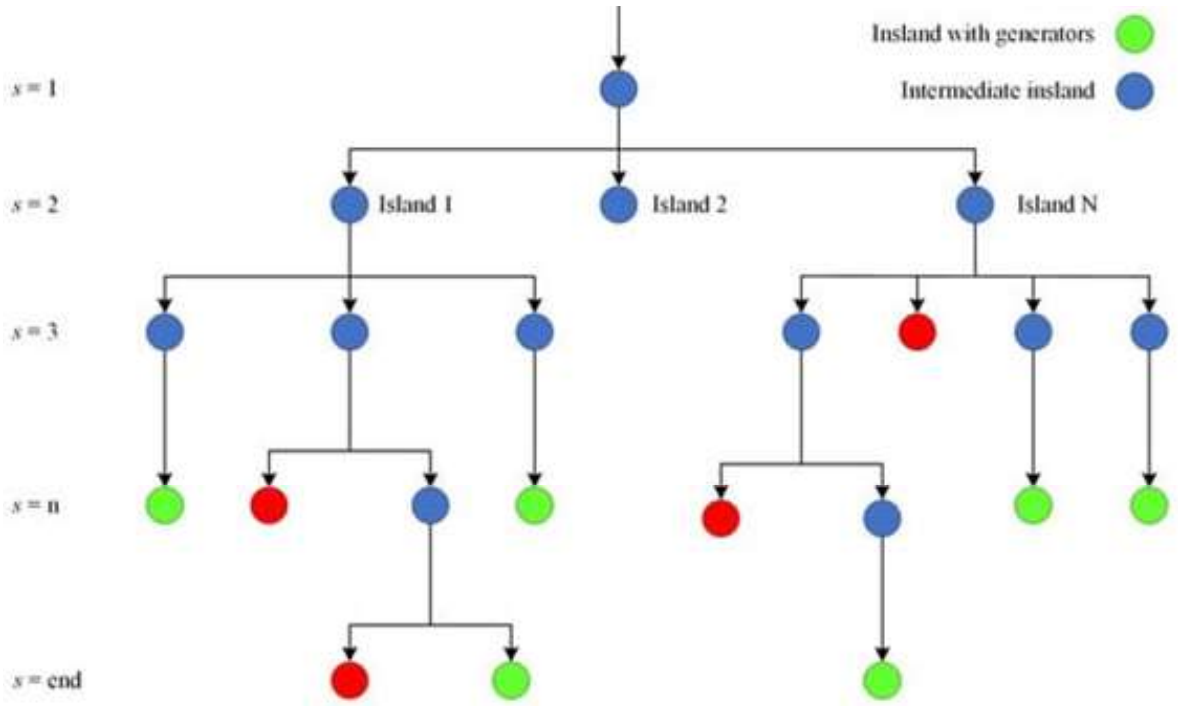

Figura 2. Estructura del árbol de proceso de fallo de cascada.

Adicionalmente, como consecuencia de la emergencia de las técnicas de inteligencia artificial, también se ha desarrollado un enfoque basado en redes neuronales de grafos tipados para resolver el problema del flujo de potencia. En este caso, las redes neuronales se entrenan en casos de referencia de la red eléctrica que se modifican al variar las inyecciones (carga y generación), las características de las ramas y la topología de red. Este método puede aplicarse para el análisis de contingencias, el despacho de tiempo real y evaluaciones tecno económicas de las redes eléctricas.

Finalmente, se optó como mejor solución por una técnica de optimización matemática mixta-entera para la programación computacional de la secuencia óptima de maniobras de operación para la restauración del sistema eléctrico. Estas operaciones incluyen tanto el redespacho de la

generación como la apertura y cierre de líneas eléctricas, en intervalos de 15 minutos.

El operador de la red de transporte eléctrica toma decisiones de recuperación en intervalos de tiempo secuenciales (es decir, primero planifica las acciones a tomar y, después de su ejecución, analiza el resultado antes de continuar con los siguientes pasos de restauración). En esta actividad, este proceso secuencial de toma de decisiones se mejora al formularlo como un problema de optimización para garantizar siempre que se seleccione el mejor conjunto de acciones de redespacho y reconfiguración a lo largo de todo el proceso de recuperación de la infraestructura. Esta formulación debería recuperar la máxima demanda en el menor tiempo posible.
Sin embargo, este último es un problema matemático complejo con múltiples decisiones posibles en cada etapa de restauración, ya que el número de acciones posibles crece exponencialmente con el número de iteraciones y tiene una complejidad computacional muy alta.

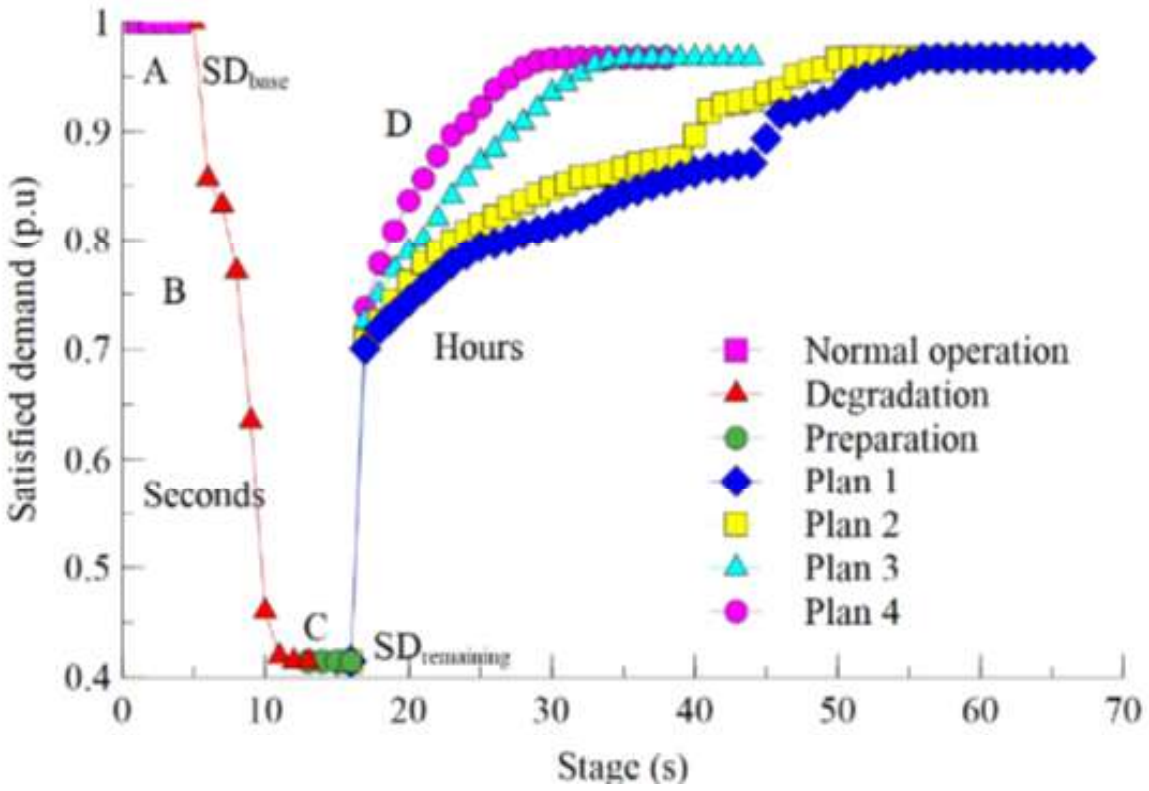

Figura 3. Curvas de recuperación para el sistema de prueba IEEE 118.

El objetivo de este trabajo es dar una primera solución a este complejo problema mediante el desarrollo de un procedimiento para determinar qué líneas eléctricas deben cerrarse en cada etapa de recuperación. El conjunto de líneas identificado no debe causar sobrecargas en los enlaces operativos y debe maximizar la carga recuperada en la red. Este proceso proporcionaría a los operadores información completa para tomar sus decisiones después de un colapso o apagón generalizado.

En definitiva, la metodología propuesta ha utilizado el estudio de robustez para determinar el estado inicial de desintegración de la red y empleó esta información de estado como datos de entrada para el estudio de resiliencia. La Figura 2 representa el proceso de fallo de cascada de la metodología que se propuso en este trabajo.

El estudio de resiliencia se ha planteado como un problema de optimización mixta-entera construido a partir de las ecuaciones de flujo de potencia de corriente continua, donde las variables enteras representan el estado operativo de las líneas eléctricas (es decir, abiertas o cerradas). En términos generales, el marco propuesto ha permito calcular los despachos de generación óptimos y determinar los enlaces a cerrar para la recuperación óptima de la topología de la red. Este último proceso está limitado por el número máximo de líneas que se pueden operar en cada paso iterativo. Durante el proceso de recuperación, se han considerado los flujos de potencia activa en las líneas eléctricas para evitar la sobrecarga de otros activos.

Para demostrar la aplicabilidad de la metodología propuesta, se ha utilizado como caso de estudio la red de prueba IEEE 118. Se analizó el impacto de las variaciones tanto en la generación como en la carga para distintos escenarios de simulación, ilustrando las diferentes condiciones operativas de la red. La Figura 3 representa las curvas de recuperación de los distintos planes obtenidos del estudio de resiliencia.

Los principales resultados obtenidos de esta actividad se publicaron en dos artículos científicos en revistas indexadas JCR con calificación Q1 y Q3, y también se presentaron en un congreso internacional:

- "**Integrated Risk Assessment for Robustness Evaluation and Resilience Optimisation of Power Systems after Cascading Failures**", Energies Vol. 14(7), 2028, 2021, https://doi.org/10.3390/en14072028

- "**Power flow analysis via typed graph neural networks**," Engineering Applications of Artificial Intelligence, vol. 117, no. June 2022, p. 105567, 2023, doi: 10.1016/j.engappai.2022.105567.

- "**Vulnerability and Resilience Assessment of Power Systems: From Deterioration to Recovery via a Topological Model based on Graph Theory**", 2020 IEEE International Autumn Meeting on Power, Electronics and Computing (ROPEC), 2020

Los resultados indicaron que la recuperación de una red podría estar relacionada con la capacidad de sobrecarga de las líneas eléctricas. En otras palabras, un sistema de potencia con alta capacidad de sobrecarga puede soportar mayores esfuerzos operativos, lo que se relaciona con una mayor robustez y un proceso de recuperación más rápido.

DESARROLLO DE ACTIVIDADES

ACTIVIDAD 3

Establecer una metodología para la integración de los indicadores de fiabilidad, robustez y restauración de sistemas eléctricos con elevada penetración de renovables ante distintos tipos de contingencias ciberfísicas, proporcionando una herramienta de decisión multicriterio (MCDM) para el diseño de topologías de red más seguras.

Los sistemas de energía eléctrica deben ser fiables y resilientes, especialmente en el actual escenario de descarbonización y electrificación. Sin embargo, los riegos para la seguridad aumentan y evolucionan al mismo ritmo que la red eléctrica. Por lo tanto, se requieren más estudios para analizar los atributos asociados a la operación del sistema y realizar un seguimiento de los cambios en el comportamiento de las redes ante la penetración de la generación renovable.

El objetivo de esta actividad es el desarrollo de una metodología basada en datos para analizar la fiabilidad, robustez y resiliencia desde una perspectiva integrada para caracterizar diferentes topologías de red eléctrica.

En una primera parte, se han analizado comparativamente los indicadores de fiabilidad, robustez y restauración del sistema eléctrico obtenidos en las actividades 1 y 2, aplicándolos a distintas redes de prueba con distinto grado de penetración de renovables.

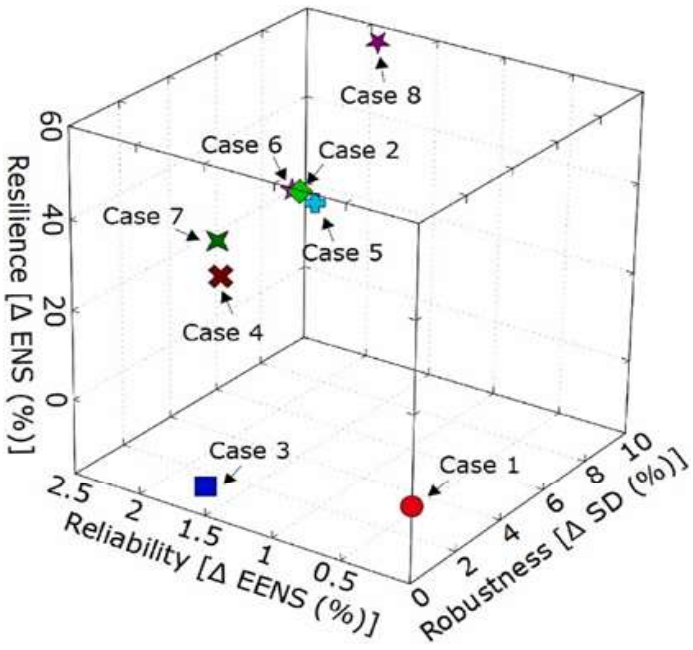

Figura 4. Resultados obtenidos integrados dentro del concepto R3.

Posteriormente, se ha evaluado conjuntamente la fiabilidad, robustez y resiliencia para cuantificar la seguridad de las topologías de las redes eléctricas. Se han construido ocho casos de estudio a partir de la red de prueba IEEE-RTS 24. La fiabilidad se ha analizado mediante la aplicación del método Monte Carlo secuencial, la robustez a través de la simulación de fallos en cascada y la resiliencia mediante un proceso de recuperación basado en optimización matemática mixta-entera. Además, se

calcularon los distintos indicadores asociados a cada uno de los tres conceptos. Los resultados obtenidos para las distintas topologías de red se comparan gráfica y cuantitativamente mediante una representación tridimensional, tal y como se indica en la Figura 4.

Los resultados mostraron que una topología más mallada del sistema eléctrico no siempre puede garantizarse como la mejor desde la perspectiva de cada criterio, pero en general ofrece los mejores resultados óptimos para la seguridad del suministro.
Los resultados obtenidos de esta actividad se presentaron en dos congresos internacionales. Además, se ha publicado un artículo científico en la revista Energy Strategy Reviews, indexada JCR con categoría Q1.

- "**Comparative evaluation of reliability and vulnerability for electrical networks with a high share of renewable generation**", 31st annual European Safety and Reliability conference – ESREL2021, 19 al 23 de septiembre de 2021, Angers, Francia.

- "**Evaluation of Reliability and Robustness of Electric Power Systems with Renewable Energies,**" 2021 IEEE International Autumn Meeting on Power, Electronics and Computing (ROPEC), 10 al 12 de noviembre de 2021, Ixtapa, México.

- "**Characterising the Security of Power System Topologies through a Combined Assessment of Reliability, Robustness, and Resilience**", Energy Strategy Reviews, Vol. 43, 2022, 100944, https://doi.org/10.1016/j.esr.2022.100944

Los resultados de esta actividad demostraron de forma clara y precisa la necesidad de realizar más estudios integrados para obtener una visión mucho más amplia del comportamiento operativo de los sistemas eléctricos. Un planificador de sistemas eléctricos puede realizar el procedimiento propuesto en esta actividad y ejecutarlo para identificar posibles inversiones o mejoras en la topología del sistema eléctrico.

DESARROLLO DE ACTIVIDADES

ACTIVIDAD 4

Aplicar la metodología MCDM al estudio de la seguridad de las interconexiones transfronterizas en la red europea de transporte de electricidad, evaluando particularmente los nuevos proyectos de interconexión España-Francia financiados por la Unión Europea bajo el programa de infraestructuras claves PCI (Projects of Common Interest).

Las infraestructuras eléctricas y gasistas desempeñan un papel clave en la transición hacia el nuevo modelo energético, con una elevada penetración de renovables, tanto para garantizar la capacidad firme de los sistemas eléctricos como para integrar todas las energías.

Dado que la Unión Europea depende en gran medida del gas y del petróleo de terceros países para su seguridad de abastecimiento energético, se están impulsando proyectos de nuevas interconexiones energéticas transfronterizas para mejorar la capacidad de suministro, reducir la actual fragmentación del mercado europeo y erradicar el aislamiento de las áreas más desfavorecidas. Además, estas interconexiones facilitan las funciones de apoyo entre sistemas vecinos ante contingencias, y reducen la dependencia de terceros países. Estos proyectos favorecen también la integración de las energías renovables y mejoran tanto la competencia en el mercado eléctrico como la seguridad del suministro eléctrico. Sin embargo, la selección de estos proyectos es una tarea compleja, ya que intervienen múltiples objetivos, criterios, participantes y alternativas.

Como consecuencia de la interdependencia entre las redes de gas y electricidad, en la primera parte de la actividad se estudió la seguridad del sistema energético europeo con la posibilidad de compartir los recursos e infraestructuras de los países vecinos frente a crisis del suministro de gas natural debido a fenómenos naturales, políticos y técnicos. Para este objetivo, se realizó un completo modelo de la red europea de infraestructuras y recursos, y se estudiaron distintos escenarios de contingencias en el abastecimiento de energía.

Por otro lado, dada la importancia de los sistemas de almacenamiento de energía para favorecer la integración de la producción eléctrica renovable, se evaluó en todos los países europeos el potencial del almacenamiento mediante bombeo hidroeléctrico para garantizar un suministro seguro de electricidad ante situaciones críticas en el abastecimiento a las centrales eléctricas alimentadas con gas natural.

Los resultados obtenidos de esta primera parte de la actividad propuesta fueron publicados en un artículo científico en una revista indexada Q1. Además, se presentaron dos artículos en congresos internacionales:

- **"Optimal cooperative model for the security of gas supply on European gas networks,"** Energy Strateg. Rev., vol. 38, p. 100706, Nov. 2021, doi: 10.1016/j.esr.2021.100706

- "**Pumped-hydro potential to enhance power system resilience under critical gas supply interruptions**", 32nd annual European Safety and Reliability conference – ESREL2022, 28 de agosto a 1 de septiembre de 2022, Dublín, Irlanda. doi: 10.3850/978-981-18-5183-4_S21-04-410-cd

- "**Robustness analysis of power systems with a high share of renewables**", 7th AIEE Energy Symposium-Current and Future Challenges to Energy Security, 12 a 16 de diciembre de 2022, Italia.

A partir de esta investigación, desde una perspectiva energética a largo plazo, está comprobado que un futuro compuesto íntegramente por generación renovable no es posible solo con la tecnología actual. Es fundamental mantener unas infraestructuras energéticas robustas mientras se completa con éxito la transición energética. Además, los objetivos de descarbonización del sector eléctrico no pueden alcanzarse sin un almacenamiento de energía que respalde la intermitencia de la generación renovable (principalmente bombeo hidroeléctrico y baterías) y un mayor número de interconexiones eléctricas para favorecer la integración de las renovables en los sistemas eléctricos y la seguridad del suministro eléctrico.

La segunda parte de la actividad se centró en el desarrollo y aplicación de una metodología de toma de decisión multicriterio con el método AHP para la evaluación de proyectos de interconexiones eléctricas transfronterizas bajo criterios técnicos, sociales, económicos y ambientales. Además, se han identificado y analizado los indicadores incluidos en los proyectos de interconexión transfronteriza que afectan a la fiabilidad, robustez y restauración de los sistemas eléctricos interconectados.

Tradicionalmente, se han utilizado herramientas de análisis de coste-beneficio (CBA) para analizar inversiones estratégicas en el sector eléctrico. Este análisis se centra en la justificación de las inversiones en términos económicos. Se contabiliza todo lo que se puede traducir en unidades monetarias. Por tanto, con esta herramienta resulta difícil valorar algunos impactos de los proyectos, como el impacto ambiental, la seguridad del sistema eléctrico y el impacto social, entre otros. Por esta razón, se eligió el método multicriterio para la evaluación y priorización de proyectos de interconexión eléctrica según distintos criterios, ya que no es necesario expresar los criterios en términos monetarios. Además, este método permite organizar eficazmente los datos sobre un problema, descomponiéndolos y analizándolos por partes, lo que proporciona un resultado objetivo y fiable.

Para verificar la aplicabilidad de esta metodología, se han evaluado los nuevos proyectos de interconexión de infraestructura eléctrica entre España-Francia financiados por la Unión Europea bajo el programa de proyectos de infraestructuras clave (PCIs). Los datos de la topología, las

características técnicas y toda la información necesaria para esta evaluación se han obtenido de los ficheros de datos disponibles en ENTSO-e para toda la red eléctrica europea. Estos proyectos pueden beneficiarse de procedimientos administrativos más rápidos, una evaluación medioambiental más adecuada y posibles ayudas financieras para su ejecución.

Además, se simularon diferentes escenarios para estudiar el efecto de los cambios de los criterios seleccionados para la evaluación y priorización de proyectos en los resultados obtenidos. El estudio de sensibilidad es una herramienta complementaria necesaria en el proceso de decisión multicriterio para reducir la subjetividad asociada a cualquier método de decisión.

Los principales resultados obtenidos de esta actividad se han recogido en un artículo científico

- "**Assessment of cross-border electricity interconnection projects using MCDA methods**" que ha sido enviado y se encuentra en fase de revisión en una revista indexada Q1.

Adicionalmente, se ha presentado un artículo en un congreso internacional:

- "T**echnical versus socio-economic and environmental criteria in power transmission projects**", 21st International Conference on Renewable Energies and Power Quality (ICREPQ' 23), 24 al 26 de mayo de 2023, Madrid.

Los resultados de esta parte de la investigación verificaron que la metodología propuesta es coherente, favorece la compresión de proyectos con un gran número de agentes implicados y ayuda en la priorización de una cartera de proyectos con un método claro y explícito. En definitiva, la herramienta desarrollada ofrece una visión completa del impacto real de los proyectos de interconexión eléctrica. Esta información ha sido compartida con los operadores de las redes eléctricas de transporte y distribución españolas.

CONCLUSIONES

La falta de metodologías y técnicas de análisis que permitan evaluar conjuntamente la fiabilidad, robustez y restauración de los sistemas eléctricos con alta penetración de energías renovables ha constituido la principal motivación para abordar este proyecto de investigación.

- El aumento de la participación de las energías renovables en el mix energético presenta importantes retos que deben abordarse integralmente para cumplir los requisitos de seguridad de las infraestructuras eléctricas. Este proyecto ha conseguido medir la influencia de la generación renovable y el impacto de las líneas de interconexión en el comportamiento operativo de los sistemas ante distintos tipos de contingencias o perturbaciones.

- El análisis conjunto de la fiabilidad y vulnerabilidad de las redes eléctricas ha permitido cuantificar el rendimiento de los sistemas con distinta penetración de generación renovable y con diferentes grados de acoplamiento de las infraestructuras eléctricas.

- En la evaluación conjunta de la robustez y resiliencia de los sistemas eléctricos, por un lado, el procedimiento de análisis de fallos en cascada ha permitido determinar el estado de desintegración de una red eléctrica y, por otro lado, se ha desarrollado un modelo matemático de optimización para identificar el despacho de generación y la topología óptimos durante el proceso de recuperación de la red. Esta metodología permite proporcionar a los operadores de red información completa para tomar las mejores decisiones tras un apagón total o parcial.

- La propuesta de un análisis integrado de fiabilidad, robustez y resiliencia ha permitido caracterizar diferentes topologías para mejorar la seguridad del suministro eléctrico. En general, la topología mallada dispone de ventajas, al permitir satisfacer una mayor demanda en caso de perturbaciones o averías, además de restablecer antes el suministro eléctrico

- Se ha desarrollado una metodología de análisis de decisión multicriterio para evaluar y priorizar una cartera de proyectos de interconexión eléctrica transfronteriza considerando criterios técnicos, económicos, medioambientales y sociales. Esta metodología puede servir como una herramienta de apoyo en el proceso de selección de alternativas de proyectos de interconexión eléctrica y ayudar a comprender mejor el comportamiento y las limitaciones de las redes eléctricas de transporte.

En definitiva, este proyecto de investigación pone de relieve la importancia de análisis integrados para obtener una visión mucho más amplia del comportamiento operativo de los sistemas eléctricos con alta penetración de energías renovables. Las herramientas propuestas pueden ayudar a los gestores de las redes a identificar posibles condiciones de riesgo en sus infraestructuras y proponer posibles inversiones y mejoras de los sistemas eléctricos.

DIFUSIÓN DE LOS RESULTADOS

PUBLICACIONES EN REVISTAS CIENTÍFICAS INTERNACIONALES

- J. Beyza and J. M. Yusta, "**Characterising the security of power system topologies through a combined assessment of reliability, robustness, and resilience,**" Energy Strateg. Rev., vol. 43, no. February, p. 100944, 2022, doi: 10.1016/j.esr.2022.100944.

- J. Beyza and J. M. Yusta, "**Integrated risk assessment for robustness evaluation and resilience optimisation of power systems after cascading failures**," Energies, vol. 14, no. 7, 2021, doi: 10.3390/en14072028.

- J. M. Yusta and J. Beyza, "**Optimal cooperative model for the security of gas supply on European gas networks,**" Energy Strateg. Rev., vol. 38, p. 100706, 2021, doi: 10.1016/j.esr.2021.100706.

- T. B. Lopez-Garcia and J. A. Domínguez-Navarro, "**Power flow analysis via typed graph neural networks,**" Eng. Appl. Artif. Intell., vol. 117, no. June 2022, p. 105567, 2023, doi: 10.1016/j.engappai.2022.105567.

- J. Beyza and J. M. Yusta, "**The effects of the high penetration of renewable energies on the reliability and vulnerability of interconnected electric power systems,**" Reliab. Eng. Syst. Saf., vol. 215, no. June, p. 107881, 2021, doi: 10.1016/j.ress.2021.107881.

- N. Naval and J. M. Yusta, "**Assessment of cross-border electricity interconnection projects using MCDA methods**," Energy Strategy Reviews (under review).

PUBLICACIONES EN CONGRESOS Y PARTICIPACIÓN EN CONFERENCIAS

- J. Beyza and J.M. Yusta, "**Comparative Evaluation of the Reliability and Vulnerability of Electrical Networks with a High Share of Renewable Generation,**" Proc. 31st Eur. Saf. Reliab. Conf. ESREL 2021, pp. 1884-1891, 2021, doi: 10.3850/978-981-18-2016-8.

- J. Beyza, J. M. Yusta, M. A. Evangelista, J. S. Artal-Sevil, and J. A. Rendon, "**Evaluation of Reliability and Robustness of Electric Power Systems with Renewable Energies**," 2021 23rd IEEE Int. Autumn Meet. Power, Electron. Comput. ROPEC 2021, no. Ropec, 2021, doi: 10.1109/ROPEC53248.2021.9668112.

- N. Naval, Y. Rqiq, and J. M. Yusta, "**Pumped-hydro potential to enhance power system resilience under critical gas supply interruptions,**" Proc. 32nd Eur. Saf. Reliab. Conf. ESREL 2022, 2022, doi: 10.3850/981-973-0000-00-0.

- N. Naval, J. J. Delgado, and J. M. Yusta, "**Robustness analysis of power systems with a high share of renewables**," in 7th AIEE Energy Symposium Current and Future Challenges to Energy Security, 2022.

- N. Naval and J. M. Yusta, "**Technical versus socio-economic and environmental criteria in power transmission projects**," in 21st International Conference on Renewable Energies and Power Quality (ICREPQ' 23), 2023.

ANEXOS

1. Comparative Evaluation of the Reliability and Vulnerability of Electrical Networks with a High Share of Renewable Generation

2. Evaluation of Reliability and Robustness of Electric Power Systems with Renewable Energies.

3. Pumped-hydro potential to enhance power system resilience under critical gas supply interruptions.

4. Robustness analysis of power systems with a high share of renewables.

5. Technical versus socio-economic and environmental criteria in power transmission projects.

6. Characterising the security of power system topologies through a combined assessment of reliability, robustness, and resilience.

7. Integrated risk assessment for robustness evaluation and resilience optimisation of power systems after cascading failures.

8. Optimal cooperative model for the security of gas supply on European gas networks.

9. Power flow analysis via typed graph neural networks.

10. The effects of the high penetration of renewable energies on the reliability and vulnerability of interconnected electric power systems.

11. Assessment of cross-border electricity interconnection projects using MCDA methods,

Comparative Evaluation of the Reliability and Vulnerability of Electrical Networks with a High Share of Renewable Generation

Jesus Beyza

Department of Electrical Engineering, University of Zaragoza, Spain. E-mail: jbeyza@unizar.es

Jose M. Yusta

Department of Electrical Engineering, University of Zaragoza, Spain. E-mail: jmyusta@unizar.es

The uncertainties associated with renewable energies can have a significant impact on the security of power systems. To address this problem, this article studies the effect of renewable sources on the reliability and vulnerability of systems with a high share of renewable generation and compares the results obtained with those measured in electrical grids mainly composed of thermal power plants. This comparison aims to quantify the influence of renewable generation on the performance and operational behavior of infrastructure under severe contingencies. Both reliability and vulnerability are assessed in parallel in two case studies: one based on the IEEE RTS-96 test system with thermal generation and the other on the IEEE RTS-GMLC test system with a high share of renewable generation. Different reliability indices are calculated using the sequential Monte Carlo method, and a vulnerability index is measured using a cascading failure approach. The simulations show that the integrated system with renewables is less reliable and more vulnerable than its purely thermal counterpart. These conclusions highlight the importance of analyzing the operational security of infrastructure from both perspectives.

Keywords: Cascading failures, critical infrastructures, power systems, reliability, renewable energies, robustness, vulnerability.

1. Introduction

In recent years, renewable generation sources such as wind energy and solar energy have increased exponentially in power systems due to the environmental problems associated with conventional power generation (Rakhshani et al. (2019)). Renewable resources are sustainable energy vectors with great environmental benefits for the planet. However, the electrical infrastructure's complexity has progressively increased with the deeper penetration of these energy sources, creating substantial challenges and risks in network security.

Renewable generators being highly dependent on weather conditions are sources of several uncertainties in the daily and continuous operation of the power grid, and expose the system vulnerabilities to cascading failures and congestion (Soder et al. (2007)). Transmission system operators must determine if energy production can safely and reliably meet the load demand. In this sense, reliability and vulnerability are the slogans used by electric utilities for managing these risks (Kadhem et al. (2017)).

The study of reliability and vulnerability in electrical systems with a high share of renewable energies has attracted much attention from researchers and academics. In general, both topics have a wide range of studies in the scientific literature.

On the one hand, reliability assessment is the most appropriate tool for the operator to assess the power system's performance, measure the frequency, duration and cost of interruptions, and compare different integration levels of renewables in the grid (Urgun and Singh (2018); Heylen et al. (2018)). There are two methods to assess reliability: the Monte Carlo simulation approach and the analytical approach (Gbadamosi and Nwulu (2020)). The first one uses statistical information on the failures and repairs of components to randomly verify the state of the network's assets. The second one uses mathematical formulations to analyze the problems associated with reliability indices.

Power systems with a high proportion of renewable energy sources must adjust their power output in a timely and adequate manner according to uncertain changes in these energy sources. This rescheduling operation aims to improve the reliability of the electrical grid (Fan et al. (2018)). To mitigate the adverse implications of intermittencies in renewable resources, some studies propose long-term generator scheduling strategies considering the sources' criticality and developing contingency tests (Kumar et al. (2020); Jiang et al. (2016)). Other studies list the benefits and challenges of incorporating renewable energy re-

Proceedings of the 31st European Safety and Reliability Conference
Edited by Bruno Castanier, Marko Cepin, David Bigaud, and Christophe Berenguer
Published by Research Publishing, Singapore.
ISBN: 978-981-18-2016-8; doi:10.3850/978-981-18-2016-8_115-cd

sources and present the different control strategies responsible for this incorporation (Ayadi et al. (2020)). Kumar et al. (2020) provide a comprehensive review of the improvements obtained in the reliability of the electrical grid thanks to renewable sources.

On the other hand, vulnerability assessment is the most appropriate tool for the operator to measure the infrastructure's capabilities in the face of critical events, quantify the entire network skeleton's structural performance, and identify the weakest buses that require significant reinforcement (Sabouhi et al. (2020); Kröger and Zio (2011)). Vulnerability can be classified into two well-established categories: functional vulnerability and structural vulnerability (Wolf et al. (2013)). The first type quantifies the technical and operational characteristics of the system during critical contingency scenarios. The second type measures the topological characteristics of the infrastructure throughout the network collapse process.

Some relevant works in the area assess vulnerability by measuring bus voltages and comparing different generation mix scenarios (Han et al. (2018)). However, others establish vulnerability indices based on short-circuit studies and centrality measures of graph theory (Zhao et al. (2020); Athari and Wang (2017)). These studies combined seek to identify and classify critical components according to their consequences, determine undesirable events and potential vulnerabilities, and propose countermeasures to reduce the degree of vulnerability of the power grid (Zio (2016); Athari and Wang (2016)). Contrary to the reliability procedure, the study of vulnerability does not consider the probabilities of asset failures during contingency events but rather considers the iterative exclusion of all network elements.

For all of the above, it is necessary to conduct both vulnerability and reliability studies and analyze the results jointly to minimize the risk of blackouts and interruptions in the energy supply of electrical systems with high penetration of renewable energies. Therefore, this study aims to analyze the effect of renewable sources on reliability and vulnerability and compare both sets of results with those obtained in power systems with coal-fired power plants. This comparison seeks to quantify how much renewable generators influence the performance and behavior of systems from both perspectives. It is important to note that research on joint reliability and vulnerability in electrical grids integrated with renewables is barely receiving attention, so more work is needed to fill the research gaps of the area under study.

The reliability study is performed by applying the sequential Monte Carlo simulation and measuring the conventional reliability indices, such as the expected energy not supplied index, the expected demand not supplied index, the expected frequency of load curtailment index, the loss of load expectancy index, the loss of load probability index and the average duration of load curtailment. The vulnerability study is carried out by randomly removing the buses, one by one, calculating optimal power flows and quantifying the disconnected load index in the infrastructure during each breakdown step. The results are compared to assess the behavior of the system with different types of generation mixes. These procedures take into account the basic guidelines found in the scientific literature. The data used for this work include the well-known IEEE Reliability Test System (RTS-96) network widely used in reliability studies and the test network of the National Renewable Energy Laboratory of the United States, NREL, which is an updated version of the previous network that incorporates a high penetration of renewable energy (Grigg et al. (1999); NREL (2016)).

The rest of this article is organized as follows: Section 2 presents the mathematical formulations and procedures to perform the reliability and vulnerability analyses applied in the study of power systems with a high share of renewables. Section 3 details the case studies based on the IEEE 24-bus test system and the IEEE 24-bus test system modified by NREL. Section 4 presents the simulations obtained, and finally, Section 5 presents the final discussion of this document.

2. Reliability and vulnerability of electrical grids with a high proportion of renewable sources

This section presents the reliability and vulnerability indices calculated in the sequential Monte Carlo approach and the cascading failure approach, respectively. The first part describes how to calculate the fundamental reliability indices in the renewable energy generation sector. The second part details the vulnerability procedure to study the collapse of the infrastructure and quantify the disconnected electrical load as a result of iterative contingencies.

2.1. *Reliability analysis*

The indices most used to assess the degree of severity of disruptive events in the electrical infrastructure are the indices of expected energy not supplied (EENS), expected demand not supplied (EDNS), expected frequency of load curtailment (EFLC), loss of load expectancy (LOLE), loss of load probability (LOLP) and average duration of load curtailment (ADLC). Here, the sequential Monte Carlo approach is used with a 1-hour temporal resolution in a year-long simulation horizon, that is, 8760 1-hour time steps each year. Of course, other temporal resolution can be used depending on the total amount of data available in

the study. The detailed mathematical formulations for each can be found elsewhere (Li et al. (2013)).

- EENS index. The sum of the energy not supplied in each of the 8760 1-hour steps [MWh/year].

$$EENS = \frac{\sum_{i=1}^{N_y} \sum_{j=1}^{N_i} E_{j,i}}{N_y} \quad (1)$$

- EDNS index. The average energy not supplied in each of the 8760 1-hour steps [MW].

$$EDNS = \frac{EENS}{8760} \quad (2)$$

- EFLC index. The frequency of the transitions from zero to zero of power not supplied [outages/year].

$$EFLC = \frac{\sum_{i=1}^{N_y} N_i}{N_y} \quad (3)$$

- LOLE index. The number of hours that the energy not supplied is above zero [hours/year].

$$LOLE = \frac{\sum_{i=1}^{N_y} \sum_{j=1}^{N_i} D_{j,i}}{N_y} \quad (4)$$

- LOLP index. The percentage of hours that the energy not supplied is above zero [%].

$$LOLP = \frac{LOLE}{8760} \quad (5)$$

- ADLC index. The average number of hours of load curtailment [hours/outage].

$$ADLC = \frac{LOLE}{EFLC} \quad (6)$$

On the other hand, it is important to model the events that cause interruptions in the infrastructure to calculate the level of reliability of the entire electrical system. Typical disturbances include power line outages, transformer problems and electrical substation failures. These events can be evaluated using the mean time to failure (MTTF) and mean time to repair (MTTR) parameters, which are inversely related to the failure (λ) and repair (μ) rates of each of the assets. The iterative procedure to carry out the reliability study can be found in (Li et al. (2013)).

$$MTTF = \frac{1}{\lambda} \quad (7)$$

$$MTTR = \frac{1}{\mu} \quad (8)$$

2.2. *Vulnerability analysis*

The vulnerability assessment requires the use of an index that allows quantifying the state of collapse of the entire electrical network as a result of multiple iterations of contingencies. The disconnected load (DL) index is an ideal measure to determine the system's decomposition in each iterative step (Beyza et al. (2020)).

- DL index. The percentage of the total load, compared to the base case, that remains connected in the electrical grid after the removal of an asset [%].

$$DL = 100 - (\frac{L_i}{L_{total}^{BC}} \times 100) \quad (9)$$

This measure is calculated as follows. Starting from a stable electrical infrastructure, a dynamic model of cascading failures is developed. The procedure begins by collecting the network's technical data, running direct current optimal power flows, measuring the total load of the infrastructure in its base case (L_{total}^{BC}) and initializing the DL index to 0. Next, the buses are removed from the system randomly and iteratively, one by one, and the power flows are calculated again to quantify the total remaining load connected to the network after each contingency i (L_i). The loss of a bus implies removing all the electrical lines connected to it and forming a new topological structure. Once the remaining load is calculated, the DL index is measured as a function of the total number of substations removed (f). Due to the randomness of the results, each experiment is repeated 1000 times to obtain an ideal statistical sample (Edwards (2007)). Once the number of samples is reached, the results are averaged, and the iterative procedure ends.

3. Test systems used

In this section, the IEEE RTS-96 test network and the IEEE RTS-GMLC test network created by NREL are described (Grigg et al. (1999); NREL (2016)). The first represents an electrical system with coal-fired power plants, while the second represents the previous infrastructure but introduces renewable generators. The objective is to use the same system but with a different generation mix.

3.1. *Description of the case studies*

In this article, two cases are considered to assess reliability and vulnerability together. The first case performs both studies without considering renewable energy alternatives. The second case considers the role of renewable sources in reliability and vulnerability indices.

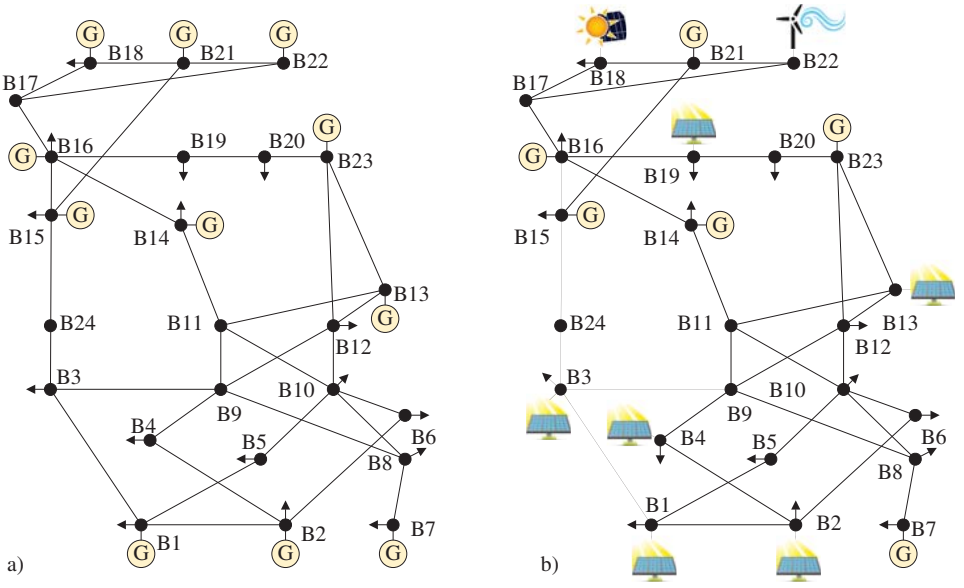

Fig. 1. Test systems under study. a) IEEE RTS network and b) IEEE RTS-GMLC network.

- Case 1) Reliability and vulnerability assessments without considering renewable energies

  This case corresponds to the well-known IEEE RTS-96 purely thermal test system composed of 24 buses, 33 generators and 38 power lines and transformers. This system has a maximum annual peak load of 2850 MW. Fig. 1 a) shows the topology of the test network. The fundamental data of the system under study, including the parameters of the lines, the general characteristics of the load, the physical constraints of the generators and the input data for the stochastic failure model for buses, transformers and lines, can be found in (Grigg et al. (1999)).

  This first system is widely used in reliability studies but does not always represent the current reality of different generations. Therefore, NREL launched a modified network of the same system known as IEEE RTS-GMLC, introducing renewable generators and updating the original thermal generators (NREL (2016)).
- Case 2) Reliability and vulnerability assessments considering renewable energies

  In this case, the impact of renewable sources is considered in both studies using the IEEE RTS-GMLC test system. In comparison with case study 1), large-scale photovoltaic (PV) generators are introduced in buses 1-4, 13 and 19, low-power rooftop photovoltaic (RTPVs) generators in bus 18 and wind (WIND) generators in bus 22. This network is located in the southwestern United States, which is an area with good solar and wind resources, demand data and hydroelectric generation. Fig. 1 b) shows the topology of the test network. The system data, such as the length of the lines, the characteristics of the load, the updated physical constraints of the generators, and the failure data of the assets, are given in (NREL (2016)). The demand and availability profiles for hydroelectric generation and the data for photovoltaic and wind generation are obtained from (Brinkman et al. (2016)) and (Lew et al. (2013)), respectively.

4. Numerical results

This section presents the simulation results obtained after applying the reliability and vulnerability assessments in the IEEE RTS-96 and RTS-GMLC test networks. The reliability indices are calculated using the PLEXOS software, and the vulnerability index is measured through the cascading failure algorithm described in Section 2.2 and implemented using MATLAB. Both simulations are run on a computer with a 3.40 GHz Intel® Core™ i7 CPU and 16 GB of RAM.

4.1. *Reliability assessment*

Table 1 shows the results obtained for the two test systems studied. A relative tolerance error of 6% in the coefficient of variation EENS was considered in the reliability study (Billinton and Sankarakrishnan (1995)). Thus, 500 iterations of one year were run for each case study, obtaining a covariance in the EENS index of 2.86% and 5.42%, as shown in Fig. 2. Additionally, the variability of renewable generation was incorporated in the reliability study of Case 2) to create a realistic model and apply the renewable resource data. Table 2 reports the statistical metrics calculated for root mean square error (RMSE), maximum absolute error (MaxAE), mean absolute error (MAE), mean bias error (MBE) and mean absolute percentage error (MAPE) (Zhang et al. (2013)). The closer the forecast is to the real value, the lower the dispersion of the metrics.

Table 1. Reliability results for the case studies.

	Case 1)	Case 2)
EENS [MWh/year]	2509.93	7717.33
EDNS [MW]	0.29	0.88
EFLC [outages/year]	4.78	10.10
LOLE [hours/year]	30.93	70.50
LOLP [%]	0.35	0.80
ADLC [hours/outage]	6.47	6.98
Computing time [h]	6.25	4.83

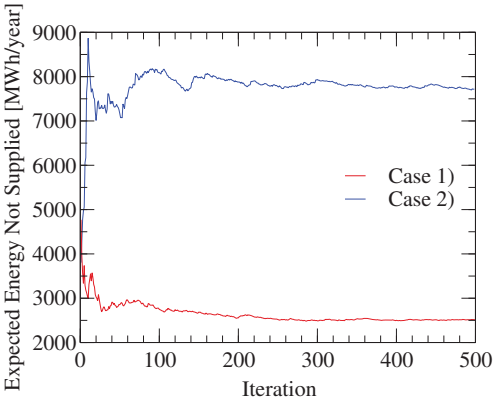

Fig. 2. Convergence of the EENS index.

Since the forecast of solar technologies is more accurate than wind technology, the renewable resource deviation from the MAPE index was used to determine the available generation in both the photovoltaic plants and the wind farm.

Table 2. Deviation in the forecasted renewable resource.

	Wind	PV	RTPV
RMSE [MW]	181.43	10.72	2.71
MaxAE [MW]	710.73	76.02	20.00
MAE [MW]	113.57	5.06	0.31
MBE [MW]	12.53	0.35	9.40
MAPE [%]	15.92	5.40	6.91

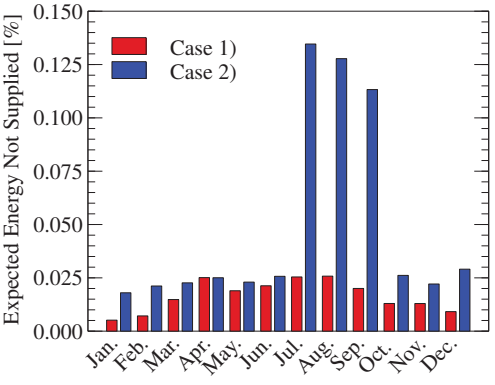

Fig. 3. Monthly percentage of energy not supplied.

On the other hand, the percentage of energy not supplied in each month compared to demand is reported in Fig. 3. The results show that the reliability of power systems decreases as renewable resources in the network increase. In Case 1), the EENS index increases in the middle months, not being excessively affected by the load variations in the rest of the year, while Case 2) has strong effects in the summer months because the energy not supplied increases enormously.

The power system with a high share of renewable sources, Case 2), is less reliable than the power system with only thermal generation, Case 1). This means that, in the case of random asset failures, the presence of renewable energy reduces the system's capability for responding and supplying all the energy demanded. In relative terms, there is three times more energy not supplied in the system with renewable generation than in the system with thermal generation.

4.2. *Vulnerability assessment*

The decomposition curves in Fig. 4 correspond to cases 1) and 2), obtained by averaging a set of 1000 samples from independent experiments.

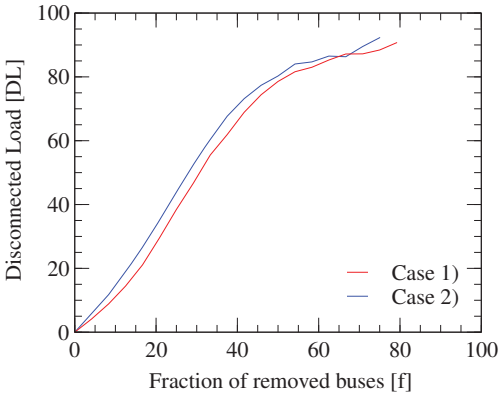

Fig. 4. Cascading failure curves for cases 1) and 2).

When the networks are initially connected, the DL index is equal to 0; then, as the systems collapse, the DL index progressively increases until 100. This indicates that the loads are completely disconnected. Note that this procedure does not consider the dynamics of the power system; however, it is valid for analysing the structural vulnerability of the network. The calculation times were 3.17 and 4.04 minutes, respectively.

The graphical results show that both networks collapse when approximately 80% of the electric buses are removed. When comparing both curves, it is observed that Case 1) is more robust than Case 2) since the plotted results are always below their counterparts. This indicates an increase in the vulnerability of the power system with a high share of renewable energies.

Table 3 shows some results corresponding to the removal of a given number of assets (f) and their impact on the disconnected load (DL) of the network.

Table 3. Impact on the disconnected load (DL).

	f=25%	f=50%	f=75%
Case 1)	38.45	78.57	88.43
Case 2)	43.86	80.28	92.28

As seen in Table 3, the DL in Case 2) is lower than that in Case 1) for all the fractions of removed assets, which again indicates that incorporating renewables does not increase the infrastructure's robustness compared to its thermal case. Instead, an increased vulnerability of the network can be inferred from the proposed iterative procedure's perspective.

5. Discussion and conclusion

There is currently a paradigm shift in the electrical system with the massive expansion of renewable energies in the generation mix. As such, challenges arise to guarantee the security of supply and the capacity of the infrastructure to respond to a gap in generation resulting from failures or contingencies. Reliability and vulnerability assessments are the main approaches in the electric power industry to address the above problems.

This work analyzed the effects of high share renewable sources on the reliability and vulnerability of electric power systems. Two networks with the same topological structure were used but with different contributions of renewable resources. The objective was to compare both sets of results to provide an overview of the infrastructure's behavior and performance.

From the strict point of view of the procedures and case studies used here, the joint results showed that the electrical system integrated with renewables experienced an increase of more than 300% in the EENS reliability index and 4% with f=75% in the DL vulnerability index. That is, the power system with renewable sources presented a lower capacity to respond to contingencies compared to the power grid with thermal generation. These differences could be due to the inability of renewable generators to satisfy the load conditions. From this, it follows that thermal power plants in the case studied have a greater generating capacity than renewable sources so that they can withstand abrupt variations in the network's operating conditions.

These findings show that new studies should include both perspectives to perform a complete analysis of the operational security of the network. This will provide operators with more complete information to make planning decisions. The results obtained here support the consolidated knowledge in this area of study.

Acknowledgement

This work was supported by the Ministry of Science and Innovation of Spain under project PID2019-104711RB-100: Smart-grid design and operation under the threat of interrupted supply from electric power transmission systems with a high penetration of renewable energies.

References

Athari, M. H. and Z. Wang (2016). Modeling the uncertainties in renewable generation and smart grid loads for the study of the grid vulnerability. In *2016 IEEE Power & Energy Society Innovative Smart Grid Technologies Conference (ISGT)*, pp. 1–5. IEEE.

Athari, M. H. and Z. Wang (2017). Impacts of wind power uncertainty on grid vulnerability to

cascading overload failures. *IEEE Transactions on Sustainable Energy 9*(1), 128–137.

Ayadi, F., I. Colak, I. Garip, and H. I. Bulbul (2020). Impacts of renewable energy resources in smart grid. In *2020 8th International Conference on Smart Grid (icSmartGrid)*, pp. 183–188. IEEE.

Beyza, J., H. F. Ruiz-Paredes, E. Garcia-Paricio, and J. M. Yusta (2020). Assessing the criticality of interdependent power and gas systems using complex networks and load flow techniques. *Physica A: Statistical Mechanics and its Applications 540*, 123169.

Billinton, R. and A. Sankarakrishnan (1995). A comparison of monte carlo simulation techniques for composite power system reliability assessment. In *IEEE WESCANEX 95. Communications, Power, and Computing. Conference Proceedings*, Volume 1, pp. 145–150. IEEE.

Brinkman, G., J. Jorgenson, A. Ehlen, and J. H. Caldwell (2016). Low Carbon Grid Study: Analysis of a 50% Emission Reduction in California.

Edwards, P. (2007). Essentials of statistics for business and economics.

Fan, M., K. Sun, D. Lane, W. Gu, Z. Li, and F. Zhang (2018). A novel generation rescheduling algorithm to improve power system reliability with high renewable energy penetration. *IEEE Transactions on Power Systems 33*(3), 3349–3357.

Gbadamosi, S. L. and N. I. Nwulu (2020). Reliability assessment of composite generation and transmission expansion planning incorporating renewable energy sources. *Journal of Renewable and Sustainable Energy 12*(2), 026301.

Grigg, C., P. Wong, P. Albrecht, R. Allan, M. Bhavaraju, R. Billinton, Q. Chen, C. Fong, S. Haddad, S. Kuruganty, et al. (1999). The ieee reliability test system-1996. a report prepared by the reliability test system task force of the application of probability methods subcommittee. *IEEE Transactions on power systems 14*(3), 1010–1020.

Han, H., C. Wu, S. Gao, and G. Zu (2018). An assessment approach of the power system vulnerability considering the uncertainties of wind power integration. In *2018 China International Conference on Electricity Distribution (CICED)*, pp. 741–745. IEEE.

Heylen, E., G. Deconinck, and D. Van Hertem (2018). Review and classification of reliability indicators for power systems with a high share of renewable energy sources. *Renewable and Sustainable Energy Reviews 97*, 554–568.

Jiang, Y., G. Wang, S. Roy, and C.-C. Liu (2016). Power system severe contingency screening considering renewable energy. In *2016 IEEE Power and Energy Society General Meeting (PESGM)*, pp. 1–5. IEEE.

Kadhem, A. A., N. I. A. Wahab, I. Aris, J. Jasni, and A. N. Abdalla (2017). Computational techniques for assessing the reliability and sustainability of electrical power systems: A review. *Renewable and Sustainable Energy Reviews 80*, 1175–1186.

Kröger, W. and E. Zio (2011). *Vulnerable Systems*. London: Springer London.

Kumar, D. S., A. Sharma, D. Srinivasan, and T. Reindl (2020). Impact analysis of large power networks with high share of renewables in transient conditions. *IET Renewable Power Generation 14*(8), 1349–1358.

Kumar, S., R. Saket, D. K. Dheer, J. Holm-Nielsen, and P. Sanjeevikumar (2020). Reliability enhancement of electrical power system including impacts of renewable energy sources: a comprehensive review. *IET Generation, Transmission & Distribution 14*(10), 1799–1815.

Lew, D., G. Brinkman, E. Ibanez, B. M. Hodge, M. Hummon, A. Florita, and M. Heaney (2013). The Western Wind and Solar Integration Study Phase 2.

Li, W. et al. (2013). *Reliability assessment of electric power systems using Monte Carlo methods*. Springer Science & Business Media.

NREL (2016). Reliability Test System Grid Modernization Lab Consortium (RTS-GMLC).

Rakhshani, E., K. Rouzbehi, A. J Sánchez, A. C. Tobar, and E. Pouresmaeil (2019). Integration of large scale pv-based generation into power systems: A survey. *Energies 12*(8), 1425.

Sabouhi, H., A. Doroudi, M. Fotuhi-Firuzabad, and M. Bashiri (2020). A novel matrix based systematic approach for vulnerability assessment. *COMPEL-The international journal for computation and mathematics in electrical and electronic engineering 40*(1), 1–17.

Soder, L., L. Hofmann, A. Orths, H. Holttinen, Y.-h. Wan, and A. Tuohy (2007). Experience from wind integration in some high penetration areas. *IEEE Transactions on energy conversion 22*(1), 4–12.

Urgun, D. and C. Singh (2018). A hybrid monte carlo simulation and multi label classification method for composite system reliability evaluation. *IEEE Transactions on Power Systems 34*(2), 908–917.

Wolf, S., J. Hinkel, M. Hallier, A. Bisaro, D. Lincke, C. Ionescu, and R. J. Klein (2013). Clarifying vulnerability definitions and assessments using formalisation. *International Journal of Climate Change Strategies and Management 5*(1), 1–17.

Zhang, J., B.-M. Hodge, A. Florita, S. Lu, H. F. Hamann, and V. Banunarayanan (2013). Metrics for Evaluating the Accuracy of Solar Power Forecasting. In *3rd International Workshop on Integration of Solar Power into Power Systems*, London, pp. 1–8.

Zhao, Y., S. Liu, Z. Lin, L. Yang, Q. Gao, and Y. Chen (2020). Identification of critical lines

for enhancing disaster resilience of power systems with renewables based on complex network theory. *IET Generation, Transmission & Distribution 14*(20), 4459–4467.

Zio, E. (2016). Challenges in the vulnerability and risk analysis of critical infrastructures. *Reliability Engineering & System Safety 152*, 137–150.

Evaluation of Reliability and Robustness of Electric Power Systems with Renewable Energies

Jesus Beyza
Department of Electrical Engineering
University of Zaragoza
Zaragoza, Spain
jbeyza@unizar.es

Jose M. Yusta
Department of Electrical Engineering
University of Zaragoza
Zaragoza, Spain
jmyusta@unizar.es

Marco A. Evangelista
Department of Electromechanical
TECNM-Costa Grande Institute of Technology
Zihuatanejo, Mexico
L17570018@costagrande.tecnm.mx

Jesus S. Artal-Sevil
Department of Electrical Engineering
University of Zaragoza
Zaragoza, Spain
jsartal@unizar.es

Jose A. Rendon
Department of Electromechanical
TECNM-Costa Grande Institute of Technology
Zihuatanejo, Mexico
jose.rc@costagrande.tecnm.mx

2021 IEEE International Autumn Meeting on Power, Electronics and Computing (ROPEC) | 978-1-6654-3427-0/21/$31.00 ©2021 IEEE | DOI: 10.1109/ROPEC53248.2021.9668112

***Abstract*—Renewable energy sources (RESs), such as wind and solar energy, are an integral part of the current process of decarbonisation of electric power systems in the vast majority of countries. Due to the stochastic and variable nature of these resources, RESs could expose an electrical network to unexpected power outages. In this context, security studies are vital for the secure and day-to-day operation of the infrastructure. This article analyses the effects of integrating renewable energies into a power system from the perspectives of reliability and robustness. For this purpose, the IEEE 14-bus test system is modified, and two case studies are proposed with a high proportion of fossil-based power generation and a high share of renewable generation, respectively. In both cases, hourly load and electricity generation profiles are considered. The reliability study is completed using the Monte Carlo probabilistic method, and the robustness study is conducted by simulating cascading failures. These assessments are carried out in the two scenarios, where the electricity system without renewable energies is considered the base case. The effects of renewable energies are analysed comparatively in terms of Loss of Load Probability (LOLP), Expected Demand Not Supplied (EDNS) and Satisfied Demand (SD).**

***Index Terms*—Cascading failures, power systems, reliability, renewable energy, robustness.**

I. Introduction

Electric power systems are an integral part of economies since the daily and continuous operation of modern activities depends on them. However, the energy sector is undergoing important changes due to the disastrous effects of climate change, which affect all segments of the electrical infrastructure, alter generation potential and efficiency, and test the physical resilience of power grids [1]. The development and transformation towards sustainable, resilient and carbon-free societies are one of the main priorities of the international agenda.

The structural change and the transition from a bulk power system with generation based on fossil resources to a power system with a high share of renewable energies presents innumerable challenges for transmission system operators and planners. Reliability and robustness studies are two of the most commonly used tools in the field of electrical engineering to analyse and manage the uncertainties associated with systems. Reliability is the ability of the electricity system to supply the aggregate electrical demand within an area at all times under normal operating conditions or in the event of failure of one or two assets [2]. Robustness is the capability of the power grid to avoid extreme adverse impact in case of multiple failures or contingencies [2], [3]. These concepts are well documented in the scientific literature [4].

Uncertainty, variability and intermittency are intrinsic characteristics of renewable energy sources that could expose an electricity system to unexpected power outages. The effect of renewable resources on the reliability and robustness of power systems is a novel field of research that requires the proposal of integrated methodological frameworks to study the different attributes associated with both concepts. Renewable energies play a key role in the security of supply, so their study and analysis is a growing concern [5], [6].

Power grids with high penetration of renewables must adjust their energy production quickly and appropriately due to uncertain changes in these sources [7]. To mitigate the adverse implications of intermittencies in renewable resources, some studies propose long-term scheduling strategies for generators, which consider both the criticality and contingencies of the generation units [8].

The operation of electrical systems is also affected by the operating status of infrastructure assets. In this sense, some researchers propose procedures to analyse potential threats and vulnerabilities, considering changes in the operation and variability of resources [9]. Other researchers point out that renewable energies could make the system more vulnerable and less reliable [10]. Some researchers propose linear programming to evaluate and improve the reliability of power systems [11]. It is believed that wind and photovoltaic generators could mitigate the interruptions caused by possible contingencies.

978-1-6654-3427-0/21/$31.00 ©2021 IEEE

Other works propose analytical approaches that highlight the ability of the system to adopt different levels of reliability according to the power of renewable generators [12].

On the other hand, one of the most critical challenges in the study of robustness is the analysis of cascading failures. Blackouts are complicated events to analyse and mitigate since they can start for countless reasons and operating conditions that studying them all is practically impossible. Graph theory could be a viable approach to model dynamic behaviour, analyse the propagation of these events and quantify the structural robustness of power grids [13]–[15].

Renewable energies could also reduce the reliability and robustness since their malfunction could cause power outages that would inevitably affect the infrastructure [16]. Some researchers propose energy hub-based methods [17], model order reduction [18], metaheuristic searching genetic algorithms [19] and multicriteria decision analysis [20] to evaluate the suitability of the generation.

Based on the above, this study aims to evaluate the reliability and robustness of both electrical power systems with high thermal generation and electrical power systems with high penetration of renewable energies. The purpose is to compare both sets of results and determine if there are significant changes in the performance of the infrastructure. This type of study is currently receiving much attention, so more work is needed to fill the research gaps in the study area.

The reliability study is completed using the probabilistic Monte Carlo method, where each generator is assigned some states that determine the probability that a generator operates at various output levels. This procedure is used because it yields relatively quick results. Of course, the sequential Monte Carlo method can also be used to simulate the actual chronological process of the power system. Likewise, each load is assigned a time-based characteristic that defines the actual hourly load in the system. In the case of wind turbines, in addition to the multistate stochastic model, a stochastic wind model described by a Weibull distribution is defined, where the mean wind speed and the beta shape factor of the distribution are adjusted to achieve the desired wind characteristic [21]. Here, the LOLP and EDNS indices are measured, and the confidence intervals of each of the indicators are quantified. The robustness study is completed by simulating cascading failures for each generation and load profile of the system. This iterative procedure consists of randomly removing an electrical line, measuring the power flows, eliminating the overloaded links, identifying the subnetworks, and measuring the SD index at each disintegration stage. This process is repeated until there are no overloaded power lines or all the assets are isolated. The reliability assessment is performed with DigSILENT POWERFACTORY 2021 SP3, and the robustness assessment is programmed in MATLAB R2021a. The IEEE 14-bus test system is used as a case study to perform the procedures described above [22].

The rest of this article is organised as follows: Section II presents the reliability and robustness procedures used to analyse the impact of renewable energy sources on bulk electrical power systems. Section III describes the two case studies based on the well-known IEEE 14-bus test system. Section IV analyses and discusses the simulation results obtained after applying the procedures described above. Finally, Section V summarises the main conclusions of this paper.

II. Analysis of Reliability and Robustness in Electrical Power Systems

This section briefly describes the procedures to evaluate the performance of the systems from the perspectives of reliability and robustness. In both cases, the fundamental statistical indicators used in this study are presented.

A. Reliability algorithm

The probabilistic Monte Carlo approach is a procedure to realistically simulate the actual and random chronological process of a system based on repetitive random sampling, which allows measuring different network performance indices [23], [24]. This procedure can be summarised in the ordered and systematic steps shown in Algorithm 1.

Algorithm 1 Monte Carlo probabilistic algorithm

Input: demand profiles, probabilistic models for generation units and temporal resolution (N), i.e. 8760 hours.
Output: LOLP and EDNS statistical indicators.
Step 1. *Generation model*: assign availability and probability states to the generation units. For wind turbines, also assign a stochastic wind model based on a Weibull distribution;
Step 2. *Load model*: establish a profile based on the time that determines the actual load level at any given time;
Step 3. *Statistical sampling*: combine the models of Steps 1 and 2 and, through a sequence of uniform random numbers, generate a system state that contains generation and demand profiles in a given time; set $N = 1$ for the first iteration;
Step 4. *Calculate demand not supplied (DNS)*: use the state calculated in Step 3 to calculate DNS in the network, that is, demand minus generation. Save the DNS value for the corresponding iteration N;
Step 5. *Iterations*: repeat Steps 3 and 4 until N;
Step 6. *Evaluate reliability indicators*: calculate the LOLP and EDNS indicators using (1) and (2).

$$LOLP = \frac{N_{DNS}}{N} \times 100\%; \text{ Unit: [\%]} \tag{1}$$

$$EDNS = \frac{\sum DNS}{N}; \text{ Unit: [MW]} \tag{2}$$

where N_{DNS} is the number of iterations where DNS>0 and N is the total number of iterations.
The LOLP index is the probability that the load is greater than the available generation capacity, while the EDNS index is the energy demand not supplied in each of the 1-hour steps;
Step 7. *End*: if the covariance between the simulation samples is less than 10%, the algorithm ends; otherwise, increase N and go to Step 3.

Basically, the reliability procedure consists of generating a random state of the system using both the demand profiles and the probabilistic models of the generators. Here, an operating state is determined that contains a corresponding output power and a corresponding demand. The demand not supplied is calculated for that state, and the process is repeated for a temporal resolution of one hour in a one-year horizon, i.e. 8760-time steps of one hour each. In the end, the LOLP and EDNS indicators are calculated as average values of all the iterations performed [25]. Note that the first index represents the expected percentage of hours where energy not supplied is

greater than zero, and the second index represents the average energy not supplied within the study horizon.

B. Robustness algorithm

In this article, robustness is measured in terms of the performance of the infrastructure against cascading failures. A cascading event is a sequence of incidents that can be initiated by multiple factors, such as voltage and frequency instabilities, malfunction of protection devices, and overloads, which can cause a series of outages in other network elements [4]. Algorithm 2 presents the proposed procedure to simulate cascading failures in an electrical power system.

Algorithm 2 Cascading failures

Input: generation profiles, demand profiles and overload tolerance parameter of the lines (α).
Output: degradation of the power grid. Satisfied Demand (*SD*) in each stage of disintegration (s).
Step 1. *Initialisation*: SD_{base} is equal to the sum of all the loads of the system;
Step 2. *Running DC power flows*: identify the flows (P) for each link (k) and determine the power threshold (P_k^{max}) of the lines using (3);

$$P_k^{max} = \alpha_k \times P_k; \text{ Unit: [MW]} \tag{3}$$

Step 3. *Initial point*: randomly eliminate a power line k;
Step 4. *Increase or decrease of flows*: determine the increases or decreases for each power line; set s = 1 for the first disintegration step;
Step 5. *Tripping the circuit breakers*: assess the condition $|P_k^s| < P_k^{max}$ for all power lines. If the condition is not met, remove all overloaded links and go to Step 6; otherwise, go to Step 10;
Step 6. *Graph transversal algorithm*: use the depth-first search algorithm to determine sub-networks (I) and isolated assets (E);
Step 7. *Energy balance*:
a) for each island I_i with generators, $g \in I_i$, evaluate
- if $\sum_{g\in I_i} P_g < \sum_{d\in I_i} P_d$, do $D_{I_i}^s = \sum_{g\in I_i} P_g$ in stage s;
- if $\sum_{g\in I_i} P_g > \sum_{d\in I_i} P_d$, do $D_{I_i}^s = \sum_{d\in I_i} P_d$ in stage s;

b) for each island I_i without generators, $g \in I_i$, do D_i^s=0 and E_i=M_i;
Step 8. *Satisfied demand*: calculate (4)

$$SD_s = \frac{\sum_{i\in I} D_{I_i}^s}{SD_{base}}; \text{ Unit: [\%]} \tag{4}$$

Step 9. *Iterations*: set $s = s + 1$ and go to Step 4;
Step 10. *End*: if all $|P_k^s| < P_k^{max}$, the algorithm ends.

This procedure begins by calculating the power flows and determining the maximum transfer capability of the power lines. Next, a link is randomly eliminated, the changes in the flows are determined, and all power lines that are overloaded as a result of the redistributed flows are eliminated. Subsequently, the sub-networks are identified, and generation and demand are balanced. The isolated elements or sub-networks without generation are considered unsatisfied loads during the disintegration process. The iterative procedure continues until there are no overloaded elements or all the assets are isolated.

III. Case Studies

A. Modified IEEE 14-bus test system

For this study, the IEEE 14-bus test system is used and modified. This test case represents a simple approximation of the United States electric power system in February 1962. It has 14 buses, 5 generators and 11 loads [22]. Fig. 1 depicts the topology of the network under study. Two case studies are considered to evaluate the reliability and robustness indices.

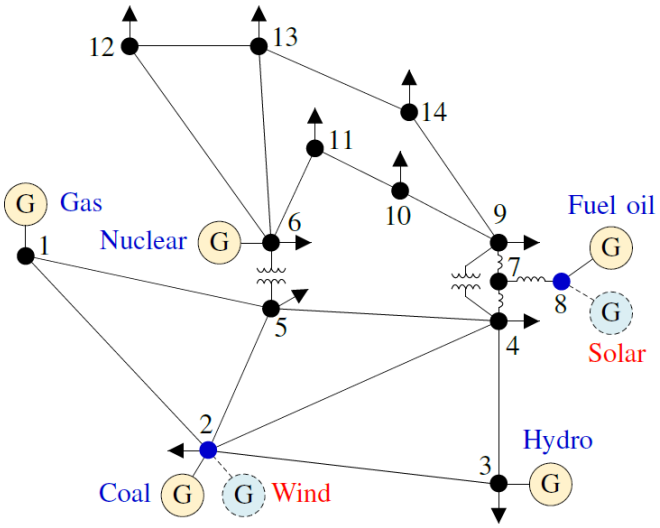

Fig. 1. Topology of the IEEE 14-bus test system. The wind farm and the photovoltaic plant correspond to the RES case.

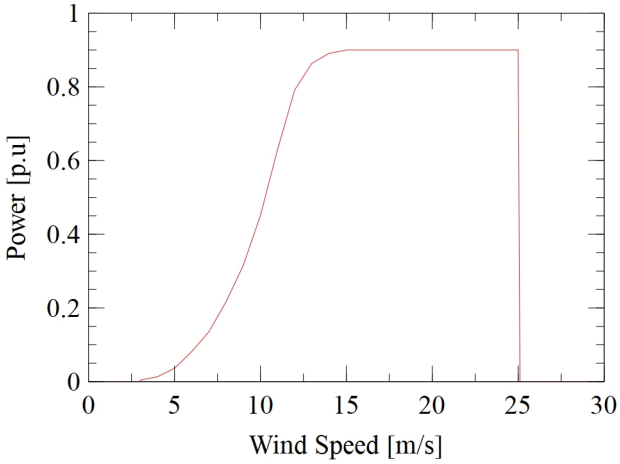

Fig. 2. Power-speed curve of the wind turbine located on Bus 2.

The first case performs both studies without considering renewable energy alternatives, and the second case considers the role of RESs.

Specifically, the base case is composed of natural gas, coal, hydroelectric, nuclear and fuel oil generators connected in buses 1, 2, 3, 6 and 8. Table I shows the basic data of conventional generators. Meanwhile, in the RES case, the coal generator and the fuel oil generator are replaced by a wind farm and a photovoltaic plant. The installed capacity of renewable resources is 180 and 60 MW, respectively. Fig. 2 shows the power curve of the wind farm.

Figs. 3 and 4 depict the power outputs of the generators for the base case and the RES case after incorporating both the temporal characteristics of the annual hourly demand and the resources of the conventional and renewable generators. The annual hourly load is obtained by adjusting the data found in [26]. These results are calculated through a quasi-dynamic

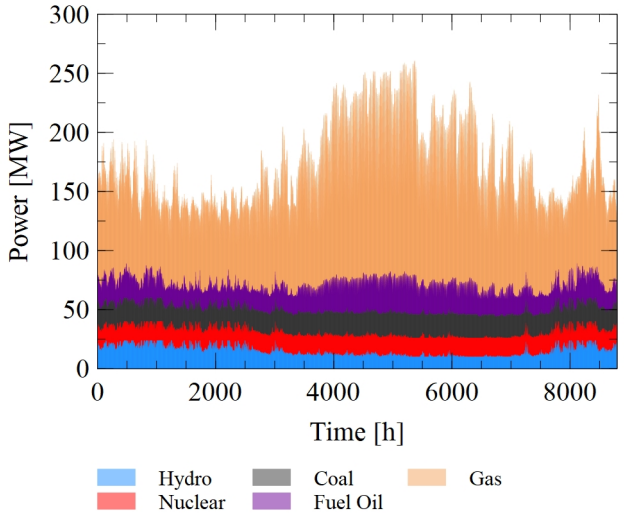

Fig. 3. Power output of the generators for the base case.

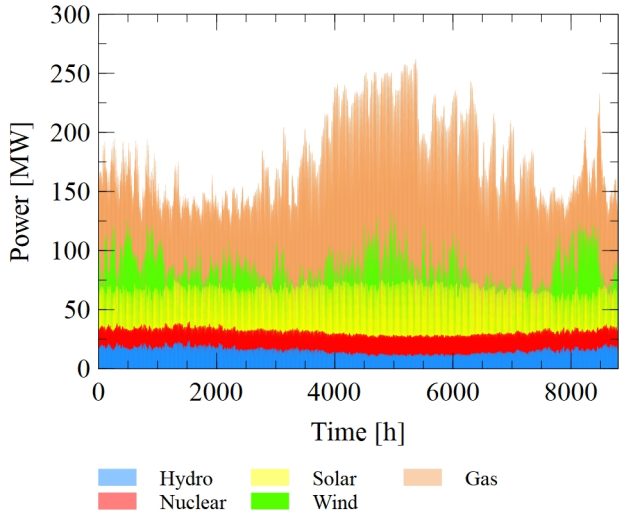

Fig. 4. Power output of the generators for the RES case.

TABLE I
GENERATOR DATA FOR THE CASE STUDIES

Generator	Type	Bus	Active Power	
			Maximum [MW]	Minimum [MW]
G1	Gas	1	192	0
G2	Coal	2	20	18
G3	Hydro	3	24	10
G4	Nuclear	6	16	10
G5	Fuel oil	8	48	15

power flow simulation. The maximum total load is 252.50 MW.

Note that wind and solar generation are not considered in the base case, and only the annual hourly demand profile is incorporated. Meanwhile, in the RES case, part of the conventional generation of the base case is replaced by renewable sources. That is, the renewable case includes profiles of electrical load and wind and solar generation. This aims to simulate the current energy transition process of electrical power systems.

IV. RESULTS AND DISCUSSIONS

This section presents the results of the LOLP, EDNS and SD indicators after sequentially applying the reliability and robustness procedures described in Section II. These indicators were calculated both for the base case integrated with fossil generation and for the RES case with a high penetration of renewable generation. The changes in the indicators imply the effects of the integration of renewable energies. The reliability study was performed in DigSILENT POWERFACTORY 2021 SP3, and the robustness study was programmed in MATLAB R2021a. Both simulations were run on a personal computer with a 3.40 GHz Intel® Core™ i7 CPU and 16 GB of RAM.

A. Discussion on the reliability study

For simulation and implementation purposes, power losses of 3% in the transmission system were considered, and the stochastic availabilities of the generators presented in Table II and the time characteristics shown in Figs. 3 and 4 were used. In Table II, the availability was the percentage of the nominal power available, and the probability was the probability that this state was valid. Thus, the total available generation capacity in % of maximum output was specified along with the probability of this availability. Note that an unlimited number of states can be considered and that the sum of the probability of all states must equal 100%. For the wind turbine, the power curve in Fig. 2 and a Weibull distribution with mean and beta coefficients of 8.862 and 2.0 were also used [21]. The computation times for the two case studies were 1.43 and 1.93 minutes, respectively.

Table III presents the reliability results along with their confidence levels for the base and renewable cases. The LOLP and EDNS indices increased with renewables, as there was three times more probability of losing load and not supplying power in the RES case than in the base case. This makes sense as wind and solar are intermittent resources dependent on weather conditions, which impacts the reliability indicators studied. The stochastic nature of these resources plays a fundamental role in the operation of a power system. The higher the penetration of renewable energy sources, the greater the impact on reliability and adequacy indices.

In general terms, the electric power system with a high share of renewable energies (RES case) was less reliable than the electric power system with fossil fuel generation (base case). In the event of failures and contingencies, renewable generators may be less able to respond and supply the total energy demand.

B. Discussion on the robustness study

A robustness study was applied for the generation and hourly demand conditions shown in Figs. 3 and 4. In all of them, a parameter α=1.5 was considered, which meant that the lines operated at 70% of their nominal capacity before

TABLE II
STOCHASTIC MODEL USED FOR CONVENTIONAL AND RENEWABLE GENERATION

Conventional generator			Photovoltaic system			Wind turbine		
State	**Availability [%]**	**Probability [%]**	**State**	**Availability [%]**	**Probability [%]**	**State**	**Availability [%]**	**Probability [%]**
1	100.00	61.55	1	100.00	55.00	1	100.00	55.00
2	80.00	13.45	2	80.00	20.00	2	85.00	25.00
3	60.00	10.00	3	65.00	10.00	3	70.00	10.00
4	40.00	10.00	4	45.00	5.00	4	55.00	5.00
5	20.00	5.00	5	20.00	10.00	5	30.00	5.00
6	0.00	0.00	6	0.00	0.00	6	0.00	0.00

TABLE III
RELIABILITY RESULTS

Grid	**Loss of Load Probability**			**Expected Demand Not Supplied**		
	Average (LOLP) [%]	**Confidence Levels**		**Average (EDNS) [MW]**	**Confidence Levels**	
		Lower	**Upper**		**Lower**	**Upper**
base case	1.199	1.181	1.217	0.301	0.295	0.307
RES case	4.441	4.407	4.475	1.404	1.389	1.418

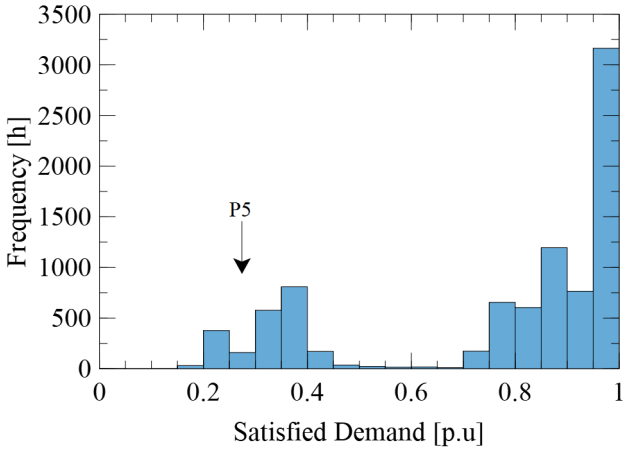

Fig. 5. Robustness results grouped for the base case. P5 represents the percentile limit.

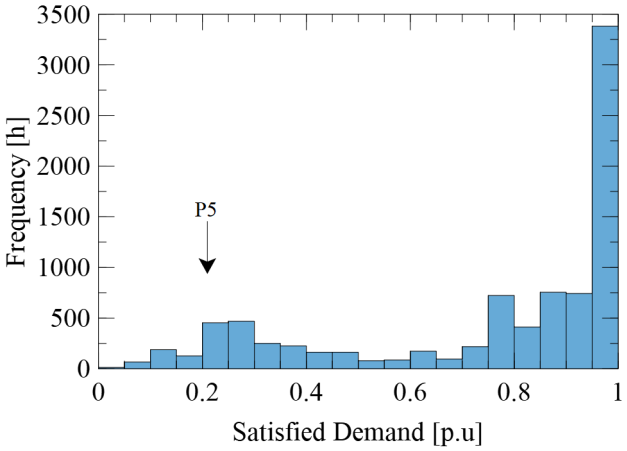

Fig. 6. Robustness results grouped for the RES case. P5 represents the percentile limit.

cascading failure. This last value was used to increase the level of disintegration of the networks in each hour. Moreover, a different power line was randomly removed to start the disintegration of the network. Note that the SD index is equal to 1 when all demand is satisfied and decreases progressively as the system disintegrates. Thus, the last SD value in each hour was used for representation purposes. The computation times for the two case studies were 12.02 and 11.31 minutes, respectively.

The grouped sets of the robustness results for the base and RES cases are shown in Figs. 5 and 6. The mean SD index was 0.769 and 0.753 with standard deviations of ± 0.265 and ± 0.289, respectively. When considering the 5th percentile in the SD index, 439 hours were below 0.274 and 0.209.

From the strict point of view of the robustness procedure used, the findings showed that the RES case maintained almost the same performance as the base case during cascading events. The latter seems to indicate that the robustness of a power system is not entirely affected by the penetration of renewable resources. Nevertheless, it is essential to note that synchronous generators can remain connected during and after a failure. In contrast, renewable generators do not precisely replace the functional behaviour of synchronous generators, which could affect the security of supply and consequently decrease the robustness.

V. CONCLUSIONS

This work studied the effect of renewable energy integration on the reliability and robustness of power systems. Two case studies with high fossil generation and high renewable energy penetration based on the IEEE 14-bus test system were used. The objective was to compare both sets of results in order to

have a broader view of the behaviour and performance of a network.

On the one hand, the reliability study showed that the case study with fossil generation was more reliable than the RES case. This could be caused by the intermittency of renewable resources, which affect the performance of a system against one or two disturbances. For example, the LOLP and EDNS indicators increased by more than 400% in the case study with renewable energies.

On the other hand, the robustness study revealed that the RES case had approximately the same robustness as the case with fossil generation since the SD values did not report significant variations. For example, the SD index decreased by only 2% in the case study with renewable energies. In other words, renewable generation may not affect the performance of a system in the face of cascading failures or multiple contingencies. However, more detailed procedures are needed to analyse robustness, incorporating the dynamics associated with the power system and the stochastic part of renewable resources during a cascading failure or blackout. This could lead to a decrease in the robustness of the systems.

Future work can focus on assessing how renewable generators with small capacity affect the reliability and robustness of electric power systems.

ACKNOWLEDGMENT

This work was supported by the Spanish Ministry of Science and Innovation under project PID2019-104711RB-100: Smart grid design and operation against the threat of interrupted supply in electric transmission systems with high penetration of renewable energies.

REFERENCES

[1] IEA, "Climate Resilience," 2021. [Online]. Available: https://www.iea.org/reports/climate-resilience

[2] ——, "Analytical frameworks for electricity security," 2021. [Online]. Available: https://www.iea.org/reports/analytical-frameworks-for-electricity-security

[3] J. Beyza, V. M. Bravo, E. Garcia-Paricio, J. M. Yusta, and J. S. Artal-Sevil, "Vulnerability and resilience assessment of power systems: From deterioration to recovery via a topological model based on graph theory," in *2020 IEEE International Autumn Meeting on Power, Electronics and Computing (ROPEC)*, 2020, pp. 1–6.

[4] J. Beyza and J. M. Yusta, "Integrated risk assessment for robustness evaluation and resilience optimisation of power systems after cascading failures," *Energies*, vol. 14, no. 7, p. 2028, 2021.

[5] V. S. Tabar, S. Ghassemzadeh, and S. Tohidi, "Increasing resiliency against information vulnerability of renewable resources in the operation of smart multi-area microgrid," *Energy*, vol. 220, p. 119776, 2021.

[6] J. Matevosyan, S. H. Huang, P. Du, N. Mago, and R. Guiyab, "Operational security: The case of texas," *IEEE Power and Energy Magazine*, vol. 19, no. 2, pp. 18–27, 2021.

[7] W. Zhu and J. V. Milanović, "Assessment of the robustness of cyber-physical systems using small-worldness of weighted complex networks," *International Journal of Electrical Power & Energy Systems*, vol. 125, p. 106486, 2021.

[8] D. S. Kumar, A. Sharma, D. Srinivasan, and T. Reindl, "Impact analysis of large power networks with high share of renewables in transient conditions," *IET Renewable Power Generation*, vol. 14, no. 8, pp. 1349–1358, 2020.

[9] L. Zhang, H. Su, E. Zio, Z. Zhang, L. Chi, L. Fan, J. Zhou, and J. Zhang, "A data-driven approach to anomaly detection and vulnerability dynamic analysis for large-scale integrated energy systems," *Energy Conversion and Management*, vol. 234, p. 113926, 2021.

[10] F. Capitanescu, "Evaluating reactive power reserves scarcity during the energy transition toward 100% renewable supply," *Electric Power Systems Research*, vol. 190, p. 106672, 2021.

[11] I. Akhtar and S. Kirmani, "Reliability assessment of power systems considering renewable energy sources," *Materials Today: Proceedings*, pp. 1–4, 2021.

[12] S. Eryilmaz, İ. Bulanık, and Y. Devrim, "Reliability based modeling of hybrid solar/wind power system for long term performance assessment," *Reliability Engineering & System Safety*, vol. 209, p. 107478, 2021.

[13] S. Yang, W. Chen, X. Zhang, and W. Yang, "A graph-based method for vulnerability analysis of renewable energy integrated power systems to cascading failures," *Reliability Engineering & System Safety*, vol. 207, p. 107354, 2021.

[14] D. Zhou, F. Hu, S. Wang, and J. Chen, "Power network robustness analysis based on electrical engineering and complex network theory," *Physica A: Statistical Mechanics and its Applications*, vol. 564, p. 125540, 2021.

[15] K. Li, K. Liu, and M. Wang, "Robustness of the chinese power grid to cascading failures under attack and defense strategies," *International Journal of Critical Infrastructure Protection*, vol. 33, p. 100432, 2021.

[16] N. A. Salim, J. Jasni, and M. M. Othman, "Reliability assessment by sensitivity analysis due to electrical power sequential tripping for energy sustainability," *International Journal of Electrical Power & Energy Systems*, vol. 126, p. 106582, 2021.

[17] W. Huang, E. Du, T. Capuder, X. Zhang, N. Zhang, G. Strbac, and C. Kang, "Reliability and vulnerability assessment of multi-energy systems: An energy hub based method," *IEEE Transactions on Power Systems*, pp. 1–12, 2021.

[18] M. B. Ndawula, I. Hernando-Gil, R. Li, C. Gu, and A. De Paola, "Model order reduction for reliability assessment of flexible power networks," *International Journal of Electrical Power & Energy Systems*, vol. 127, p. 106623, 2021.

[19] A. N. Abdalla, M. S. Nazir, M. Jiang, A. A. Kadhem, N. I. A. Wahab, S. Cao, and R. Ji, "Metaheuristic searching genetic algorithm based reliability assessment of hybrid power generation system," *Energy Exploration & Exploitation*, vol. 39, no. 1, pp. 488–501, 2021.

[20] F. Ezbakhe and A. Pérez-Foguet, "Decision analysis for sustainable development: The case of renewable energy planning under uncertainty," *European Journal of Operational Research*, vol. 291, no. 2, pp. 601–613, 2021.

[21] C. Ozay and M. S. Celiktas, "Statistical analysis of wind speed using two-parameter weibull distribution in alaçatı region," *Energy Conversion and Management*, vol. 121, pp. 49–54, 2016.

[22] ICSEG, "IEEE 14-Bus System." [Online]. Available: https://icseg.iti.illinois.edu/ieee-14-bus-system/

[23] A. A. Kadhem, N. I. A. Wahab, I. Aris, J. Jasni, and A. N. Abdalla, "Computational techniques for assessing the reliability and sustainability of electrical power systems: A review," *Renewable and Sustainable Energy Reviews*, vol. 80, pp. 1175–1186, 2017.

[24] P. Zhou, R. Jin, and L. Fan, "Reliability and economic evaluation of power system with renewables: A review," *Renewable and Sustainable Energy Reviews*, vol. 58, pp. 537–547, 2016.

[25] DIgSILENT, "Reliability analysis functions," 2021. [Online]. Available: https://www.digsilent.de/en/reliability-analysis.html

[26] Texas A&M University, "Texas 2000-Bus System ACTIVSg2k," 2020. [Online]. Available: https://egriddata.org/dataset/texas-2000-bus-system-activsg2k

Pumped-hydro potential to enhance power system resilience under critical gas supply interruptions

Natalia Naval

Department of Electrical Engineering, University of Zaragoza, Spain. naval@unizar.es

Yassine Rqiq

Department of Electrical Engineering, University of Zaragoza, Spain. yassinerqiq@gmail.com

Jose M. Yusta

Department of Electrical Engineering, University of Zaragoza, Spain. jmyusta@unizar.es

Currently, the security of electricity systems depends largely on gas supply, as this source, along with renewables, plays a key role to accelerate the energy transition and decarbonization of the economy. Europe's high dependence on external gas suppliers and the continuing and growing trade and political tension between Ukraine and Russia make Europe vulnerable to a supply crisis. This article assesses the potential of pumped hydropower to improve the security of the European power system against gas shortages under highly severe climatic and technical conditions. A mathematical optimization approach is applied to maximize the coverage of the electricity demand while fostering cooperative strategies among countries in the event of critical gas shortages. To test the proposed model, data from January 18, 2017, are used as the peak demand for both electricity and gas occurred on this day in Europe. The results indicate that exploiting the potential of pumped hydro storage in different countries can reduce the high external dependence on gas and thus avoid the negative consequences of an interruption in gas supply. Ultimately, this paper argues that pumping hydro plants can improve the stability and security of power systems.

Keywords: Pumped hydro, Resilience, Gas shortages, Cooperation model, Power system, Gas network.

1. Introduction

Renewable energy is solidifying itself as the main energy source for the coming years. However, this process still requires time to achieve an energy mix with 100% renewable production. Photovoltaic and wind energy have reached a high degree of technological development, but these renewable sources still require support to overcome their intermittency issues and variable nature. In this regard, storage systems are essential to enable the integration of renewables into the electricity system, but their development and implementation are still in progress. Meanwhile, gas-fired power plants have become the main source to support renewables and accelerate the energy transition by functioning as backup generation.

The European Union (EU) is highly dependent on gas and especially from Russia, which is the country with the largest natural gas reserves worldwide. Europe receives more than 40% of its natural gas through the network of pipelines connecting to Russia (Yusta and Beyza 2021).

The ongoing trade and political conflicts between Russia and Ukraine, which have increased in recent years, have made the security of gas supply one of the EU's main concerns. The risk of Russia completely disrupting supplies to the EU is growing.

Proceedings of the 32nd European Safety and Reliability Conference
Edited by Maria Chiara Leva, Edoardo Patelli, Luca Podofillini, and Simon Wilson
 Published by Research Publishing, Singapore
ISBN: 981-973-0000-00-0 :: doi: 10.3850/981-973-0000-00-0_esrel2022-paper

Regarding gas crises, the EU has promoted policies to favor coordination and efficient cooperation among different countries. The focus is on sharing all available resources and infrastructures in the event of a gas supply crisis and thus reducing the harmful effects of supply interruptions in the most vulnerable countries ("Regulation (EU) 2017/1938 of the European Parliament and of the Council of 25 October 2017 Concerning Measures to Safeguard the Security of Gas Supply" n.d.). Rodríguez-Fernández, Fernández Carvajal, and Ruiz-Gómez (2020) assess the progress of gas supply security in EU countries after the gas crises of 2006 and 2009.

Sesini, Giarola, and Hawkes (2022) examine solidarity measures in the event of high-impact and low-probability disruptions to the EU's gas supply. As a consequence of this gas supply uncertainty, Europe is paying high prices for liquefied natural gas transported by sea, mainly from the United States. This issue stems from geopolitical reasons of supply diversification to avoid supply shortages.

In addition to cooperation mechanisms among countries, it is essential to promote the use of other technologies such as pumped hydropower to ensure a balance between electricity consumption and generation. This technology can provide flexibility in the electricity system in case of possible critical gas supply interruptions affecting gas-fired power plants, and thus guaranteeing the supply of reliable electricity in combination with renewable energy. Currently, pumped hydro technology is the most efficient system for large-scale energy storage, though it is dependent on orographic factors. Pumped hydro technology is more convenient for maintaining the stability and security of the power system than other types of storage (e.g., batteries, hydrogen) because it generates a large amount of energy with a very fast response time. Some previous studies (Deane, Ó Gallachóir, and McKeogh 2010), (Lu et al. 2018), (Kucukali 2014) propose different methodologies for locating suitable sites for the development of pumped-hydro energy storages worldwide.

This paper aims to analyze the potential of pumped hydropower to improve the resilience of the European energy system in the face of gas supply disruptions under highly severe climatic and technical conditions. The proposed mathematical optimization model maximizes the demand coverage by using cooperation mechanisms among EU countries in the event of critical gas disruption and harnessing the available pumping hydro capacity of each country. The methodology is applied to a case study involving the maximum demand previously recorded in both the gas and electricity systems in Europe. Here we follow the ENTSO-G methodology for gas supply and infrastructure disruption scenarios, one of which is the one day (peak day) of exceptionally high demand ("ENTSO-G. Union-wide SoS simulation report 2021." n.d.). The high demand cases are meant to capture the capability of the gas system to cope with the most challenging demand situation (peak day / Design Case).

The remainder of this paper is organized as follows: Section 2 formulates the optimization model. Section 3 describes the European gas system. Section 4 analyzes the results obtained and discusses the pumped-hydro potential. Finally, Section 5 summarizes the main conclusions.

2. Mathematical formulation of the model

The proposed model is based on the approach used by (Rqiq and Yusta 2020) but including an analysis of the potential for new pumping hydro plants in all EU and neighboring countries in the event of a gas supply shortage. Interconnections, together with storage systems, help to balance generation in countries with different renewable production profiles, alleviating surpluses and shortages among countries.

The optimization problem is completely formulated by means of an objective function and a set of constraints stated in Eq. (1)-(8).

The following assumptions are considered for the modeling:

- Both the interruption of gas from Russia and the supply of liquefied natural gas by sea;
- The use of cooperation mechanisms among EU and neighboring countries (i.e., all countries share all available resources and infrastructures).

The objective function maximizes the daily natural gas demand coverage in each country *i* in the event of a critical gas supply disruption, C_i, (Eq. (1)). All gas uses are considered into the gas demand, also gas for electricity generation. This variable must be within the range of 0 and the maximum natural gas demand that the system seeks to satisfy, $C_{i,max}$ (Eq. (2)).

$$\max(\text{demand coverage}) = \sum_{i=1}^{n} C_i \quad (1)$$

$$0 \le C_i \le C_{i,max} \quad (2)$$

$$P_i + St_i + IMP_i + LNG_i - \sum X_{ij} - C_i = 0 \quad (3)$$

$$0 \le P_i \le P_{i,max} \quad (4)$$

$$0 \le St_i \le St_{i,max} \quad (5)$$

$$0 \le IMP_i \le IMP_{i,max} \quad (6)$$

$$0 \le LNG_i \le LNG_{i,max} \quad (7)$$

$$-X_{ji,max} \le X_{ij} \le X_{ij,max} \quad (8)$$

Eq. (3) establishes the balance of all possible sources of gas in each country *i*.

Eq. (4) states that the daily gas production of each country *i* (P_i) must be less than or equal to the maximum production of each country ($P_{i,max}$). The amount of gas from underground storage in each country *i* (St_i) must be within the range of 0 and the maximum allowable extraction, $St_{i,max}$, as indicated in Eq. (5).

Eq. (6) sets the limits of the daily import of natural gas in each country *i* from external gas suppliers (IMP_i). This variable must not exceed the maximum admissible import by the system's gas pipeline network ($IMP_{i,max}$).

Countries with access to the sea have regasification plants for the supply of liquefied natural gas; therefore, this capacity can be used to help meet the demand of different countries. The amount of daily liquefied natural gas that can be injected into the pipelines of each country *i* (LNG_i) must be less than or equal to its maximum capacity ($LNG_{i,max}$), as stated by Eq. (7).

Interconnections between countries may allow gas to be exchanged in one direction or in both directions. Therefore, the daily gas flow is limited to the maximum amount of gas that can be exchanged depending on the direction of the flow (Eq. (8)). The values of $X_{ji,max}$ and $X_{ij,max}$ are the sum of the technical limits of all cross-border interconnections from country *i* to *j* and viceversa.

According to the mathematical formulation of the problem, the optimization model is linear due to its inclusion of continuous variables in addition to the objective function and constraints also being linear. The problem is programmed and executed using MATLAB software since its optimization toolbox incorporates an efficient linear programming solver. The simulation runs on a computer with an Intel® Core i7 processor, 3.00 GHz CPU, and 16 GB of RAM.

3. Definition of the case study

The case study for the validation of the model consists of the European gas network (see Fig. 1). This system incorporates 28 countries connected by 35 cross-border interconnections, 18 of which were bi-directional in 2017. In recent years, energy security in the EU has become a priority due to the high dependence on external gas and the conflicts between Ukraine and Russia that have caused severe natural gas supply problems; the most serious was in the winter of 2006 and 2009, which led to the shutdown of all gas pipelines crossing Ukraine.

The EU has promoted the diversification of gas suppliers and the increase of interconnections between countries. The EU has also encouraged the use of cooperation and solidarity mechanisms to minimize the impact of a gas supply crisis.

On the power system side, pumped hydro storage is the main large-scale electricity storage technology used in most EU countries due to its efficiency and flexibility. There is high potential in pumping hydroelectric plants, which would allow for greater integration of renewable energy into the electricity system and reduce dependence on gas.

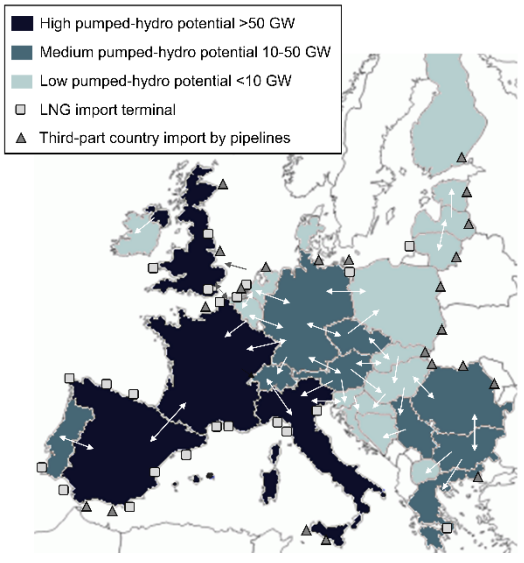

Fig. 1. European gas network and pumped hydropower potential in 2017.

During the winter of 2016/2017, Europe coped with an extreme cold spell, atypically reaching simultaneous peak demand for both gas and electricity on January 18, 2017. As a result of the low availability of nuclear power plants and renewable generation, in the consumption of natural gas for electricity generation reached its highest levels in the last years. To illustrate the proposed methodology, data from January 18, 2017, are chosen to assess the influence of existing and new pumped hydro plants in the event of gas supply disruptions that affect Europe's electricity supply.

More specifically, this study uses available data from 19:00 on January 18, 2017 from the European Network of Transmission System Operators for Electricity (ENTSO-E) Winter Outlook ("ENTSO-E. Winter Outlook 2016/2017 and Summer Review 2016" n.d.).

ENTSO-E is responsible for the reliable and coordinated operation of the European electricity system and provides data on generation capacity, electricity demand, planned shortages, etc. All data are recorded at 19:00 on the Wednesday of each week during the winter months for each European country. In this case study, severe system conditions are assumed. This means that the climatic conditions are extreme according to both demand (i.e., higher than normal conditions) and reduced production (i.e., lower wind generation or restrictions on conventional power plants).

Data on the potential of pumping hydropower are based on the 2013 European Commission report (Lacal-Arántegui and Gimeno-Gutiérrez 2013). This report includes a model focused on a topographic description and data on existing reservoirs, electrical networks, transport infrastructures, land use, etc.

Table 1 indicates the available technical gas capacities of the European system as well as the pumping potential for each country.

4. Discussion of the results

This section presents the results obtained under severe climatic conditions after the application of the model to the European power system.

As a consequence of decarbonization and increases in renewable generation in different countries, gas-fired power plants have emerged as a back-up technology for the European power system. This highlights a growing interdependence between the gas and electricity systems.

Table 2 indicates the percentage of gas not supplied in each country from the optimization performed. It also presents the remaining generation capacity calculated after a gas shortage and the influence of the available pumping capacity. Importable or exportable electricity capacities have not been considered since this case study is carried out under the most possible severe conditions.

Table 1. Gas system capacities on January 18, 2017 and pumping potential (GW).

Country	**Demand**	**Production**	**Underground storage extraction**	**Import**	**Liquefied natural gas injection**	**Capacity cross-border interconnections**		**Pumping hydro potential**
i	$C_{i,max}$	$P_{i,max}$	$St_{i,max}$	$IMP_{i,max}$	$LNG_{i,max}$	$X_{ij,max}$	$X_{ji,max}$	-
Austria	746	41	1050	0	0	2382	2290	24
Belgium	1168	0	170	488	515	2380	2658	1
Bosnia	13	0	0	0	0	0	15	7
Bulgaria	222	4	36	777	0	158	362	15
Croatia	225	49	61	0	0	0	129	9
Czech	713	6	703	0	0	1923	1690	16
Denmark	224	129	194	0	0	33	61	0
Estonia	28	0	0	48	0	0	63	0
Finland	152	0	0	249	0	0	0	0
France	3699	1	2506	570	1030	695	1667	126
Germany	6520	207	7159	4133	0	5111	5384	28
Greece	316	0	0	49	150	0	109	22
Hungary	872	50	837	605	0	270	283	1
Ireland	240	112	27	0	0	0	432	2
Italy	5325	174	2970	1716	543	41	1807	127
Latvia	96	0	315	179	0	128	68	0
Lithuania	132	0	0	325	121	68	65	0
Macedonia	26	0	0	0	0	0	27	0
Netherlands	2478	1352	2791	0	399	4288	2009	0
Poland	1139	135	574	312	158	932	194	3
Portugal	268	0	86	0	336	80	144	20
Romania	851	335	347	360	0	364	73	17
Serbia	28	14	57	0	0	15	142	22
Slovakia	369	14	479	2080	0	2285	1111	1
Slovenia	68	0	0	0	0	75	141	2
Spain	1748	2	215	732	1900	369	245	183
Switzerland	135	0	0	0	0	635	828	39
UK	5148	1454	1455	1499	2089	1062	1297	150

The remaining capacity is expressed as the difference between the available generation capacity and the electric load. This defined term corresponds to the power system's remaining generation capacity to meet the electricity demand in the event of unexpected, unplanned gas supply interruptions in each country.

First, in a situation with gas interruptions, high electricity demand and low generation availability, eleven countries in total would face problems with meeting electricity demand. This fact is due to the reduction of available gas capacity to facilitate the supply of gas-fired power plants, and thus the optimal operation of the European electricity system cannot be ensured.

Second, without considering the existing pumping hydro capacity, seventeen countries would face problems with meeting their electricity demand (Austria, Belgium, Denmark, Finland, France, Greece, Hungary, Italy, Lithuania, Macedonia, Poland, Portugal, Slovakia, Slovenia, Spain, Switzerland, and the United Kingdom).

Furthermore, several countries are highly dependent on natural gas from Russia, such as Finland and Lithuania, in addition to having few domestic resources.

Table 2. The impact of a gas supply interruption with pumped hydropower potential on the European power system.

Country	**Gas shortage (%)**	**Remaining capacity after gas shortage (GW)**	**Remaining capacity after gas shortage without available pumping hydropower (GW)**	**Remaining capacity after gas shortage with pumping hydropower potential (GW)**
Austria	0	4.73	-3.43	28.73
Belgium	0	-0.46	-1.77	0.34
Bosnia	0	1.08	1.08	8.28
Bulgaria	78	1.45	0.59	16.65
Croatia	0	0.36	0.08	9.76
Czech	0	3.85	2.69	19.65
Denmark	0	-0.26	-0.26	-0.26
Estonia	0	0.93	0.93	0.93
Finland	100	-4.61	-4.61	-4.61
France	0	-3.57	-6.54	122.63
Germany	0	9.3	4.41	37.10
Greece	75	-2.53	-2.97	19.47
Hungary	0	-1.16	-1.16	-0.56
Ireland	0	1.97	1.68	3.77
Italy	0	0.69	-3.81	127.29
Latvia	0	0.17	0.17	0.17
Lithuania	51	-0.94	-1.84	-0.94
Macedonia	67	-0.54	-0.54	-0.54
Netherlands	0	3.04	3.04	3.04
Poland	21	0.14	-1.32	3.14
Portugal	50	-1.56	-3.33	18.24
Romania	19	0.06	0.06	16.66
Serbia	0	0.69	0.07	22.49
Slovakia	0	0.01	-0.91	0.61
Slovenia	0	-0.35	-0.35	1.85
Spain	39	0	-2.39	183
Switzerland	0	0.88	-0.62	40.28
UK	0	-2.60	-5.43	147.40

In contrast, other countries such as Macedonia and Greece cannot meet their electricity demand due to poor connections with other countries in the system. In this situation, in global terms, there would be a total deficit of the remaining generation capacity of -26.48 GW, which would make it difficult to meet the electricity demand of several European countries. These results show that the role of existing pumping hydropower might be key for many countries to keep their electric power systems in operation under critical conditions.

On the other hand, a few European countries have potential to build new pumping hydro plants. The European Commission (Lacal-Arántegui and Gimeno-Gutiérrez 2013) has already assessed pumped-hydro potential in all European countries. Table 2 also includes the results of the remaining generation capacity after a gas supply interruption and considers the pumping hydropower potential of each country.

The results regarding expected gas shortages under the gas cooperation model of the case study highlight that the availability of new pumping hydro plants can solve the electricity demand coverage in six out of eleven countries mentioned above. This potential depends on the availability of sites and varies considerably from one country to another. France, Greece, Portugal, and the United Kingdom are able to meet electricity demand due to their high potential pumped-hydro storage capacity and can maintain the stability of the electricity system.

However, while Belgium and Slovenia display significantly lower potential than other countries, their strong connections to neighboring countries along with the exploitation of the new pumping hydropower plants can satisfy their demand in the event of severe gas disruptions.

From the results obtained, the authors conclude that the combination of cross-border interconnections and the development of new pumping plants can contribute to the flexibility, security, and stability of the European electricity system. This combination allows countries to benefit from each other's resources and thus avoid the negative impacts of gas disruptions.

5. Conclusions

The interdependence of the gas and electricity systems is an issue of concern due to the increase in gas-fired power plants to overcome the intermittency problems of solar and wind resources. It is essential to promote the implementation of large-scale storage systems to ensure a secure supply of electricity regardless of possible gas interruptions.

This paper presents an assessment of pumping hydropower to minimize the impact of gas shortages on the electricity system based on a mathematical model that maximizes the demand coverage of different countries under a cooperative approach. To validate the model, the authors apply it to the European power system. Specifically, this paper uses data from one day under severe conditions that shows peak demands recorded for both electricity and gas.

Pumped hydro storage is the main large-scale storage solution in the European Union. The results show that the availability of new pumping hydropower plants would reduce the number of countries unable to meet their demand in the event of a gas supply crisis by half.

Nevertheless, the development of new exploitable plants includes certain drawback. For instance, it is difficult to find suitable sites due to their dependence on orographic conditions. Therefore, the available storage potential varies significantly among different countries.

In short, pumping hydropower plants allow for the integration of renewables, reduce the dependence on gas in the power system, and quickly adapt their production to keep generation and consumption balanced at all times. Thus, these plants are key to ensuring the stability and continuous operation of European power grids.

References

Deane, J. P., B. P. Ó Gallachóir, and E. J. McKeogh. 2010. “Techno-Economic Review of Existing and New Pumped Hydro Energy Storage Plant.” Renewable and Sustainable Energy Reviews 14 (4): 1293–1302. https://doi.org/10.1016/j.rser.2009.11.015.

“ENTSO-E. Winter Outlook 2016/2017 and Summer Review 2016.” n.d. Accessed February 12, 2022. https://docs.entsoe.eu/dataset/winter-outlook-

Proceedings of the 32nd European Safety and Reliability Conference
Edited by Maria Chiara Leva, Edoardo Patelli, Luca Podofillini, and Simon Wilson

ISBN: 981-973-0000-00-0 :: doi: 10.3850/981-973-0000-00-0_esrel2022-paper

2016-2017-and-summer-review-2016/resource/94c803fe-7213-4c11-a4dc-d944a94e7544.

"ENTSO-G. Union-wide SoS simulation report." n.d. Accessed June 13, 2022. https://www.entsog.eu/security-of-supply-simulation#union-wide-simulation-of-supply-and-infrastructure-disruption-scenarios-2021.

Kucukali, Serhat. 2014. "Finding the Most Suitable Existing Hydropower Reservoirs for the Development of Pumped-Storage Schemes: An Integrated Approach." Renewable and Sustainable Energy Reviews 37: 502–8. https://doi.org/10.1016/j.rser.2014.05.052.

Lacal-Arántegui, Roberto, and Marcos Gimeno-Gutiérrez. 2013. "Assessment of the European Potential for Pumped Hydropower Energy Storage."

Lu, Bin, Matthew Stocks, Andrew Blakers, and Kirsten Anderson. 2018. "Geographic Information System Algorithms to Locate Prospective Sites for Pumped Hydro Energy Storage." Applied Energy 222 (July): 300–312. https://doi.org/10.1016/j.apenergy.2018.03.177.

"Regulation (EU) 2017/1938 of the European Parliament and of the Council of 25 October 2017 Concerning Measures to Safeguard the Security of Gas Supply." n.d. Accessed February 12, 2022. https://eur-lex.europa.eu/eli/reg/2017/1938/oj.

Rodríguez-Fernández, Laura, Ana Belén Fernández Carvajal, and Luis Manuel Ruiz-Gómez. 2020. "Evolution of European Union's Energy Security in Gas Supply during Russia–Ukraine Gas Crises (2006–2009)." Energy Strategy Reviews 30 (July): 100518. https://doi.org/10.1016/j.esr.2020.100518.

Rqiq, Yassine, and Jose M. Yusta. 2020. "Impact Assessment of Gas Shortages on the European Power System under Extreme Weather Conditions." In 2020 IEEE International Conference on Environment and Electrical Engineering and 2020 IEEE Industrial and Commercial Power Systems Europe , 1–5.

Sesini, Marzia, Sara Giarola, and Adam D. Hawkes. 2022. "Solidarity Measures: Assessment of Strategic Gas Storage on EU Regional Risk Groups Natural Gas Supply Resilience." Applied Energy 308 (February): 118356. https://doi.org/10.1016/j.apenergy.2021.118356.

Yusta, Jose M., and Jesus Beyza. 2021. "Optimal Cooperative Model for the Security of Gas Supply on European Gas Networks." Energy Strategy Reviews 38 (November): 100706. https://doi.org/10.1016/j.esr.2021.100706.

Natalia Naval, Jorge J. Delgado and Jose M. Yusta

ROBUSTNESS ANALYSIS OF POWER SYSTEMS WITH A HIGH SHARE OF RENEWABLES

Natalia Naval, University of Zaragoza, EINA, Spain, email: naval@unizar.es
Jorge J. Delgado, Blue Power Partners, Spain, email: jda@bluepp.dk
Jose M. Yusta, University of Zaragoza, EINA, C/ Maria de Luna 3, 50018, Spain
Phone: +34 976761922, Fax: + 34976762226, email: jmyusta@unizar.es

Overview
The objective of this research work is to evaluate the behaviour of power systems with different levels of renewable energy share under contingencies in the electrical grid. Papers [1], [2], [3] study the influence of renewables on the robustness of the electricity system, although our contribution additionally considers the effect of the interdependence between the electricity and gas systems. Today, both infrastructures are closely related, since natural gas has become the main backup source to meet energy demand when sufficient renewable generation is not available.

Method
The assessment of the robustness of electricity systems with integration of renewable generation must consider the interactions between gas and electricity transmission networks. This article uses the software SAInt (Scenario Analysis Interface for Energy Systems), [4]. This tool is based on a mathematical formulation of models for electrical networks with a quasi-dynamic behavior, for gas networks with a time evolution of the fluid conditions in the pipelines, and a formulation to represent the interconnections between both systems.

Results
The robustness analysis is applied to a case study of Belgium, since the general data are public (generation, electricity and gas consumption, and technical constraints of each infrastructure component) [5], [6], [7]. The study is carried out during the 24 hours of a critical day for electricity demand and gas consumption with low generation availability. Due to the big cold wave during the study day, the Belgian electricity system suffered several contingencies such as the freezing of wind turbines, failures in the gas supply to gas-fired power plants, and failures of several transmission lines. This paper analyzes four cases:

- Base case without contingencies (Case 1)
- Base case with contingencies (Case 2)
- Case with higher share of renewables and without contingencies (Case 3)
- Case with higher share of renewables and with contingencies (Case 4)

In Cases 3 and 4, renewable energy represent 38% of the electricity generation mix compared to 21% in Cases 1 and 2.

From the results of the simulation of the electrical system, the electricity that could not be supplied in the network demand buses in each hour has been obtained. Similarly, the evolution of the gas not supplied in the consumption nodes of the gas network is also obtained. Case 2 presents an increase of 14% of the electricity not supplied regarding case 1, as several simultaneous contingencies occur, including line outages and generator shutdowns. In addition, in this case, the contingencies in the grid has a more significant effect on the gas system by affecting buses that fed compressor stations, causing a lack of gas supply.

In the cases with a higher share of renewable generation, there have been significant changes. Case 3 reduces average gas consumption because of the renewables contribution, which has an impact on the fluid stored in the network's gas pipelines by 2% with respect to Case 1. Case 4 increases the electricity not supplied due to the lack of generation assets to mitigate the imbalances derived from the simulated events.

It should be noted that as renewable generation increases in the grid, more critical problems appear in the supply, where variability in generation defines the system performance.

Conclusions

From a long-term energy perspective, it is verified that a future consisting entirely of renewable generation is not possible with today's technology. Robust energy infrastructures must remain in place while the energy transition is successfully completed. The objectives of decarbonization of the electricity sector cannot be achieved without energy storage to back up the intermittency of renewable generation (large-capacity electrical batteries, hydroelectric pumping or Power-To-Gas facilities).

Acknowledgements

This work was funded by the Spanish Ministry of Science and Innovation MCIN/AEI/ 10.13039/501100011033 under the project PID2019-104711RB-100: Smart-grid design and operation under the threat of interrupted supply from electric power transmission systems with a high penetration of renewable energies.

References

[1] J. Beyza, J. M. Yusta, M. A. Evangelista, J. S. Artal-Sevil, and J. A. Rendon. Evaluation of Reliability and Robustness of Electric Power Systems with Renewable Energies. *2021 23rd IEEE Int. Autumn Meet. Power, Electron. Comput. ROPEC 2021*. 2021. no. Ropec. doi: 10.1109/ROPEC53248.2021.9668112.

[2] F. Hu, L. Chen, and J. Chen. Robustness evaluation of complex power grids containing renewable energy. *Int. J. Electr. Power Energy Syst.* 2021. vol. 132, no. October 2020. p. 107187. doi: 10.1016/j.ijepes.2021.107187.

[3] F. Gutierrez-Garcia, A. Arcos-Vargas, and A. Gomez-Exposito. Robustness of electricity systems with nearly 100% share of renewables: A worst-case study. *Renew. Sustain. Energy Rev.* 2022. vol. 155. p. 111932. doi: 10.1016/j.rser.2021.111932.

[4] Saint User Manual, 2018. https://saintnet.net/ (accessed Aug. 30, 2022).

[5] ENTSOE. https://www.entsoe.eu/ (accessed Aug. 30, 2022).

[6] ENTSOG | ENTSOG. https://www.entsog.eu/ (accessed Aug. 30, 2022).

[7] J. Munoz, N. Jimenez-Redondo, J. Perez-Ruiz, and J. Barquin. Natural gas network modeling for power systems reliability studies. *2003 IEEE Bol. PowerTech - Conf. Proc.* 2003. vol. 4. pp. 20–27. doi: 10.1109/PTC.2003.1304696.

21th International Conference on Renewable Energies and Power Quality (ICREPQ'23)
Madrid (Spain), 24th to 26th May 2023
Renewable Energy and Power Quality Journal (RE&PQJ)
ISSN 2172-038 X, Volume No.21, July 2023

Technical versus socio-economic and environmental criteria in power transmission projects

N. Naval[1] and J.M Yusta[1]

[1] Department of Electrical Engineering
EINA, University of Zaragoza
María de Luna 3, 50018, Zaragoza (Spain)
Phone/Fax number:+0034 976761922, e-mail: naval@unizar.es, jmyusta@unizar.es

Abstract. In recent years, the efforts of countries to reach agreements on the development of cross-border electricity interconnection have intensified because they optimize energy resources and constitute the most significant instantaneous support for the security and continuity of electricity supply. In addition, interconnections play a key role in the integration of electricity markets. However, the planning of European electricity infrastructures constitutes complex analyses due to the large number of factors involved. This article applies a multicriteria methodology for the evaluation and prioritization of cross-border interconnection projects with the simulation of different scenarios, in total 12 scenarios, to study the effect of changes in the selected criteria on the results obtained. To test the defined methodology, the variation in the weight of different criteria in the assessment of a new cross-border electrical interconnection project between Spain and France is studied. It was verified that the tool is coherent and that the analysis developed improves the understanding of such large and complex projects and can facilitate the prioritization of project portfolios with a clear and explicit method.

Keywords. Cross-border electricity interconnections, multi-criteria technique, Analytic Hierarchy Process, power system security, scenarios.

1. Introduction

Cross-border electrical interconnection represents a key solution to address renewable energy variability and grid stability problems. On the one hand, from a technical perspective, electrical interconnections facilitate support functions between interconnected electrical systems and increase inertia in these systems. Therefore, interconnection lines improve power grid security and stability. On the other hand, from the economic perspective, cross-border interconnections allow a greater power exchange commercially to take advantage of the differences in energy prices in interconnected systems, greater competitive strength in electricity markets, more efficient management of losses and a lower operating reserve capacity, therefore lowering investment in generation plants [1].

The European Union promotes cross-border interconnections through its regulations to ensure uninterrupted electricity supply in the face of extended supply crises, favors the integration of renewable energies, promotes competition in the internal market and connects the most disadvantaged areas [2], [3], among others. In this context, the European Network of Transmission System Operators for Electricity, taking into account technological, market and political developments, proposes a portfolio of projects that provide socioeconomic well-being and help Europe meet its climate objectives [4]. Projects of Common Interest (PIC) are energy infrastructure projects necessary for the development of priority and strategic areas in the European Union. These projects have a short commissioning time and are funded by community grants [5].

Most of the reviewed works on electrical systems use multicriteria decision techniques, as they are efficient methods to handle decision-making problems under different and conflicting criteria. The works [6], [7] classify the main decision-making methods. There are numerous classifications based on the various characteristics of the methods (number of criteria, environment, alternatives or number of decision-makers). The main classification to consider is the one that refers to the number of alternatives. In this way, multicriteria methods are classified into continuous (multiobjective decision-making, MODM) and discrete (multiattribute decision-making, MADM) methods [8]. Continuous multicriteria methods are those in which the number of alternatives is not countable and therefore try to optimize the value of a technical parameter. On the other hand, discrete multicriteria methods are those in which the number of alternatives is countable and they are fundamentally explicitly defined.

Discrete multicriteria methods are divided into three categories: value measurement models, goal and preference levels models, and overclassification models. First, value measurement models are those that assign a numerical value to each alternative, thus establishing an order of preference. Each criterion or subcriterion is assigned a weight based on the importance of this criterion for decision-makers. This category includes the analytic hierarchy process (AHP) method [9], the analytic network process (ANP) method [9], and the multiattribute utility

theory (MAUT) or multiattribute value theory (MAVT) [10]. Second, the preference level models are those that seek to select the alternative that is closest to the ideal solution or to the level of preference. The methods that make up this category are VIKOR [11] and the Technique for Order-Preference by Similarity to Ideal Solution (TOPSIS) [12]. Finally, overclassification methods are those that compare the alternatives in the form of pairs in such a way that they determine which of them is preferred with respect to the previous criterion. Within this group, the preference ranking organization MeTHod for enrichment evaluations (PROMETHEE) [13] and ELECTRE [14] can be found.

Regarding the objective of the multicriteria analysis applied in the previous articles on the electricity sector, the works [15] - [18] mainly evaluate different energy sources to achieve an optimal energy system in different areas, such as Iran [15], India [16], Lithuania [17], and Bangladesh [18]. Other articles evaluate and prioritize different alternatives for the electrical planning of isolated areas [19], [20].

Based on the literature reviewed, the lack of sensitivity studies that validate the methodologies developed through a multicriteria decision process to reduce the subjectivity associated with any decision method is verified. Sensitivity analysis makes it possible to determine how the selection of alternatives changes when the relative weight of the criteria or requirements considered as determining factors in the selection process changes.

Therefore, sensitivity analysis is a necessary complementary tool in analyzing decisions. Based on the application of multicriteria techniques for the evaluation of electrical interconnection infrastructure projects, this article proposes to carry out a sensitivity analysis (changes in the weight assigned to the criteria and modification of the proposed criteria) to study the influence of the variation of the input data on the effect of the results obtained. The methodology is applied to a project of common interest for the cross-border interconnection of Spain-France that will be put into service in the coming years. It must be taken into account that if small variations in the inputs produce large changes in the results, the decision-makers should assess the validity of the judgments issued. Therefore, this research allows a complete and realistic analysis of the results, studies the importance of each of the selected criteria (social, economic, environmental and technical) and verifies which are the most important.

The rest of the article is structured as follows: Section 2 presents the multicriteria methodology. Section 3 defines the case study along with the proposed scenarios. Section 4 analyzes the results obtained. Finally, Section 5 summarizes the main conclusions of this research.

2. Methodology

Selecting the most beneficial project from a range of alternatives is one of the greatest difficulties faced by electrical infrastructure planners. The consideration of a large number of factors that intervene in the process and the variety of criteria, objectives and participants makes it necessary to plan a multidimensional decision process in which economic, technical, social and environmental aspects are involved.

Multicriteria techniques help in the analysis or decision- making thanks to dividing the problem into parts or subparts that are studied in isolation and that are easier to address that way. In addition to facilitating the selection ofthe best alternative through an in-depth study of the problem, multicriteria analysis can provide other advantages and benefits, even generating new alternatives that are better than those initially proposed [21].

In this article, the AHP method is used since it has many advantages over other defined techniques, such as the possibility of decomposing and analyzing the problem in parts and measuring quantitative and qualitative criteria using a common scale, including the involvement of different stakeholders, generate a synthesis and perform sensitivity analysis. In short, it is a simple and flexible method that can solve complex problems with multiple criteria.

Figure 1 represents the main steps that make up the methodology used to apply the AHP technique correctly and obtain the prioritization of cross-border interconnection projects.

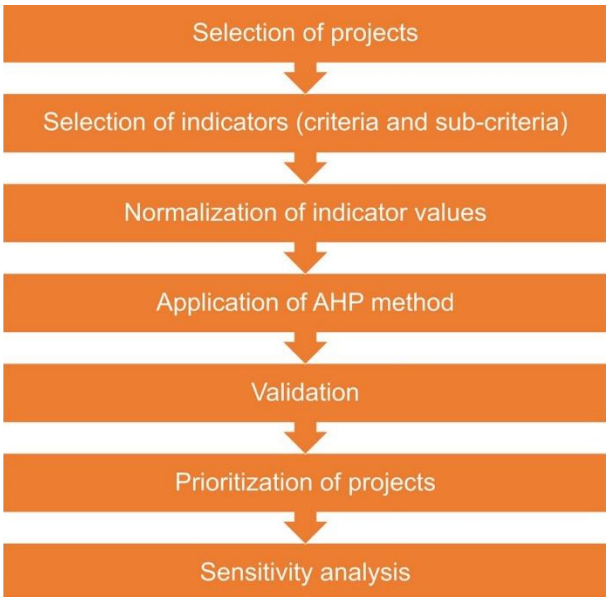

Fig. 1. Summary diagram of the multicriteria methodology.

Next, the stages of the proposed methodology are briefly defined:

- First, you must select the alternatives on which you want to apply the multicriteria tool.
- Subsequently, the indicators that directly affect the selection of one project or another are identified, and their values are normalized with respect to the target country.
- Then, once the alternatives to be evaluated andthe different indicators have been selected, they are weighed through surveys of the different groups of experts. The total set of decision- makers must consist of professionals or specialists with different backgrounds in the planning of electrical infrastructures,

socioeconomic and environmental impact of energy systems, planning and land use planning, among others.

- The next step is to validate the results obtained through the consistency of judgments. The consistency ratio is calculated, which must be less than 0.1. If this does not happen, it is necessary to coordinate with the decision-maker to make the corrections where the inconsistency occurs until a consistency ratio of less than 0.1 is achieved.
  Equations (1)-(3) indicate the calculation of the consistency index of the comparison matrix (CI), the random consistency index (RI) and the consistency ratio (CR). Here, λmax is the maximum eigenvalue and n corresponds to number of criteria.

$$CI = \frac{\lambda max - n}{n - 1} \quad (1)$$

$$RI = \frac{1.98 \cdot (n - 2)}{n} \quad (2)$$

$$RC = \frac{CI}{RI} \quad (3)$$

- Once the results are adequate, each of the projects selected for each of the subcriteria are compared.
- Finally, the evaluation and prioritization of the projects is obtained. The project with the highest AHP weighting value is the one selected.
- Finally, it is essential to carry out a sensitivity analysis through which the reliability of the results obtained is verified.

Figure 2 presents the criteria and subcriteria that are used to assess cross-border electrical interconnection projects. Consistent energy planning requires the implementation oftechnical, economic, environmental and social criteria. In addition, subcriteria must be established and linked to each of the criteria for decision-making. Therefore, in this case, four criteria and twelve subcriteria are chosen.
For a more detailed explanation of the indicators, see document [4].

3. Case study

To test the proposed methodology in various scenarios, it is applied to a new project of common interest for cross-border electrical interconnection between Spain and France [5]. The level of electrical interconnection in Spain is very low, and it is a priority to promote new interconnections to reduce Spain's isolation from the restof the European system.
Table I indicates the main characteristics of the capacity and costs of the project that is taken as a case study in this article. This project consists of a new HVDC (high-voltage direct current) interconnection by means of a direct current submarine cable in the Bay of Biscay. In addition, there is a converter station at each end of the electric transmission line to transform direct current into alternating current to connect to the electricity transmission network of each country.

Table I. Study project characteristics.

Substations	Capacity increase (MW)	Length (km)	CAPEX (€ M)	OPEX (€ M)
Gatika (Spain) - Cubnezais (France)	2200	370	1750	10.2

The scenarios that are proposed in this article to evaluate the importance of each criterion and obtain an adequate assessment of the judgments made are indicated in Table II.

Table II. Proposed scenarios.

Scenarios	Technical criterion (%)	Environmental criterion (%)	Social criterion (%)	Economic criterion (%)
1	100	0	0	0
2	0	100	0	0
3	0	0	100	0
4	0	0	0	100
5	50	50	0	0
6	50	0	50	0
7	50	0	0	50
8	33.33	33.33	33.33	0
9	33.33	33.33	0	33.33
10	33.33	0	33.33	33.33
11	25	25	25	25
12	35.50	33.46	16.22	14.82

Each of the criteria is modified separately, always ensuring a sum of 100% is met to observe the effects that the modifications have on decision-making. If only one criterion is considered, the analysis ceases to be multicriteria, but that is how the effects of conditioning decision-making on a single criterion can be analyzed.
Subsequently, criteria are added to evaluate the impact on their combination, generating different scenarios.
The technical criterion is considered the most influential in cross-border electrical interconnection projects since, with the increase in the flow of electricity transfer capacity, the study system achieves important benefits. The new interconnection allows greater stability and continuity of the electricity supply in the event of phenomena that endanger supply availability between the two countries, progress toward achieving the energy transition objectives and to creating a more efficient system with greater savings that benefit all consumers.

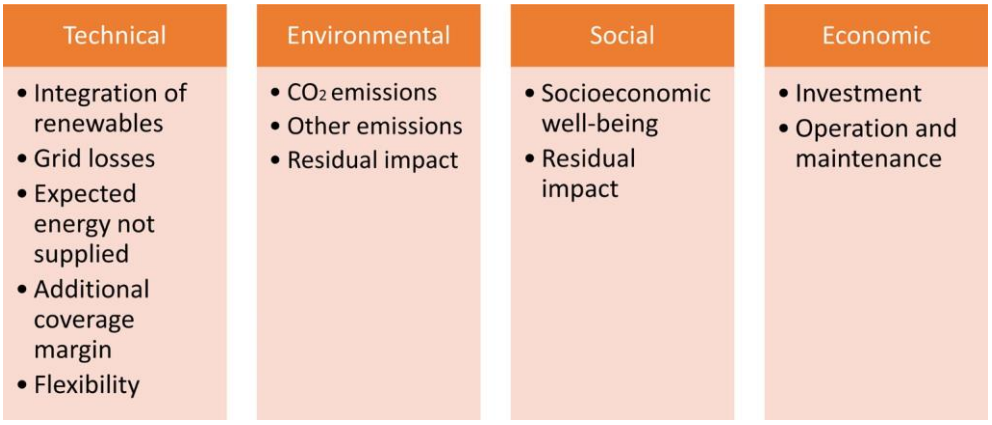

Fig. 2. Outline of the proposed criteria and subcriteria.

4. Results

Table III presents the results obtained from the AHP method when applying the weights of the criteria indicatedin Table II through the proposed methodology.

Table III. Results obtained in the different study scenarios.

Scenarios	Study project
1	0.9643
2	0.8795
3	1.0000
4	0.6299
5	0.7763
6	0.9821
7	0.7971
8	0.8507
9	0.8926
10	0.8646
11	0.9201
12	0.8937

It should be noted that the results shown are the result of the application of the criteria for the different scenarios, keeping the weights in the subcriteria. Scenario 12 represents the base case with the four criteria selected, and its weight is obtained through surveys carried out with groups of experts.

In the scenarios where the economic criterion was weighted more (scenarios 4 and 7), the score of the project decreases with respect to the base case since the investment and operation costs are high as a consequence of the use of submarine cables over the greater portion of the route in addition to the fact that the necessary transmission line is long (almost 400 km).

By increasing the weight of the social criterion, the AHP score of the study project increases. This project is at a very advanced stage for commissioning in the coming years, which is why it has been subjected to several public consultations throughout the planning process to ensure a rational use of natural resources, the prevention and reduction of pollution and strengthening social cohesion. For cross-border electrical interconnection projects, the citizen involvement during all stages through access to comprehensive and easy-to-understand information is critical for achieving greater social consensus and the best solution for the territory.

As a result, the final layout of this project avoids proximity to population centers and areas with potential urban development, as well as isolated homes, where noise emissions can become annoying for people. In addition, the increase in energy exchange capacity that this project allows translates into a reduction in the expected congestion at the border, as well as the use of cheaper energy at all times, due to the increase in flow in both directions, providing a greater socioeconomic benefit throughout Europe.

Similarly, by increasing the weight of the technical criterion, the score of the project increases, since, as obtained in the base scenario (scenario 12), it is the most important criterion. The increase in energy transfer capacity between countries (2200 MW) provides a better mesh with the rest of the European system with the consequent improvement of the quality and security of the electrical system and the possibility of mutual support in case of incidents and extreme situations. In addition, it avoids having to install backup generation in the Spanish and French systems with the possibility of sharing balancing mechanisms, achieving a more efficient European global system.

Regarding the increase in weight of the environmental criterion, a similar score is obtained in the project compared to the base case (scenario 12). In scenario 12, the groups of experts already scored high on the environmental criteria (33.46%) together with the technical criteria (35.50%). Cross-border electrical interconnection projects can affect vegetation, protected natural spaces, fauna and places with protected or endangered species. Therefore, it is essential to minimize this impact. The layout of this study project uses submarine cables that avoid affecting the mountainous system of the Pyrenees, which have vast areas outfitted for leisure highlighted by their beauty, species and climate. In addition, the project avoids fishing areas. Additionally, with this electrical interconnection, a greater integration of renewable energies is achieved with the consequent reduction of CO_2 emissions.

In summary, from this evaluation, the power of the tool for analyzing various case studies and the importance of conducting sensitivity studies to be able to visualize the influence of each of the criteria more clearly and validate the decisions taken emerge.

5. Conclusion

Cross-border electrical interconnections allow greater stability and security of the electricity supply as the number of interconnections increases with an increase in the energy exchange capacity and, consequently, a greater possibility of sharing resources and their more efficient use. This article aims to apply a multicriteria methodology for the evaluation of large and complex cross-border electrical interconnection infrastructure projects with the simulation of various scenarios to validate the prioritization of projects and study the influence of the different proposed criteria (technical, environmental, social and economic).
A new electrical interconnection project between Spain and France has been chosen as a case study. The impulse and political support for these interconnections is essential for Spain to reach the minimum value of 10% of the interconnection ratio established as a target in the European Union.
From the results obtained, the following conclusions have been drawn:

- The methodology allows simulating different scenarios and assessing the consequences of different decisions made.
- The study of scenarios allows a more consistent and exhaustive evaluation of electrical interconnection projects.
- An important criterion in the evaluation of this type of project is the technical one. This project presents good technical characteristics with the incorporation of the latest HVDC technology, greater integration of renewables and increased electrical security. Of similar importance is the environmental criterion, for which the new electrical interconnections must minimize the negative impact on the environment with the appropriate selection of its route.
- The methodology is valid since the evaluation of several scenarios shows that the proposed variations in the weights of the criteria do not leadto large changes in the project score.

In summary, the application of the multicriteria methodology to different study scenarios provides as complete a view as possible of the real impact of cross-border electricity infrastructure projects. In addition, it allows us to analyze in detail the variation of the different criteria and improve the selection process and, thus, beable to validate the prioritization of some alternatives over others.

Acknowledgment

This work was funded by the Spanish Ministry of Science and Innovation MCIN/AEI/ 10.13039/501100011033 under the project PID2019-104711RB-100: Smart-grid design and operation under the threat of interrupted supply from electric power transmission systems with a high penetration of renewable energies.

References

[1] International Renewable Energy Agency (IRENA). Outlook for the global energy transition. 2021.
[2] E. Parliament. Directiva 2009/72/CE. 2009. pp. 1–39. [Online]. Available: http://eur-lex.europa.eu/LexUriServ/LexUriServ.do?uri=OJ:L:2009:211:0055:0093:PT:PDF.
[3] European Commission. Electricity interconnections with neighbouring countries. pp. 1–40, 2018.
[4] ENTSOE. https://www.entsoe.eu/ (accessed Aug. 30, 2022).
[5] TYNDP 2020 Project Collection. https://tyndp2020-project-platform.azurewebsites.net/projectsheets (accessed May 13, 2022).
[6] E. Løken. “Use of multicriteria decision analysis methods for energy planning problems”. Renewable and Sustainable Energy Reviews. 2007. vol. 11, no. 7. pp. 1584–1595.
[7] J. J. Wang, Y. Y. Jing, C. F. Zhang, and J. H. Zhao. “Review on multi-criteria decision analysis aid in sustainable energy decision-making”. Renewable and Sustainable Energy Reviews. 2009. vol. 13, no. 9. pp. 2263–2278.
[8] R. Abu Taha and T. Daim. “Multi-Criteria Applications in Renewable Energy Analysis, a Literature Review”. Green Energy and Technology. 2013. vol. 60. pp. 17–30.
[9] M. R. Asadabadi, E. Chang, and M. Saberi. “Are MCDM methods useful? A critical review of Analytic Hierarchy Process (AHP) and Analytic Network Process (ANP)”. Cogent Engineering. 2019. vol. 6, no. 1.
[10] J. Ananda and G. Herath. “A critical review of multi-criteria decision making methods with special reference to forest management and planning”. Ecological Economics. 2009. vol. 68, no. 10. pp. 2535–2548.
[11] A. Mardani, E. K. Zavadskas, K. Govindan, A. A. Senin, and A. Jusoh. “VIKOR technique: A systematic review of the state of the art literature on methodologies and applications”. Sustainability. 2016. vol. 8, no. 1. pp. 1–38.
[12] L. Ren, Y. Zhang, Y. Wang, and Z. Sun. “Comparative analysis of a novel M-TOPSIS method and topsis”. Applied Mathematics Research EXpress. 2007. vol. 2007. pp. 1–10.
[13] J.-P. Brans and Y. De Smet. PROMETHEE methods Chapter 1 PROMETHEE METHODS, no. January. 2016.
[14] X. Yu, S. Zhang, X. Liao, and X. Qi. “ELECTRE methods in prioritized MCDM environment”. Information Sciences. 2018. vol. 424. pp. 301–316.
[15] F. Katal and F. Fazelpour. “Multi-criteria evaluation and priority analysis of different types of existing power plants in Iran: An optimized energy planning system”. Renewable Energy. 2018. vol. 120. pp. 163–177.
[16] J. Vishnupriyan and P. S. Manoharan. “Multi-criteria decision analysis for renewable energy integration: A southern India focus”. Renewable Energy. 2018. vol. 121. pp. 474–488.
[17] D. Štreimikiene, J. Šliogeriene, and Z. Turskis. “Multi-criteria analysis of electricity generation technologies in Lithuania”. Renewable Energy. 2016. vol. 85. pp. 148–156.
[18] I. Khan. “Power generation expansion plan and sustainability in a developing country: A multi-criteria decision analysis”. Journal of Cleaner Production. 2019. vol. 220. pp. 707–720.

[19] T. Jamal, T. Urmee, and G. M. Shafiullah. “Planning of off-grid power supply systems in remote areas using multi-criteria decision analysis”. Energy. 2020. vol. 201, 117580
[20] F. Fuso Nerini, M. Howells, M. Bazilian, and M. F. Gomez. “Rural electrification options in the Brazilian Amazon. A multi-criteria analysis”. Energy for Sustainable Development.2014. vol. 20, no. 1. pp. 36–48.
[21] J. C. Rojas-Zerpa and J. M. Yusta. “Application of multicriteria decision methods for electric supply planning in rural and remote areas”. Renewable and Sustainable Energy Reviews. 2015. vol. 52. pp. 557–571.

Energy Strategy Reviews 43 (2022) 100944

Contents lists available at ScienceDirect

Energy Strategy Reviews

journal homepage: www.elsevier.com/locate/esr

Characterising the security of power system topologies through a combined assessment of reliability, robustness, and resilience

Jesus Beyza [a], Jose M. Yusta [b,*]

[a] National Centre for Energy Control, Blvd. Adolfo López Mateos 2157, Los Alpes, Álvaro Obregón, 01010, Mexico City, CDMX, Mexico
[b] University of Zaragoza, Department of Electrical Engineering, C/ María de Luna 3, 50018, Zaragoza, Spain

ARTICLE INFO

Keywords:
Cascading failure
R3 concept
Power system
Reliability
Resilience
Restoration
Robustness

ABSTRACT

Electricity has a prominent role in modern economies; therefore, ensuring the availability of electricity supply should be a top priority for policymakers. The joint assessment of reliability, robustness, and resilience can be a useful criterion to characterise different topologies and improve the security of supply. This paper proposes a novel integrated analysis of these three attributes to quantify the security of power grid topologies. Hence, eight case studies with different topologies created using the IEEE 24-bus reliability test system were analysed. Reliability was evaluated by applying the sequential Monte Carlo approach, robustness was evaluated by simulating cascading failures, and resilience was evaluated by analysing recovery curves. The different indicators associated with each of the three evaluations were then calculated. The results obtained were discussed both graphically and quantitatively in a novel three-dimensional representation, where the importance of joint analysis was also highlighted. The proposed method can serve as an additional tool for planners to identify possible investments or improvements in power system topologies.

1. Introduction

Electrical power systems should be reliable, robust, and resilient. In the current decarbonisation process in modern societies, they have become increasingly important for the continuous operation of daily activities. Thus, threats and disruptions to electricity security are increasing and evolving at the same rate as in the power grid [1]. Therefore, more studies are required to analyse the associated attributes, ensure that systems are increasingly secure on a daily basis, and track the changing patterns of systems under different threats that affect the sector.

The distinction between the concepts of reliability, robustness, and resilience in a power system is clearly defined in the scientific literature [2]. According to Georges Zissis's message in the IEEE Industry Applications Magazine [3], "reliability is the probability that a system will perform in a satisfactory manner for a given period when it is used under specified operating conditions". This attribute evaluates the network performance in the event of a loss of one or two assets. In contrast, "robustness is the ability of a system to avoid malfunctioning when a fraction of its elements fail, or the ability of a system to perform the intended task under unexpected disturbances" [4,5]. More aggressive than reliability, this attribute considers the elimination of multiple assets and quantifies the network performance in the event of cascading failures. Finally, "resilience is a system's ability to withstand, adapt, and absorb from a major disruption within acceptable degradation parameters and recover within a satisfactory timeframe". This concept generally analyses HILP events, such as extreme natural disasters [6–8]. These three joint attributes are currently known as the "R3 concept" [3]. Fig. 1 outlines as an example of the R3 concept.

Currently, there is a strong desire to improve the performance and quality of electrical networks.

This desire results from the development and transformation of more sustainable, resilient, and carbon-free societies. The R3 concept is a field of research that requires the proposal of new integrated methodological frameworks to study the different interrelated attributes that encompass reliability, robustness, and resilience. The scientific literature describes methods to study some of these attributes [10]; for example, previous studies used energy hub-based methods, models order reduction, metaheuristic searching genetic algorithms, multicriteria decision analysis, advanced intelligent strategies, and linear programming [11–16].

However, one of the largest challenges in studying R3 concept is cascading failures. These events are complicated to study because they can result from countless reasons or causes; thus, studying them is

* Corresponding author.
E-mail addresses: jesus.beyza@cenace.gob.mx (J. Beyza), jmyusta@unizar.es (J.M. Yusta).

https://doi.org/10.1016/j.esr.2022.100944
Received 21 February 2022; Received in revised form 9 August 2022; Accepted 21 August 2022
Available online 30 August 2022

Nomenclature

Abbreviations

DC	Direct current
DFS	Depth-first search algorithm
HILP	High-impact low-probability

Indices

n, m	Nodes or buses
d	Loads
g	Generators
i	Islands
j	Number of closed power lines
k	Lines
p	Disruption
q	Year
r	Recovery stage
s	Steps

Variables

Δ_n	Voltage angle at node n [radians]
P_k, P_g, P_n	Power flow through line k, power of the generator g, and power demand at node n [MW]
μ_k	Binary variable indicating the open or closed state of the power line (open, $\mu_k = 0$, closed, $\mu_k = 1$)
D_i	Demand on each island i [MW]
SD_s	Satisfied demand in step s [p.u]
RD_r	Recovered demand in stage r [p.u]
$MTTF$	Meantime to failure [h]
$MTTR$	Meantime to repair [h]
TTR	Time to repair [h]
TTF	Time to failure [h]
r	Random number uniformly distributed between [0,1]
ADLC	Average duration of load curtailment [h/outage]
Dd	Duration of disruption [h]
E	Energy not supplied for reliability assessment [MWh]
EDNS	Expected demand not supplied [MW]
EENS	Expected energy not supplied [MWh/yr]
EFLC	Expected frequency of load curtailment [outages/yr]
ENS	Energy not supplied for resilience assessment [MWh]
LOLE	Loss of load expectancy [h/yr]
LOLP	Loss of load probability [%]
N	Number of disruptions
RD	Recovered demand [p.u]
SD	Satisfied demand [p.u]

Parameters

P_k^{max}, P_k^{min}	Maximum and minimum capacity of the power line k [MW]
P_g^{max}, P_g^{min}	Maximum and minimum capacity of the generator g [MW]
Δ_n^{max}, Δ_m^{min}	Maximum and minimum voltage angle at node n [radians]
N_y	Number of simulated years
B_k	Susceptance of the power line k [p.u]
N_c	Maximum number of power lines to be closed
α_k	Overload tolerance parameter of the power line k
λ	Failure rate of the assets
μ	Repair rate of the assets

Sets

D	System loads
E	Isolated elements
G	Generators
I	Islands
K	Power lines
L	Closed power lines
M	Nodes or buses

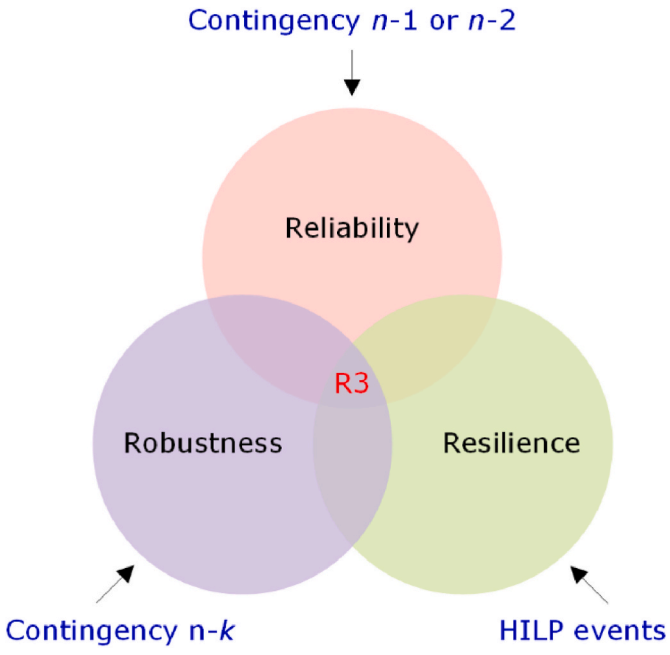

Fig. 1. Schematic representation of the R3 concept [9].

unfeasible. Hence, the complex network theory (or graph theory) may be suitable for modelling the dynamic behaviour, analysing the propagation of disturbances, and quantifying the structural robustness of a system [17–20]. Furthermore, note that this technique has the potential to identify both critical assets and the events that can trigger cascading failures [21–26].

Some studies more focused on extreme disturbances have indicated that both reliability and robustness studies should consider the impact of weather conditions because they can severely impact the system and sectors linked to it. Under this premise, some studies proposed metrics, protection strategies, and theoretical frameworks to analyse this problem in detail [27–29].

Resilience is an entirely new area of research that encompasses procedures and techniques to solve problems associated with protecting and restoring the services provided by a power system. Some academics have evaluated the resilience of networks considering the strengths and weaknesses of both the topology and power transfer capacities of transmission lines under different disturbances, such as natural disasters, earthquakes, and floods [30–32]. Owing to the increase in disruptions, it is important to evaluate the resilience of a network after a high-impact disturbance [33,34], which is related to the concept of resilience. Therefore, some researchers have proposed procedures to plan the iterative recovery of a system after a disruptive event [35–37].

Another factor considered in some combined robustness and resilience studies is the fundamental change in the structure and generation mix of power systems. For example, some articles have reviewed cutting-edge practices, whereas others have offered integrated analyses of

decision-making [38,39]. The main aim is to analyse the different reconfiguration options and select the optimal solution for its implementation. Additionally, other studies have provided definitions, metrics, guidelines, practical challenges, and technical problems related to the attributes of resilience [40–43].

In summary, the following deficiencies can be identified in the existing literature related to the reliability, robustness, and resilience of power systems:

1. No related articles has proposed an integrated study of the three concepts on the topology of power systems. Most existing publications correspond to the study of these concepts individually, and very few others correspond to the analysis of only two of the concepts [2,7,11,27,44]. All the studies examined different problems from the one proposed in this paper.
2. The concepts of reliability, robustness, and resilience are used to evaluate power systems from different perspectives; therefore, the conclusions of the studies already published can be expanded and improved by considering a joint and integrated vision.
3. The characteristics and relationships between the concepts must be explored; for example, identifying how a certain improvement in one indicator does not necessarily imply improvements in the other indicators. Published studies did not address this problem.

Reliability, robustness, and resilience are discussed in several aspects and from different perspectives in the scientific literature; however, few studies considered these three concepts in an integrated manner. The latter motivated the specific objective of this study, which was to develop a theoretical and data-based methodological framework to explore the characteristics and relationships between all concepts in an electrical power system. Combined studies of reliability, robustness, and resilience could better reflect the performance of a network. Including the three attributes in a joint analysis can be an incentive for future research in this area. However, it is important to note that this document does not discuss how to improve the study of these attributes but rather emphasises the critical role of these concepts in an electrical network. A reliable power system may not be robust or resilient to other threats or disturbances; therefore, the task of ensuring electricity security should be a priority for decision-makers.

The main contributions of this article can be summarised as follows:

1. An integrated reliability, robustness, and resilience assessment is performed to quantify the security of the power system topologies.
2. A novel three-dimensional representation is proposed to represent the integrated results and provide an additional strategy to the traditional procedures. Here, we seek to provide a visual representation of the relationship between these concepts.
3. Different case studies with different topologies are analysed to demonstrate the performance of the proposed approach and to obtain integrated results.

Based on the above and the provisions and guidelines in the scientific literature, the reliability assessment was performed by applying the sequential Monte Carlo technique and measuring the indices of EENS, EDNS, EFLC, LOLE, LOLP, and ADLC. The robustness evaluation was completed by simulating cascading failures and quantifying the SD index at each stage of system disintegration. This iterative procedure eliminates an asset, quantifies the power flows in the network, removes the system's overloaded links, and identifies and balances the resulting subsystems to determine whether a cascading event continues or ends. A resilience study was performed using a mixed-integer optimisation problem, where the integer variables represent the operational state of the power lines, and the real variables represent the scheduled dispatch of the generators. This procedure uses the system's state of disintegration at the end of the cascading failure as input data and determines the power lines that must be closed iteratively and the redispatch of generation plants for the optimal recovery of network connectivity. The RD index was measured at each recovery stage, whereas the ENS index was measured at the end of the recovery process.

The three previous procedures use a standard model of DC power flows because they yield rapid solutions. While other methods can be used depending on the required accuracy sought in the results, the only objective here was to establish an integrated framework for future development; therefore, this model is adequate. The proposal made here is novel and original in the field of power system security. The reliability, robustness, and resilience procedures were programmed using MATLAB R2021a platform. The different results obtained were discussed both graphically and numerically in a sequential study framework. Subsequently, a joint analysis of the three concepts was presented. The proposed approach can significantly positively impact the performance and quality of a power network, improve consumer satisfaction, and inform planners in the decision-making process for better investment in network topologies. Numerical tests to investigate the similarities and differences between the concepts were conducted in eight case studies based on the IEEE 24-bus reliability test system (RTS) [45].

The remainder of this article is organised as follows: Section 2 describes the reliability, robustness, and resilience procedures used to evaluate of a power system in an orderly and systematic manner. Section 3 presents case studies based on a well-known IEEE 24-bus RTS. Section 4 discusses the simulation results obtained by applying the procedures described above. Finally, Section 5 summarises the main conclusions of this study.

2. Reliability, robustness, and resilience methodologies

In this section, the procedures used to evaluate the reliability, robustness, and resilience of an electrical power system are described. In general terms, the reliability is evaluated by applying the sequential Monte Carlo technique, the robustness is evaluated by simulating cascading failures, and the resilience is evaluated by developing a mixed-integer optimisation problem. These three procedures follow the foundations of scientific literature.

2.1. Reliability procedure

Reliability is divided into two areas that are well established in the scientific literature: adequacy and security. On the one hand, adequacy evaluates whether the generation capacity adjusts to the demand and constraints of the system. On the other hand, security studies focus on the performance of a power system against the outage of one or two components. This study focused on the security of power systems. This type of evaluation can be performed from an analytical or simulation perspective. The first one requires initial assumptions to simplify the problem and produce an analytical; hence, the resulting analysis may lose its relevance. The second one simulates the random behaviour of the system through multiple experiments and considers all possible contingencies in the network. The Monte Carlo technique is a simulation approach [46,47]; therefore, it was used in this research work. In the Monte Carlo technique, two main techniques, non-sequential and time-sequential, are used. The former considers each time step or system state independently, whereas the latter realistically simulates both the actual chronological process and the random behaviour of the system [48,49]. This study used the sequential Monte Carlo technique for reliability assessment because it is flexible, accurate, and enables the calculation of different indicators. For a more detailed description, please refer to Refs. [46,47]. The implementation of the sequential Monte Carlo technique for the reliability analysis is presented in Algorithm 1.

Algorithm 1. Reliability

Input: technical data of the power system and N.

(*continued on next page*)

(*continued*)

Output: statistical indicators EENS, EDNS, EFLC, LOLE, LOLP and ADLC.
Step 1. Start: establish the operational state of the assets, that is, normal or failure.
Step 2. Modelling of outages: these events are modelled using the MTTF and MTTR indices. These indicators are inversely related to λ and μ of the assets,

$$MTTF = \frac{1}{\lambda}; \quad (1)$$

$$MTTR = \frac{1}{\mu}; \quad (2)$$

Step 3. Time between states: quantify the time that the assets spend in normal and failure state, that is, TTR and TTF,

$$TTR = -\ln(r) \times MTTR; \quad (3)$$

$$TTF = \frac{-\ln(r)}{\lambda} \times 8760; \quad (4)$$

This step is repeated for a specific time, frequently one year.
Step 4. Overlapping time: calculate the overlapping times of failures of the elements (when several components are simultaneously out of service) for a temporal resolution of 1 h in a time horizon of 1 year, that is, 8760-time steps of 1 h each.
Step 5. Power flows: conduct a DC power flow study considering the operational state of the components throughout the year.
Step 6. Reliability indicators: evaluate the security of the power system through reliability indices (5)–(10), using the results from Step 5.

$$EENS = \frac{\sum_{p=1}^{N_y}\sum_{q=1}^{N_q} E_{p,q}}{N_y}; \quad (5)$$

$$EDNS = \frac{EENS}{8760}; \quad (6)$$

$$EFLC = \frac{\sum_{p=1}^{N_y} N_p}{N_y}; \quad (7)$$

$$LOLE = \frac{\sum_{p=1}^{N_y}\sum_{q=1}^{q} Dd_{p,q}}{N_y}; \quad (8)$$

$$LOLP = \frac{LOLE}{8760}; \quad (9)$$

$$ADLC = \frac{LOLE}{EFLC}; \quad (10)$$

Step 7. Iterations: repeat the previous steps until a covariance of less than 6% is obtained for the EENS index [50].

Generally, this procedure assumes that each asset of an electrical system can have two states: operational and failure. It is assumed that the residence time of the component is exponentially distributed and that the state transition is determined by both its current state and the transition rates. The transition rates between the two states are the failure and repair rates of the components. The random samples of the state of each component are statistically dependent, that is, they are related to the previous sample. Subsequently, when the overlapping times are determined, it executes the DC power flows and calculates the reliability indicators of the studied electrical system. According to previous studies [50,51], this procedure is repeated several times until the covariance of the EENS indicator is less than 6%.

2.2. Robustness procedure

The robustness of power systems, including cascading phenomena, is an active field of research. Most of the contributions in the literature evaluate the robustness of the power grid with respect to the modelling and analysis of cascading failures, in particular for cascading effects due to line overloads under faults or targeted attacks [11,17–19,21,52]. Blackouts are disastrous events generally caused by cascading failures, which includes a series of iterative events that can include voltage problems and the disconnection of power lines and loads. These events are complicated to model because they encompass hundreds of highly dynamic events. However, it is important to analyse and model them because they affect hundreds of thousands of people and cause enormous economic losses [17]. In this study, the robustness was measured in operational areas both before and after cascading failure [53]. The SD index was used to measure the functionality of an electrical power system during such disturbances. This index varies between 1 and 0 and is measured according to the assets isolated during the disintegration of the network. As the SD index decreases, the impact on disconnected loads increases. Algorithm 2 describes the ordered and systematic steps used to model cascading failures in an electrical power system.

Algorithm 2. Robustness

Input: technical data of the power system and α.
Output: degradation of the electrical power system. SD in s, I, E, and μ_k, i.e. open or closed.
Step 1. Start: $SD_{base} = D_{load}$, I = { · } and E = { · }. At the beginning, all the power lines are operational.
Step 2. DC power flows: calculate P in each k within the network and determine P_k^{max} of the lines using (11).

$$P_k^{max} = \alpha_k \times P_k; \quad (11)$$

Step 3. Initiating event: randomly remove an asset from the system. The latter represents the event that triggers the cascading failure.
Step 4. Increase or decrease flows: determine the increases or decreases in each power line; initialise s = 1 as the first disintegration stage.
Step 5. Triggering of switches: evaluate the condition $|P_k^s| < P_k^{max}$ in all power lines of the system. Remove all overloaded links, i.e. $|P_k^s| > P_k^{max}$, and go to Step 6; otherwise, go to Step 10.
Step 6. Transversal graph algorithm: use DFS to determine I and E formed after the activation of the switches.
Step 7. Energy balance:
a) for each island I_i with generators g ∈ I_i evaluate
- if $\sum_{g\in I_i} P_g < \sum_{d\in I_i} P_d$, then do $D_{I_i}^s = \sum_{g\in I_i} P_g$ in stage s.
- if $\sum_{g\in I_i} P_g > \sum_{d\in I_i} P_d$, then do $D_{I_i}^s = \sum_{d\in I_i} P_d$ in stage s.

b) for each subnet I_i without generators g ∈ I_i; do $D_i^s = 0$, respectively.
Step 8. Satisfied *demand*: calculate (12),

$$SD_s = \frac{\sum_{i\in I} D_{I_i}^s}{SD_{base}} \text{ in } s; \quad (12)$$

Step 9. Iterations: iterate s = s + 1 and go to Step 4.
Step 10. End: if $|P_k^s| < P_k^{max}$ ∀k, the algorithm ends.

The procedure begins by collecting the technical data of the electrical network and calculating the power flows to determine the maximum transfer capacity of the lines. Next, it randomly removes an asset, determines the changes in the flows, and removes all overloaded power lines resulting from the redistributed network flows. Note that the cascading failure initiation event is random, such as involuntary human errors or technical failures in the equipment and hardware. The constant tripping of protection mechanisms in the power lines resulting from the propagation of the cascading failure can result in the formation of different islands in the system. Therefore, this procedure incorporates a transversal graph algorithm to identify subsets formed during the disintegration stages. The DFS algorithm was used here to simplify the resolution of this problem [54]. This technique is widely recognised as an effective tool for solving various graphs problems. The algorithm starts at the root node and scans each branch before backtracking. Fig. 2 shows the tree structure of the cascading failure process used in Algorithm 2. Islands without generators are considered dead and are marked in red, while islands with generations are marked in green. The intermediate islands where cascading failure continues are marked in blue.

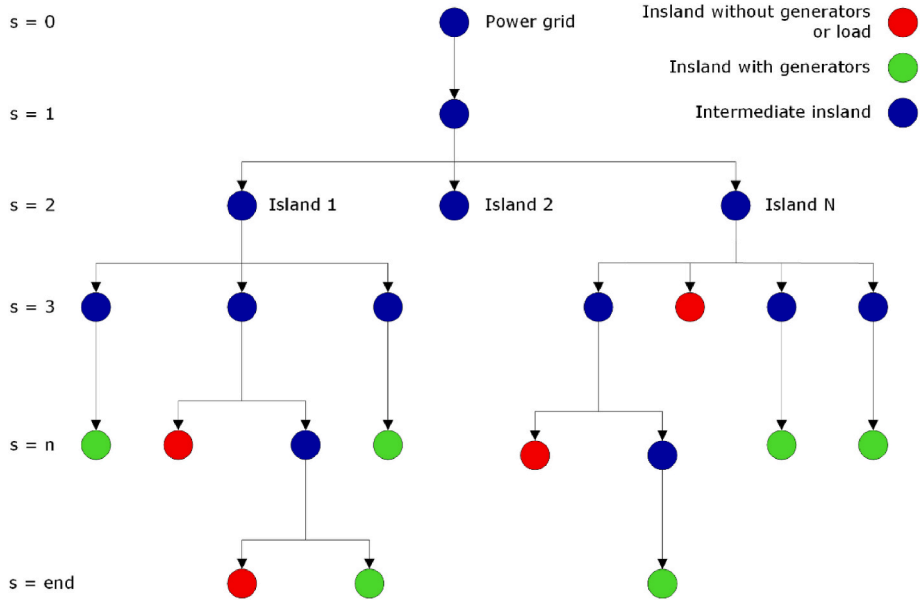

Fig. 2. Tree structure of the cascading failure process.

The tree structure shows how an island can undergo changes during the process and disintegrate into more islands, where some remain operational and others are deeply affected. Cascading failure continues on all intermediate islands in blue. The constant redistribution of flows can cause further overloads on other links; thus, each intermediate island can result in an additional group of islands where the cascading event also continues simultaneously. Thus, each time one or more power lines are disconnected during the disintegration stage, the DFS algorithm identifies and orders each island for a correct simulation. Similarly, these islands must comply with the balance between demand and generation; thus, load shedding is used to satisfy the energy balance. Isolated elements or subnets without generation are considered unsatisfied loads during the disintegration process. The iterative procedure continues until no overloaded elements remain or all assets are isolated.

2.3. Resilience procedure

After a major disturbance, the degradation of an electrical system is a function of robustness; thus, resilience depends on both the robustness and rapid recovery of the disconnected load. Therefore, a mixed-integer optimisation problem is proposed to recover both the loads and connectivity of the system after cascading failure. The optimisation output is the quantified optimal resilience characteristic and state of the transmission lines. For demonstration, the RD index is used to represent the resilience of the system. The optimisation objective is to maximise this resilience metric after the cascading failure is modelled using Algorithm 2. This optimisation problem is subject to several constraints. Algorithm 3 describes the iterative procedure for determining the power lines that must be closed in each recovery stage of the power system.

Algorithm 3 uses the final disintegration of a power system as input data to initialise both the recovered demand and initial operational state of the power lines. Similarly, it considers the maximum number of lines that can be reconnected and the redispatch of generators in each recovery stage. It then constructs an optimisation problem based on the standard DC power flow equations and establishes the minimum and maximum thresholds for the different equations. The maximum threshold of the power lines is calculated using Algorithm 2. When the set of equations is constructed, the objective function for the corresponding recovery stage is maximised. The output consists of the recovered demand and power lines, which must be closed during the restoration stage. Finally, these results are saved, and new closed power lines are set in their corresponding equations. If all power lines are closed, the algorithm ends; otherwise, the algorithm repeats the procedure until all remaining lines are closed.

Algorithm 3. Resilience

Input: outputs of Algorithm 2, i.e., SD in the last *s*, *I*, E, and μ_k. Similarly, N_c in each r.
Output: recovery of the electrical power system. RD and μ_k in each r.
Step 1. Start: initialise $RD_r = SD_{s_{final}}$ and $\mu_k = 1$ for closed lines and $\mu_k = 0$ for open lines at r = 1. The initial satisfied demand and the states of the lines correspond to the final disintegration state obtained with Algorithm 2.
Step 2. Optimisation problem based on the standard model of DC power *flows:* consider (13) to (21)

$$max\ (RD_r - RD_{r-1}) \tag{13}$$

subject to:

$$P_g^{min} \le P_g^r \le P_g^{max}\ \forall g \in G \tag{14}$$

$$P_k^{min} \cdot \mu_k^r \le P_k^r \le P_k^{max} \cdot \mu_k^r\ \forall k \in K \tag{15}$$

$$\Delta_n^{min} \le \Delta_n^r \le \Delta_n^{max}\ \forall n \tag{16}$$

$$-\sum_{k\in K} P_k^r - \sum_{g\in G} P_g^r - \sum_{d\in D} P_d^r = 0\ \forall n \tag{17}$$

$$B_k\left(\Delta_n^r - \Delta_m^r\right) - P_k^r \ge 0\ \forall k \tag{18}$$

$$-B_k\left(\Delta_n^r - \Delta_m^r\right) - P_k^r \le 0\ \forall k \tag{19}$$

$$\sum_{k\in K} \mu_k^r \le N_c \tag{20}$$

$$RD_r = \sum P_n^r\ \forall n \tag{21}$$

The maximum thresholds of (15) are initially determined in Algorithm 2.
Step 3. Solve the optimisation problem: maximise (13), subject to constraints (14)–(21) in each r.
Step 4. Solution: save the results of RD_r and μ_k^r; set the variables μ_k^r restored as constants $\mu_k^r = 1$ for all subsequent iterations.

(*continued on next page*)

(*continued*)

Step 5. Evaluation: if $\forall k \in (K - k')$: $\mu_k^s = 1$ go to Step 7; otherwise, go to Step 6.
Step 6. Iterations: iterate r = r +1 and go to Step 3.
Step 7. End: if $\forall k \in (K - k')$: $\mu_k^s = 1$; the algorithm ends.
Step 8. Energy not supplied: calculate the ENS index for the resilience curve, i.e. the area above the curve.

3. Case studies

This section describes the IEEE 24-bus RTS through which eight case studies with different topologies were constructed [45]. That is, the original system was used, and lines were added to obtain different networks for comparison. First, the case studies are presented, and then the guidelines followed for the reliability, robustness, and resilience simulations are described.

3.1. Test system

Fig. 3 shows the IEEE 24-bus RTS. This network is composed of 24 buses, 33 generators and 38 power lines, and transformers. The maximum demand is 2850 MW. The parameters of the lines, load characteristics, and input data for the stochastic failure model for the buses, transformers, and lines are described in Ref. [45]. This test network has been well documented in the scientific literature.

Eight different case studies based on the previous system were used to assess reliability, robustness, and resilience. The case studies included adding and combining three different power lines to the original system (14–15, 14–24, and 6–9). The objective was to obtain different topologies of the same system and to perform comparative evaluations between them. The lines added to the original system satisfied type n-1 and n-2 contingencies according to the provisions provided in Ref. [55]. Considering the representation of the test system shown in Fig. 3, the eight case studies were as follows:

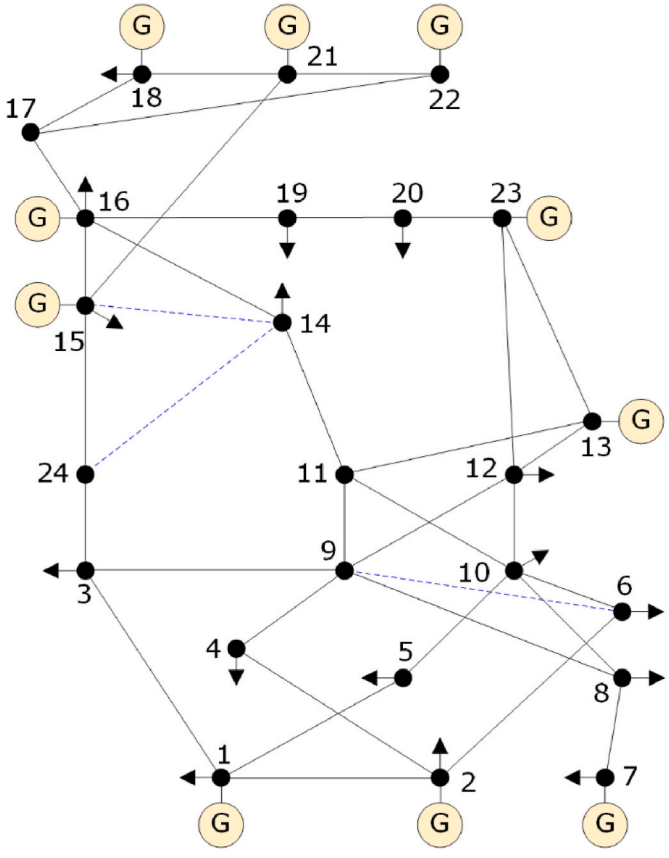

Fig. 3. Topology of the IEEE 24-bus RTS. The lines in blue represent the additional power lines.

- **Case 1:** the original system.
- **Case 2:** addition of line 14–15 to the original system.
- **Case 3:** addition of line 14–24 to the original system.
- **Case 4:** addition of line 6–9 to the original system.
- **Case 5:** addition of lines 14–15 and 14–24 to the original system.
- **Case 6:** addition of lines 14–15 and 6–9 to the original system.
- **Case 7:** addition of lines 14–24 and 6–9 to the original system.
- **Case 8:** addition of lines 14–15, 14–24, and 6–9 to the original system.

3.2. Simulation guidelines in the analysis of reliability, robustness, and resilience

Different guidelines were followed when applying Algorithms 1, 2, and 3 to the eight case studies described above to perform a comprehensive and accurate analysis of the different indicators studied. As reliability evaluation is a classic analysis in power systems, this study followed the already published studies in this field of research. That is, 1500 one-year iterations were executed in each network, obtaining covariance values lower than 6% in all cases [44].

Robustness evaluation is a complex procedure that involves different parameters and characteristics of the studied system. For example, an electrical system can have different levels of robustness depending on where the initial failure occurs, level of congestion of the lines, operational assets, load level, etc. Therefore, some researchers prefer to characterise robustness from a topological and structural perspective; thus, it is invariant to other factors that occur in the network [56]. This type of analysis is also advantageous because it offers another perspective on the system. To conduct a complete evaluation of robustness, in this study, we eliminated the lines adjacent to the buses (except for buses 6, 9, 14, 15, and 24 because new lines were added) to begin the network disintegration process.

Furthermore, because the system had a constant load, we also considered different levels of overload in the links for the same scenario to obtain different states of disintegration for the initiating event. Therefore, 114 scenarios were executed with α = 1, 1.1, 1.2, 1.3, 1.4, and 1.5 in each case study, that is, a total of 912 simulations for the eight cases. Finally, the robustness of each case was measured by averaging the set of results obtained, which provided an overview of system performance.

In contrast, the resilience evaluation was performed from the averaged states of disintegration of the eight cases after applying the robustness procedure. We assumed that the maximum number of lines that could change state in each recovery stage was three. The number of lines that can operate to recover a collapsed electrical system depends on the physical characteristics of the network and the procedures applied by each control centre. In this study, only three power lines were used for simulation. Finally, the ENS index was calculated for each case, assuming that each interval of redispatch and reconfiguration required approximately 15 min on average, because it was necessary to plan, execute, and verify the manoeuvres. Although other times could be used, the time between the manoeuvres and redispatch used in this study corresponded to a value close to reality.

4. Simulation results

This section discusses the simulation results obtained after the reliability, robustness, and resilience were evaluated in the eight case studies described above. The three procedures were programmed in MATLAB R2021a and executed on a personal computer with a 3.40 GHz Intel® Core™ i7 CPU and 16 GB of RAM. The run times for the reliability, robustness and resilience studies were 294.99 h, 167.91 s, and

31.81 s, respectively.

Table 1 shows the different reliability indicators calculated for the eight cases after applying Algorithm 1, and Fig. 4 presents the convergence results of the EENS indicator. Case 6 was the best case, in which an improvement of 2.19% was obtained compared with Case 1. Note that Case 5 also had a very similar percentage improvement to Case 6, although owing to decimal point values, this case was positioned after Case 6. In Case 8, the improvement was 1.86% over that of the original system, indicating an improvement in the system performance. However, Cases 2 and 7 had EENS values very close to each other, although Case 7 was more connected than the others. This was because line 14–15 reduced the congestion of two lines adjacent to bus 14. This line also coincided with Case 6. The same occurred when line 6–9 was added in Case 6, which was the most reliable case. However, the focus was on line 14–15 because it decongested the links adjacent to the generator connected to bus 15. The remaining indicators exhibited similar behaviours to the analysis performed previously. The results showed that the reliability was improved by adding lines to the original system; however, certain lines located on buses with poor connectivity exhibited better results. From highest to lowest, the reliability was in the order of Cases 6, 5, 8, 2, 7, 4, 3, and 1.

Fig. 5 shows the dispersion of the last value of the robustness indicator SD after applying Algorithm 2 and the mean values obtained in the eight cases. The mean values of the SD index for Cases 1–8 were 0.34, 0.38, 0.34, 0.35, 0.40, 0.39, 0.35, and 0.40 p.u, respectively. The plotted results show that the cases had different satisfied demand values at the end of the network collapse, indicating that the redistributed flows after the initial disturbance differed in each case. However, when averaging the set of results for each case, the robustness of Case 8 improved by 9.43% compared with that of Case 1. That is, the most connected case was the most robust to cascading failures. This was reasonable as the power lines were less congested. The results also showed that all the cases in which one or two lines were added improved the robustness of the original system. Cases 3 and 4 had improvements of 0.52% and 1.17%, respectively, when considering less-connected cases compared with Case 1. However, Case 2 improved by 5.71% compared with the original system and was even better than Case 7 with two lines. Note that Case 2 corresponded to the addition of line 14–15, which was also identified as an asset that improved the reliability of the system. The robustness of the cases was ordered, from highest to lowest, as Cases 8, 5, 6, 2, 7, 4, 3, and 1. These findings suggest that complex meshed topologies are more robust against the propagation of cascading failures than less meshed topologies, provided that there are vital assets that increase the energy transfer or reduce link congestion.

The curves in Fig. 6 illustrate the general concept and demonstrate the advantages of the restoration strategy proposed in Algorithm 3. The cases started began with different values of satisfied demand and different states of disintegration for greater realism. Numerically, Cases 1 and 5 began from topologies in which 27 and 32 power lines were lost, respectively. The results indicated that each system recovered its disrupted loads; however, some of them were superior because they required fewer manoeuvres to restore the load more promptly. The ENS indices for Cases 1–8 were 3277.82, 2108.23, 3701.65, 2233.49, 2564.52, 2371.71, 2110.90, and 1359.00 MWh, respectively. Considering this indicator, Case 8 was the most resilient because it improved by

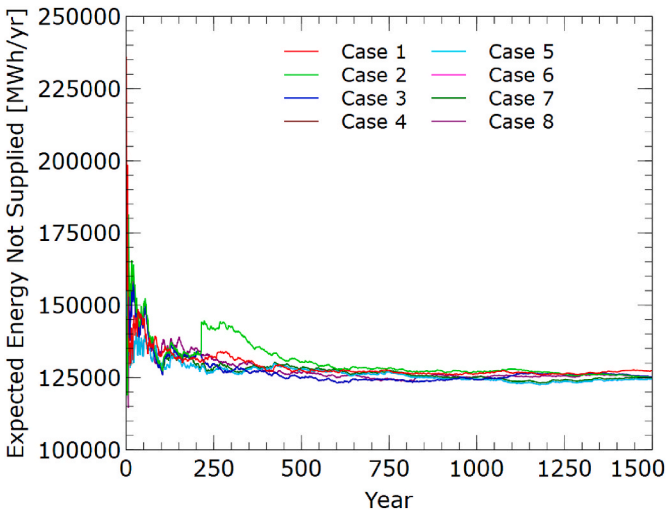

Fig. 4. Convergence of the EENS indicator for the eight cases.

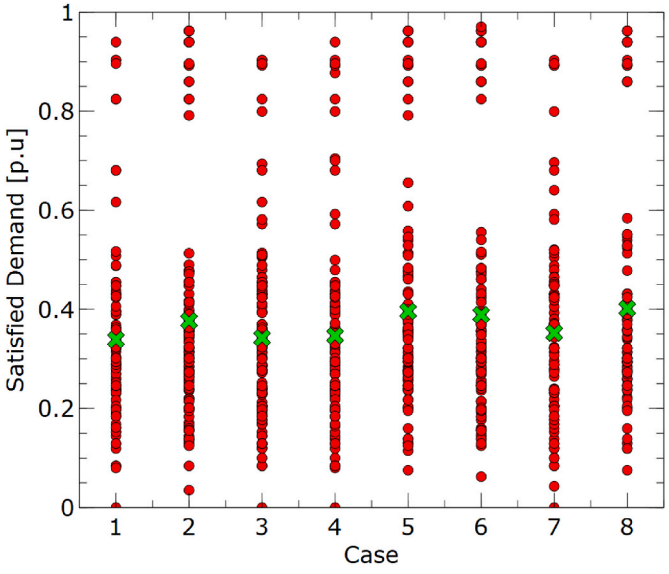

Fig. 5. Dispersion of the robustness results for the eight cases.

58.53% compared with Case 1, whereas Case 3 was the least resilient because it worsened by 12.93% compared with Case. 1. Cases 2 and 7 improved by 35.68% and 35.60%, respectively, compared with the original system, which placed them in the second and third positions, respectively. The cases can be ordered from highest to lowest resilience as Cases 8, 2, 7, 4, 6, 5, 1, and 3. Note that the order of the cases is not directly related to the meshing of the network as it is to the robustness, although Case 8 with the addition of three links was the most resilient, and Case 3 with the addition of a single link was the least resilient. As far as this study is concerned, the cases had between 32 and 33

Table 1
Reliability results.

	Case 1	Case 2	Case 3	Case 4	Case 5	Case 6	Case 7	Case 8
EENS	127,285.95	124,988.11	125,259.72	125,258.70	124,504.17	124,504.00	125,029.97	124,921.43
EDNS	14.53	14.27	14.30	14.30	14.21	14.21	14.27	14.26
EFLC	19.07	18.93	19.06	19.05	18.93	18.93	18.83	18.97
LOLE	731.41	721.78	726.59	726.60	720.12	720.13	720.79	723.20
LOLP	8.35	8.24	8.29	8.29	8.22	8.22	8.23	8.26
ADLC	38.35	38.14	38.13	38.13	38.03	38.03	38.28	38.12

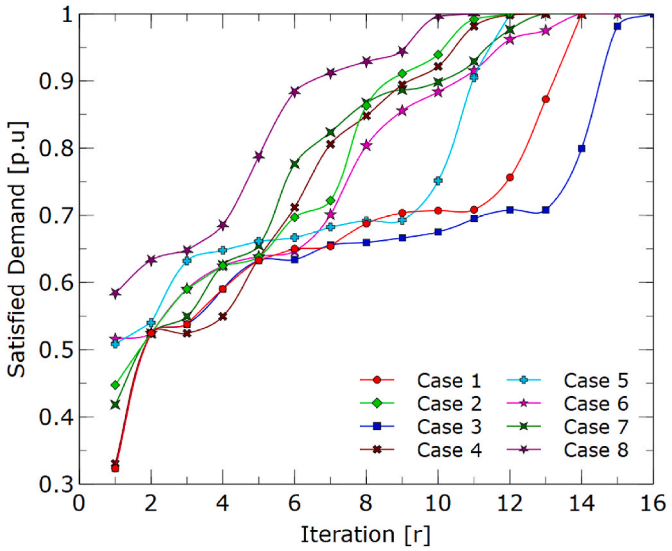

Fig. 6. Optimal recovery curves for the eight cases.

disconnected lines, but their combinations were completely different in each case; thus, the subsequent reconnection strongly influenced both the recovery and ENS index. This appeared to indicate that resilience can be influenced by several factors, such as the topological state of disintegration, load distribution, energy transfer limits, and loss of critical assets. Therefore, it is reasonable that the order of the cases obtained here was different, which again confirmed the requirement for joint and integrated studies to characterise the behaviour of power system topologies. The resilience evaluation demonstrated that the network topology influenced the recovery of the system. For example, Cases 1 and 3 had different recovery curves, although they began from similar values of satisfied demand. In other words, the topology has a fundamental role in the design of resilient systems.

Examining the results more comprehensively, Table 2 shows the improvement percentages of the EENS, SD, and ENS indices for reliability, robustness, and resilience evaluations. These values are expressed as percentages of the increases or decreases compared with the original system (Case 1). Fig. 7 shows a three-dimensional representation of these results. On the one hand, the results indicated that most of the topologies improved on reliability, robustness, and resilience, except for Case 3, which exhibited the worst performance in terms of resilience. Similarly, the topology of Case 8 was the most robust and resilient of all the systems but slightly less reliable than the topologies of Cases 5 and 6 because it had 0.33% more ENS. The topologies of Cases 2, 5, and 6 were intermediate among the three attributes. On the other hand, although the topologies of Cases 4 and 7 exhibited good performance in terms of reliability and resilience, they had a slightly poor performance in terms of robustness because their improvement percentages were minimal compared with the more robust topologies. However, the performance of these two topologies was superior to that

Table 2
Percentages of increase in the EENS, SD and ENS indicators in the reliability, robustness, and resilience evaluations compared with Case 1.

	Reliability [Δ EENS (%)]	Robustness [Δ SD (%)]	Resilience [Δ ENS (%)]
Case 1	0.00	0.00	0.00
Case 2	1.81	5.71	35.68
Case 3	1.59	0.52	−12.93
Case 4	1.59	1.17	31.86
Case 5	2.19	8.61	21.76
Case 6	2.19	7.58	27.64
Case 7	1.77	2.02	35.60
Case 8	1.86	9.43	58.52

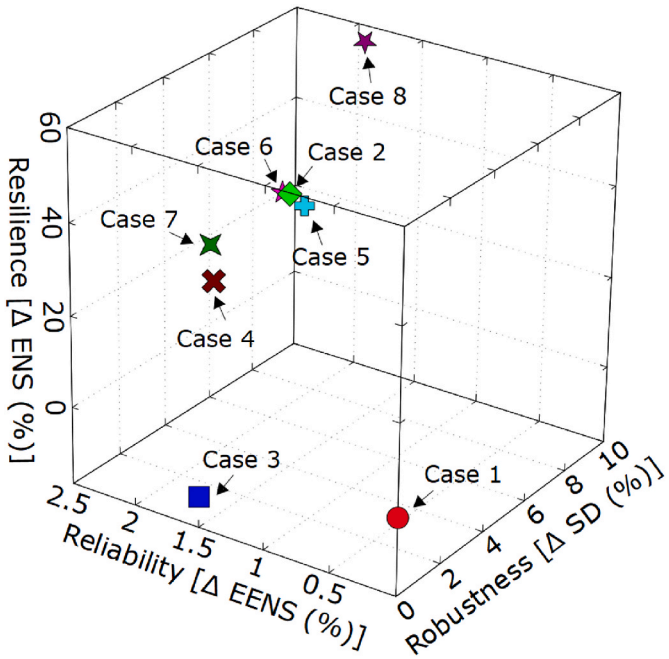

Fig. 7. Results obtained integrated into an R3 concept.

of Case 3.

The results integrated into the R3 concept also demonstrated that the addition of lines mostly had a positive impact on the operating conditions of the original system because they enabled an increase in the power transfer capacity between different zones and reduced congestion in the power lines. They also aided in the adaptation to the different disturbances simulated in the network and facilitated optimal resource management during the recovery process. Generally, and corresponding with other related publications, reliability is improved by adding more power lines and meshing the network; however, the network can become less robust because it is more exposed to cascading failures. Similarly, a less robust system implies greater disintegration because of a cascading event, which directly influences resilience. However, it is important to note that some lines were more beneficial than others; thus, the R3 concept can offer a better compromise solution for the design of electrical power systems.

Finally, the results obtained in the R3 framework can be used to make investment decisions or improvements in the power grid topology from an integrated perspective of the three concepts. For example, a decision-maker can determine a compromise solution for a power system by weighing reliability, robustness, and resilience in an integrated manner, as considering the concepts separately can result in contradictory views on the problem and, to some extent, impact the security of supply. Note that these conclusions do not invalidate other transmission network planning strategies under other criteria for improving system capacity to ensure optimal technical and economic performance. This is because the conclusions reached in this manuscript do not replace the conclusions obtained with the methods of analysis widely used and recognised in the industry, mainly focused on traditional adequacy and security criteria. Instead, the R3 framework can be an additional strategy for the traditional tools already used in power systems.

Additionally, renewable energy sources are an integral part of the current process of decarbonisation of power systems and, as such, recent articles consider these assets in their studies. Here, the results could be different depending on how the simulation is performed, what guidelines are considered, or even what percentage of renewable resources are available in each case study. For example, in terms of reliability, the case study with renewables would be expected to be less reliable than the case study with fossil generation, mainly due to the stochastic nature

of renewable resources. In terms of robustness, the case studies with and without renewables could have similar behaviour because cascading events can happen irrespective of the type of generation, as they are influenced by the operation of the protection devices. However, it would be important to note that synchronous generators can remain connected during and after a fault; in contrast, challenges arise in maintaining adequate frequency response as the share of inverter-based renewables increases. In terms of resilience, the case study with renewables could recover the load of the system faster than the case study with fossil generation because the first one could have distributed generation to restore inoperative areas (if sufficient wind or solar resources were available). Nevertheless, renewable energy sources do not represent any obstacle in the proposal presented here, as it is possible to consider them [57,58].

Other areas for improvement in this research include the following:

1. The robustness study could be improved with a more complex methodology to capture both the frequency dynamics and the triggering mechanisms of the protection devices in a cascading event.
2. The integration of indicators could be further extended by considering multi-criteria techniques for a better ranking of network topologies.

5. Conclusions

This paper proposes a methodological framework based on data to analyse the reliability, robustness, and resilience of a power system from an integrated perspective. A sequential Monte Carlo technique was applied to evaluate the reliability, a cascading failure procedure was used to quantify the robustness, and a recovery procedure based on a mixed-integer optimisation problem was used to calculate a resilience metric. For this analysis, eight case studies were used based on the well-known IEEE 24-bus RTS, in which different indicators of reliability, robustness, and resilience were calculated. The results obtained were presented both graphically and numerically and were comprehensively discussed in a three-dimensional representation that considered the ranking of each case in each concept. This representation demonstrated the advantage of representing the three concepts in an integrated manner rather than separately. The findings showed that most meshed topology of an electrical system cannot always be guaranteed as the best from the perspective of each criterion, but generally, it offers the best optimal results for the security of supply. For example, the reliability study indicated that Case 6, with only two lines, was more reliable than Case 8 with three lines by 0.33% in relation to the ENS index. Although this is a small value, the unavailability of energy has strong economic repercussions in modern economies. In contrast, Case 8 was more robust and resilient than Case 6 by 2.50% and 42.70%, respectively, which could indicate that a meshed topology has advantages because it enables higher demand to be satisfied in the event of disturbances or failures and the power supply to be restored earlier. The results also showed that a power line can have a favourable impact on the security of supply, as demonstrated by Cases 1 and 2, where Case 2 had improvements of 1.81% in reliability, 10.53% in robustness, and 35.68% in resilience. The findings presented here clearly and accurately demonstrated the requirement for more integrated studies to obtain a much broader view of the operational behaviour of power systems. A planner can perform this procedure and run it to identify possible investments or improvements in the power system topology. A power system planner can use these results to identify possible investments or improvements in power system topology. This paper is a starting point for future developments. Future work will incorporate other methods of analysis and consider other strategies for integrating indicators.

Credit author statement

Jesus Beyza: Conceptualization; Investigation; Methodology; Writing - original draft. **Jose M. Yusta**: Conceptualization; Funding acquisition; Project administration; Writing - review & editing.

Declaration of competing interest

The authors declare that they have no known competing financial interests or personal relationships that could have appeared to influence the work reported in this paper.

Acknowledgements

This work was funded by the Spanish Ministry of Science and Innovation MCIN/AEI/10.13039/501100011033 under the project PID2019-104711RB-100: Smart-grid design and operation under the threat of interrupted supply from electric power transmission systems with a high penetration of renewable energies.

References

[1] IEA, Analytical Frameworks for Electricity Security, 2021. https://www.iea.org/reports/analytical-frameworks-for-electricity-security.
[2] E. Hossain, S. Roy, N. Mohammad, N. Nawar, D.R. Dipta, Metrics and enhancement strategies for grid resilience and reliability during natural disasters, Appl. Energy 290 (February) (2021), 116709, https://doi.org/10.1016/j.apenergy.2021.116709.
[3] G. Zissis, The R3 concept: reliability, robustness, and resilience [President's Message], IEEE Ind. Appl. Mag. 25 (1) (2019) 5–6, https://doi.org/10.1109/MIAS.2019.2909374.
[4] Y. Koç, M. Warnier, P. Van Mieghem, R.E. Kooij, F.M.T. Brazier, The impact of the topology on cascading failures in a power grid model, Phys. A Stat. Mech. its Appl. 402 (2014) 169–179, https://doi.org/10.1016/j.physa.2014.01.056.
[5] Y. Koc, A. Raman, M. Warnier, T. Kumar, in: Structural Vulnerability Analysis of Electric Power Distribution Grids 31, Jun. 2015, pp. 1–20 [Online]. Available: http://arxiv.org/abs/1506.08641.
[6] S. Ahmadi, A.H.F. Khorasani, A. Vakili, Y. Saboohi, G. Tsatsaronis, Developing an innovating optimization framework for enhancing the long-term energy system resilience against climate change disruptive events, Energy Strategy Rev. 40 (Mar. 2022) 100820, https://doi.org/10.1016/j.esr.2022.100820.
[7] T. Kemabonta, G. Mowry, A syncretistic approach to grid reliability and resilience: Investigations from Minnesota, Energy Strategy Rev. 38 (Nov. 01) (2021), https://doi.org/10.1016/j.esr.2021.100726.
[8] IEA, Analytical Frameworks for Electricity Security, 2021. https://www.iea.org/reports/analytical-frameworks-for-electricity-security.
[9] K. Kapur, D. Reed, Integration of Reliability, Robustness and Resilience for Engineered System Motivation, Jun. 2014. http://depts.washington.edu/hursandy/Pub/ISERC2014_Presentation.pdf.
[10] N.A. Salim, J. Jasni, M.M. Othman, Reliability assessment by sensitivity analysis due to electrical power sequential tripping for energy sustainability, Int. J. Electr. Power Energy Syst. 126 (2021), 106582, https://doi.org/10.1016/j.ijepes.2020.106582.
[11] W. Huang, et al., Reliability and Vulnerability Assessment of Multi-Energy Systems: An Energy Hub Based Method, IEEE Trans. Power Syst. 8950 (2021) 1–12, https://doi.org/10.1109/TPWRS.2021.3057724.
[12] M.B. Ndawula, I. Hernando-Gil, R. Li, C. Gu, A. De Paola, Model order reduction for reliability assessment of flexible power networks, Int. J. Electr. Power Energy Syst. 127 (2021), 106623, https://doi.org/10.1016/j.ijepes.2020.106623.
[13] A.N. Abdalla, et al., Metaheuristic searching genetic algorithm based reliability assessment of hybrid power generation system, Energy Explor. Exploit. 39 (1) (2021) 488–501, https://doi.org/10.1177/0144598720959749.
[14] F. Ezbakhe, A. Pérez-Foguet, Decision analysis for sustainable development: The case of renewable energy planning under uncertainty, Eur. J. Oper. Res. 291 (2) (2021) 601–613, https://doi.org/10.1016/j.ejor.2020.02.037.
[15] I. Akhtar, S. Kirmani, M. Jameel, Reliability Assessment of Power System Considering the Impact of Renewable Energy Sources Integration into Grid with Advanced Intelligent Strategies, IEEE Access 9 (2021) 32485–32497, https://doi.org/10.1109/ACCESS.2021.3060892.
[16] I. Akhtar, S. Kirmani, Reliability assessment of power systems considering renewable energy sources, Mater. Today Proc. (2021) 1–4, https://doi.org/10.1016/j.matpr.2021.01.326.
[17] S. Yang, W. Chen, X. Zhang, W. Yang, A Graph-based Method for Vulnerability Analysis of Renewable Energy integrated Power Systems to Cascading Failures, Reliab. Eng. Syst. Saf. 207 (2021), 107354, https://doi.org/10.1016/j.ress.2020.107354.
[18] D. Zhou, F. Hu, S. Wang, J. Chen, Power network robustness analysis based on electrical engineering and complex network theory, Phys. A Stat. Mech. its Appl. 564 (2021), 125540, https://doi.org/10.1016/j.physa.2020.125540.
[19] K. Li, K. Liu, and M. Wang, "Robustness of the Chinese power grid to cascading failures under attack and defence strategies," Int. J. Crit. Infrastruct. Prot., p. 100432, doi: 10.1016/j.ijcip.2021.100432.

[20] J. Beyza, J.M. Yusta, Integrated Risk Assessment for Robustness Evaluation and Resilience Optimisation of Power Systems after Cascading Failures, Energies 14 (7) (2021) 2028, https://doi.org/10.3390/en14072028.
[21] W. Zhu, J.V. Milanović, Assessment of the robustness of cyber-physical systems using small-worldness of weighted complex networks, Int. J. Electr. Power Energy Syst. 125 (2) (2021), 106486, https://doi.org/10.1016/j.ijepes.2020.106486.
[22] D. Zhu, R. Wang, J. Duan, W. Cheng, Comprehensive weight method based on game theory for identify critical transmission lines in power system, Int. J. Electr. Power Energy Syst. 124 (2021), 106362, https://doi.org/10.1016/j.ijepes.2020.106362.
[23] S. Wang, W. Lv, J. Zhang, S. Luan, C. Chen, X. Gu, Method of power network critical nodes identification and robustness enhancement based on a cooperative framework, Reliab. Eng. Syst. Saf. 207 (2021), 107313, https://doi.org/10.1016/j.ress.2020.107313.
[24] I.B. Sperstad, E.H. Solvang, S.H. Jakobsen, A graph-based modelling framework for vulnerability analysis of critical sequences of events in power systems, Int. J. Electr. Power Energy Syst. 125 (2021), 106408, https://doi.org/10.1016/j.ijepes.2020.106408.
[25] Y. Liu, N. Zhang, D. Wu, A. Botterud, R. Yao, and C. Kang, "Searching for Critical Power System Cascading Failures with Graph Convolutional Network," IEEE Trans. Control Netw. Syst., vol. 5870, 2021, doi: 10.1109/TCNS.2021.3063333.
[26] T. Nguyen, B.H. Liu, N. Nguyen, B. Dumba, J. Te Chou, Smart Grid Vulnerability and Defense Analysis Under Cascading Failure Attacks, IEEE Trans. Power Deliv. 8977 (2021) 1–9, https://doi.org/10.1109/TPWRD.2021.3061358.
[27] E. Hossain, S. Roy, N. Mohammad, N. Nawar, D.R. Dipta, Metrics and enhancement strategies for grid resilience and reliability during natural disasters, Appl. Energy 290 (2021), 116709, https://doi.org/10.1016/j.apenergy.2021.116709.
[28] D. Zhou, F. Hu, S. Wang, J. Chen, Robustness analysis of power system dynamic process and repair strategy, Elec. Power Syst. Res. 194 (2021), 107046, https://doi.org/10.1016/j.epsr.2021.107046.
[29] I.B. Sperstad, G.H. Kjølle, O. Gjerde, A comprehensive framework for vulnerability analysis of extraordinary events in power systems, Reliab. Eng. Syst. Saf. 196 (2020), 106788, https://doi.org/10.1016/j.ress.2019.106788.
[30] T. Tapia, Á. Lorca, D. Olivares, M. Negrete-Pincetic, A.J. Lamadrid L, A Robust Decision-Support Method Based on Optimization and Simulation for Wildfire Resilience in Highly Renewable Power Systems, Eur. J. Oper. Res. (2021), https://doi.org/10.1016/j.ejor.2021.02.008.
[31] A. Shahbazi, J. Aghaei, S. Pirouzi, T. Niknam, M. Shafie-khah, J.P.S. Catalão, Effects of resilience-oriented design on distribution networks operation planning, Elec. Power Syst. Res. 191 (2021), 106902, https://doi.org/10.1016/j.epsr.2020.106902.
[32] N. Zhao, et al., Full-time scale resilience enhancement framework for power transmission system under ice disasters, Int. J. Electr. Power Energy Syst. 126 (2021), 106609, https://doi.org/10.1016/j.ijepes.2020.106609.
[33] G.E. Alvarez, A novel strategy to restore power systems after a great blackout. The Argentinean case, Energy Strategy Rev. 37 (2021), 100685, https://doi.org/10.1016/j.esr.2021.100685.
[34] H.H. Alhelou, M.E. Hamedani-Golshan, T.C. Njenda, P. Siano, A survey on power system blackout and cascading events: Research motivations and challenges, Energies 12 (4) (2019) 1–28, https://doi.org/10.3390/en12040682.
[35] C.W. Zobel, C.A. MacKenzie, M. Baghersad, Y. Li, Establishing a frame of reference for measuring disaster resilience, Decis. Support Syst. 140 (2021), 113406, https://doi.org/10.1016/j.dss.2020.113406.
[36] Y. Almoghathawi, A.D. González, K. Barker, Exploring Recovery Strategies for Optimal Interdependent Infrastructure Network Resilience, Network. Spatial Econ. (2021), https://doi.org/10.1007/s11067-020-09515-4.
[37] A. Senkel, C. Bode, G. Schmitz, Quantification of the resilience of integrated energy systems using dynamic simulation, Reliab. Eng. Syst. Saf. 209 (2021), 107447, https://doi.org/10.1016/j.ress.2021.107447.
[38] P. Jamborsalamati, R. Garmabdari, J. Hossain, J. Lu, P. Dehghanian, Planning for resilience in power distribution networks: A multi-objective decision support, IET Smart Grid 5 (1) (2021) 45–60, https://doi.org/10.1049/stg2.12005.
[39] A. Najafi Tari, M. S. Sepasian, and M. Tourandaz Kenari, "Resilience assessment and improvement of distribution networks against extreme weather events," Int. J. Electr. Power Energy Syst., vol. 125, 2021, doi: 10.1016/j.ijepes.2020.106414.
[40] D. K. Mishra, M. J. Ghadi, A. Azizivahed, L. Li, and J. Zhang, "A review on resilience studies in active distribution systems," Renew. Sustain. Energy Rev., vol. 135, 2021, doi: 10.1016/j.rser.2020.110201.
[41] Y. Cheng, E.A. Elsayed, X. Chen, Random Multi Hazard Resilience Modeling of Engineered Systems and Critical Infrastructure, Reliab. Eng. Syst. Saf. 209 (2021), 107453, https://doi.org/10.1016/j.ress.2021.107453.
[42] T. Aziz, Z. Lin, M. Waseem, S. Liu, Review on optimization methodologies in transmission network reconfiguration of power systems for grid resilience, Int. Trans. Electr. Energy Syst. (2021) 1–38, https://doi.org/10.1002/2050-7038.12704.
[43] R. Cantelmi, G. Di Gravio, R. Patriarca, Reviewing Qualitative Research Approaches in the Context of Critical Infrastructure Resilience, Springer US, 2021, 0123456789.
[44] J. Johansson, H. Hassel, E. Zio, Reliability and vulnerability analyses of critical infrastructures: Comparing two approaches in the context of power systems, Reliab. Eng. Syst. Saf. 120 (2013) 27–38, https://doi.org/10.1016/j.ress.2013.02.027.
[45] Reliability Test System Task, The IEEE reliability test system -1996 a report prepared by the reliability test system task force of the application of probability methods subcommittee, IEEE Trans. Power Syst. 14 (3) (1999) 1010–1020, https://doi.org/10.1109/59.780914.
[46] A. Ali Kadhem, N.I. Abdul Wahab, I. Aris, J. Jasni, A.N. Abdalla, Computational techniques for assessing the reliability and sustainability of electrical power systems: A review, Renew. Sustain. Energy Rev. 80 (2017) 1175–1186, https://doi.org/10.1016/J.RSER.2017.05.276.
[47] P. Zhou, R.Y. Jin, L.W. Fan, Reliability and economic evaluation of power system with renewables: A review, Renew. Sustain. Energy Rev. 58 (2016) 537–547, https://doi.org/10.1016/J.RSER.2015.12.344.
[48] R. Billinton, W. Li, Reliability Assessment of Electric Power Systems Using Monte Carlo Methods, Springer US, Boston, MA, 1994.
[49] R. Billinton, R.N. Allan, Reliability Evaluation of Power Systems, Springer US, Boston, MA, 1996.
[50] W. Wangdee, Bulk Electric System Reliability Simulation and Application, 2005. December.
[51] R. Billinton, A. Sankarakrishnan, Comparison of Monte Carlo simulation techniques for composite power system reliability assessment, IEEE WESCANEX Commun. Power, Comput. 1 (95) (1995) 145–150, https://doi.org/10.1109/wescan.1995.493961.
[52] L. Zhang, et al., A data-driven approach to anomaly detection and vulnerability dynamic analysis for large-scale integrated energy systems, Energy Convers. Manag. 234 (2021), 113926, https://doi.org/10.1016/j.enconman.2021.113926.
[53] J. Beyza, H.F. Ruiz-Paredes, E. Garcia-Paricio, J.M. Yusta, Assessing the criticality of interdependent power and gas systems using complex networks and load flow techniques, Phys. A Stat. Mech. its Appl. 540 (2020), 123169, https://doi.org/10.1016/j.physa.2019.123169.
[54] S. Even, "Depth-First Search," Graph Algorithms, pp. 46–64, doi: 10.1017/CBO9781139015165.006.
[55] Z. Wu, Y. Liu, W. Gu, Y. Wang, C. Chen, Contingency-constrained robust transmission expansion planning under uncertainty, Int. J. Electr. Power Energy Syst. 101 (2018) 331–338, https://doi.org/10.1016/j.ijepes.2018.03.020.
[56] S. Kang, S. Yoon, Topological and Statistical Analysis for the High-Voltage Transmission Networks in the Korean Power Grid, vol. 42, 2017, pp. 923–931, 4.
[57] S. Kosai, J. Cravioto, Resilience of standalone hybrid renewable energy systems: The role of storage capacity, Energy 196 (2020), 117133, https://doi.org/10.1016/J.ENERGY.2020.117133.
[58] L. Xing, Cascading Failures in Internet of Things: Review and Perspectives on Reliability and Resilience, IEEE Internet Things J. 8 (1) (2021) 44–64, https://doi.org/10.1109/JIOT.2020.3018687.

energies

MDPI

Article

Integrated Risk Assessment for Robustness Evaluation and Resilience Optimisation of Power Systems after Cascading Failures

Jesus Beyza * and Jose M. Yusta

Department of Electrical Engineering, University of Zaragoza, Maria de Luna 3, 50018 Zaragoza, Spain; jmyusta@unizar.es
* Correspondence: jbeyza@unizar.es

Abstract: Power systems face failures, attacks and natural disasters on a daily basis, making robustness and resilience an important topic. In an electrical network, robustness is a network's ability to withstand and fully operate under the effects of failures, while resilience is the ability to rapidly recover from such disruptive events and adapt its structure to mitigate the impact of similar events in the future. This paper presents an integrated framework for jointly assessing these concepts using two complementary algorithms. The robustness model, which is based on a cascading failure algorithm, quantifies the degradation of the power network due to a cascading event, incorporating the circuit breaker protection mechanisms of the power lines. The resilience model is posed as a mixed-integer optimisation problem and uses the previous disintegration state to determine both the optimal dispatch and topology at each restoration stage. To demonstrate the applicability of the proposed framework, the IEEE 118-bus test network is used as a case study. Analyses of the impact of variations in both generation and load are provided for 10 simulation scenarios to illustrate different network operating conditions. The results indicate that a network's recovery could be related to the overload capacity of the power lines. In other words, a power system with high overload capacity can withstand higher operational stresses, which is related to increased robustness and a faster recovery process.

Keywords: cascading failures; power systems security; resilience; restoration; robustness

Citation: Beyza, J.; Yusta, J.M. Integrated Risk Assessment for Robustness Evaluation and Resilience Optimisation of Power Systems after Cascading Failures. *Energies* **2021**, *14*, 2028. https://doi.org/10.3390/en14072028

Academic Editor: Pietro Romano

Received: 5 March 2021
Accepted: 29 March 2021
Published: 6 April 2021

1. Introduction

Critical infrastructure systems are integral to the everyday activities of modern life. Among these systems, power transmission networks are responsible for reliably and safely meeting power demands at different points in a power system. In daily operation, these networks can experience attacks, failures, natural disasters, etc., all of which can severely degrade the entire function of the infrastructure [1]. The transmission system operator (TSO) must adjust the network topology to increase the power transfer capacity between different areas.

Figure 1 depicts the behaviour of the power system when it is subject to failures or natural disasters. In this figure, the variable t represents the transitions in time between the different phases and P(t) represents variations in the load over time. Note that the sequence consists mainly of five states. In the normal operation state ($t_0 \rightarrow t_{NO}$), the power grid is operating and satisfying the electrical demand safely (P_{NO}) before an unwanted event occurs. Disruption is the phase experienced by the infrastructure immediately after a failure or high-impact, low-probability (HILP) event occurs and is followed by severe degradation of network function ($t_{NO} \rightarrow t_D$). At this point, the load is only partially maintained (P_d). In the preparation stage ($t_D \rightarrow t_{FP}$), the TSO assesses the conditions of the infrastructure and determines which actions must be implemented during the recovery stage ($t_{FP} \rightarrow t_{FR}$). The process ends once the network returns to the load levels that were present before the disruptive event (P_{NO}). This final stage can take hours or even days.

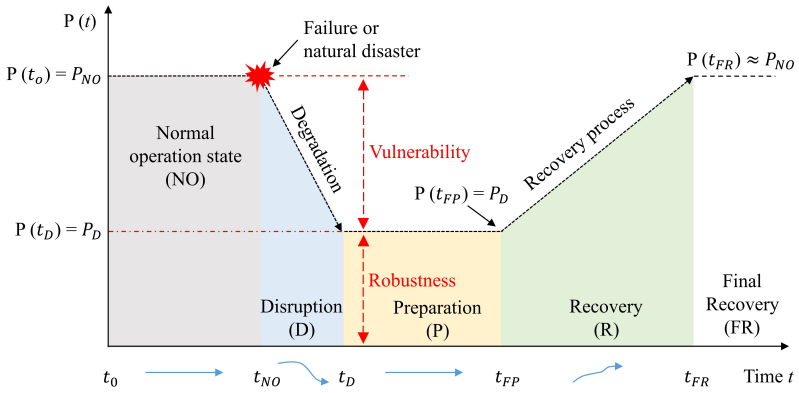

Figure 1. Power system behaviour during failures or natural disasters (representation adapted from [1,2]).

In the field of electrical engineering, robustness studies assess the performance of a network against the loss of multiple assets, while resilience studies analyse the ability of a system to rapidly recover from such disruptive events and adapt its operation and structure to prevent or mitigate the impact of similar events in the future [3,4]. Both concepts are important because they describe the performance of a power system during and after a disturbance or contingency.

Robustness assessment is the most appropriate tool to measure the performance of infrastructure during extreme events, quantify the structural performance of the entire network skeleton and identify the weakest buses that require significant reinforcement [5]. Resilience assessment is the most appropriate tool to analyse the capacity of the system to anticipate, absorb, adapt and recover from such events [6].

Resilience is a novel field of research that requires techniques to solve different problems associated with the protection and recovery of electrical infrastructure. Some researchers have assessed resilience by considering system topology, link switching capabilities and different human-made disaster scenarios [7]. Other researchers have proposed optimal design frameworks to improve resilience and protect the network against extreme weather events such as earthquakes, floods and ice storms [8,9].

Moreover, due to the increasing occurrence of outages and the growing interdependencies between networks, it is vital to understand the resilience of critical infrastructure systems. The most notable existing studies have presented improved approaches to measure resilience and have proposed better decision-making processes for recovery planning after a disruptive event [10–12]. These works have not only identified faster recovery but have also proposed mechanisms to improve the responsiveness of a network.

Other works have considered how renewable resources may be essential to improving the resilience of power systems. In this context, some academics have indicated that the performance of PV systems and hybrid systems composed of wind, PV and batteries can increase operational efficiency and improve reliability and resilience after a natural disaster [13–15].

Similarly, the increase in power outages due to climate deterioration has accelerated research in this area. Several researchers and decision-makers have indicated that more coordinated studies are needed to improve grid resilience and reliability [16]. Other scholars have suggested that optimal restoration strategies that incorporate resilience indicators are also required [17].

Fundamental changes in generation structure and profiles alongside increased demands for robustness and resilience have created the need for new operational and planning practices for modern networks. Cicilio et al. [18] reviewed research that explores the changing generation profile, cutting-edge practices to address resilience and the combination of both topics. Other scholars have offered integrated decision-making analyses

to characterise resilience, robustness, restoration agility and load criticality [19,20]. The objective of this existing work is to evaluate different infrastructure reconfiguration options and select the optimal solution for implementation in both cases.

Resilience also involves a process of detection, anticipation, learning and reconfiguration. In this context, some academics have proposed to reconfigure the power grid using economic model predictive control algorithms [21], deep learning and robust optimisation [22], data-driven batch-constrained reinforcement learning algorithms [23] and Markov decision process models [24].

Smart grid resilience is another relatively young field of research which has not yet been adequately defined. Plotnek and Slay [25] proposed guidelines to orient additional research in this area of study.

The authors of [26–31] provided a comprehensive classification of definitions, metrics, guidelines, practical challenges and technical and practical problems in power system resilience research.

After a contingency or cascading failure, the state of disintegration of the power system is a function of robustness, whereas resilience depends on robustness and the speed of the recovery of the lost load. Most works ignore the initial decay of system conditions, which could be composed of multiple islands and isolated assets. Therefore, new procedures should consider the extent of initial disintegration to improve the recovery process.

This paper postulates that the concepts of robustness and resilience should be integrated within a sequential decision framework to study the impact of disturbances on power systems in detail. Joint analysis of robustness and resilience studies can improve network structural performance, system planning, reliability and even security of supply. A contingency or event in a power network with low robustness can affect the restoration time of isolated assets. In such situations, resilience studies must consider the initial state of disintegration or decay of the infrastructure. The objective of this work is to demonstrate that disintegration plays an important role in the recovery process, as a large number of isolated assets makes it difficult to determine the optimal order in which to reconnect network assets.

Thus, the main purpose of this article is to propose an integrated framework to study both the robustness and resilience of an electrical power system. A system can function under normal operating conditions until one element is lost, triggering adverse effects such as cascading failures that impact a significant portion of the network. Actions are subsequently taken to recover the lost electricity demand in a coordinated manner both in the dispatch of generation and in the optimal reconfiguration of the infrastructure topology.

The robustness described in this work is conducted by running an iterative cascading failure procedure that involves initially removing a link, running direct current power flows, identifying and eliminating overloaded links, quantifying the number of islands and isolated elements and measuring whether demand is satisfied within the network with each iteration of decomposition. On the other hand, the resilience study is a mathematical optimisation problem that considers the optimal redispatch of generation and optimal reconfiguration of the topology. In real-world situations, the TSO makes recovery decisions in sequential time intervals (i.e., the TSO first plans the actions to be taken and, after their execution, analyses the outcome before proceeding to the next restoration steps). In this paper, this sequential decision-making process is improved by formulating it as an optimisation problem to always ensure the best set of redispatch and reconfiguration actions are selected throughout the entire infrastructure recovery process. This formulation should recover maximum demand in the shortest possible time.

However, the latter is a complex mathematical problem with multiple possible decisions at each restoration stage, as the number of possible actions grows exponentially with the number of iterations and has very high computational complexity. The aim of this work is to provide the first solution to this complex problem by developing a procedure to determine which power lines should be closed at each recovery stage. The set of lines identified should not cause overloads on operational links and should maximise the recovered

load on the network. This process would provide operators with complete information to make their decisions after a widespread collapse or blackout.

In short, the proposed sequential framework uses the robustness study to determine the initial state of disintegration of the network and uses this state information as input data for the resilience study. The resilience study is posed as a mixed-integer optimisation problem constructed from the direct current power flow equations, where the integer variables represent the operational state of the power lines (i.e., open or closed). In general terms, the proposed framework calculates optimal generation dispatches and determines the links to be closed for optimal recovery of the network topology. The latter process is limited by the maximum number of lines that can be operated in each iterative step. During the recovery process, active power flows on power lines are considered to avoid overloading other assets.

Notably, this proposal does not address the reactive power limits of the generators or the voltage magnitudes in each of the buses of the electrical network. Instead, the developed procedure could complement other work already published in the scientific literature.

The simulation framework runs on the well-known IEEE 118-bus test system, from which different simulation scenarios are built to demonstrate the scope of the proposed methodology [32]. This network was chosen because it is a sufficiently meshed system and can be applied to many studies with a reasonable solution time but is sufficiently detailed to reflect the real complexities of robustness and resilience studies. This system includes the main generation and transmission facilities, representing a simple and representative model of a real grid. The basic notion is to best illustrate some configurations that can be found in a disintegrated power system. Of course, the simulation framework can be applied and expanded to any other electrical power system.

The rest of the article is organised as follows. Section 2 describes the cascading failure model for determining the initial disintegration state of a power grid. Section 3 details the mathematical model of power system restoration based on a mixed-integer optimisation problem. Section 4 describes the case study and presents the simulation results obtained after applying the two procedures described in the previous sections. Finally, Section 5 draws the main conclusions of this paper and presents some future research directions.

2. Degradation of the Power System

This section presents the procedure developed to assess the robustness of a power system. A cascading failure model, which incorporates models of the protection mechanisms for power lines, is combined with a graph traversal algorithm. The proposed framework accurately captures the state of infrastructure degradation resulting from a failure or HILP event.

Robustness is an internal characteristic of power grids that measures the a system's ability to withstand the effects of faults [33] and is often quantified in terms of the largest connected component, both before and after cascading events [34]. A cascading failure is a sequence of events that begins with one or more disturbances, causing a series of outages in other network components [35]. Cascading can be initiated by multiple factors, such as voltage and frequency instabilities, malfunctioning control devices, human errors, line overloads or deliberate attacks.

To determine the impact of cascading failures, the performance of the network is measured as a function of the connected load after several outages. Here, the satisfied demand (SD) index is used [36,37], and a cascading failure simulation algorithm is proposed.

2.1. Basis of the Cascading Interruption Modelling

The power system can be represented as a graph composed of nodes and links, where the former represent buses, generators and loads, while the latter represent transformers and electric transmission lines (see Figure 2a).

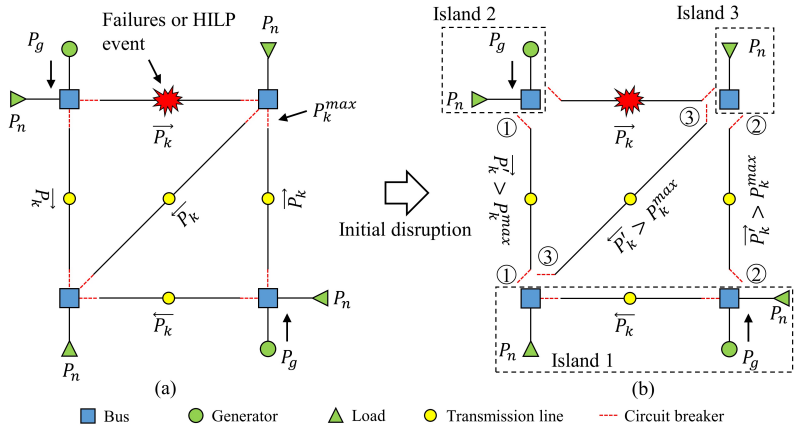

Figure 2. Initial interruption. Operation of power line circuit breakers: (**a**) initial state; and (**b**) first interruption state.

Power flows are a function of Kirchhoff's laws, where the physical parameters of the lines and the voltages and angles of the buses determine the flows within the infrastructure. In this manuscript, the direct current power flow (DCPF) equations are used for simulation purposes [38].

The maximum power transfer capacity (P_k^{max}) of the lines is generally determined using stability constraints, voltage drops and thermal effects. This document assumes that the maximum flow is related to the initial power flow (P_k), as shown in (1), where $\alpha_k > 1$.

$$P_k^{max} = \alpha_k \cdot P_k \qquad \forall k \in K \tag{1}$$

Equation (1) models the protection mechanisms of the power lines by introducing a tolerance parameter, α_k. A circuit breaker generally trips when the power flow on the line exceeds an overload threshold. Circuit breakers are assumed to operate when $P_k > P_k^{max}$. Note that the overload tolerance parameter in (1) is defined so that the MVA rating for a power line is not violated.

Cascading failure propagation can lead to the formation of multiple islands, as shown in Figure 2b. In these situations, the load flow problem may not converge, so it is necessary to incorporate a graph traversal algorithm to identify subsets formed in the decomposition stage. The depth-first search (DFS) algorithm is used to solve this problem [39]. This algorithm identifies and sorts the islands each time one or more power lines are disconnected.

2.2. Cascading Failure Algorithm

Algorithm 1, also depicted in the flowchart in Figure 3, defines the proposed procedure for evaluating the disruption stage using the simulation assumptions presented above.

The iterative procedure starts by calculating the power flows and determining the maximum power transfer capacity of the lines with (1). The most loaded power line is then disconnected due to an HILP event, the changes in P_k are determined and the constraint $|P_k| < P_k^{max}$ $\forall k \in K$ is verified. If this constraint is not met, the circuit breakers are tripped according to the scheme in Figure 2, and the DFS algorithm immediately monitors the formation of the islands. This technique is used because it is a method for scanning a finite, undirected graph and is widely recognised as a powerful technique for solving various graph problems. The algorithm starts at a root node and scans along each branch before backtracking [39].

Algorithm 1: Disruption stage. Cascading failures.

Input: Technical data of the electrical network and α
Output: Degradation of the power grid. Set of islands I, state of branches μ_k, set of isolated elements E, and satisfied demand SD_s
Step 1. *Initialisation*: $E = \emptyset$ and $SD_{base} = \sum_{d \in D} d$;
Step 2. *Power flows*: calculate $P_k^s \in K$ for all power lines of the infrastructure in stage s; determine P_k^{max} with (1);
Step 3. *Starting point*: eliminate the most loaded power line, k'; set $\mu_k' = 0$;
Step 4. *Calculate power flows*: determine the increases or decreases in each P_k^s $\forall K$, using DC power flows; set $s = 1$ for the first step;
Step 5. *Trigger mechanisms for circuit breakers*: evaluate the condition $|P_k^s| < P_k^{max}$ $\forall K$. If the condition is not met, set $\mu_k^s = 0$ for the triggered power lines k and go to Step 6; otherwise, go to Step 10;
Step 6. *Graph traversal algorithm*: use DFS to determine islands $I = \{I_1, I_2, \ldots, I_N\}$ and isolated elements E;
Step 7. *Energy balance*:
(a) for each island I_i with generators, $g \in I_i$, evaluate
- if $\sum_{g \in I_i} P_g < \sum_{d \in I_i} P_d$, set $D_{I_i}^s = \sum_{g \in I_i} P_g$ in stage s;
- if $\sum_{g \in I_i} P_g > \sum_{d \in I_i} P_d$, set $D_{I_i}^s = \sum_{d \in I_i} P_d$ in stage s;

(b) for each island I_i without generators, $g \in I_i$; set $D_i^s = 0$ and $E_i = M_i$;
Step 8. *Satisfied demand*: Calculate $SD_s = \frac{\sum_{i \in I} D_{I_i}^s}{SD_{base}}$ for iteration s;
Step 9. *Iterations*: set $s = s + 1$ and go to Step 4;
Step 10. *Termination*: if $|P_k^s| < P_k^{max}$ $\forall k$ or $E = M$, the algorithm ends.

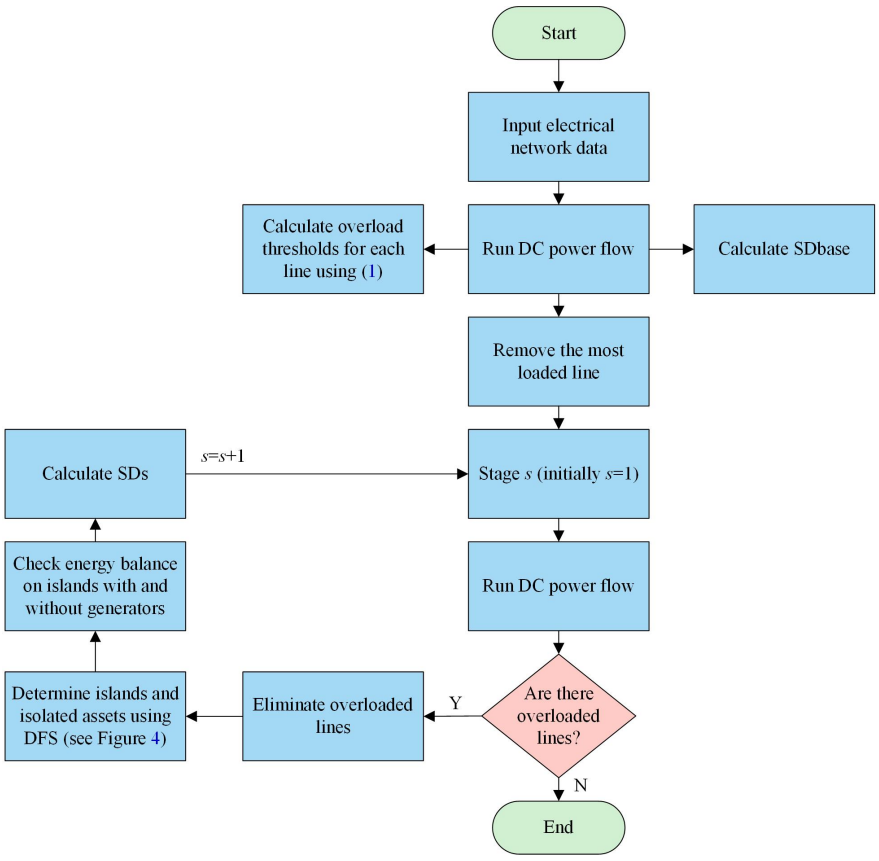

Figure 3. Flowchart of Algorithm 1.

Figure 4 presents the tree structure of the cascading failure process used in Algorithm 1. Here, islands without generation are considered dead and are marked in red, while islands

with generation are marked in green. All intermediate islands where cascading failures continue are marked in blue. The tree structure demonstrates how an island can undergo changes during the cascading failure process (*s*) and disintegrate into several islands, some of which remain operational, and others of which are deeply affected by the disintegration. The cascading failure continues and is repeated on all the intermediate islands marked in blue. The redistribution of the power flows may cause additional overloads on other power lines in the network. Consequently, each intermediate island may result in the formation of different islands, so the procedure continues simultaneously on these new islands.

The SD index used in Algorithm 1 measures the robustness of the power grid by quantifying the SD at each stage of network disintegration. This measure varies between 0 and 1; therefore, as the SD indicator decreases, so does the robustness of the infrastructure.

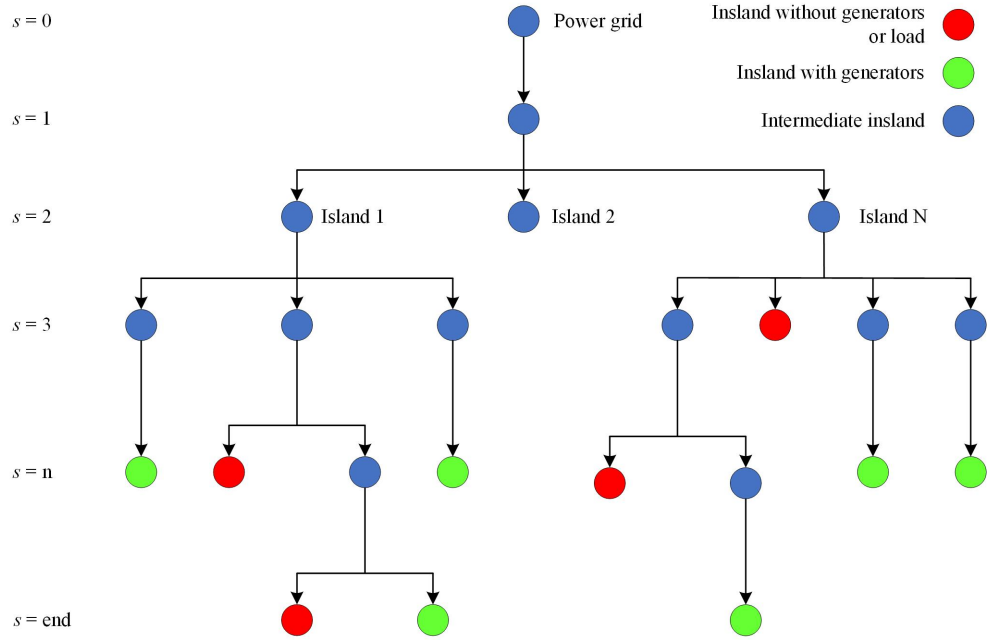

Figure 4. A tree structure of the cascading failure process.

3. Recovery of the Power System

Power system restoration is a highly complex tasks, as the TSO must be prepared with a restoration plan that enables fast and safe recovery of the system. Moreover, the TSO must carefully attend to the energy balance, active and reactive power control, voltage condition and power system stability [40].

Section 3 presents the proposed methodology for recovering a disintegrated electrical network composed of multiple islands and isolated assets. The developed algorithm is based on mixed-integer linear programming and uses the DCPF equations. Here, voltage magnitudes and standing phase angles may not be a major concern, so DCPF studies provide sufficient accuracy in the results, as indicated in [41].

DC Power Flows with Line Drive Incorporation

DCPF is an estimate of power flows in AC power systems. DCPF only considers active power flows and neglects reactive power flows. This method is convergent and non-iterative and is used whenever fast estimates of power flows are required [38]. This formulation is used and power line switching is also incorporated.

The proposed mixed-integer optimisation problem maximises the recovered satisfied demand ($SD_s - SD_{s-1}$) at each step *s*, as shown in Equation (2), by dispatching generation units and reconnecting power lines.

For each step *s*:

$$max\ (SD_s - SD_{s-1}) \quad (2)$$

subject to:

$$P_g^{min} \leq P_g^s \leq P_g^{max} \quad \forall g \in G \tag{3}$$

$$P_k^{min} \cdot \mu_k^s \leq P_k^s \leq P_k^{max} \cdot \mu_k^s \quad \forall k \in K \tag{4}$$

$$\Delta_n^{min} \leq \Delta_n^s \leq \Delta_n^{max} \quad \forall n \tag{5}$$

$$-\sum_{k \in K} P_k^s - \sum_{g \in G} P_g^s - \sum_{d \in D} P_d^s = 0 \quad \forall n \tag{6}$$

$$B_k \cdot (\Delta_n^s - \Delta_m^s) - P_k^s \geq 0 \quad \forall k \tag{7}$$

$$-B_k \cdot (\Delta_n^s - \Delta_m^s) - P_k^s \leq 0 \quad \forall k \tag{8}$$

$$\sum_{k \in K} \mu_k^s \leq N_c \tag{9}$$

$$SD_s = \sum P_n^s \quad \forall n \tag{10}$$

In this formulation, power lines have binary variables μ_k, which represent the switching states of the links (open, $\mu_k = 0$, and closed, $\mu_k = 1$). Moreover, Constraint (9) is included to limit the maximum number of lines to be closed in each recovery iteration.

Constraint (3) limits the power produced by the generators between their maximum and minimum limits; Constraint (4) controls the power passing through the links; Constraint (5) determines the angles of each bus; Constraint (6) incorporates the nodal balance equations; and Constraints (7) and (8) include the Kirchhoff's laws. Finally, Constraint (9) determines the lines operated in each iterative step, as identified by the binary variable $\mu_k^s = \{0, 1\} \forall k \in K$. There is no industry consensus on the maximum number of lines that can be switched during each stage of power grid restoration, as the latter depends on the physical characteristics of the infrastructure and the procedures applied by each control centre.

The output of the optimisation problem consists of the recovered satisfied demand ($SD_s - SD_{s-1}$), the energy produced by the generators (P_g) and the switching states of the power lines (μ_k) for each restoration stage s.

Algorithm 2 describes the iterative procedure for determining power system recovery. This algorithm uses the output of Algorithm 1 as its input. Figure 5 presents the flowchart of Algorithm 2.

Algorithm 2: Recovery process. Mixed-integer optimisation problem.

Input: the output of Algorithm 1 (set of islands I, state of branches μ_k, set of isolated elements E and remaining satisfied demand $SD_{remaining}$) and the number of lines to be reconnected N_c in each step s.
Output: SD_s and μ_k^s $\forall k$ in each recovery step s
Step 1. *Inicialisation*: set $SD_s = SD_{remaining}$;
Step 2. *Build the problem*: set the minimum and maximum parameters of the constraints (3)–(5). The thresholds of (4) are initially determined in Algorithm 1;
Step 3. *Solve the mixed-integer optimisation problem*: maximise (2), subject to the constraints in (3)–(10);
Step 4. *Solution*: save the results of SD_s and μ_k^s; set the restored variables μ_k^s as constants μ_k^s=1 for all subsequent stages;
Step 5. *Evaluation*: if $\forall k \in (K - k')$: $\mu_k^s = 1$ and go to Step 7; otherwise, go to Step 6;
Step 6. *Iterations*: set $s = s + 1$ and go to Step 3;
Step 7. *Termination*: if $\forall k \in (K - k')$ and $\mu_k^s = 1$; the algorithm ends.

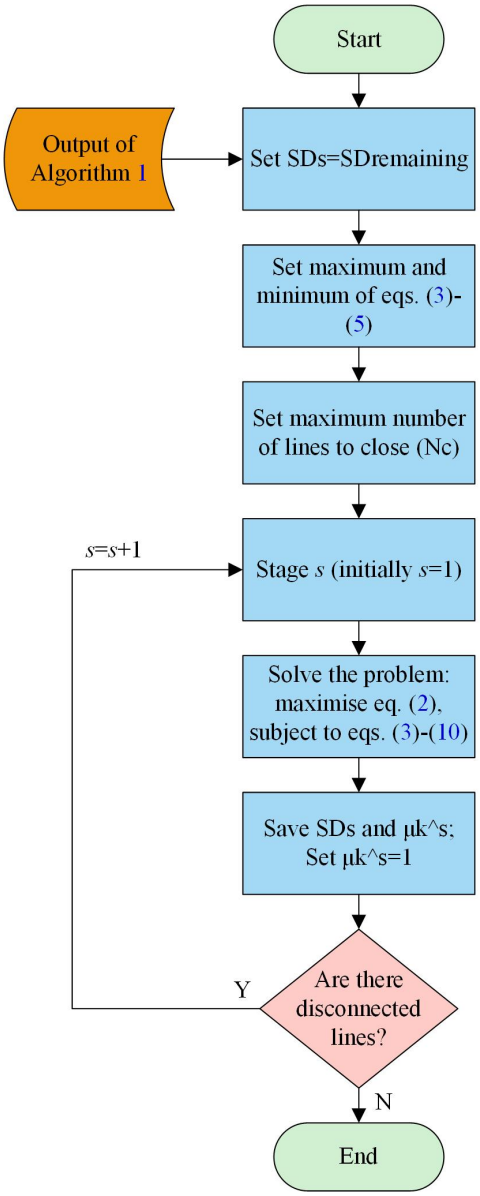

Figure 5. Flowchart of Algorithm 2.

4. Simulation and Results

The simulation results obtained after applying the two developed algorithms to the well-known IEEE 118-bus test network are presented below. Here, costs of generators were not considered, line resistances were ignored and power losses were neglected. Both algorithms were programmed and executed on the MATLAB platform, using a personal computer with an Intel® Core^{TM} i7 3.40 GHz CPU and 32 GB of RAM.

4.1. Normal Operation State: IEEE 118-Bus Test System

This IEEE 118-bus test case represents a simple approximation of the American Electric Power system (in the U.S. Midwest) and contains 54 generators, 186 lines, 14 capacitors and 99 loads. The technical data of the system can be found in [32].

In the normal operation state, the system safely satisfies a load of 4242 MW, and the coupled generators can produce up to 9721 MW. A parameter α = 1.5 is applied such that the maximum capacity of the lines is 1.5 times the base flow; therefore, the lines operate at about 70% of their capacity. Moreover, the Δ_n^{min} and Δ_n^{max} for the angles are limited to between -0.6 and -0.6 radians. The P_g^{min} and P_g^{max} for the generators can be found in [38]. Figure 6 depicts this system condition (State A).

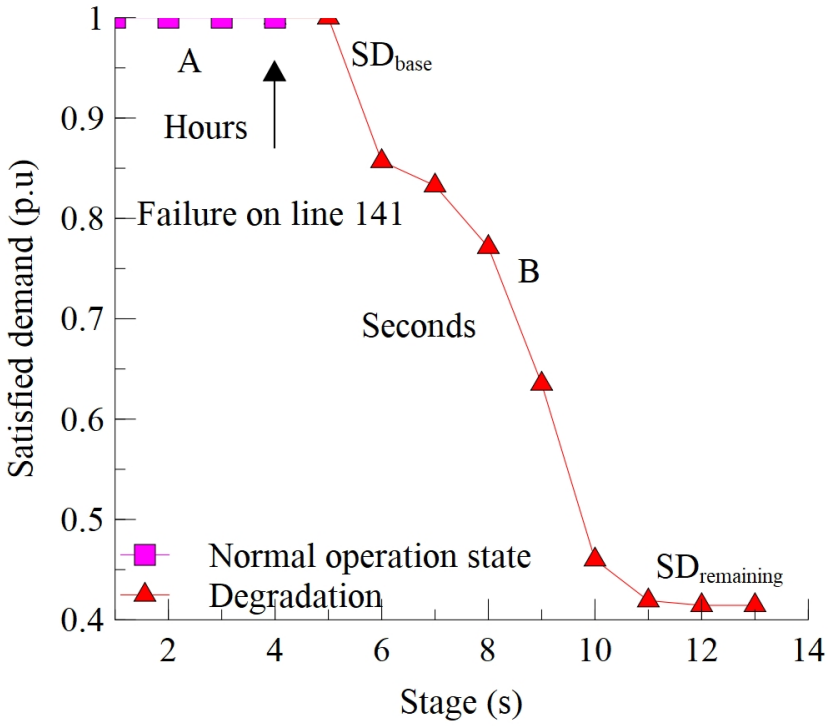

Figure 6. Degradation of the IEEE 118-bus test network. Results obtained using Algorithm 1.

4.2. Disruption State: Degradation of the Power System

Figure 6 plots the degradation of the studied network (State B) due to the non-trivial loss of line 141 (89–92) at stage $s = 4$ ($k' = 141$ and $\mu_{141}{}' = 0$). As this line was the most loaded line, it was assumed that an HILP event occurred there. The plotted results were obtained after applying Algorithm 1, as described in Section 2.2. The computational time for Algorithm 1 was 0.12 min.

The curve represents the satisfied demand as a function of the cascading stages s. When all assets were initially connected, the SD index had a value of 1. Subsequently, the SD index gradually decreased to a value of 0 as the power system disintegrated due to circuit breakers operations. At this point, the infrastructure may have been composed of islands with and without generation and isolated assets.

The results indicate that the IEEE 118-bus test network reached its maximum degradation point at stage $s = 13$, at which point approximately 40% of the load remained connected. Likewise, the damage caused by the loss of link 141 caused the system to disintegrate into 15 islands. Here, four islands had a load of 1092 MW. In parallel, these four islands had a load shedding of 196 MW to satisfy the conditions of balance between generation and load (666 MW). Similarly, seven islands with a load of 1000 MW were inoperative, and 71 lines were open due to overloading. There were 44 isolated buses with a total load of 1288 MW. Figure 7 presents the topology of the IEEE 118-bus test network and the various islands in the system.

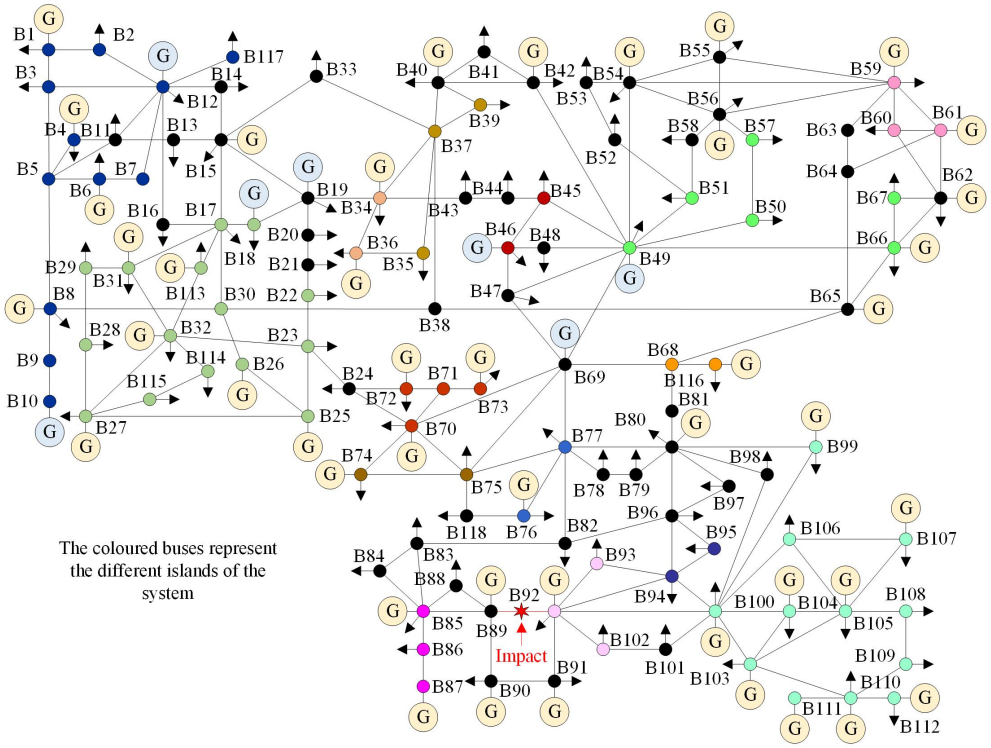

Figure 7. Schematic representation of the power system under study after the cascading failures took place.

The above results were obtained by applying a tolerance parameter $\alpha = 1.5$. Depending on this value, different degradation states of the electrical network can be obtained due to line overloads. For example, Figure 8 presents the final SD for different values of alpha between $\alpha = 1$ and $\alpha = 2$. Note that, as the overload parameter α increases, the satisfied demand also increases. Thus, the recovery process is related to the overload capacity of the power lines, as infrastructure with high overload capability can withstand higher operational efforts, which is related to less degradation and, consequently, to a faster recovery process.

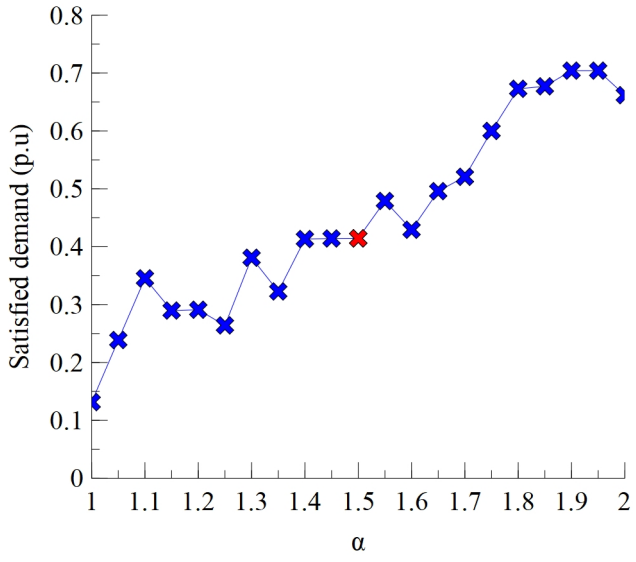

Figure 8. Overload tolerance parameter.

On the contrary, an electrical infrastructure with low overload capability achieves lower SD percentages at the end of the degradation process, which is related to a slower recovery process. A tolerance parameter α = 1.5 was chosen in this paper because it is an acceptable intermediate value for the case studies, as indicated in Figure 8.

4.3. Preparation State

In this phase, the TSO analyses the state of the network after the cascading failure and prepares the necessary actions or manoeuvres to quickly and safely recover the load and reconnect the isolated assets.

In the engineering field, the TSO could prioritise the reconnection of some loads or some generators or utilise all infrastructure facilities [42–45]. Certain assets may not be available if they have suffered irreversible damage. The TSO carefully evaluates and uses all available resources to quickly restore the network.

In this case study, the disintegrated power grid consisted of 15 islands, 71 open lines, 44 isolated buses and a disconnected load of more than 2000 MW. Three stages were considered to plan recovery actions (s = 14 to s = 16).

4.4. Recovery Process

The aim of the recovery process is to develop a methodology to restore the operating conditions of the electrical infrastructure after a major disruption. This recovery must comply with several security parameters to avoid further line outages. Algorithm 2 can be applied to determine the optimal recovery of the network under study.

To obtain different recovery plans, the maximum number of lines N_c to be closed at each restoration stage is limited. In this case, values of N_c = 1, 3, 5 and 7 were considered. One or seven lines were closed for simulation purposes only; closing three or five lines corresponds to the usual number of safe manoeuvres performed by the TSO. Moreover, line 89–92 could not be reconnected during the recovery process because it was badly damaged.

Figure 9 displays the recovery curves for the different plans obtained using Algorithm 2. Unlike Figure 6, in this case, higher SD values indicate a greater recovered load.

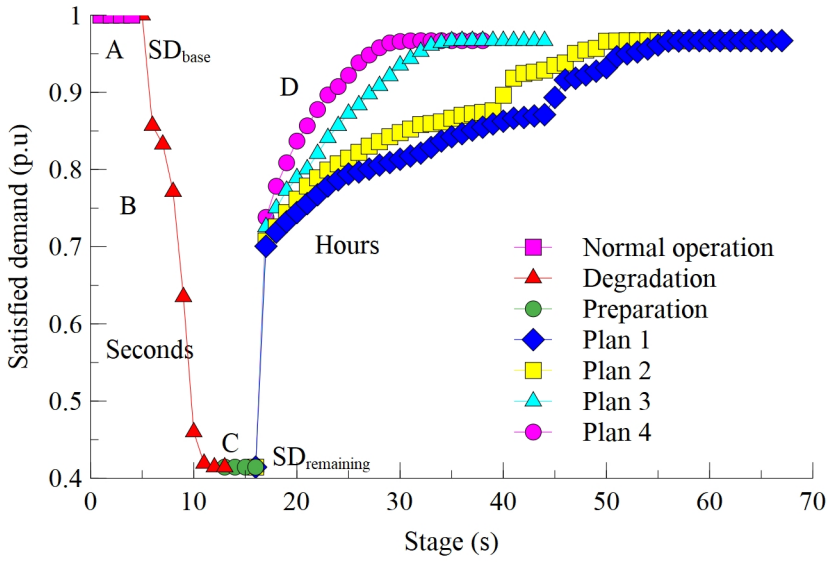

Figure 9. Recovery curves for the IEEE 118-bus test system.

The developed methodology found the optimal solution at each stage to recover the disconnected loads and reconnect the islands and isolated buses. The plans restored the operational network conditions fairly quickly. In the proposed system, manoeuvres are managed in minutes, so the actions that could be taken during this simulation were limited. For example, only one line was reconnected, and the corresponding generation redispatch

was performed with N_c = 1. The next action was then executed, and the procedure was repeated. However, recovery would be faster if more manoeuvres could be performed at each interval.

Table 1 reports the different recovery plans according to the number of lines reconnected in each iteration. For illustration purposes, only the lines corresponding to the first recovery iteration are shown (i.e., s = 17). The values of recovered load, satisfied demand and computation times are included for each plan.

Table 1. Optimal recovery plans obtained using Algorithm 2 in stage s = 17.

Plan	Number of Lines to Be Closed (N_c)	Closed Lines (L)	Recovered Load (MW)	Satisfied Demand (SD_s)	Computation Times (min)
State C				0.414	
1	1	18	1214	0.701	7.357
2	3	18, 63, 80	1243	0.707	37.085
3	5	16, 18, 63, 64, 80	1320	0.726	67.619
4	7	16, 18, 63, 64, 80, 91, 114	1373	0.738	71.649

The first manoeuvre resulted in values of satisfied demand that were similar across the different recovery plans. However, the topological configuration was not the same in each case; therefore, generation redispatch influenced the recovery of isolated loads. Additionally, the calculation time increased with the number of lines to be reconnected because more combinations had to be considered to find the optimal solution.

Recovery was slow when a power line was reconnected (Plan 1), but the system quickly recovered the load and the meshed structure of the network when three power lines were reconnected (Plan 2).

The outcomes of Plans 3 and 4 were almost similar, as were the outcomes of Plans 1 and 2. However, Plans 3 and 4, which involved the reconnection of five and seven lines, respectively, offered better results than Plans 1 and 2. Some topological configurations are evidently better for network meshing since line constraints influence the recovered load. For example, as shown in Figure 9, if the TSO were to follow Plan 3 in the order indicated, 29 stages would be sufficient to recover almost 100% of the load and bring all lines into operation. However, if Plan 1 or 2 was followed, approximately 50 stages would be required.

Table 2 presents the Energy Not Supplied (ENS) results for each recovery plan. The ENS metric is quantified by measuring the area above the recovery curves and considering time intervals of 15 min for each stage s and 20 h of repair time for line 89–92. As the ENS decreases, the recovery plan becomes more efficient. Considering these times and the number of stages, an average time to restore the infrastructure can be obtained. For example, Plan 4 required 23 stages, that is, 5.75 h plus an additional 20 h to repair power line 89–92. In contrast, the proposed study framework obtained the complete solution in approximately 1.2 h (Table 1), so each set of lines computed per iteration required about three minutes. The results can therefore be obtained in parallel to the execution of the corresponding manoeuvres, with an additional 12-min reserve. Of course, other factors that could influence the speed of the recovery of the power system must be considered; however, the times between switching, redispatching and repairing the damaged line correspond to values close to reality. In short, the proposed procedure determined the required manoeuvres before their execution. The TSO could consequently analyse the results and determine the most appropriate and accurate actions, which would guarantee the highest load recovery and the best-operating conditions of the system.

Table 2. Energy Not Supplied for each recovery plan.

Plan	Number of Stages s	Energy not Supplied (MWh)
Base network		0
1	52	135.65
2	49	114.56
3	29	77.06
4	23	63.71

4.5. Variations in Generation and Load

To test the usefulness of the developed algorithms under various generation and load conditions, 10 simulation scenarios were additionally applied, using $\alpha = 1.5$ and $N_c = 5$ as parameters during each recovery stage. Five lines were chosen for this analysis (Plan 3) because five lines is a safer switching number than seven lines (Plan 4) for the considered time interval of 15 min.

Table 3 summarises each of the scenarios studied in this analysis. In the case of generation variation, Scenario G_{89} evaluated the system's degradation and recovery without Generator 89. Scenario G_{89+80} corresponds to the same system, but without Generators 89 and 80. The rest of the scenarios followed the same scheme as above, eliminating the generators with the highest capabilities in descending order. Meanwhile, in the case of load variation, Scenario $L_{+5\%}$ evaluated the system's degradation and recovery with a 5% load increase, while Scenario $L_{+10\%}$ evaluated the system's performance with a 10% load increase. This process was repeated successively for subsequent scenarios until the load increased reached 25%.

Table 3. Study scenarios.

Variation	Scenarios
Generation	$G_{89} \rightarrow G_{89+80} \rightarrow G_{89+80+69} \rightarrow G_{89+80+69+10} \rightarrow G_{89+80+69+10+66}$
Load	$L_{+5\%} \rightarrow L_{+10\%} \rightarrow L_{+15\%} \rightarrow L_{+20\%} \rightarrow L_{+25\%}$

Figure 10 indicates that the base case maintained a satisfied demand of more than 40% after the cascading event. In the rest of the cases analysed with variations in generation and load, the networks collapsed more significantly. The 10 scenarios studied had worse performance than the base case, as the curves always went below in both degradation and recovery. These scenarios show that the IEEE 118-bus test system in its base case is more robust than when it has less generation or more load.

Similar robustness values were obtained in the generation and load scenarios. For example, the satisfied demand after the system degradation process was close to 20% for both the lowest generation scenario ($G_{89+80+69+10+66}$) and the highest load scenario ($L_{+25\%}$).

The curves in Figures 9 and 10 demonstrate that the developed study framework provides optimal recovery strategies for collapsed networks composed of multiple islands and isolated elements. The results also indicate that generation availability conditions could severely affect cascading failures propagation and electrical network recovery.

The conducted simulations demonstrate that the developed procedures can be applied to different operating conditions and disintegration states of power systems. Although the procedures are applied to scenarios of variation in generation and demand, the robustness and resilience models could be combined with other proposals to extend the results presented here.

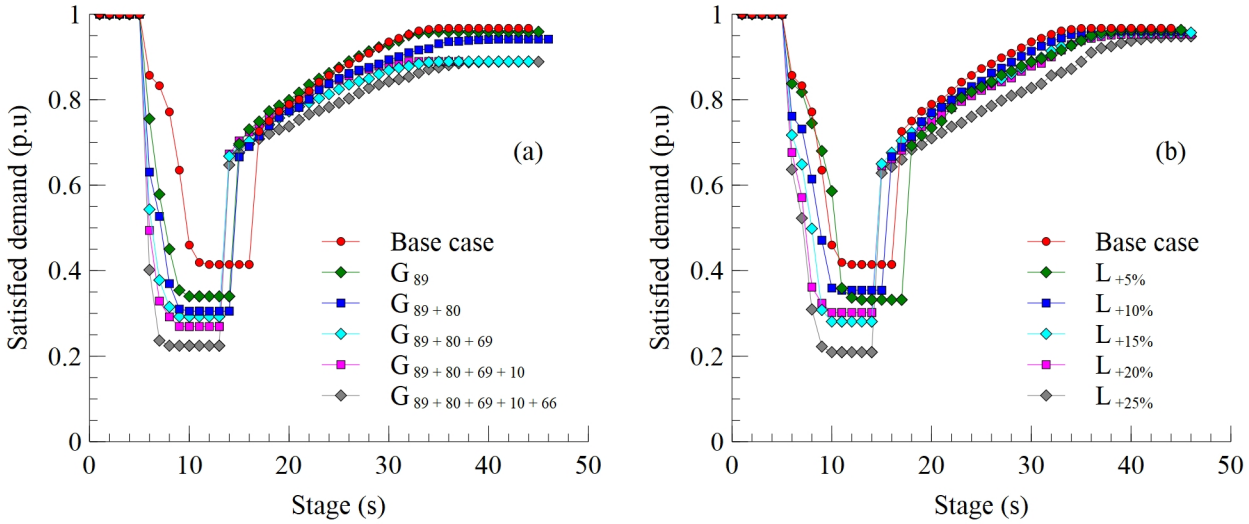

Figure 10. Process of disintegration and recovery of the IEEE-118 bus test system with variations in: (**a**) generation; and (**b**) load.

5. Conclusions

This paper proposes a joint framework for assessing both the robustness and resilience of electric power systems. A cascading failure procedure id used to determine the state of disintegration of a power grid and a mixed-integer optimisation problem id applied to identify the optimal dispatch and topology during the network recovery process. The cascading failure procedure considers the dynamic disintegration of the infrastructure due to the tripping of the circuit breakers of the power lines. The restoration procedure determines the level of generation and the power lines to be closed or opened at each stage of system recovery. In both cases, the satisfied demand index is measured to quantify the power supply within the infrastructure.

The effectiveness and applicability of the proposed framework, which aims to quantify robustness and resilience, was verified using the IEEE 118-bus test system. This paper provides a detailed discussion of the numerical results, demonstrating the efficacy of the proposed procedures and their benefit to end-users and utilities. The TSO could apply different strategies or plans to recover a disconnected load after a high impact event, depending on the switching actions taken.

Renewable energies are becoming increasingly important in the current energy transition scenario of power systems. This considerable increase in renewable generation could affect the performance of a network in the case of a high-impact, low-probability event. Thus, future research and development efforts should explore computationally efficient mathematical methodologies to assess the robustness and resilience of power systems with a high share of renewable energy. The random nature of renewable energies necessitates stochastic models to analyse different operating conditions of a power grid. The resulting models should integrate both indicators and provide solutions for transmission system planners and operators.

Author Contributions: Methodology, J.B. and J.M.Y.; investigation, J.B. and J.M.Y.; validation, J.B. and J.M.Y.; writing—original draft preparation, J.B.; and writing—review and editing, J.B. and J.M.Y. All authors have read and agreed to the published version of the manuscript.

Funding: This research was funded by Ministry of Science and Innovation, Spain, under project PID2019-104711RB-100: Smart-grid design and operation under the threat of interrupted supply from electric power transmission systems with a high penetration of renewable energies.

Institutional Review Board Statement: Not applicable.

Informed Consent Statement: Not applicable.

Data Availability Statement: Not applicable.

Acknowledgments: The authors would like to thank Carlos Alcaine-Baquedano, Department of Global Infrastructure Networks, ENEL, for helpful discussions on this and related topics.

Conflicts of Interest: The authors declare no conflict of interest.

Abbreviations

The following abbreviations are used in this manuscript:

Indices

n,m	Nodes or buses
k	Lines
g	Generators
d	Loads
j	Number of closed power lines
i	Islands
s	Steps

Variables

Δ_n	Voltage angle at node n (radians)
P_k, P_g, P_n	Power flow through line k, generator g, and power demand at node n
μ_k	Binary variable indicating the open or closed state of the power line (open, $\mu_k = 0$, closed, $\mu_k = 1$)
D_i	Demand on each island i
SD_s	Satisfied demand in step s (MW)

Parameters

P_k^{max}, P_k^{min}	Maximum and minimum capacity of the power line k (MW)
P_g^{max}, P_g^{min}	Maximum and minimum capacity of the generator g (MW)
Δ_n^{max}, Δ_n^{min}	Maximum and minimum voltage angle at node n (radians)
B_k	Susceptance of the power line k
N_c	Maximum number of power lines to be closed at each step s
α_k	Overload tolerance parameter of the power line k

Sets

D	System loads
E	Isolated assets
G	Generators
I	Islands
K	Power lines
L	Closed power lines
M	Nodes or buses

References

1. Jamborsalamati, P.; Moghimi, M.; Hossain, M.; Taghizadeh, S.; Lu, J.; Konstantinou, G. A framework for evaluation of power grid resilience case study: 2016 South Australian blackout. In Proceedings of the 2018 IEEE International Conference on Environment and Electrical Engineering and 2018 IEEE Industrial and Commercial Power Systems Europe (EEEIC/I&CPS Europe), Palermo, Italy, 12–15 June 2018; pp. 1–6.
2. Dehghanian, P.; Aslan, S.; Dehghanian, P. Maintaining electric system safety through an enhanced network resilience. *IEEE Trans. Ind. Appl.* **2018**, *54*, 4927–4937. [CrossRef]
3. Chen, Q.; McCalley, J.D. Identifying high risk Nk contingencies for online security assessment. *IEEE Trans. Power Syst.* **2005**, *20*, 823–834. [CrossRef]
4. Noebels, M.; Preece, R.; Panteli, M. AC Cascading Failure Model for Resilience Analysis in Power Networks. *IEEE Syst. J.* **2020**, 1–12. [CrossRef]
5. Sabouhi, H.; Doroudi, A.; Fotuhi-Firuzabad, M.; Bashiri, M. A novel matrix based systematic approach for vulnerability assessment. *COMPEL Int. J. Comput. Math. Electr. Electron. Eng.* **2020**, *40*, 1–17. [CrossRef]

6. Stankovic, A. *The Definition and Quantification of Resilience*; IEEE PES Industry Technical Support Task Force: Piscataway, NJ, USA, 2018; pp. 1–4.
7. Tapia, T.; Lorca, Á.; Olivares, D.; Negrete-Pincetic, M.; Lamadrid L, A.J. A Robust Decision-Support Method Based on Optimization and Simulation for Wildfire Resilience in Highly Renewable Power Systems. *Eur. J. Oper. Res.* **2021**, 1–11. [CrossRef]
8. Shahbazi, A.; Aghaei, J.; Pirouzi, S.; Niknam, T.; Shafie-khah, M.; Catal ao, J.P. Effects of resilience-oriented design on distribution networks operation planning. *Electr. Power Syst. Res.* **2021**, *191*, 106902. [CrossRef]
9. Zhao, N.; Yu, X.; Hou, K.; Liu, X.; Mu, Y.; Jia, H.; Wang, H.; Wang, H. Full-time scale resilience enhancement framework for power transmission system under ice disasters. *Int. J. Electr. Power Energy Syst.* **2021**, *126*, 106609. [CrossRef]
10. Zobel, C.W.; MacKenzie, C.A.; Baghersad, M.; Li, Y. Establishing a frame of reference for measuring disaster resilience. *Decis. Support Syst.* **2021**, *140*, 113406. [CrossRef]
11. Almoghathawi, Y.; González, A.D.; Barker, K. Exploring Recovery Strategies for Optimal Interdependent Infrastructure Network Resilience. *Netw. Spat. Econ.* **2021**, *21*, 229–260. [CrossRef]
12. Senkel, A.; Bode, C.; Schmitz, G. Quantification of the resilience of integrated energy systems using dynamic simulation. *Reliab. Eng. Syst. Saf.* **2021**, *209*, 107447. [CrossRef]
13. Bai, X.; Liang, L.; Zhu, X. Improved Markov-chain-based ultra-short-term PV forecasting method for enhancing power system resilience. *J. Eng.* **2021**, *2021*, 114–124. [CrossRef]
14. Tawfiq, A.A.; Osama abed el Raouf, M.; Mosaad, M.I.; El-Gawad, A.A.; Farahat, M.A. Optimal reliability study of grid-connected PV systems using Evolutionary Computing Techniques. *IEEE Access* **2021**, *9*, 42125–42139. [CrossRef]
15. Samy, M.M.; Mosaad, M.I.; El-Naggar, M.F.; Barakat, S. Reliability Support of Undependable Grid Using Green Energy Systems: Economic Study. *IEEE Access* **2020**, *9*, 14528–14539. [CrossRef]
16. Hossain, E.; Roy, S.; Mohammad, N.; Nawar, N.; Dipta, D.R. Metrics and enhancement strategies for grid resilience and reliability during natural disasters. *Appl. Energy* **2021**, *290*, 116709. [CrossRef]
17. Yu, Z.; Li, Z.; Qian, T.; Huang, K.; Chen, X.; Tang, W. Optimal Restoration Strategy Based on Resilience Improvement for Power Transmission Systems Under Extreme Weather Events. In Proceedings of the 2020 International Conference on Smart Grid and Energy Engineering, Guilin, China, 13–15 November 2021; IOP Publishing: Bristol, UK, 2021, Volume 645, pp. 1–8.
18. Cicilio, P.; Glennon, D.; Mate, A.; Barnes, A.; Chalishazar, V.; Cotilla-Sanchez, E.; Vaagensmith, B.; Gentle, J.; Rieger, C.; Wies, R.; et al. Resilience in an Evolving Electrical Grid. *Energies* **2021**, *14*, 694. [CrossRef]
19. Jamborsalamati, P.; Garmabdari, R.; Hossain, J.; Lu, J.; Dehghanian, P. Planning for resilience in power distribution networks: A multi-objective decision support. *IET Smart Grid* **2021**, *4*, 45–60. [CrossRef]
20. Tari, A.N.; Sepasian, M.S.; Kenari, M.T. Resilience assessment and improvement of distribution networks against extreme weather events. *Int. J. Electr. Power Energy Syst.* **2021**, *125*, 106414.
21. Liberati, F.; Di Giorgio, A.; Giuseppi, A.; Pietrabissa, A.; Priscoli, F.D. Efficient and risk-aware control of electricity distribution grids. *IEEE Syst. J.* **2020**, *14*, 3586–3597. [CrossRef]
22. Zheng, W.; Huang, W.; Hill, D.J. A deep learning-based general robust method for network reconfiguration in three-phase unbalanced active distribution networks. *Int. J. Electr. Power Energy Syst.* **2020**, *120*, 105982. [CrossRef]
23. Gao, Y.; Wang, W.; Shi, J.; Yu, N. Batch-constrained reinforcement learning for dynamic distribution network reconfiguration. *IEEE Trans. Smart Grid* **2020**, *11*, 5357–5369. [CrossRef]
24. Wang, C.; Lei, S.; Ju, P.; Chen, C.; Peng, C.; Hou, Y. MDP-based distribution network reconfiguration with renewable distributed generation: Approximate dynamic programming approach. *IEEE Trans. Smart Grid* **2020**, *11*, 3620–3631. [CrossRef]
25. Plotnek, J.J.; Slay, J. Power systems resilience: Definition and taxonomy with a view towards metrics. *Int. J. Crit. Infrastruct. Prot.* **2021**, *33*, 100411. [CrossRef]
26. Mahzarnia, M.; Moghaddam, M.P.; Baboli, P.T.; Siano, P. A review of the measures to enhance power systems resilience. *IEEE Syst. J.* **2020**, *14*, 4059–4070. [CrossRef]
27. Naghshbandi, S.N.; Varga, L.; Purvis, A.; Mcwilliam, R.; Minisci, E.; Vasile, M.; Troffaes, M.; Sedighi, T.; Guo, W.; Manley, E.; et al. A review of methods to study resilience of complex engineering and engineered systems. *IEEE Access* **2020**, *8*, 87775–87799. [CrossRef]
28. Mishra, D.K.; Ghadi, M.J.; Azizivahed, A.; Li, L.; Zhang, J. A review on resilience studies in active distribution systems. *Renew. Sustain. Energy Rev.* **2021**, *135*, 110201. [CrossRef]
29. Cheng, Y.; Elsayed, E.; Chen, X. Random Multi Hazard Resilience Modeling of Engineered Systems and Critical Infrastructure. *Reliab. Eng. Syst. Saf.* **2021**, *209*, 107453. [CrossRef]
30. Aziz, T.; Lin, Z.; Waseem, M.; Liu, S. Review on optimization methodologies in transmission network reconfiguration of power systems for grid resilience. *Int. Trans. Electr. Energy Syst.* **2021**, *31*, 1–38. [CrossRef]
31. Cantelmi, R.; Di Gravio, G.; Patriarca, R. Reviewing qualitative research approaches in the context of critical infrastructure resilience. *Environ. Syst. Decis.* **2021**, 1–36. [CrossRef]
32. IEEE. IEEE 118-Bus System. Available online: https://electricgrids.engr.tamu.edu/electric-grid-test-cases/ieee-118-bus-system/ (accessed on 6 April 2021).
33. Kröger, W.; Zio, E. *Vulnerable Systems*; Springer: London, UK, 2011; p. XIV-204.
34. Albert, R.; Barabási, A.L. Statistical mechanics of complex networks. *Rev. Mod. Phys.* **2002**, *74*, 1–54. [CrossRef]

35. Vaiman, M.; Bell, K.; Chen, Y.; Chowdhury, B.; Dobson, I.; Hines, P.; Papic, M.; Miller, S.; Zhang, P. Risk assessment of cascading outages: Methodologies and challenges. *IEEE Trans. Power Syst.* **2012**, *27*, 631–641. [CrossRef]
36. Bier, V.M.; Gratz, E.R.; Haphuriwat, N.J.; Magua, W.; Wierzbicki, K.R. Methodology for identifying near-optimal interdiction strategies for a power transmission system. *Reliab. Eng. Syst. Saf.* **2007**, *92*, 1155–1161. [CrossRef]
37. Haidar, A.M.; Mohamed, A.; Hussain, A. Vulnerability assessment of a large sized power system considering a new index based on power system loss. *Eur. J. Sci. Res.* **2007**, *17*, 61–72.
38. Zimmerman, R.D.; Murillo-Sánchez, C.E.; Thomas, R.J. MATPOWER: Steady-state operations, planning, and analysis tools for power systems research and education. *IEEE Trans. Power Syst.* **2010**, *26*, 12–19. [CrossRef]
39. Even, S. *Graph Algorithms*; Cambridge University Press: Cambridge, UK, 2011; pp. 1–189.
40. Martins, N.; de Oliveira, E.J.; Moreira, W.C.; Pereira, J.L.R.; Fontoura, R.M. Redispatch to reduce rotor shaft impacts upon transmission loop closure. *IEEE Trans. Power Syst.* **2008**, *23*, 592–600. [CrossRef]
41. Wood, A.J.; Wollenberg, B.F.; Sheblé, G.B. *Power Generation, Operation, and Control*; John Wiley & Sons: Hoboken, NJ, USA, 2013; pp. 1–656.
42. Panteli, M.; Trakas, D.N.; Mancarella, P.; Hatziargyriou, N.D. Power systems resilience assessment: Hardening and smart operational enhancement strategies. *Proc. IEEE* **2017**, *105*, 1202–1213. [CrossRef]
43. Bie, Z.; Lin, Y.; Li, G.; Li, F. Battling the extreme: A study on the power system resilience. *Proc. IEEE* **2017**, *105*, 1253–1266. [CrossRef]
44. Chanda, S.; Srivastava, A.K. Quantifying resiliency of smart power distribution systems with distributed energy resources. In Proceedings of the 2015 IEEE 24th International Symposium on Industrial Electronics (ISIE), Buzios, Brazil, 3–5 June 2015; pp. 1–6.
45. Panteli, M.; Mancarella, P. Influence of extreme weather and climate change on the resilience of power systems: Impacts and possible mitigation strategies. *Electr. Power Syst. Res.* **2015**, *127*, 259–270. [CrossRef]

Energy Strategy Reviews 38 (2021) 100706

Contents lists available at ScienceDirect

Energy Strategy Reviews

journal homepage: www.elsevier.com/locate/esr

Optimal cooperative model for the security of gas supply on European gas networks

Jose M. Yusta *, Jesus Beyza

University of Zaragoza, Department of Electrical Engineering, C/Maria de Luna 3, 50018, Zaragoza, Spain

ARTICLE INFO

Keywords:
European natural gas system
Optimisation
Resilience
Risk assessment
Security of supply

ABSTRACT

Natural gas infrastructures play a key role in the transition towards the new energy model, with a high share of renewable energies, both ensuring the firm capacity of electric power systems and integrating all energy vectors. The European Union (EU) strongly depends on external natural gas suppliers and is thus particularly vulnerable. In the event of supply problems due to natural phenomena, technical failures or other threats, cooperation between EU countries would be essential to best solve a supply crisis. This study proposes an EU cooperative model to meet the gas demand over a fourteen-day crisis, using a mathematical optimisation approach for resources and infrastructure. The model considers the dynamic management of underground gas storage facilities, limiting daily withdrawal based on the amount of working gas available in each storage facility. The ability of the model to make quick decisions is illustrated in six gas-demand case studies of the European cold wave in January 2017 and hypothetical supply disruptions.

1. Introduction

As part of the new international policy to reduce pollutant emissions, most developed countries are closing coal-fired power stations. These power stations are being replaced by other, more modern, power production technologies, which mainly use natural gas and renewable energy sources. The International Energy Agency estimates that replacing coal-with gas-fired power stations could reduce up to 1.2 gigatons of CO_2 because the latter emit 50% less pollutants than the former [1]. The creation of international emissions markets and regulations has remarkably raised the cost of coal-fired power generation, rendering gas-fired power generation increasingly attractive. In fact, low natural gas prices have accelerated this trend in 2020 [2].

While many countries are setting ambitious decarbonisation targets for 2030 and 2050, the transition towards 100% renewable energy requires power generation technologies that provide electric power systems with firm capacity. Until commercially viable, large-scale electricity storage technologies are available, electric power systems will depend on predictable and reliable energy generation sources like gas-fired power plants [3]. In addition, gas infrastructures do allow seasonal energy storage, which also provides significant value in ensuring electricity supply through combined-cycle gas plants. Therefore, these stations play a key role in the security of electricity supply.

Notwithstanding the importance of natural gas as a transition fuel for supporting renewable energy development in the short and medium term, the demand for gas is expected to decline in the long term [4,5]. This perspective can limit future investments in new gas transmission and storage infrastructure projects even though the gas sector is promoting alternatives for the use of existing networks with new energy vectors, such as hydrogen, to address its decreasing importance from 2030 [6,7].

As the world's largest importer of natural gas and, therefore, highly dependent on other countries, the European Union (EU) is a very unique case. Its annual consumption is approximately 500,000 million m^3, and its dependence on external suppliers reached 90% in 2019 [8]. Russia is the main natural gas supplier to the EU (45%), followed by Norway (21%) and Algeria (12%) [9]. Liquefied natural gas (LNG) imports to the EU increased for geopolitical reasons of supply diversification, reaching 22% of total gas imports in 2019. However, pipeline gas imports remain the main source of foreign gas entry into the EU, and some major projects for new international gas pipelines running from Russia and Caspian countries to Europe are under development, such as Nord Stream 2, TurkStream and TANAP-TAP (Trans-Anatolian Natural Gas Pipeline - Trans Adriatic Pipeline).

In addition to improving the natural gas supply infrastructures, the EU has proposed new cooperative mechanisms to reduce the impact of supply crises by increasing cross-border pipeline gas exchange when

* Corresponding author.
E-mail addresses: jmyusta@unizar.es (J.M. Yusta), jbeyza@unizar.es (J. Beyza).

https://doi.org/10.1016/j.esr.2021.100706
Received 7 June 2021; Received in revised form 16 August 2021; Accepted 25 August 2021

Nomenclature

$C_{i,d}$	daily gas demand satisfied in country i (GWh/d)
$P_{i,d}$	daily gas production of country i (GWh/d)
$ST_{i,d}$	daily working gas available in storage every day in country i (GWh)
$SWR_{i,d}$	daily gas storage withdrawal from underground storage in country i (GWh/d)
$IMP_{i,d}$	daily gas pipeline imports from third-party countries to country i (GWh/d)
$LNG_{i,d}$	daily gas injected from regasification plants into the pipes of country i (GWh/d)
$X_{ij,d}$	daily gas flow through cross-border pipelines between countries i and j (GWh/d)

necessary [10,11]. These regulations do not aim to replace the national energy policies, but rather to facilitate mutual support between natural gas-producing countries, LNG-importing countries, pipeline gas transit countries and the other EU countries. Similar cooperative mechanisms have also been proposed for risk-preparedness in the electricity sector [12].

Intentional attacks, cold waves, or technical failures can affect gas supply. However, when operators of national transmission systems face these crises, they usually make decisions considering their endogenous resources, overlooking possible collaborative actions with neighbouring countries. In turn, given the dynamic nature of gas production, storage and flows in networks, establishing contingency plans for all possible scenarios during an energy supply crisis is practically impossible. In addition, such a crisis may require continuously updating the interventions in the infrastructure, especially if the crisis lasts for a long period.

Thus, this study proposes a novel approach to developing strategies to optimally respond to possible crises, beyond the classical simulation approach for risk assessment. For this purpose, mathematical optimisation tools are used to apply cooperative strategies towards meeting as much as possible the demand in all EU-28 member states and in some neighbouring countries. The mathematical problem is formulated considering the daily production and storage capacities, cross-border interconnections and third-party country LNG or gas pipeline imports of each country. The EU network model of gas transmission infrastructures captures the different characteristics of national systems and manages gas exchange between countries to determine the best possible solution for global EU supply.

Another novelty of this research is the application of the proposed mathematical model to identify the best strategy for a two-week winter gas supply crisis by calculating the most adequate daily use of resources and infrastructures while maximising the satisfied demand over the entire fourteen-day period. The effects of emptying gas reservoirs and reducing the daily withdrawal with the decrease in stored working gas volume are analysed. The two-week case study is a common research strategy in studies simulating the security-of-supply of natural gas conducted by the European Network of Transmission System Operators for Gas (ENTSO-G) in Europe because this design makes it possible to capture the effect of a cold wave on gas supply and, especially, on gas storage [13].

This article is organised as follows: Section 2 presents a review of the main gas system models. Section 3 describes the optimisation model proposed to determine the optimal management of a fourteen-day natural gas supply crisis in the EU. Section 4 presents six case studies based on possible supply outages in the European gas transmission network. Section 5 discusses the findings, and, last, Section 6 outlines the main conclusions of this paper.

2. Modelling of gas systems for the security of supply: state of the art

The most widely used approach in risk assessment studies for interconnected natural gas systems is the set of probabilistic methods known as Monte Carlo. The Monte Carlo method has been used to evaluate the behaviour of natural gas networks in different events [14,15]. This method is based on repetitive simulations of how the system operates under different assumptions of accidental or intentional contingencies in gas supply and transportation infrastructures. Each possible contingency is assigned a specific probability. Hence, the method makes it possible to evaluate all possible consequences by estimating the input uncertainties of the model, running the model under different values of input parameters and by describing the consequences in statistical terms [16].

The risk assessment studies for interconnected gas systems frequently rely on a simplified mass balance model in which the equations are obtained by applying the principle of mass conservation at each network node [14,15], rather than on a dynamic hydraulic model of the gas transmission system [17] since the latter requires extensive knowledge of the parameters and technical characteristics of the networks. If this information would be available, specific software programs such as SAInt can simulate the dynamic operation of gas networks for assessing the security of supply [18].

While simulation models analyse the consequences of different system contingencies, there is a lack of research providing strategies to optimally respond to possible gas supply crises. Using mathematical optimisation rather than probability-based approaches may be appropriate if the time frame for making decisions about available resources is limited because traditional probabilistic simulation models used to determine the impact of disturbances on gas supply take a long time to run. Therefore, a mathematical optimisation approach makes it possible to obtain the best possible operation of an interconnected gas infrastructure under different supply disruption conditions.

Some models apply optimisation in gas systems, but they aim to examine how markets function, to reduce costs or to analyse the impact of different changes in regulatory frameworks on market participants. Among these, the GASMOD model is formulated as a two-stage game of natural gas exports and wholesale trade within Europe [19]. Other works propose multilevel models for the gas market, including infrastructure constraints under perfect competition and assuming interaction between the operator and traders [20]. Similarly, the European Gas Market Model (EGMM) is a market equilibrium model for analysing the production, trade, storage, and natural gas consumption in Europe [21]. Meanwhile, the Global Gas Model is a model for studying European gas markets, which maximises the profit of market players and the behaviour of operators, and includes security of supply concerns [22,23]. Additionally, a minimum cost dispatch for the gas supply chain can be found in Ref. [24].

On the other hand, other studies propose models based on mathematical programming techniques to evaluate investments in new infrastructure within the EU. For example, the GASTALE model uses game theory, and the EUGAS and MAGELAN models use dynamic programming to optimise investments in production and infrastructure capacity on a yearly basis [25,26]. Likewise, the COLUMBUS model optimises production, transport and storage capacities based on monthly resolution [27], the TIGER model minimises supply-demand transmission costs also with monthly granularity [28,29], and the GASMOPEC model enhances the decision-making process from a market perspective [30].

Despite analysing gas markets and infrastructures, these optimal models do not solve supply crises in the short term, but rather aim to assess the adequacy of the infrastructure in the long term. Therefore, it is essential to propose an optimal cooperative management model for the security of supply, which allows establishing the best strategies for dealing with crisis scenarios in case of disruptions in gas supply to the EU.

3. Proposed mathematical model

Contingency plans to recover critical energy infrastructure after a severe failure are developed primarily at the national level. However, European energy infrastructures are interconnected between countries, and intentional attacks, natural hazards or limited third-party country supply can lead to restrictions on demand. In these cases, cooperative strategies may be implemented, instead of individual solutions, to jointly meet as much as possible the demand of all countries.

The EU has proposed regulations to prepare and establish preventive and emergency action plans, seeking a cooperative approach among member states to reduce the impact of severe disruption scenarios. Regulation (EU) 2017/1938 on measures to safeguard the security of gas supply is currently being implemented to develop joint measures and facilitate the bi-directional capacity of cross-border interconnections under a cooperation framework between EU countries [11].

Given the dynamic nature of gas production flows, storage and networks, establishing contingency plans for all possible scenarios during a power supply crisis is practically impossible. In addition, infrastructure interventions may require updating, especially if the crisis lasts for a long period. This study proposes a formulation for managing interconnected natural gas infrastructures towards improving resilience when facing a supply crisis, that is, maintaining the maximum amount of gas supply to consumers during a two-week study period. Gas storage facilities and exchange between countries play a key role in this problem because they can extend gas supply for more days if used optimally. Using mathematical optimisation techniques instead of probabilistic approaches is appropriate when decisions concerning available resources need to be quick since traditional probabilistic simulation models used for determining the disturbance impact on gas supply are more time-consuming.

The proposed model maximises the daily coverage of the natural gas demand for fourteen days in a group of interconnected countries by providing collaborative solutions to supply crises due to technical, political or natural phenomena. Later, in Section 4, this model is applied to a series of case studies in the European gas transmission network. The mathematical equations of the model are derived by applying the principle of mass balance at each node of the network. Each country is represented by a node in a graph, following the Monte Carlo-based Gas Energy Network for Europe, Russia, and the Commonwealth of Independent States (MC-GENERCIS) and Gas Emergency Flow (GEMFLOW) models proposed by the Joint Research Centre of the European Commission [14,31]. Such models can be applied to draw significant conclusions about gas system capacities even when a hydraulic model of the system is not used. They are used to assess the security of natural gas supply in the event of disruptions in the external supply of natural gas to the EU through cooperative mechanisms between member countries. Hydraulic models cannot be used due to the lack of detailed information on the infrastructures of these countries.

In the model presented here, each country i is represented as a node in the natural gas transmission system. The resources involved every day d are the demand, $C_{i,d}$, the production, $P_{i,d}$, the daily storage facility's withdrawal rate, $S_{i,d}$, natural gas pipeline imports, $IMP_{i,d}$, LNG shipping, $LNG_{i,d}$, and the interconnection capacities between neighbouring countries $X_{ij,d}$.

The mathematical model uses the available capacities of each country once the internal demand has been met to identify the best solution for the fourteen days of the case study, that is, to get as close as possible to meeting the demand of the countries belonging to the interconnected natural gas system. Cross-border interconnections have a physical capacity that limits the flow and they can be uni-o bi-directional. Previous optimisation models for this problem have only solved gas supply for one day, and without sharing gas stored in the countries [32].

The mathematical optimisation problem is defined by the objective function of eq. (1) and by the set of constraints that are shown in eqs. (2)–(10). $C_{i,d}^{max}$ is the natural gas demand that the system seeks to meet every day, d, in each country, i, and $C_{i,d}$ is the demand that is actually met.

The maximum technical capacity for endogenous natural gas production in each country ($P_{i,d}^{max}$) is a value which generally remains relatively stable over time and which is not affected in the two-week case study. The withdrawal rate of gas storage in each country results from solving the mathematical problem, and a different value is calculated for each day of the fourteen-day study period.

The amount of third-party country pipeline natural gas imports is defined as the daily maximum available technical capacity from gas pipelines, in the direction of entry, to the countries in the network.

The countries of the system with access to the sea may have receiving terminals and regasification plants for liquefied natural gas (LNG) supply. The possibility of using the nominal capacity of a regasification plant ($LNG_{i,d}^{max}$) to supply the gas entry to natural gas transmission networks for fourteen days depends on the ability to maintain the supply flow to the terminal through LNG tankers because the storage capacity of LNG maritime terminals is usually limited to a few days.

$$max \sum_{d=1}^{14} \sum_{i=1}^{n} C_{i,d} \tag{1}$$

when

$$0 \le C_{i,d} \le C_{i,d}^{max} \tag{2}$$

$$0 \le P_{i,d} \le P_{i,d}^{max} \tag{3}$$

$$0 \le IMP_{i,d} \le IMP_{i,d}^{max} \tag{4}$$

$$0 \le LNG_{i,d} \le LNG_{i,d}^{max} \tag{5}$$

The amount of natural gas exchanged between countries helps to solve the possible shortage of domestic gas supply in some countries. The may vary with the direction of gas flow, as indicated in eq. (6). Balancing all possible gas resources in each country is expressed in eq. (7).

$$-X_{ji,d}^{max} \le X_{ij,d} \le X_{ij,d}^{max} \tag{6}$$

$$P_{i,d} + SWR_{i,d} + IMP_{i,d} + LNG_{i,d} - C_{i,d} - \sum X_{ij,d} = 0 \tag{7}$$

Gas storage is a strategic resource for each country. However, under a cooperative scheme, gas storage can be decisive in supporting other countries in the system during a crisis. The underground gas storage capacity differs considerably between countries because it depends on the geological conditions and on the investments in infrastructure. There are three main types of underground storage: aquifer, salt cavern and depleted gas reservoir. The amount of gas available each day from an underground gas storage is characterised by the maximum withdrawal rate, $SWR_{i,d}^{max}$, and varies with the amount of working gas, $ST_{i,d}$, available in storage every day. In this model, the relationship between $SWR_{i,d}^{max}$ and $ST_{i,d}$ was estimated by linear regression, as mathematically expressed in eq. (9). The daily storage balance is indicated in eq. (10).

$$0 \le SWR_{i,d} \le SWR_{i,d}^{max} \tag{8}$$

$$SWR_{i,d}^{max} = a_i ST_{i,d} + b_i \tag{9}$$

$$-SWR_{i,d-1} + ST_{i,d-1} - ST_{i,d} = 0 \tag{10}$$

The mathematical optimisation problem defined in eqs. (1)–(10) is linear because the objective function is linear, the constraints are linear, and all variables are continuous. The optimisation problem is programmed and solved using the Optimisation Toolbox™ of MatlaB R2019a by applying the linear programming function *linprog* and the

Table 1
Mean data from the European natural gas system from the 14th to the 27th of January of 2017, and peak gas consumption on the 18th of January of 2017 (GWh/d).

	Daily averages from the 14th to the January 27, 2017				UGS		Cross-border capacity		Gas demand on the January 18, 2017
	C^{max}	P^{max}	IMP^{max}	LNG^{max}	$ST_{d=1}$	$SWR_{d=1}$	X_{ij}^{max}	X_{ji}^{max}	C^{max}
Austria	517	44	0	0	23,657	998	2382	2290	550
Belgium	929	0	488	225	2046	170	2380	2658	988
Bosnia	10	0	0	0	0	0	0	15	11
Bulgaria	142	3	766	0	1463	36	158	362	151
Croatia	150	37	0	0	1383	58	0	129	159
Czechia	511	5	0	0	9358	682	1923	1690	543
Denmark	135	170	0	0	3075	194	33	61	144
Estonia	21	0	48	0	0	0	0	63	22
Finland	101	0	249	0	0	0	0	0	107
France	2964	0	570	615	33,638	2205	695	1667	3152
Germany	4347	189	3280	0	65,072	6657	5111	5384	4623
Greece	215	0	49	75	0	0	0	109	229
Hungary	598	68	605	0	16,781	812	270	283	636
Ireland	181	120	0	0	0	0	0	432	192
Italy	3840	171	1695	272	46,894	2703	41	1807	4084
Latvia	62	0	179	0	6380	287	128	68	66
Lithuania	89	0	325	61	0	0	68	65	95
Macedonia	15	0	0	0	0	0	0	27	16
Netherlands	1960	1936	0	218	37,700	2400	4288	2009	2084
Poland	745	74	1336	79	8300	528	932	194	792
Portugal	222	0	0	178	893	78	80	144	236
Romania	624	314	370	0	8165	315	364	73	664
Serbia	83	15	0	0	1133	52	15	142	88
Slovakia	268	0	2080	0	9002	436	2285	1111	285
Slovenia	45	0	0	0	0	0	75	141	48
Spain	1412	3	732	956	7905	129	369	245	1502
Switzerland	206	0	0	0	0	0	635	828	219
UK	3612	2007	1499	823	12,703	1324	1062	1297	3841

Table 2
Capacity of the cross-border interconnections of the European natural gas system in January of 2017.

			Capacity max	Capacity min				Capacity max	Capacity min
Unidirectional	Belgium	France	870	0	Bidirectional	Spain	France	225	−165
	Germany	France	571.8	0		Spain	Portugal	144	−80
	France	Switzerland	260.4	0		Belgium	Germany	313.1	−320.1
	Belgium	Netherlands	122	0		Netherlands	Germany	889.7	−1615.9
	Germany	Switzerland	554.4	0		UK	Belgium	630.1	−803.4
	Switzerland	Italy	634.7	0		Germany	Austria	581.3	−638.7
	Netherlands	Germany	1466.8	0		Czechia	Slovakia	696.8	−400.4
	Netherlands	UK	494	0		Latvia	Lithuania	65.1	−67.6
	Netherlands	Belgium	1041.5	0		Austria	Slovakia	320.2	−1684.7
	UK	Ireland	431.7	0		Belgium	Netherlands	271.2	−396
	Germany	Austria	24.2	0		Italy	Slovenia	28.5	−21.5
	Slovenia	Croatia	53.3	0		Germany	Denmark	60.6	−32.7
	Austria	Italy	1150.5	0		Germany	Poland	166.3	−931.6
	Austria	Slovenia	112.5	0		Hungary	Romania	51.5	−2.5
	Austria	Hungary	153.1	0		Slovakia	Czechia	73.1	−93.9
	Latvia	Estonia	63	0		Bulgaria	Romania	21.6	−1.6
	Czechia	Germany	906.9	0		Germany	Czechia	135.5	−197.5
	Hungary	Croatia	76	0					
	Hungary	Serbia	142.1	0					
	Romania	Bulgaria	751.2	0					
	Bulgaria	Greece	109.3	0					
	Bulgaria	Macedonia	27.4	0					
	Serbia	Bosnia	15	0					
	Germany	Czechia	1081.2	0					
	Czechia	Poland	28	0					
	Slovakia	Hungary	127	0					
	France	Belgium	270	0					
	Italy	Switzerland	12.9	0					
	Austria	Germany	6.9	0					

interior-point algorithm. The simulation framework runs on a computer with a 3.40 GHz CPU Intel® Core™ i7 processor and with 16 GB of RAM.

The data on the technical capacities of different variables are subjected to a pre-treatment before solving the optimisation problem. In reality, each country tries to meet its demand by first using its own resources and then, under the cooperative scheme of the proposed model, making its surplus capacities available to the other countries in the system. Usually, the countries use their own resources in the following order: production, imported LNG and imported pipeline gas. Gas in underground storage is always the last resort since it is a more strategic resource.

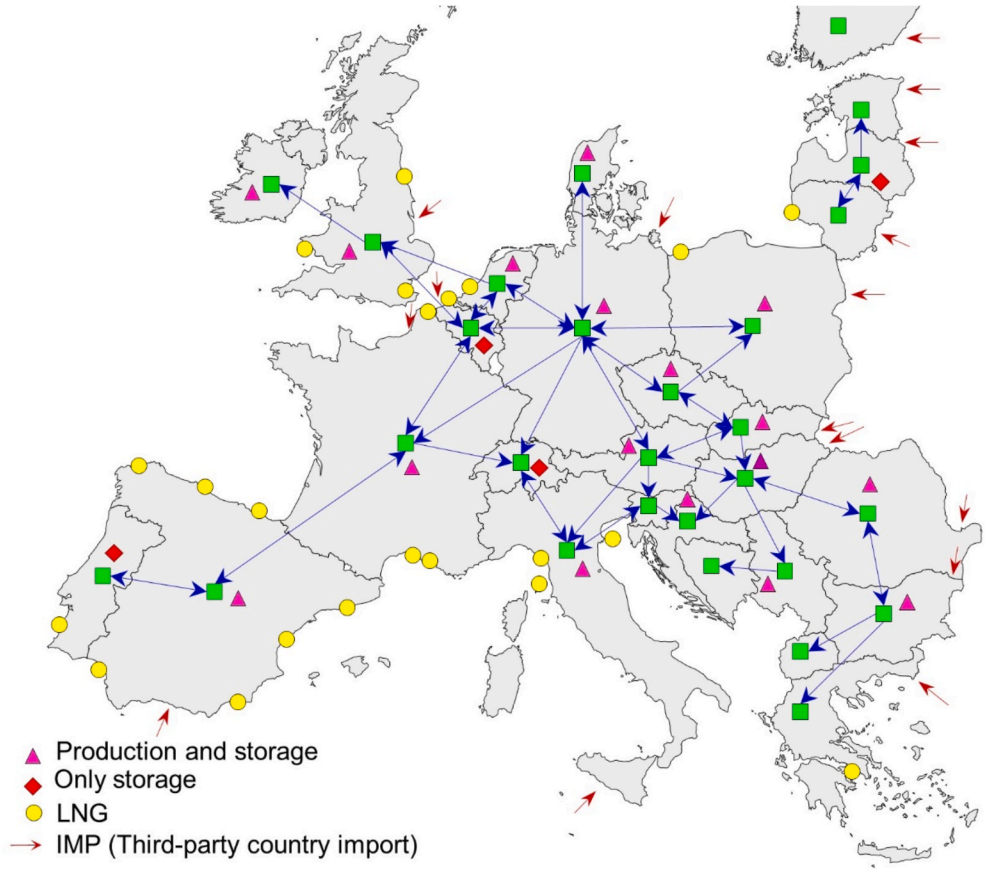

Fig. 1. Natural gas transmission system of the European Union in 2017.

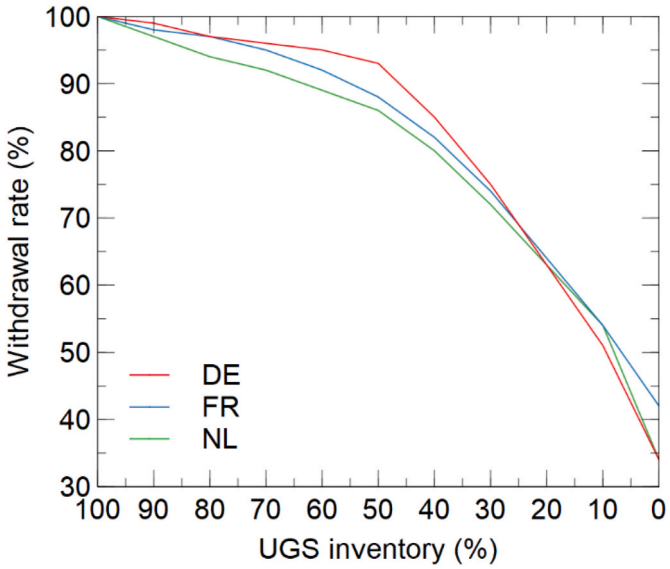

Fig. 2. Withdrawal capacity versus UGS inventory level of some EU countries [41].

4. Case studies

The sharp demand in gas that occurred during the European cold wave of January 2017 lasting several weeks was used as an application example to show the utility of the proposed model. The demand for gas shows a strong seasonal pattern in Europe, with a higher demand in winter. These variations are largely due to the temperature-related demand for heating in the residential and tertiary sectors.

As mentioned in Section 1, the two-week case study is a common design among simulation studies on the security of natural gas supply in Europe. Other studies analyse system capacities in the very short term, on the day of peak gas demand [32], and in the very long term, assuming supply crisis from one to three months [33]. However, the most interesting case is that of two weeks because this period makes it possible to assess the effect of a cold wave [13].

Almost 90% of the natural gas consumption in the EU derives from third countries [8]. If, in addition to a high demand for natural gas in several countries, additional constraints are imposed on natural gas imports, the system may enter into severe stress. This extreme situation may be exacerbated if the underground gas storage is low, which usually occurs in late winter. Therefore, to demonstrate the applicability of the mathematical model for optimal management presented in Section 3, the consumption data recorded from the 14th to the 27th of January of 2017 was used here together with the scenarios of total or partial disruption of gas imports to the EU.

The average demand during the fourteen-day peak demand period from the 14th to January 27, 2017, was 24,000 GWh/d. The peak gas demand in the EU was reached on the January 18, 2017, which was 25,521 GWh/d [34]. Interestingly, the peak electricity demand in the EU, that is, 581,276 MW, was also reached on the same day [35]. The interaction between the gas system and the electric power system must be considered because combined-cycle gas-fired power stations play a key role in maintaining the electricity supply as a backup for renewables during dark doldrums, a cold period such as a two-week cold wave with very low renewable electricity generation.

Another reason for selecting the cold wave of the 2017 Winter is that the storage inventory level in January and February 2017 was at historic lows, reducing the contribution from underground gas storage (UGS) to safeguarding the supply in the event of additional unforeseen

Table 3
Parameters a_i and b_i of eq. (9), modelling UGS inventory lower than 50% for each country.

Country *i*	a_i	b_i
Austria	0.01953	535.52
Belgium	0.06297	40.68
Bosnia	0.00000	0.00
Bulgaria	0.01584	13.03
Croatia	0.03593	8.48
Czechia	0.04585	253.18
Denmark	0.04425	58.32
Estonia	0.00000	0.00
Finland	0.00000	0.00
France	0.03427	1052.52
Germany	0.06491	2433.92
Greece	0.00000	0.00
Hungary	0.02246	435.46
Ireland	0.00000	0.00
Italy	0.03483	1069.20
Latvia	0.02716	113.40
Lithuania	0.00000	0.00
Macedonia	0.00000	0.00
Netherlands	0.03850	948.89
Poland	0.03666	223.91
Portugal	0.05280	30.84
Romania	0.02335	124.76
Serbia	0.02768	20.52
Slovakia	0.02929	172.57
Slovenia	0.00000	0.00
Spain	0.00651	77.22
Switzerland	0.00000	0.00
UK	0.06301	523.89

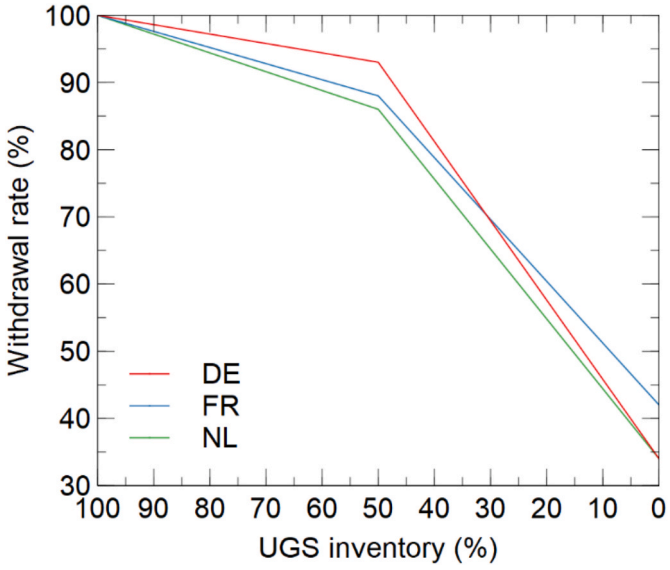

Fig. 3. Withdrawal capacity versus UGS inventory level of some EU countries upon linear approximation.

contingencies [34].

Data from the European natural gas system in January 2017 are outlined in Tables 1 and 2. The gas demand values were retrieved from Ref. [36], while the values of natural gas production, imports, LNG and cross-border capacity were gathered from Ref. [37]. The UGS data were collected from Ref. [38]. In the case study, EU countries and the following neighbouring countries were considered: Bosnia-Herzegovina, North Macedonia, Switzerland and Serbia.

The natural gas system represented in Fig. 1 includes 28 countries, which, in 2017, were connected by 35 cross-border interconnections, 18 of which were bi-directional. These infrastructures have been expanded in recent years to improve the European security of natural gas supply.

A few EU countries, such as Italy, France, Germany and the Netherlands, have the highest underground gas storage capacity. For geological reasons, Eastern and South-Eastern European countries have only a small gas storage capacity [39]. Therefore, properly using interconnection capacities between countries by optimally managing cross-border gas pipelines for trading gas from underground storage can improve the ability of EU and other neighbouring countries to meet the gas demand.

In this study, a model of underground gas storage is applied, assessing the UGS inventory effect on the withdrawal rate using deliverability curves. The amount of gas that can be withdrawn from a storage facility decreases with the decrease in stored gas [40]. Fig. 2 shows the curves of three EU countries built using the data provided by the Gas Storage Europe [41]. These curves represent a weighted average of the facilities in each country (salt caverns, aquifers or depleted gas reservoirs).

Fig. 2 shows an inflexion point in the curves when storage is higher than 50% inventory level, and the relation between the withdrawal rate and the stored gas is approximately linear when this level continues to decrease. For this reason, in the mathematical model of Section 3, a linear equation was proposed to relate the withdrawal rate to the UGS inventory between 0% and 50% of the UGS stock, as shown in eq. (9). The parameters of the equations for each country, calculated in Table 3, were determined by linear approximation in two sections of the data provided in Ref. [41] for UGS lower than 50% inventory level. The representation of eq. (9) in Fig. 3, for the same countries of Fig. 2, shows the goodness-of-fit of the linear approximation.

The mathematical optimisation tool developed in this research identified the best daily solution for gas resources (especially the use of UGS and cross-border capacities between countries) to meet as much as possible the natural gas demand for two weeks, not by maximising the demand met each day but by maximising the demand over the entire fourteen-day period. That is, a global solution to the problem was offered, instead of providing daily solutions that may not be optimal in the medium term. In addition, the solution ensures the best cooperation between the EU countries with the common goal of supplying natural gas to their end consumers, thereby meeting the demand.

Case studies were defined to assess the impact of various scenarios of gas supply disruption coupled with a low initial storage level during very high demand events:

- **Case 1.** Demand from the 14th to the 27th of January of 2017 and 50% initial storage
- **Case 2.** Russian pipeline gas supply disruption and 50% initial storage
- **Case 3.** LNG supply disruption and 50% initial storage
- **Case 4.** Demand from the 14th to the 27th of January of 2017 and 20% initial storage.
- **Case 5.** Russian pipeline gas supply disruption and 20% initial storage.
- **Case 6.** LNG supply disruption and 20% initial storage.

Case 1 analyses the capacity of the gas system to cope with a situation of high demand and half empty gas storage, that is, 50% inventory level. This was the real scenario in January of 2017 because an unusually cold winter quickly emptied UGS facilities, which only had 50% working gas stored at the beginning of the second half of January [34].

Cases 2 and 3, in addition to the situation of high gas demand,

Table 4
Breakdown of the main results by country in Case 1.

	Demand satisfied		Production used		LNG imports used		Pipeline imports used		UGS ST 100%	UGS ST 50%	UGS SWR 50%	UGS ST final	
	GWh	%	GWh	%	GWh	%	GWh	%	GWh	GWh	GWh/d	GWh	%
Austria	7274	100%	616	100%	0		0		47,315	23,657	998	19,760	42%
Belgium	13,066	100%	0		3143	100%	6832	100%	4092	2046	170	1610	39%
Bosnia	145	100%	0		0		0		0	0	0	0	
Bulgaria	1997	100%	42	100%	0		2499	23%	2926	1463	36	1312	45%
Croatia	2103	100%	518	100%	0		0		2765	1383	58	1056	38%
Czechia	7181	100%	70	100%	0		0		18,715	9358	682	7979	43%
Denmark	1904	100%	2031	85%	0		0		6150	3075	194	2920	47%
Estonia	291	100%	0		0		291	43%	0	0	0	0	
Finland	1415	100%	0		0		1415	41%	0	0	0	0	
France	41,684	100%	0		8610	100%	7980	100%	67,275	33,638	2205	24,408	36%
Germany	61,138	100%	2646	100%	0		45,926	100%	130,144	65,072	6657	30,986	24%
Greece	3028	100%	0		1050	100%	680	100%	0	0	0	0	
Hungary	8411	100%	952	100%	0		7730	91%	33,563	16,781	812	15,957	48%
Ireland	2539	100%	1680	100%	0		0		0	0	0	0	
Italy	54,010	100%	2394	100%	3801	100%	23,730	100%	93,787	46,894	2703	35,303	38%
Latvia	873	100%	0		0		873	35%	12,760	6380	287	6380	50%
Lithuania	1256	100%	0		854	100%	402	9%	0	0	0	0	
Macedonia	212	100%	0		0		0		0	0	0	0	
Netherlands	27,560	100%	27,104	100%	1217	40%	0		75,399	37,700	2400	30,630	41%
Poland	10,474	100%	1036	100%	1106	100%	9701	52%	16,601	8300	528	7113	43%
Portugal	3121	100%	0		2492	100%	0		1785	893	78	623	35%
Romania	8781	100%	4396	100%	0		4385	85%	16,329	8165	315	7714	47%
Serbia	1160	100%	211	100%	0		0		2265	1133	52	962	42%
Slovakia	3769	100%	0		0		6398	22%	18,003	9002	436	7799	43%
Slovenia	635	100%	0		0		0		0	0	0	0	
Spain	19,864	100%	42	100%	13,377	100%	7281	71%	15,810	7905	129	7388	47%
Switzerland	2896	100%	0		0		0		0	0	0	0	
UK	50,796	100%	28,098	100%	11,515	100%	12,483	59%	25,406	12,703	1324	11,031	43%
TOTAL	337,583	100%	71,836	100%	47,165	96%	138,606	69%	591,090	295,548	20,064	220,931	37%

included a hypothetical disruption of either gas imports from Russia to Central Europe by pipeline (Case 2) or LNG supply by sea (Case 3) during the fourteen-day study period. These situations are unlikely, but not impossible as similar events have already been recorded on different occasions in the past, particularly disruption of gas supply from Russia [42]. Any problem related to gas supply from Russia greatly impacts the downstream EU countries because Russia is the main supplier, with a 40% import quota for pipeline gas and 17% for LNG [43]. Russian natural gas is exported to the European market through five main pipelines, of which the two most important transit the Ukraine. Tense relations between Russia and Ukraine result in a high-risk scenario [44].

On the other hand, a global LNG supply crisis is possible, as recent events in January 2021 demonstrated when LNG shipments were diverted from Europe to Asia for commercial reasons in an unprecedented event during a severe cold snap. Europe had to increase the gas extraction from its storage reserves and use the import capacity of pipeline gas to overcome the lack of LNG supply. As a result, current gas storage levels in Europe decreased to a minimum after winter and inventory levels required for next winter were at risk.

To illustrate the behaviour of the mathematical model proposed for the European natural gas infrastructure, the previous cases were repeated in the scenario with the lowest level of gas storage (20%), that is, Cases 4, 5 and 6. These scenarios are not that unlikely because, for example, UGS stock levels reached 18.4% by the end of the 2018 winter [45].

5. Simulation results

This section presents the results of the six case studies defined above to illustrate how the tool proposed in this research can facilitate strategies for the best use of resources and infrastructures in the event of a two-week gas supply crisis. In each case, the formulation of the linear optimisation problem defined by eqs. (1)–(10) was applied to data from the European gas system outlined in Table 1 and to the 2017 capacities of the unidirectional and bidirectional gas pipelines of the interconnections of Fig. 1 and Table 2.

- **Case 1 (demand from the 14th to the 27th of January of 2017 and 50% initial storage)**

Table 4 outlines the results of the base case, defined with the gas demand data recorded from the 14th to the 27th of January of 2017. During this period, the storage inventory level in European countries was approximately 50%, that is, 294,000 GWh. The results indicate that the best solution to cooperatively meet the demand for gas during those two weeks, under the assumptions explained in Section 3, would consist of using 100% of the available gas production resources of countries from the system (mainly the Netherlands and the United Kingdom), 96% of the resources contributed by LNG terminals and 69% of the capacity of pipeline gas imports. Underground gas reservoirs would be emptied to 37% storage level.

The use rate of cross-border interconnections would average 37% of the available capacity in unidirectional and bidirectional gas pipelines (see Table 9); that is, to meet the average daily demand of 24,000 GWh/d during the two-week study period, 8700 GWh/d would have to be exchanged between the countries of the system, highlighting the importance of gas transit for ensuring the availability of each country to the other members of the system.

Underground gas storage also plays a key role in the optimal strategy to meet the demand. The results from using UGS outlined in Table 5 showed that withdrawal would increase in the first five days but would decrease in the following days. These findings are consistent because the

Table 5
Optimal UGS management in Case 1.
• **Case 2 (demand from the 14th to the 27th of January of 2017, 50% initial storage and Russian pipeline gas supply disruption)**

	Withdrawal rate - SWR (GWh/d)													
	Day 1	Day 2	Day 3	Day 4	Day 5	Day 6	Day 7	Day 8	Day 9	Day 10	Day 11	Day 12	Day 13	Day 14
Austria	143	238	252	269	328	294	303	317	329	341	352	362	369	240
Belgium	25	25	26	28	31	31	33	35	36	38	40	43	45	57
Bosnia	0	0	0	0	0	0	0	0	0	0	0	0	0	0
Bulgaria	13	11	11	11	12	11	11	11	12	12	12	12	12	13
Croatia	26	25	25	25	29	25	25	25	25	25	25	25	25	26
Czechia	13	57	71	89	110	105	108	114	122	132	143	154	163	201
Denmark	12	11	11	11	12	12	12	12	12	12	12	12	13	12
Estonia	0	0	0	0	0	0	0	0	0	0	0	0	0	0
Finland	0	0	0	0	0	0	0	0	0	0	0	0	0	0
France	467	591	629	632	820	662	692	708	748	790	817	833	839	898
Germany	3493	3200	3064	2944	3110	2696	2579	2469	2349	2232	2109	1975	1865	1537
Greece	0	0	0	0	0	0	0	0	0	0	0	0	0	0
Hungary	53	64	64	64	74	64	64	64	64	63	63	63	62	55
Ireland	0	0	0	0	0	0	0	0	0	0	0	0	0	0
Italy	732	766	798	814	1053	874	901	926	936	941	946	953	951	985
Latvia	0	0	0	0	0	0	0	0	0	0	0	0	0	0
Lithuania	0	0	0	0	0	0	0	0	0	0	0	0	0	0
Macedonia	0	0	0	0	0	0	0	0	0	0	0	0	0	0
Netherlands	344	448	468	490	590	529	545	561	574	585	615	646	673	732
Poland	18	44	65	74	91	87	92	99	106	115	123	132	140	155
Portugal	19	17	17	18	22	20	21	21	22	22	23	23	24	27
Romania	32	34	34	34	40	34	34	34	35	35	35	35	35	33
Serbia	13	12	12	12	14	13	13	13	13	14	14	14	15	17
Slovakia	21	56	61	73	97	90	95	101	108	116	123	129	133	145
Slovenia	0	0	0	0	0	0	0	0	0	0	0	0	0	0
Spain	30	31	32	35	44	39	41	42	43	44	45	45	46	47
Switzerland	0	0	0	0	0	0	0	0	0	0	0	0	0	0
UK	46	84	88	104	165	141	147	151	154	154	150	147	141	183
TOTAL	5500	5714	5728	5727	6642	5727	5716	5703	5688	5671	5647	5603	5551	5363
	UGS level - ST (GWh)													
	Day 1	Day 2	Day 3	Day 4	Day 5	Day 6	Day 7	Day 8	Day 9	Day 10	Day 11	Day 12	Day 13	Day 14
Austria	23,657	23,514	23,277	23,024	22,755	22,427	22,133	21,829	21,513	21,184	20,843	20,491	20,129	19,760
Belgium	2046	2021	1996	1970	1943	1911	1880	1847	1813	1777	1738	1698	1655	1610
Bosnia	0	0	0	0	0	0	0	0	0	0	0	0	0	0
Bulgaria	1463	1450	1439	1428	1416	1405	1393	1382	1371	1359	1347	1336	1324	1312
Croatia	1383	1357	1332	1308	1283	1254	1229	1204	1179	1155	1130	1105	1081	1056
Czechia	9358	9344	9288	9217	9128	9019	8914	8806	8692	8570	8439	8296	8142	7979
Denmark	3075	3063	3052	3041	3029	3017	3005	2993	2981	2969	2957	2945	2932	2920
Estonia	0	0	0	0	0	0	0	0	0	0	0	0	0	0
Finland	0	0	0	0	0	0	0	0	0	0	0	0	0	0
France	33,638	33,170	32,579	31,950	31,318	30,498	29,836	29,144	28,435	27,687	26,897	26,080	25,247	24,408
Germany	65,072	61,579	58,379	55,315	52,371	49,262	46,566	43,987	41,518	39,168	36,936	34,827	32,851	30,986
Greece	0	0	0	0	0	0	0	0	0	0	0	0	0	0
Hungary	16,781	16,729	16,665	16,601	16,537	16,463	16,399	16,336	16,272	16,208	16,145	16,082	16,019	15,957
Ireland	0	0	0	0	0	0	0	0	0	0	0	0	0	0
Italy	46,894	46,162	45,396	44,598	43,783	42,730	41,856	40,955	40,029	39,093	38,152	37,207	36,254	35,303
Latvia	6380	6380	6380	6380	6380	6380	6380	6380	6380	6380	6380	6380	6380	6380
Lithuania	0	0	0	0	0	0	0	0	0	0	0	0	0	0
Macedonia	0	0	0	0	0	0	0	0	0	0	0	0	0	0
Netherlands	37,700	37,355	36,907	36,439	35,949	35,359	34,830	34,285	33,724	33,150	32,565	31,950	31,304	30,630

(*continued on next page*)

Table 5 (*continued*)

Poland	8300	8282	8238	8172	8098	8007	7920	7828	7729	7622	7508	7385	7253	7113
Portugal	893	873	857	839	821	799	779	758	737	716	693	671	647	623
Romania	8165	8133	8099	8065	8031	7991	7956	7922	7887	7853	7818	7784	7749	7714
Serbia	1133	1120	1108	1096	1084	1070	1058	1045	1032	1019	1005	991	977	962
Slovakia	9002	8981	8925	8864	8791	8694	8604	8509	8407	8299	8183	8061	7932	7799
Slovenia	0	0	0	0	0	0	0	0	0	0	0	0	0	0
Spain	7905	7874	7843	7812	7776	7733	7693	7653	7611	7568	7524	7479	7434	7388
Switzerland	0	0	0	0	0	0	0	0	0	0	0	0	0	0
UK	12,703	12,657	12,573	12,485	12,381	12,216	12,075	11,928	11,777	11,623	11,470	11,319	11,172	11,031
TOTAL	295,548	290,044	284,333	278,604	272,874	266,235	260,506	254,791	249,087	243,400	237,730	232,087	226,482	220,931

gas demand of the European system peaked on the 18th of January. In the breakdown of the data by country outlined in Table 4, the extensive use of UGS in Germany stands out. As a result, its storage stock would reach 24% at the end of the study period, a very low value that could compromise supply in the remaining weeks of winter. Germany is a country with a large storage capacity and a strategic position in Central Europe, with many gas pipelines interconnecting with neighbouring countries. For these reasons, Germany represents 45% of total deliverability from natural gas storage in the EU during the two-week period.

Table 6 outlines the results of Case 2, considering a total disruption of the pipeline gas supply to Central Europe from Russia. The main conclusion of this hypothetical case study is that, even with the best possible strategy for gas supply, it would not be possible to meet the demand in five countries, and South-Eastern European countries would be the most affected (see Fig. 4). This supply crisis would occur despite increasing the use of all available resources: 100% own production, 97% LNG regasification capacity and 86% available capacity to import pipeline gas (mainly from Norway and Algeria because importing gas from Russia would not be available in this case). Underground gas storage use would also increase, leaving the available UGS working gas reserves at 29% by the end of the fourteen-day study period.

These results are in line with the forecasting studies conducted by operators of the European networks at the beginning of the 2016/2017 winter [46]. Those studies predicted a possible gas supply drop in South-Eastern European countries if the Russian gas transit through Ukraine was disrupted. In our case study, the situation is even more critical because supply through Belarus is also disrupted.

- Case 3 (demand from the 14th to the 27th of January of 2017, 50% initial storage and LNG supply disruption).

This case illustrates a scenario of prolonged disruption of LNG shipping, which could occur for commercial or meteorological reasons. The results outlined in Table 7 show that Spain, Portugal and Greece would not meet their demand for natural gas. In other words, the LNG shortage would affect only the three countries located in the corners of the continent as they are more dependent on LNG and have weak gas pipeline interconnections with their European neighbours. The analysis of the results from Spain in more detail shows that, surprisingly, only 20% storage is used because gas withdrawal is limited by a low daily deliverability due to the type of underground storage existing in the country [41].

- Cases 4, 5 and 6 (20% instead of 50% initial storage).

As indicated in the description of the case studies, the calculations made in three new scenarios are repeated assuming that the UGS inventory status is 20% instead of 50% at the beginning of the fourteen-day study period.

The mathematical tool provides the best possible solution to meet the demand, optimising the management of all capacities of the European natural gas system. As expected, the results clearly showed an increased use of available resources (see Table 8) and cross-border capacities between the countries of the system (see Table 9). In particular, UGS would be intensively used, leaving the inventory levels of working gas of the storage facilities at minimum values, lower than 8%. Nevertheless, only 10 of the 28 countries would be able to meet the national demand for natural gas, while five countries would not be able to meet 80% of the demand. Bulgaria and Bosnia would be the most affected countries, meeting only 50% of consumer needs during the two-week study period (see Fig. 5). In order to graphically present some of the findings, Fig. 6 shows the main comparative results of the case studies.

The analysis of Cases 2 and 5 shows some relevant differences in the use of cross-border interconnections from the other cases. The disruption of the Russian pipeline gas supply forces the internal gas pipelines in the EU system to reconfigure, reducing the use of unidirectional pipelines and increasing the use of bidirectional pipelines (see Table 9). This shift occurs because some unidirectional pipelines of the EU system are designed for gas transit from Russia to other European countries. However, in Cases 2 and 5, bidirectional pipelines gain prominence by

Table 6
Breakdown of the main results by country in Case 2.

	Demand satisfied		Production used		LNG imports used		Pipeline imports used		UGS ST 100%	UGS ST 50%	UGS SWR 50%	UGS ST final	
	GWh	%	GWh	%	GWh	%	GWh	%	GWh	GWh	GWh/d	GWh	%
Austria	7274	100%	616	100%	0		0		47,315	23,657	998	17,434	37%
Belgium	13,066	100%	0		3143	100%	6832	100%	4092	2046	170	1475	36%
Bosnia	145	100%	0		0		0		0	0	0	0	
Bulgaria	1304	65%	42	100%	0		0		2926	1463	36	1035	35%
Croatia	2103	100%	518	100%	0		0		2765	1383	58	1011	37%
Czechia	7181	100%	70	100%	0		0		18,715	9358	682	6174	33%
Denmark	1904	100%	2028	85%	0		0		6150	3075	194	2914	47%
Estonia	291	100%	0		0		0		0	0	0	0	
Finland	1415	100%	0		0		1415	41%	0	0	0	0	
France	41,684	100%	0		8610	100%	7980	100%	67,275	33,638	2205	20,964	31%
Germany	61,138	100%	2646	100%	0		23,943	100%	130,144	65,072	6657	20,661	16%
Greece	2510	83%	0		1050	100%	680	100%	0	0	0	0	
Hungary	8411	100%	952	100%	0		0		33,563	16,781	812	10,078	30%
Ireland	2539	100%	1680	100%	0		0		0	0	0	0	
Italy	54,010	100%	2394	100%	3801	100%	23,730	100%	93,787	46,894	2703	30,566	33%
Latvia	873	100%	0		0		0		12,760	6380	287	4925	39%
Lithuania	1256	100%	0		854	100%	0		0	0	0	0	
Macedonia	130	61%	0		0		0		0	0	0	0	
Netherlands	27,560	100%	27,104	100%	1387	45%	0		75,399	37,700	2400	24,247	32%
Poland	10,324	99%	1036	100%	1106	100%	0		16,601	8300	528	3179	19%
Portugal	3121	100%	0		2492	100%	0		1785	893	78	606	34%
Romania	7207	82%	4396	100%	0		0		16,329	8165	315	4593	28%
Serbia	1160	100%	211	100%	0		0		2265	1133	52	877	39%
Slovakia	3769	100%	0		0		0		18,003	9002	436	6748	37%
Slovenia	635	100%	0		0		0		0	0	0	0	
Spain	19,864	100%	42	100%	13,377	100%	7368	72%	15,810	7905	129	7293	46%
Switzerland	2896	100%	0		0		0		0	0	0	0	
UK	50,796	100%	28,098	100%	11,515	100%	12,550	60%	25,406	12,703	1324	8958	35%
TOTAL	334,566	99%	71,833	100%	47,335	97%	84,498	86%	591,090	295,548	20,064	173,738	29%

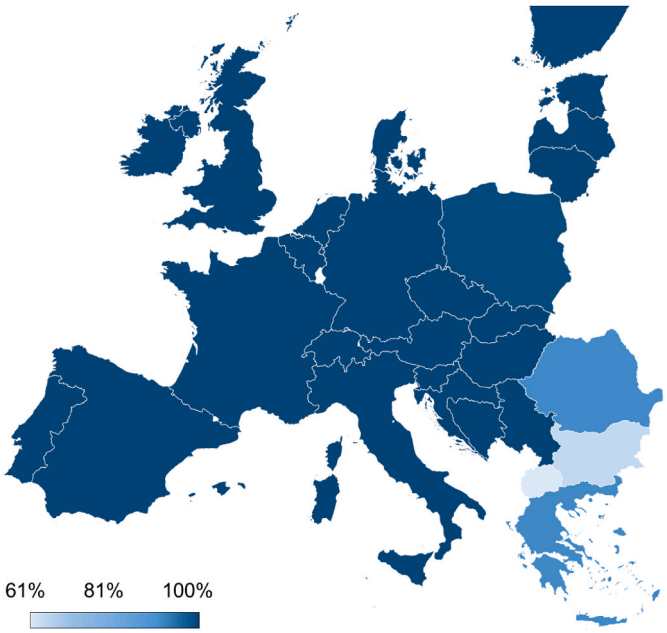

Fig. 4. Demand met by country in Case 2 study.

compensating for the loss of the Russian supply and by rebalancing internal gas flows in the EU system with the increase in the use of UGS and other sources of natural gas supply.

6. Conclusions

This article proposed a mathematical tool to maximise the coverage of global demand for natural gas during a fourteen-day supply crisis in the European natural gas system. The tool offers collaborative solutions to crises spurred by political events or natural phenomena, facilitating strategies for the optimal use of available resources and facilities, such as liquefied natural gas, underground storage and cross-border interconnections. The tool makes it possible to quickly update the decision-making process in the event of a supply crisis because its computation only requires seconds, while other techniques take hours or days to reach solutions as those based on simulation methods.

Six case studies were applied evaluate the impact of various gas supply disruption scenarios considering two different levels of initial storage during high-demand events. The findings demonstrated the applicability of the proposal, identifying optimal solutions throughout the entire interconnected gas infrastructure.

The mathematical model developed here can be applied to any interconnected gas system but is particularly relevant for the EU. Gas shortages can have significant economic and social effects in the EU, as it is highly dependent on external supplies. Therefore, the proposed tool offers means to meet the challenging objectives of Regulation (EU) 2017/1938, i.e. to provide a more cooperative approach, reduce the impact of gas supply disruptions and address the potential vulnerabilities in some member states revealed in this research for a two-week supply crisis. As observed in the case studies, South Eastern European countries are highly vulnerable to gas disruptions from Russia, while the Iberian Peninsula and Greece are more exposed to LNG shortages. These findings are quite similar to those already obtained in other studies developed by the European Network of Transmission System Operators for Gas (ENTSO-G) [47].

Table 7
Breakdown of the main results by country in Case 3.

	Demand satisfied		Production used		LNG imports used		Pipeline imports used		UGS ST 100%	UGS ST 50%	UGS SWR 50%	UGS ST final	
	GWh	%	GWh	%	GWh	%	GWh	%	GWh	GWh	GWh/d	GWh	%
Austria	7274	100%	616	100%	0	0%	0		47,315	23,657	998	19,212	41%
Belgium	13,066	100%	0		0	0%	6832	100%	4092	2046	170	1538	38%
Bosnia	145	100%	0		0	0%	0		0	0	0	0	
Bulgaria	1997	100%	42	100%	0	0%	2580	24%	2926	1463	36	1293	44%
Croatia	2103	100%	518	100%	0	0%	0		2765	1383	58	1035	37%
Czechia	7181	100%	70	100%	0	0%	0		18,715	9358	682	7059	38%
Denmark	1904	100%	2029	85%	0	0%	0		6150	3075	194	2921	47%
Estonia	291	100%	0		0	0%	291	43%	0	0	0	0	
Finland	1415	100%	0		0	0%	1415	41%	0	0	0	0	
France	41,684	100%	0		0	0%	7980	100%	67,275	33,638	2205	15,976	24%
Germany	61,138	100%	2646	100%	0	0%	45,926	100%	130,144	65,072	6657	30,127	23%
Greece	2210	73%	0		0	0%	680	100%	0	0	0	0	
Hungary	8411	100%	952	100%	0	0%	7702	91%	33,563	16,781	812	15,831	47%
Ireland	2539	100%	1680	100%	0	0%	0		0	0	0	0	
Italy	54,010	100%	2394	100%	0	0%	23,730	100%	93,787	46,894	2703	32,592	35%
Latvia	873	100%	0		0	0%	873	35%	12,760	6380	287	6380	50%
Lithuania	1256	100%	0		0	0%	1256	28%	0	0	0	0	
Macedonia	212	100%	0		0	0%	0		0	0	0	0	
Netherlands	27,560	100%	27,104	100%	0	0%	0		75,399	37,700	2400	28,145	37%
Poland	10,474	100%	1036	100%	0	0%	11,658	62%	16,601	8300	528	6561	40%
Portugal	1274	41%	0		0	0%	0		1785	893	78	145	8%
Romania	8781	100%	4396	100%	0	0%	4385	85%	16,329	8165	315	7642	47%
Serbia	1160	100%	211	100%	0	0%	0		2265	1133	52	955	42%
Slovakia	3769	100%	0		0	0%	8236	28%	18,003	9002	436	7375	41%
Slovenia	635	100%	0		0	0%	0		0	0	0	0	
Spain	13,840	70%	42	100%	0	0%	10,248	100%	15,810	7905	129	6295	40%
Switzerland	2896	100%	0		0	0%	0		0	0	0	0	
UK	50,796	100%	28,098	100%	0	0%	20,987	100%	25,406	12,703	1324	9233	36%
TOTAL	328,894	97%	71,834	100%	0	0%	154,779	77%	591,090	295,548	20,064	200,315	34%

Table 8
Main results of the case studies.

		Demand satisfied		Production used		LNG imports used		Pipeline imports used		UGS final	
		GWh	%	GWh	%	GWh	%	GWh	%	GWh	%
Case 1	Base case, UGS level at 50%	337,583	100%	71,836	100%	47,165	96%	138,606	69%	220,931	37%
Case 2	Disruption from Russia, UGS level at 50%	334,566	99%	71,833	100%	47,335	97%	84,498	86%	173,738	29%
Case 3	LNG disruption, UGS level at 20%	328,894	97%	71,834	100%	0	0%	154,779	77%	200,315	34%
Case 4	Base case, UGS level at 20%	337,583	100%	71,830	100%	47,329	97%	143,463	72%	47,926	8%
Case 5	Disruption from Russia, UGS level at 20%	327,797	97%	71,929	100%	49,000	100%	191,689	96%	9053	2%
Case 6	LNG disruption, UGS level at 20%	326,759	97%	71,835	100%	0	0%	166,150	83%	35,268	6%

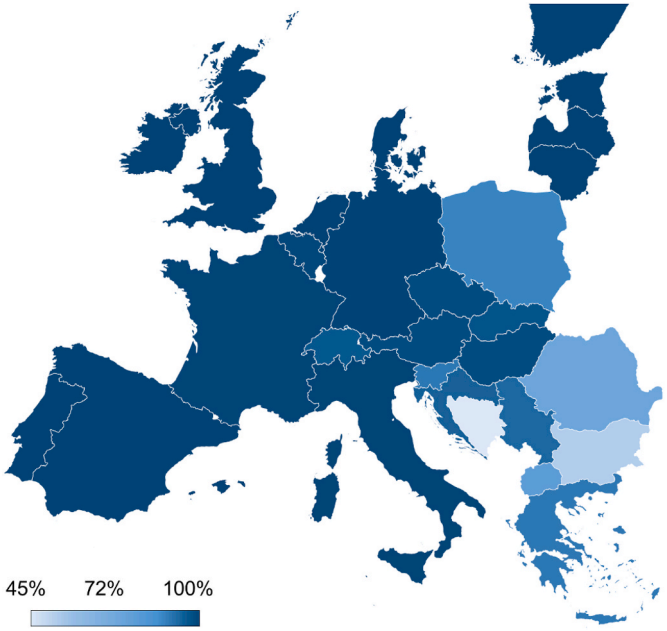

Fig. 5. Demand met by country in Case Study 5.

Given the dynamic nature of demand, production, storage and network flows, it is challenging to establish contingency plans in advance for all possible scenarios during a supply crisis. In fact, it may be necessary to continuously update the actions to be taken on the infrastructure, even if the crisis continues for an extended period. The cooperative solution resulting from the proposed mathematical model would enable rapid recovery of transnational gas infrastructures after a

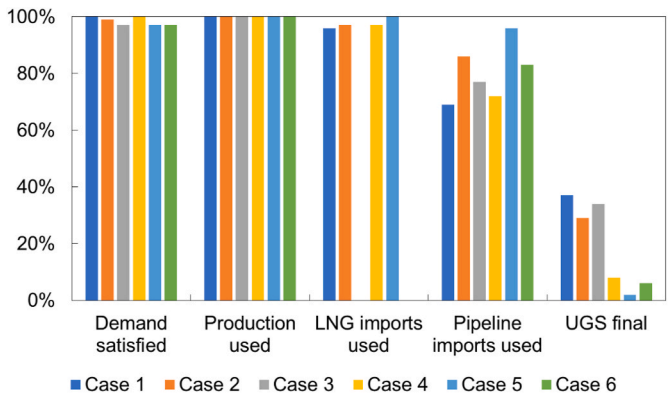

Fig. 6. Comparative results of the case studies.

Table 9
Average daily use of cross-border capacities.

	Unidirectional		Bidirectional		Average
	GWh/d	%	GWh/d	%	%
Capacity max	11,558		4674		
Capacity min			−7453		
Case 1	6193	54%	1661	36%	37%
			−897	12%	
Case 2	5603	48%	2709	58%	36%
			−233	3%	
Case 3	6418	56%	1342	29%	39%
			−1517	20%	
Case 4	6283	54%	1588	34%	38%
			−1060	14%	
Case 5	5251	45%	2975	64%	36%
			−284	4%	
Case 6	6539	57%	928	20%	40%
			−2067	28%	

partial or total outage caused by intentional threats, technical failures or natural disasters. In this way, the proposal could be helpful for transmission system operators, public authorities, utilities and other stakeholders. Moreover, measures taken for the security and resilience of gas systems could also benefit electrical infrastructure and minimise cascading effects across the energy sector as natural gas and power systems become increasingly interconnected.

Credit author statement

Jose M. Yusta: Conceptualization, Methodology, Software, Formal analysis, Writing - Original Draft, Writing - Review & Editing, Funding acquisition. **Jesus Beyza:** Methodology, Software, Writing - Review & Editing.

Declaration of competing interest

The authors declare that they have no known competing financial interests or personal relationships that could have appeared to influence the work reported in this paper.

Acknowledgements

This study was supported by the Ministry of Science and Innovation of Spain, under project PID2019-104711RB-100: Smart-grid design and operation under the threat of interrupted supply from electric power transmission systems with a high penetration of renewable energies.

References

[1] IEA, The Role of Gas in Transforming Energy, 2019.
[2] A. Agosta, N. Browne, G. Bruni, N. Tan, How COVID-19 and Market Changes Are Shaping LNG Buyer Preferences, 2020.
[3] C. Franza, L. de Jong, Van der Linde, The Future of Gas: the transition fuel? in: M. E. H, N.S. Silvia Colombo (Eds.), In *the Future Of Natural Gas. Markets And Geopolitics*, Hof Van Twente Lenthe/European Energy Review, The Netherlands, 2016, pp. 25–40.
[4] A. Safari, N. Das, O. Langhelle, J. Roy, M. Assadi, Natural gas: a transition fuel for sustainable energy system transformation? Energy Sci. Eng. 7 (4) (2019) 1075–1094.
[5] B. Gillessen, H. Heinrichs, J.-F. Hake, H.-J. Allelein, Natural gas as a bridge to sustainability: infrastructure expansion regarding energy security and system transition, Appl. Energy 251 (Oct. 2019) 113377.
[6] A. Buttler, H. Spliethoff, Current status of water electrolysis for energy storage, grid balancing and sector coupling via power-to-gas and power-to-liquids: a review, Renew. Sustain. Energy Rev. 82 (Feb. 2018) 2440–2454.
[7] J. Stern, "The Future of Gas in Decarbonising European Energy Markets : the Need for a New Approach, 2017.
[8] Eurostat, Natural Gas Supply Statistics, 2020.
[9] Eurostat, EU Imports of Energy Products - Recent Developments, 2020.
[10] European Parliament, Regulation (EU) No 994/2010 of the European Parliament and of the Council of 20 October 2010 Concerning Measures to Safeguard Security of Gas Supply and Repealing Council Directive 2004/67/EC, No. 12.11.2010, 2010, pp. 1–22.
[11] EU, Regulation (EU) 2017/1938 of the European Parliament and of the Council of 25 October 2017 Concerning Measures to Safeguard the Security of Gas Supply and Repealing Regulation (EU) No 994/2010, 2017, p. 56.
[12] European Parliament, Regulation (EU) 2019/941 of the european parliament and of the council of 5 june 2019 on risk-preparedness in the electricity sector L158/1 (14.06.2019) (2019) 1–21.
[13] ENTSO-G, TYNDP 2020 SCENARIO BUILDING GUIDELINES, 2020.
[14] F. Monforti, A. Szikszai, A MonteCarlo approach for assessing the adequacy of the European gas transmission system under supply crisis conditions, Energy Pol. 38 (5) (May 2010) 2486–2498.
[15] M. Flouri, C. Karakosta, C. Kladouchou, J. Psarras, How does a natural gas supply interruption affect the EU gas security? A Monte Carlo simulation, Renew. Sustain. Energy Rev. 44 (Apr. 2015) 785–796.
[16] R. Bolado, F. Gracceva, P. Zeniewski, P. Zastera, L. Vanhoorn, A. Mengolini, Best Practices and Methodological Guidelines for Conducting Gas Risk Assessments, Publications Office of the European Union, Luxembourg, 2012.
[17] K.A. Pambour, R. Bolado-Lavin, G.P.J. Dijkema, An integrated transient model for simulating the operation of natural gas transport systems, J. Nat. Gas Sci. Eng. 28 (2016) 672–690.
[18] K.A. Pambour, B. Cakir Erdener, R. Bolado-Lavin, G.P.J. Dijkema, "SAInt – a novel quasi-dynamic model for assessing security of supply in coupled gas and electricity transmission networks, Appl. Energy 203 (2017) 829–857.
[19] F. Holz, C. von Hirschhausen, C. Kemfert, A strategic model of European gas supply (GASMOD), Energy Econ. 30 (3) (May 2008) 766–788.
[20] V. Grimm, L. Schewe, M. Schmidt, G. Zöttl, A multilevel model of the European entry-exit gas market, Math. Methods Oper. Res. 89 (2) (Apr. 2019) 223–255.
[21] REKK, European gas market model (EGMM) [Online]. Available: https://rekk.hu/modeling/gas-market-modeling, 2021. (Accessed 27 April 2021). Accessed.
[22] R. Egging, Benders Decomposition for multi-stage stochastic mixed complementarity problems-Applied to a global natural gas market model, Eur. J. Oper. Res. 226 (2) (2013) 341–353.
[23] P.M. Richter, F. Holz, All quiet on the eastern front? Disruption scenarios of Russian natural gas supply to Europe, Energy Pol. 80 (May 2015) 177–189.
[24] M. Sesini, S. Giarola, A.D. Hawkes, The impact of liquefied natural gas and storage on the EU natural gas infrastructure resilience, Energy 209 (Oct. 2020) 118367.
[25] M.G. Boots, B.F. Hobbs, F.A.M. Rijkers, Trading in the downstream European gas market: a successive oligopoly approach, Energy J. 25 (3) (2004) 73–102.
[26] J. Perner, A. Seeliger, Prospects of gas supplies to the European market until 2030 - results from the simulation model EUGAS, Util. Pol. 12 (4) (2004) 291–302.
[27] H. Hecking, T. Panke, "COLUMBUS – a global gas market model, EWI Work. Pap. 12 (2012).
[28] S. Lochner, D. Bothe, From Russia with gas an analysis of the Nord Stream pipeline's impact on the European gas transmission system with the tiger-model from Russia with gas, Inst. Econ. Univ. Col. (2007) 1–16.
[29] B. Petrovich, H. Rogers, H. Hecking, S. Schulte, F. Weiser, Future European gas transmission bottlenecks in differing supply and demand scenarios, Oxford Inst. Energy Stud. NG 119 (2017).
[30] A. del Valle, S. Wogrin, J. Reneses, Multi-objective bi-level optimization model for the investment in gas infrastructures, Energy Strateg. Rev. 30 (2020) 100492.
[31] A. Szikszai, F. Monforti, GEMFLOW: a time dependent model to assess responses to natural gas supply crises, Energy Pol. 39 (9) (Sep. 2011) 5129–5136.
[32] Y. Rqiq, J. Beyza, J.M. Yusta, R. Bolado-Lavin, Assessing the impact of investments in Cross-border pipelines on the security of gas supply in the EU, Energies 13 (11) (2020).
[33] N. Rodríguez-Gómez, N. Zaccarelli, R. Bolado-Lavín, European ability to cope with a gas crisis. Comparison between 2009 and 2014, Energy Pol. 97 (Oct. 2016) 461–474.
[34] ENTSO-G, Winter Supply Review 2016/2017, Brussels, Belgium, 2017.
[35] ENTSO-E, ENTSO-E's Statistical Factsheet 2017, 2018.
[36] Eurostat, European database [Online]. Available: https://ec.europa.eu/eurostat/data/database, 2017. (Accessed January 2021). Accessed, 27.
[37] Gas Infrastructure Europe (GIE), System Development Map 2017, 2017 [Online]. Available: https://www.entsog.eu/sites/default/files/2018-12/ENTSOG_GIE_SYSDEV_2017-2018_1600x1200_FULL.pdf. Accessed: 27-Jan-2021.
[38] Gas Infrastructure Europe (GIE), Storage database [Online]. Available: https://www.gie.eu/index.php/gie-publications/databases/storage-database, 2021. Accessed: 27-Jan-2021.
[39] European Commission, Liquefied Natural Gas and gas storage will boost EU's energy security, EU Liq. Nat. Gas Gas Storage Strat. (2016) [Online]. Available: https://ec.europa.eu/commission/presscorner/detail/en/MEMO_16_310.
[40] U.S. Energy Information Administration, The Basics of Underground Natural Gas Storage, 2015 [Online]. Available: https://www.eia.gov/naturalgas/storage/basics/.
[41] ENTSO-G, Winter Supply Outlook 2017/2018, " Brussels, Belgium, 2017.
[42] A.N. Stulberg, Natural gas and the Russia-Ukraine crisis: strategic restraint and the emerging Europe-Eurasia gas network, Energy Res. Soc. Sci. 24 (Feb. 2017) 71–85.
[43] BP, Statis. Rev. World Energy 2020 (2020) 66.
[44] V. Kutcherov, M. Morgunova, V. Bessel, A. Lopatin, Russian natural gas exports: an analysis of challenges and opportunities, Energy Strateg. Rev. 30 (2020) 100511.
[45] ENTSO-G, Winter Supply Review 2019/2020, " 2019.
[46] ENTSO-G, Winter Supply Outlook 2016/2017, 2017.
[47] ENTSO-G, Security of Supply Simulation Report, 2017.

Engineering Applications of Artificial Intelligence 117 (2023) 105567

Contents lists available at ScienceDirect

Engineering Applications of Artificial Intelligence

journal homepage: www.elsevier.com/locate/engappai

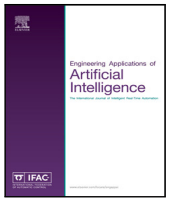

Power flow analysis via typed graph neural networks

Tania B. Lopez-Garcia, José A. Domínguez-Navarro *

University of Zaragoza, C. María de Luna, Zaragoza, 50018, Spain

ARTICLE INFO

Keywords:
Power flow
Graph neural networks
Unsupervised learning
Physics-informed neural networks

ABSTRACT

Power flow analyses are essential for the correct operation of power grids, however, electricity systems are becoming increasingly complex to analyze with the conventional numerical methods. The present work proposes a typed graph neural network based approach to solve the power flow problem. The neural networks are trained on benchmark power grid cases which are modified by varying the injections (load and generation), branch characteristics and topology. The solution to the power flow analysis is found when all voltage values are known. The proposed system infers the voltage magnitude and phase and is trained so that the obtained values minimize the violation of the physical laws that govern the system, this way the training is achieved in an unsupervised manner. The proposed solver has linear time complexity and is able to generalize to grids with considerably different conditions, including size, from the grids available during training. Though the training is unsupervised and does not suppose any ground truth data, the solutions obtained are found to have a close correlation with the conventional Newton–Raphson method. The results are additionally validated by finding the root mean square deviation from the Newton–Raphson method, and the faster, though less accurate, DC approximation method.

1. Introduction

For correct power system operation, power flow analyses must be executed frequently, as they are necessary for many procedures such as power systems planning, security assessment, management and optimization, Glover et al. (2012). Conventionally, the power flow analysis is carried out by determining and solving a set of non-linear algebraic equations with iterative numerical analysis methods; most known methods of this type have been tested at some point to solve the power flow problem, Stott (1974) and van Amerongen (1989). In recent years both the importance and complexity of software modeling of the electrical grid have increased due to higher electrical demand and the need to increase the sustainability of the conventional power grid, Smith et al. (2022). These issues arise from the ambitious, yet necessary, goals for emission reduction. Electrification of diverse energy sectors, such as heating and transport, has become a strategy for decarbonization, this phenomenon has consequently increased the demand and the dependence on electricity, Xie et al. (2021). In parallel, the use of variable renewable energy sources (VRES), such as solar and wind, is expanding. VRES are non-dispatchable and require power systems to become more flexible; they may cause loading in sections of the grid where it is usually not expected and cause instability, Babatunde et al. (2020). Many of the methods currently used for power system modeling were developed before widespread integration of VRES and the electrification of transport and heating, furthermore, most are computationally intensive. The increasing complexity of the electricity system may become too convoluted to describe in a timely and precise manner with conventional PF analysis approaches, thus requiring the investigation of new tools for power system modeling (Tovar-Facio et al., 2021).

With the emergence of artificial intelligence, many systems such as decision trees, neural networks and fuzzy logic methods have been applied to power system problems, Vankayala and Rao (1993) and Lopez-Garcia et al. (2020). Amongst these approaches, artificial neural networks (NNs) have shown promise to a certain extent, due to their ability to synthesize complex mappings accurately and rapidly, along with the possibility to continuously learn. However, most NNs used for power system modeling, such as in Hu et al. (2021) and Fikri et al. (2018), implement multi-layer perceptrons (MLPs). MLPs usually suffer from local minima and over-fitting issues, in addition to not scaling well to larger power grids; MLP based models cannot be used for grids of different size or configuration from the ones they are trained on.

Recently, graph neural networks (GNNs) have gained popularity for learning structured data and transferring learned information beyond training conditions (Battaglia et al., 2018). These methods convey strong relational inductive biases by establishing the GNN architecture directly on the structure of the analyzed system, which guides these approaches towards learning not only about the elements of the system, but also the relationships between them. By basing the proposed solver on GNNs, several advantages are introduced, such as scaling well to

* Corresponding author.
E-mail addresses: lopez.200916947@gmail.com (T.B. Lopez-Garcia), jadona@unizar.es (J.A. Domínguez-Navarro).

https://doi.org/10.1016/j.engappai.2022.105567
Received 8 June 2022; Received in revised form 11 October 2022; Accepted 25 October 2022
Available online 15 November 2022

larger power grids, and having the ability to generalize decently on grids of different size and configuration from the grids seen during training.

There are a few other works that apply GNNs (or NNs in general) for power grid analysis. The work in Owerko et al. (2020) uses GNNs but is based on imitation learning, and thus the GNN is burdensome to train and does not generalize well outside similar cases to those seen in training. A pioneering work by Donon et al. (2020) also applies GNNs, and training is carried out in an unsupervised manner, however the model is complicated and does not consider changes in grid topology during training.

The proposed model presents a simple GNN based solver to calculate the AC power flow in a way that allows to solve many different scenarios in parallel, considering the continuously changing balance between energy supply and demand, and does this in linear time as opposed to the exponential time needed for conventional methods that solve Jacobian matrices. The proposed solver is based on a generalization of GNNs called typed graph networks (TGNs) (Avelar et al., 2019), which allows different types of elements to be defined instead of the usual nodes and edges. The use of TGNs allows to obtain more faithful representations of the different elements present in electrical grids, such as the branches and the different types of buses, by considering each of them as different node types in the corresponding graph representation. Like other GNN based models, the presented solver can generalize to electrical grids of different sizes and parameters, yet it additionally considers changes in the grid topology during training, making it specially adequate for analyzing different scenarios of possible line outages, which is essential for security assessments. Additionally, the training is carried out in an unsupervised manner, applying physics-informed neural networks by incorporating information of the physical system in the loss function and aiming to minimize the violation of the physical laws that govern the system, thus eliminating the time consuming need of solving the training cases beforehand with other solvers to produce targets. The solver is modular in nature, allowing to connect different node types in any desired configuration. Additionally the time complexity of the proposed solver is linear, in contrast with common methods, such as the Newton–Raphson, which has exponential time complexity.

In summary, the proposed method consists of a TGN based system that abstracts the relationship between the different elements in the electrical grid to solve the steady state power flow problem for dynamical networks, i.e. considering different grid configurations, injections and branch characteristics. Thus, the presented work presents a valuable step towards developing a machine learning based system that is able to assist in analyzing flexible electrical grids of increasing complexity, while improving speed and reducing the computational burden of essential power flow analyses.

2. Preliminaries

In this section the basic components and power flow formulation are described, along with a general description of TGNs, which are the basis of the proposed model and solver. The description of the variables used to describe the electrical grid can be found in Table 1, and the definition of the main components used in the proposed solver are found in Table 2.

2.1. Power flow formulation

This work focuses on solving the power flow problem of power grids in a steady-state condition. Power grids are basically formed by buses, branches, loads and generators. The buses are the nodes to which the other elements are connected. Branches connect two buses and are modeled internally using the standard π transmission line model. The branch series impedance is given by the complex value: $z_k = r_k + ix_k$, where the resistance of the branch model constitutes the real part, and the equivalent reactance, the imaginary part. The shunt susceptance of the equivalent branch model is represented by b_k; this general model can include an ideal phase shifting transformer located at the sender end of the branch. The objective of the power flow analysis is to determine the voltage magnitude and phase at all buses for a given load, generation, and grid configuration state.

Table 1
Power grid nomenclature.

Variable	Units	Definition
n	–	Bus ID index
m	–	Generator bus ID index
k	–	Branch ID index
from_k	–	Sender bus ID of branch k
to_k	–	Receiver bus ID of branch k
V_n	kV	Voltage magnitude at bus n
θ_n	rad	Voltage phase at bus n
Pd_n	MW	Active power load at bus n
Qd_n	MVAr	Reactive power load at bus n
Pg_m	MW	Active power generation at generation bus m
Vg_m	kV	Voltage magnitude setpoint at generation bus m
r_k	Ω	Series resistance for branch k
x_k	Ω	Series reactance for branch k
b_k	S	Total line charging susceptance for branch k
τ_k	–	Transformer tap ratio
θ_k^{shift}	rad	Transformer phase shift

The power that flows through the grid depends on the power imbalances at the buses and the impedance of the branches, while the power balance at each bus is determined by the possible loads, generators and branches attached to it. Loads and generators constitute the external injections of the power grid, loads as a specified power demand, and generators as a specified power source. Given the grid topology, the specified values of the injections and line characteristics, the proposed power flow solver computes the resulting voltages in the buses and hence the current flow through the branches can be determined. The relationship between the branch characteristics, the voltages of the buses and the currents is given by:

$$\begin{bmatrix} i_{\text{from}_k} \\ i_{\text{to}_k} \end{bmatrix} = Y_{br,k} \begin{bmatrix} v_{\text{from}_k} \\ v_{\text{to}_k} \end{bmatrix} \tag{1}$$

where i_{from_k} and i_{to_k} represent the complex current injections at the sender and receiver sides of branch k, respectively; v_{from_k} and v_{to_k} are the complex voltage values at the sender and receiver sides of branch k, respectively; the k branch admittance matrix $Y_{br,k}$ given by:

$$Y_{br,k} = \begin{bmatrix} \left(y_k + i\frac{b_k}{2}\right)\frac{1}{\tau_k^2} & -y_k \frac{1}{\tau_k e^{-i\theta_k^{\text{shift}}}} \\ -y_k \frac{1}{\tau_k e^{-i\theta_k^{\text{shift}}}} & y_k + i\frac{b_k}{2} \end{bmatrix} \tag{2}$$

where the series admittance element y_k is denoted by $y_k = \frac{1}{z_k}$.

It should be noted that before the load flow is solved, the network losses are unknown, thus, a generator bus, called the slack bus, is designated to compensate for these losses. The voltage magnitude and phase are given beforehand for the chosen slack bus ($n = 0$), and the power needed to compensate for the total grid losses must be determined. In addition to the slack bus, two other types of buses are defined: PV buses constitute the set of buses directly connected to a generator (that are not the slack bus); the remaining non-generation buses are classified as PQ buses. For each PV bus n_{PV}, the voltage magnitude is given by $Vg_{n_{PV}}$ and the generated active power is given by $Pg_{n_{PV}}$; for these buses the voltage phase $\theta_{n_{PV}}$, and the generated reactive power $Qg_{n_{PV}}$, must be determined. For each PQ bus n_{PQ}, the active and reactive powers are given by: $P_{n_{PQ}} = -Pd_{n_{PQ}}$ and $Q_{n_{PQ}} = -Qd_{n_{PQ}}$; for these buses both voltage magnitude and phase, $V_{n_{PQ}}$ and $\theta_{n_{PQ}}$, must be found.

For a solution to be obtained, the power balance in all nodes must be achieved by solving a non-linear equation system of the form $\Delta S = 0$,

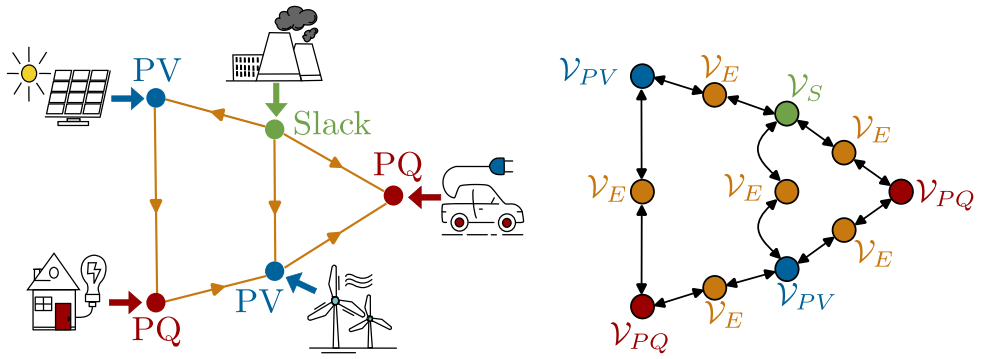

(a) Power grid toy example (b) TGN representation

Fig. 1. Relationship between a power grid toy example and the corresponding TGN layer.

Table 2
Proposed solver components.

Component	Definition
$\mathcal{G}$	A graph
ζ	Set of node types
$\mathcal{V}_i$	Set of type i nodes
d_i	Embedding dimension of type i nodes
$\mathbf{A}$	Adjacency matrix
L	Total message passing iterations
T	Total TGN layers

which is deconstructed into nodal power balance equations as functions of unknown voltage values, as shown below for a bus n:

$$\Delta P_n(V_n,\theta_n) = Pg_n - Pd_n - \mathrm{Re}\left[\left(\sum_{\substack{k\in\mathcal{N}(n)\\ n=\mathrm{from}_k}} i_{\mathrm{from}_k} + \sum_{\substack{k\in\mathcal{N}(n)\\ n=\mathrm{to}_k}} i_{\mathrm{to}_k}\right)\cdot v_n\right] \tag{3}$$

$$\Delta Q_n(V_n,\theta_n) = Qg_n - Qd_n - \mathrm{Im}\left[\left(\sum_{\substack{k\in\mathcal{N}(n)\\ n=\mathrm{from}_k}} i_{\mathrm{from}_k} + \sum_{\substack{k\in\mathcal{N}(n)\\ n=\mathrm{to}_k}} i_{\mathrm{to}_k}\right)\cdot v_n\right] \tag{4}$$

where $k \in \mathcal{N}(n)$ represents all the branches that are connected to bus n.

There are $N_{pv} + 2N_{pq}$ voltage values that must be found (only phase for PV buses and both phase and magnitude for PQ buses), where N_{pv} and N_{pq} are the number of PV and PQ buses, respectively. Afterwards, $N_{pv} + 1$ reactive power balance equations are solved to find the generator reactive power injections, and this way all unknown variables are found.

2.2. Typed graph networks

It results straightforward to represent a power grid as a graph, the approach taken in this work is illustrated with a toy example in Fig. 1. The toy power grid shown in Fig. 1(a) includes PV, PQ and slack nodes, the branches that connect them and the external injections; Fig. 1(b) shows how the proposed solver architecture is directly related to the grid structure. The goal of the presented system is to infer the voltage values by representing the power grid as graph structured data and learning the relationships between the different elements; in other words, the proposed system takes a relational data graph as input, and outputs nodal voltage predictions. To achieve said goal, TGNs are employed; a brief description is found below.

Normally, a graph is defined as $\mathcal{G} = (\mathcal{V}, \mathcal{E})$, with $\mathcal{V} = \{1, \ldots, N\}$ a finite set of nodes, and $\mathcal{E} = \{1, \ldots, K\} \subseteq \mathcal{V} \times \mathcal{V}$ a set of edges defined as nodal pairs. In a single sample of a graph signal, an input vector x_n from the graph input $\mathbf{x} \in \mathbb{R}^N$ is assigned to each node in $\mathcal{V}$. The graph structure, or topology of the graph, is represented in matrix form, typically by an adjacency matrix $\mathbf{A} \in \mathbb{R}^{N\times N}$, defined as:

$$A_{i,j} = \begin{cases} 1, & \text{if } (i,j) \in \mathcal{E} \\ 0 & \text{otherwise} \end{cases} \tag{5}$$

The generally accepted graph network model proposed by Battaglia et al. (2018) projects the nodes, edges, and possibly the entire graph to a d-dimensional space. The nodal embedded states iteratively add information from their k-hop neighborhood over numerous message-passing steps, in which nodes are updated as a function of the embedded values of neighboring nodes and their own previous state. Information is propagated between nodes, edges and possibly the whole graph (Gilmer et al., 2017). The broadcasting of signals on the graph is computed as a series of local operations, commonly matrix multiplications with adjacency matrices are employed. Taking $z_n^{(l)} \in \mathbb{R}^d$ as the embedded state of node n on iteration l, the embedding, updating and outputting steps are:

$$\mathbf{z}^{(0)} = \mathbf{x} \tag{6}$$

$$\mathbf{z}^{(l+1)} = f\left(\mathbf{z}^{(l)}, \bar{\mathbf{A}}\right) \tag{7}$$

$$\mathbf{z}^{(L)} = \mathbf{y} \tag{8}$$

where $\mathbf{z}$ represents the embedded state of the graph, $\mathbf{y}$ the nodal prediction output, f a non-linear state update function that depends on the accumulated messages of neighboring nodes and the previous state of the nodes themselves; $\bar{\mathbf{A}} = \mathbf{A} + I$, with I as the identity matrix, is an adjacency matrix augmented with self loops (to allow the incorporation of information from the nodes themselves, and not just from neighboring nodes) (Kipf and Welling, 2017).

The elements of the power grid are related through the grid topology, and the state of the grid depends on both external injections and this configuration, it is thus evident that a natural correspondence between power grids and graph networks exists. However, the defined bus types are fundamentally different in that each has different characteristics and a different number of expected outputs. Furthermore, the branch characteristics are important factors in determining the resulting voltages, such that they cannot be treated as simple edges, but are not expected to produce an output. In essence, the different grid elements should be treated as distinct node types, as shown in Fig. 1(b).

TGNs are a generalization of GNNs, in that instead of defining nodes and edges as the graph elements, the concept of node types is adopted. This way the edges can be defined as a type of node, and a finite number of additional node types can be designated. This outlook presents several advantages; each node type can have different output, projected state dimensions, and update function parameters.

This way a relevant difference with respect to conventional GNNs is the way the message-passing and update iterations are computed. For a TGN with a ζ set of node types, message passing functions are defined

for node types that have at least one pair of adjacent nodes, to compute messages from one projection dimension to the other:

$$\mathcal{M} = \{\mu : \mathbb{R}^{d_j} \rightarrow \mathbb{R}^{d_i} |\ i, j \in \zeta,\ A_{i,j} \neq \mathbf{0}\} \tag{9}$$

The outputs from the message passing functions are propagated via matrix multiplication with adjacency matrices that indicate the sparsity pattern between the different node types, e.g. an adjacency matrix between types i and j nodes is represented as $A_{i,j} \in \mathbb{R}^{d_i \times d_j}$. For each node type i, their corresponding update function, ϕ_i concatenates their previous state with the propagated messages from neighboring node types, such that:

$$\phi_i : \mathbb{R}^{d_i + D_i} \rightarrow \mathbb{R}^{d_i} \tag{10}$$

$$D_i = \sum_{\substack{\mu : \mathbb{R}^{d_j} \rightarrow \mathbb{R}^{d_i} \\ j \in \mathcal{N}(i)}} d_i \tag{11}$$

where $\mathcal{N}(i)$ represents the set of all node types that directly interact with type i nodes, and D_i is the dimension of the final accumulation of messages that are concatenated from the neighboring node types. Thus the update function input for each node consists of the final accumulation of messages concatenated with their previous node state.

This way, the TGN structure takes as input a feature vector for every node of every node type, i.e. $\mathbf{x}_i \in \mathbb{R}^{f_i}$, for a node type i, where f_i is the dimension of the input features. All nodes are projected to their corresponding embedding space through a linear function, $\gamma_i : \mathbf{x}_i \rightarrow \mathbf{z}_i \in \mathbb{R}^{d_i}$. Then message passing and node update functions are repeated iteratively for L message passing steps. The nodal outputs are obtained from a final mapping, $\varphi_i : \mathbf{z}_i \rightarrow \mathbf{y}_i \in \mathbb{R}^{o_i}$; where o_i is the desired output dimension for i type nodes.

3. Methodology

In this section a description of how the TGN framework is applied to solve the power flow problem is presented. It is shown that by training four small MLPs, the power flow problem can be solved in linear time, robust to changes in topology (in particular to single branch line outages) and different branch characteristics. The training is not supervised, but physics-informed, and the solver architecture is modular in nature. First a description of the proposed TGN based model is reported, and then the training mechanism is explained.

3.1. TGN based power flow solver

In the proposed method, a predefined number T of TGN layers is used to iteratively approximate the missing voltage values at every node of the power grid. The message passing and update functions, μ and ϕ, are small fully connected neural networks; their parameters are the only ones that must be learned. These functions are the same for all nodes of the same type in the same layer, supporting the concept of combinatorial generalization, this way, the same TGN architecture can operate with input graphs of different sizes and shapes.

While the embedding, message passing, update and output functions of each TGN layer are independently parameterized, the layers are structurally the same; each one is defined by four types of nodes: branch nodes ($\mathcal{V}_E$) to include branch characteristics, PV nodes ($\mathcal{V}_{PV}$) for generator buses, PQ nodes ($\mathcal{V}_{PQ}$) for load buses, and slack nodes ($\mathcal{V}_S$) for slack buses. Different input features are defined for each type of node, as shown below for a layer t:

$$\mathbf{x}_{PV}\begin{cases} V_i(t) \\ \theta_i(t) \\ \Delta P_i(t) \\ Qg_i(t), \end{cases} \quad \mathbf{x}_{PQ}\begin{cases} V_j(t) \\ \theta_j(t) \\ \Delta P_j(t) \\ \Delta Q_j(t), \end{cases} \quad \mathbf{x}_{S}\begin{cases} V_s \\ \theta_s \\ Pg_s(t) \\ Qg_s(t), \end{cases} \quad \mathbf{x}_{E}\begin{cases} \rho(r_k, x_k) \\ \delta(r_k, x_k) \\ b_k \end{cases} \tag{12}$$

$\forall i \in \mathcal{V}_{PV}, \forall j \in \mathcal{V}_{PQ}, \forall s \in \mathcal{V}_S, \forall k \in \mathcal{V}_E$

As was mentioned in Section 2.1, the branch series impedance is given by the complex value: $z_k = r_k + ix_k = |z_k| \angle \varphi$, however, making reference to the conventional admittance matrix, the branches admittance magnitude and phase are chosen as features. The admittance is given by: $y_k = \frac{1}{z_k} = \frac{1}{|z_k|} \angle -\varphi = \rho \angle \delta$. Defining the magnitude and phase of the series admittance of each branch as ρ and δ, respectively, the first two branch node features are thus established as:

$$\rho(r_k, x_k) = \frac{1}{\sqrt{r_k^2 + x_k^2}} \tag{13}$$

$$\delta(r_k, x_k) = -\arctan\left(\frac{x_k}{r_k}\right) \tag{14}$$

The last branch node feature b_k corresponds to the total line charging susceptance. These branch input features remain unchanged throughout all TGN layers. Concerning the other features, the rotating angle of the buses is measured relative to the chosen slack bus, as is common in power flow analyses, i.e. $\theta_n = \theta_s,\ \forall n \in \left(\mathcal{V}_{PV} \bigcup \mathcal{V}_{PQ}\right)$. Apart from this, an initial 'flat' guess of voltage magnitude values is established, with $V_j = 1$ (per unit), $\forall j \in \mathcal{V}_{PQ}$. This initial voltage state is used for the first TGN layer, and the following TGN layers receive the voltage approximation of the previous layer; after each approximation, the power balance error (ΔP and ΔQ) is calculated at each bus and is used as part of the input features for the next TGN layer. The reactive power at generator buses is locally compensated, such that $\Delta Q_j = 0$, this does not provide additional information and is thus excluded from the $\mathcal{V}_{PV}$ input features. A similar situation happens with the slack node where both active and reactive powers are compensated; thus, the calculated powers generations are used as input features. Furthermore, the same adjacency matrices are used for every layer of the TGN based solver since the configuration of the power grid is not altered between layers.

For the message-passing steps three distinct adjacency matrices are defined: between $\mathcal{V}_E$ nodes and $\mathcal{V}_{PV}$, $\mathcal{V}_{PQ}$ and $\mathcal{V}_S$ nodes, as shown in Eq. (15). Only three adjacency matrices are needed because bus type nodes cannot be directly connected to each other, but instead are always connected through branch type nodes. The adjacency matrices may be transposed depending on whether information is moving from a branch node to a bus node, or vice versa.

$$\begin{aligned} \mathbf{A}_{PV,\ E} &\in \mathbb{R}^{|\mathcal{V}_{PV}| \times |\mathcal{V}_E|} \\ \mathbf{A}_{PQ,\ E} &\in \mathbb{R}^{|\mathcal{V}_{PQ}| \times |\mathcal{V}_E|} \\ \mathbf{A}_{S,\ E} &\in \mathbb{R}^{1 \times |\mathcal{V}_E|} \end{aligned} \tag{15}$$

A predefined number L of message passing and state update steps is set; for this procedure, the same NNs μ and ϕ, are applied at each iteration to propagate and aggregate information across the graph, and update the graph state. At the final update step, each node has shared information with neighboring nodes L−hops away (Battaglia et al., 2018). This iterative message-passing and updating process is illustrated in Fig. 2. The output of each TGN layer is obtained by decoding the final states of the $\mathcal{V}_{PV}$ and $\mathcal{V}_{PQ}$ node types. The layer outputs correspond to the inferred change in voltage values, ΔV and $\Delta\theta$, with respect to the input voltage values, for the corresponding TGN layer, as shown below:

$$\mathbf{y}_{PV}\begin{cases} \Delta\theta_i \end{cases}, \quad \mathbf{y}_{PQ}\begin{cases} \Delta V_j \\ \Delta\theta_j \end{cases}, \tag{16}$$

$\forall i \in \mathcal{V}_{PV}, \forall j \in \mathcal{V}_{PQ}$

The voltage values after every TGN layer are updated by:

$$\hat{V}(t+1) = \Delta V + \hat{V}(t) \tag{17}$$

$$\hat{\theta}(t+1) = \Delta\theta + \hat{\theta}(t) \tag{18}$$

With the updated voltage values, Eqs. (3) and (4) are used to calculate the power balance error in each bus, the reactive power

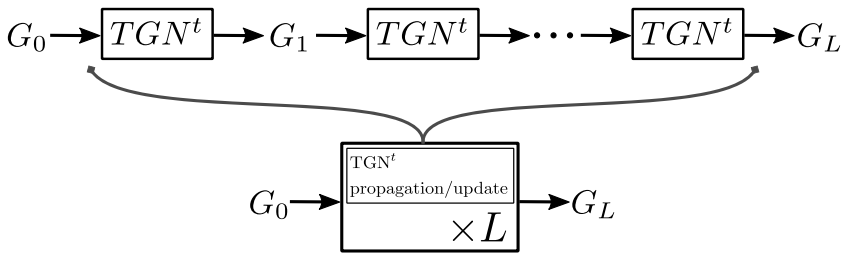

Fig. 2. Message passing and update state procedure (shared weights).

compensation in generator buses, and both active and reactive power compensation in the slack bus. If the last layer has not been reached, the voltage values and power balance error values are used to determine the graph input for the next TGN layer, otherwise, they are used to evaluate the cost function. The iterative portion of the proposed power solver structure is summarized by Algorithm 1 and illustrated in Fig. 3. If the model is being trained, the final voltage inference is used with the power equilibrium equations to calculate the loss function and then the Adam optimization algorithm is applied to find new NN parameters, as is explained in Section 3.3. If the model is not being trained, the process ends with the final voltage inference values.

Algorithm 1 TGN based PF solver

Require: $\mathcal{G} = \bigcup_{i\in\zeta} \mathcal{V}_i, \quad A_{i,j} \in \mathbb{R}^{d_i \times d_j} | i,j \in \zeta, \quad \zeta = \{PV, PQ, S, E\}$

Input: S = grid state (injections, branch characteristics, topology)

$\hat{V}_{PQ}^{(0)} = 1,\ \hat{\theta}_{PV,PQ}^{(0)} = 0$ ▷ Flat start

$t = 0$

while $t \leq T$ **do** ▷ Iterate over a predefined number of TGN layers

  $\Delta P^{(t)} = P_g - P_d - P_{bus}(\hat{V}^{(t)}, \hat{\theta}^{(t)})$ ▷ Power balance error

  $\Delta Q^{(t)} = Q_g - Q_d - Q_{bus}(\hat{V}^{(t)}, \hat{\theta}^{(t)})$

  for each $i \in \zeta$ **do** ▷ For all node types

    $\mathbf{x}_i = \mathbf{f}_i(\hat{V}^{(t)}, \hat{\theta}^{(t)}, \Delta P^{(t)}, \Delta Q^{(t)}, S)$ ▷ Input features: $\mathbf{x}_i \in \mathbb{R}^{N_i \times f_i}$

    $\mathbf{z}_i^{(0)} = \gamma_i(\mathbf{x}_i)$ ▷ Node embedding: $\mathbf{z}_i \in \mathbb{R}^{N_i \times d_i}$

    $l = 0$

    while $l \leq L$ **do** ▷ L message-passing steps

      $\bar{\mu}_i = \text{concat}\left(A_{i,j} \cdot \mu_i\left(\mathbf{z}_j^{(l)}\right)\right), \forall j \in \mathcal{N}(i)$ ▷ Message aggregation

      $\mathbf{z}_i^{(l+1)} = \phi_i\left(\mathbf{z}_i^{(l)}, \bar{\mu}_i\right)$ ▷ Update $\forall i \neq S$

      $l \leftarrow l + 1$

    end while

  end for

  $\hat{V}_{PV}^{(t)} = \varphi_{PV}\left(\mathbf{z}_{PV}^{(L)}\right)$ ▷ Outputs: $\mathbf{y}_i \in \mathbb{R}^{N_i \times o_i}$

  $\hat{V}_{PQ}^{(t)}, \hat{\theta}_{PQ}^{(t)} = \varphi_{PQ}\left(\mathbf{z}_{PQ}^{(L)}\right)$

  $t \leftarrow t + 1$

end while

Output: $\hat{\theta}_{PV}^{(T)}, \hat{V}_{PQ}^{(T)}, \hat{\theta}_{PQ}^{(T)}$ ▷ Final voltage inference

3.2. Model computational complexity

Each TGN layer is composed of four main functions: encoding, message passing, updating and decoding. The four functions are defined by small MLPs, with either one or two layers. All MLPs with two layers have one layer with a hyperbolic tangent activation function, and a linear layer; the MLPs with a single layer are linear. Different instances of the encoding MLPs are defined for each of the four node types ($\mathcal{V}_{PV}$, $\mathcal{V}_{PQ}$, $\mathcal{V}_E$, $\mathcal{V}_S$); these MLPs have a single layer of size $f_x \times d_x$ for each node type x, where f_x and d_x are the corresponding feature vector size and embedding dimension, respectively. Five message passing functions are defined: two to exchange information to and from $\mathcal{V}_{PV}$ and $\mathcal{V}_E$, two to exchange information between $\mathcal{V}_{PQ}$ and $\mathcal{V}_E$, and one for passing information from $\mathcal{V}_S$ to adjacent $\mathcal{V}_E$ nodes. The message passing MLPs have two layers, the first of size $d_{IN} \times d_{IN}$, and the second of size $d_{IN} \times d_{OUT}$. When a type x node casts information unto a type y node ($\mathcal{V}_x \rightarrow \mathcal{V}_y$), d_{IN} and d_{OUT} represent the embedding size of the type x and type y nodes, respectively. Only $\mathcal{V}_{PV}$, $\mathcal{V}_{PQ}$ and $\mathcal{V}_E$ are updated; $\mathcal{V}_S$ nodes pass their corresponding information through the $\mathcal{V}_E$ nodes but do not need to be updated, as no information is sent to them and no output is required from them. $\mathcal{V}_E$ nodes receive information from $\mathcal{V}_S$, $\mathcal{V}_{PV}$ and $\mathcal{V}_{PQ}$; $\mathcal{V}_{PV}$ and $\mathcal{V}_{PQ}$ nodes only receive information from $\mathcal{V}_E$. The aggregating and update function for $\mathcal{V}_E$ has two layers, one of size $(d_E + d_{PV} + d_{PQ} + d_S) \times d_E$, and the other of size $d_E \times d_E$. The update functions for generator and load bus type nodes also have two layers, one of size $(d_x + d_E) \times d_x$, and the other of size: $d_x \times d_x$, where $x = PV$ or $x = PQ$. Only $\mathcal{V}_{PV}$ and $\mathcal{V}_{PQ}$ require an output, their decode MLPs consist of a single layer of size $d_x \times o_x$, where $o_{PV} = 1$ and $o_{PQ} = 2$. In total, each TGN layer has the following number of trainable parameters P:

$$P = (4d_{PV} + 4d_{PQ} + 4d_E + 2d_S)d_E + 3d_{PV}^2 + 3d_{PQ}^2 + d_S^2 + (F_{PV} + G_{PV})d_{PV} + (F_{PQ} + G_{PQ})d_{PQ} + F_E d_E + F_S d_S \quad (19)$$

If all embedding dimensions are the same d value, then:

$$P = 21d^2 + (F_{PV} + G_{PV})d + (F_{PQ} + G_{PQ})d + F_E d + F_S d \quad (20)$$

In this particular case, for simplicity, all nodes were embedded to the same dimension, with $d = 16$, so that $P = 5648$. This value is independent of the size of the electrical grid.

With N_x representing the cardinality of a type x node set, the encoding function for a type x node has complexity $\mathcal{O}(f_x N_x d_x)$, and since f_x and d_x are predefined constants, this translates to a $\mathcal{O}(N_x)$ complexity. Similarly, each decoding and message passing function has complexity $\mathcal{O}(N_x)$. The update function includes an aggregation procedure which involves the multiplication of sparse adjacency matrices, with dense matrices that represent messages passed from one type of node to another. The total amount of values in all sparse matrices is $2N_E$, the complexity of the aggregation multiplications for a type x node is at most $\mathcal{O}(2N_E d_x)$. The total amount of nodes $N = N_{PV} + N_{PQ} + N_S + N_E$ depends on the particular case of electrical grid, but as all operations have at most $\mathcal{O}(DN) = \mathcal{O}(N)$ complexity (with D being some constant dependent on the chosen hyperparameters), the time complexity of the proposed solver is linear with respect to the size of the electrical grid.

3.3. Model training

The proposed TGN solver is trained in batches, the independent NNs of the TGN layers are trained simultaneously based on a cost function that only considers the final voltage inference and the resulting power balance error. The cost function is given by:

$$\frac{1}{H}\sum_{h=1}^{H}\left(\frac{1}{N}\sum_{n=1}^{N}\left(\Delta P_{n,h}^2 + \Delta Q_{n,h}^2\right)\right) \quad (21)$$

where N represents the total number of buses, and H the total number of samples (n and h being the node and sample indices, respectively). The gradients of this cost function with respect to the parameters of the

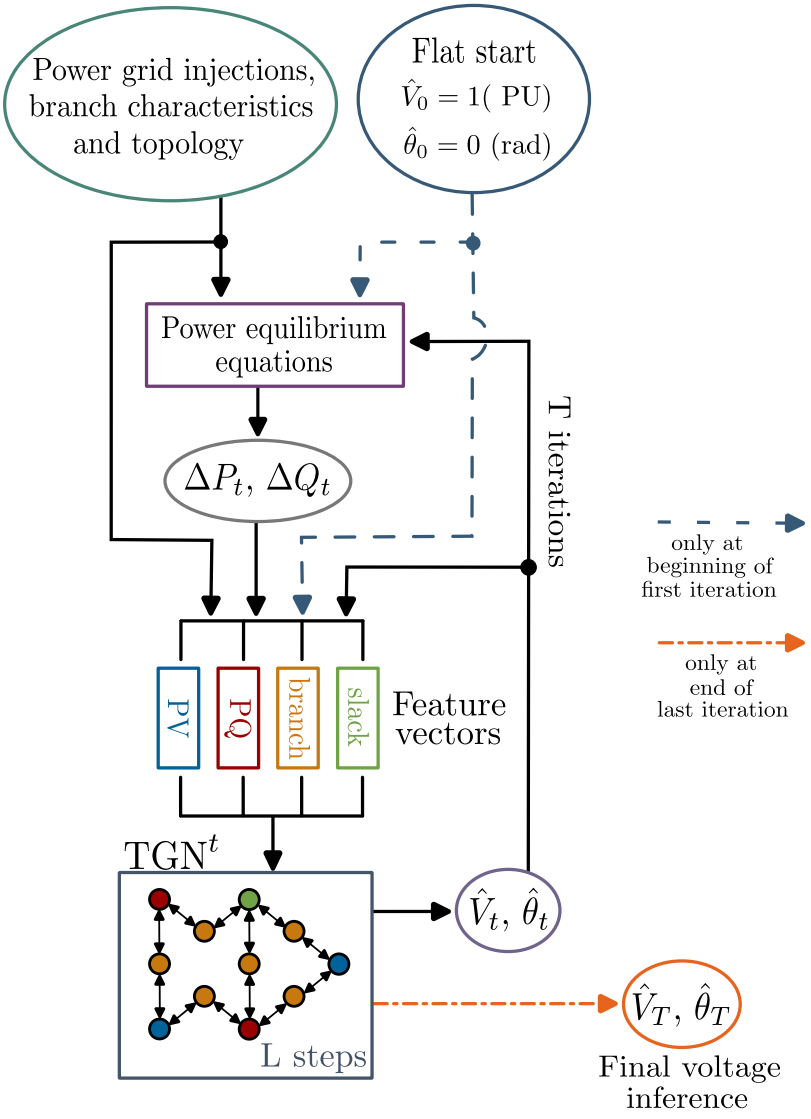

Fig. 3. TGN based power solver structure.

embedding, message-passing, update and output NNs is calculated with the backpropagation algorithm. These gradients are used to modify the values of the NN parameters via the Adam optimization algorithm, afterwards a new batch of data is introduced to the TGN model and the process is repeated until the cost function converges to a minimum value. This way, as is evident, the learning is unsupervised; the goal of the cost function is to enforce Kirchhoff's current law by minimizing the power balance error in all nodes.

4. Numerical tests and discussion

In this section the design of the experiments performed to validate the proposed TGN based power flow solver is described, along with the results obtained.

4.1. Dataset

The data for all experiments is based on benchmark IEEE test cases, similar to the default test cases available for Matpower (Zimmerman et al., 2011); perturbations are added to the injections, branch characteristics and grid topology for each sample.

The information of the IEEE test cases is imported through three two dimensional arrays, with information for the buses, generators, and branches, respectively. From the bus array, the values of the active and reactive power demand are extracted, and a proper ID number is assigned to each substation. Uniform noise is added to the value of the active and reactive power loads, Pd and Qd, so that the resulting values vary between 50% and 150% of the original value. The power load is restricted so that the rare case of the total load demand being higher than the sum of the maximum power generation limits is avoided. From the branch array, the indices of the buses at each side of the branch is collected, as well as the resistance, reactance, susceptance and tap ratio values of the branch. Similarly as with the bus perturbations, uniform noise is added to these values so that they are between 90% and 110% of the test case value. An important aspect of the presented work is the introduction of change to the electrical grid topology in the different samples during training of the system; to this effect, in each sample a different random branch is disconnected. This way both injection and topology changes are involved during training. From the generator array, the ID of the generator bus is considered, along with the maximum permitted active power generation and the nominal voltage magnitude of these buses. The voltage magnitude is uniformly sampled between 90% and 110% of the nominal value, the active power generation is uniformly sampled between 25% and 75% of the allowed range. All voltage magnitude values from load buses are initialized to 1 P.U. and all voltage phase values are set to the slack bus angle reference.

This way, a group of objects that represent a batch of electrical grid samples is formed. Said representation is structured so that it is ready to be used to calculate adjacency matrices and the inputs to the proposed TGN based model.

4.2. Model construction

In the following tests, three electrical grid sizes are employed based on the case 30, case 57 and case 118 standard IEEE power grids. For this reason, three instances of the proposed solver are generated, each trained on an electrical grid of fixed size. The three instances of the TGN based power solver share the same hyperparameters: number of TGN layers, number of message passing and update steps, embedded dimension of node types, and learning rate. The number of TGN layers is empirically chosen to produce a precise enough solution while maintaining the overall size of the solver relatively small; this number is set at $T = 15$. Furthermore, to avoid the distortion of messages being propagated from distant nodes (Topping et al., 2022), only two message passing and update steps are defined ($L = 2$) for each TGN layer. As once mentioned previously, the embedded dimension for all types of nodes is set to $d = 16$. The optimizer used is the Tensorflow (Abadi et al., 2015) implementation of the Adam algorithm, with a learning rate of $1e-4$, and all other parameters are left with the default values. The three instances are trained relatively quickly, with only 1250, 1500 and 1500 learning iterations for the TGN instances trained on case 30, case 57 and case 118 grids, respectively.

4.3. Conventional test

The first experiment consists of testing the three instances of the proposed solver on electrical grids of the same size as the ones they are trained on, changing power grid injections and disconnecting random branches. For each grid size, 20 power grid states are generated; the corresponding TGN instance is applied to infer the missing voltage values at each node. To validate the obtained results, they are compared with the solutions calculated with the trusted and conventional Newton–Raphson (N–R) method using Matpower (Zimmerman et al., 2011). Because of the way the batch samples are generated, some input samples result in non-feasible grid states that do not converge with the N–R method, for these cases the proposed solver does infer some solution, but in the presented results only those that converged with the N–R method are considered.

To further explain the inference procedure, Fig. 4 shows the absolute difference between the final N–R based result and the outputs obtained at distinct TGN iterations of the proposed method, for a single sample of the case 118 grid. This way, *iter* 0 corresponds to the output of the first TGN layer; *iter t* represents an intermediate layer, in this case $t = 7$; *iter T* represents the final output, with $T = 15$. The abundance of low error vertices on the magnitude side of the first layer is due to the quantity of generator (PV) nodes, for which the voltage magnitude is known from the original state of the grid. As the iterations advance, it is shown that the output of each node approaches the N–R output, even though the learning is not supervised and the N–R result is not known during training.

To exemplify the similarity between the resulting voltage values obtained with the N–R method and the proposed TGN based solver Figs. 5 to 7 illustrate the final voltage magnitude and phase results of a single sample, obtained with the proposed TGN based solver and the N–R method. Fig. 5 shows the results for a sample state of case 30 grids, displaying the voltage magnitude and phase of each substation on the left and right graphs, respectively. Figs. 6 and 7 show similar experiments for case 57 and case 118 grids, respectively. These are purely illustrative graphs, since they only show the outputs of a single power grid instance.

In order to show a more general perspective of the precision of the proposed solver, Figs. 8 to 10 show scatter plots with the N–R based solutions and the proposed solver solutions, for test batches with 20 samples. The value of the correlation coefficient between the two results is also shown in the bottom right of the scatter plots. Fig. 8 shows the correlation between the proposed solver solution and the N–R based solution, for magnitude (PU) on the left and for phase on the right (radians). That is, the N–R based solutions, for all the buses in all the samples of the test batch, are compared to the corresponding values obtained with the proposed method. Figs. 9 and 10 show similar plots for case 57 and case 118, respectively. In all cases, there is a high level of correlation with all coefficients being above 0.98; the least correlated case is the one corresponding to the voltage phase solution of the case 118 grids. The most correlated case corresponds to the voltage magnitude solution of the case 118 grids, although this can be partly explained by the high rate of generator nodes in that specific case (the voltage magnitude values are known beforehand).

Table 3
Voltage magnitude RMSE.

	Test size		
	Case 30	Case 57	Case 118
DC	0.040139	0.045667	0.028195
TGN Trained on case 30	**2.5092e−04**	3.9902e−03	1.7344e−03
TGN Trained on case 57	8.5203e−03	**2.3706e−03**	2.0319e−03
TGN Trained on case 118	3.6260e−04	3.9346e−03	**2.3699e−04**

Table 4
Voltage phase RMSE.

	Test size		
	Case 30	Case 57	Case 118
DC	0.012974	0.016247	0.079729
TGN Trained on case 30	**2.2852e−03**	0.068866	0.017480
TGN Trained on case 57	0.01229	**4.4389e−03**	**1.2320e−03**
TGN Trained on case 118	6.1418e−03	0.01686	0.010423

4.4. Extrapolation to different grid sizes

One of the crucial points of the proposed model is the capability to be tested on grids of different size from the ones they are trained on, due to the graph structure representation of the system. To evaluate the generalization performance of the proposed solver when faced with different grid sizes, each of the three TGN instances is tested on batches of the other two grid sizes that do not correspond to the ones they were trained on. Each grid in the test batch is obtained as described in Section 4.3, with varying injections, line characteristics and grid configuration through the elimination of a random branch.

To add another point of comparison to the results, the test samples are additionally solved using the DC approximation method, which does not consider the reactive power in the electrical grid and uses linear network equations that relate real power to bus voltage angles (instead of complex bus voltages). The DC approximation is simple and robust, and for these reasons, sometimes used for contingency or real-time dispatch analyses (Van Hertern et al., 2006).

In Tables 3 and 4, the solutions obtained with the proposed method and the DC approximation are compared to the results obtained with the N–R method, which is considered the correct solution. The comparison is measured using the root mean square error (RMSE):

$$RMSE = \sqrt{\frac{\sum_{i=1}^{H}\left(\sum_{j=1}^{N}(x_{i,j} - \hat{x}_{i,j})^2\right)}{NH}} \tag{22}$$

where $x_{i,j}$ represents the solution obtained with the newton raphson method for a bus j at test sample i, $\hat{x}_{i,j}$ represents the corresponding solution obtained with either the DC approximation method or the proposed TGN based method, N represents the total number of buses of the tested grid and H represents the total number of samples in the test batch.

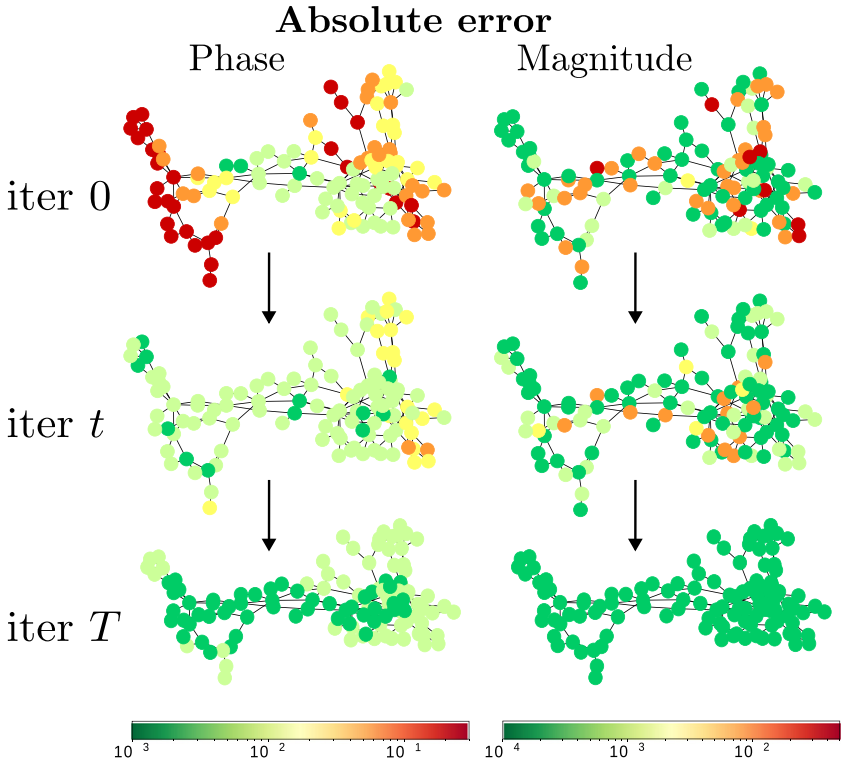

Fig. 4. Evolution of the absolute difference between the proposed method outputs throughout the TGN layers and the final N–R based output, for a single sample of the case 118 grid, showing voltage phase difference in radians (left) and voltage magnitude in P.U. (right).

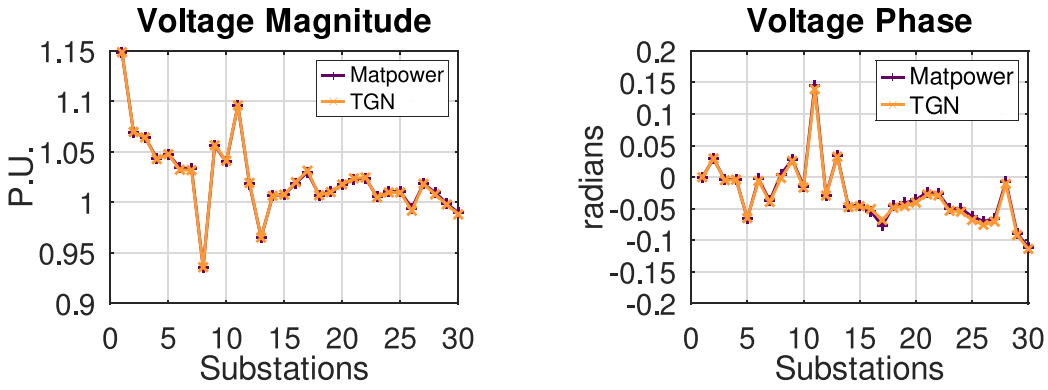

Fig. 5. Voltage magnitude and phase solutions for a single sample of the case 30 grid.

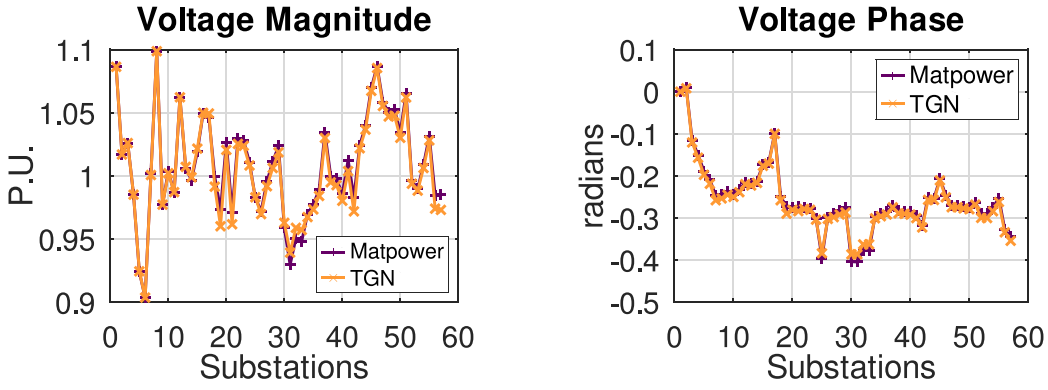

Fig. 6. Voltage magnitude and phase solutions for a single sample of the case 57 grid.

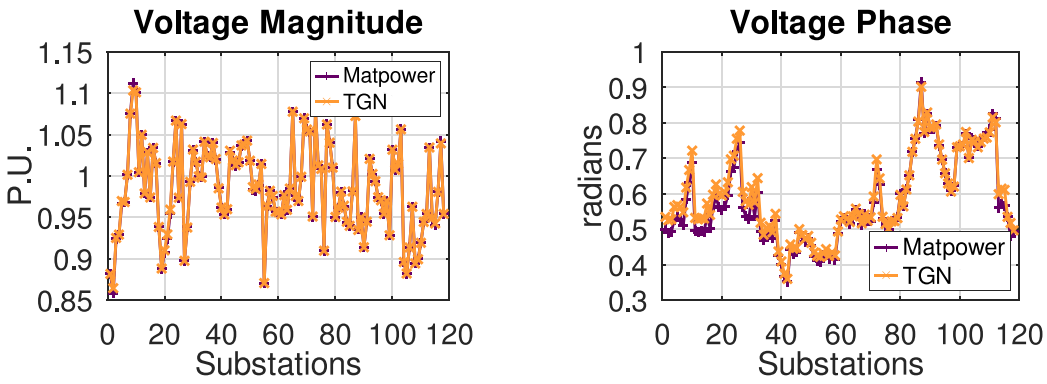

Fig. 7. Voltage magnitude and phase solutions for a single sample of the case 118 grid.

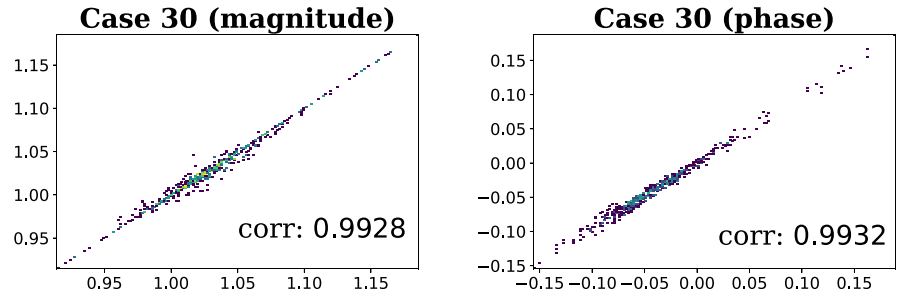

Fig. 8. Correlation of TGN based power solver with Matpower's Newton Raphson solution for case 30 V magnitude (left) and phase (right).

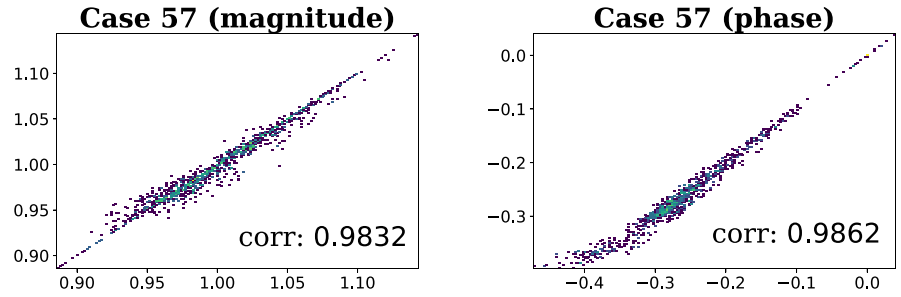

Fig. 9. Correlation of TGN based power solver with Matpower's Newton Raphson solution for case 57 V magnitude (left) and phase (right).

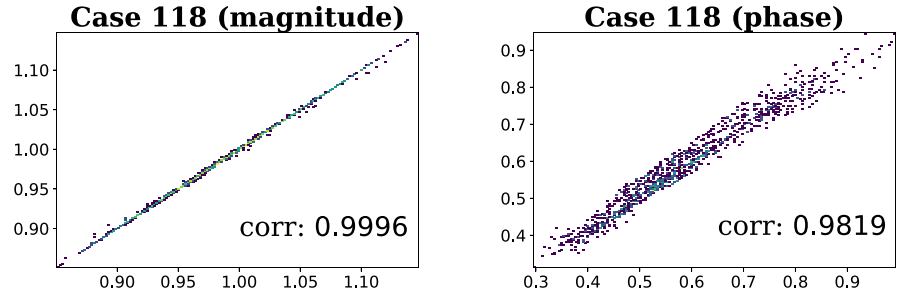

Fig. 10. Correlation of TGN based power solver with Matpower's Newton Raphson solution for case 118 V magnitude (left) and phase (right).

The first row of Table 3 shows the voltage magnitude RMSE of the DC approximation results and the N–R method results, tested on grids from the three different test case sizes. The following rows show the RMSE of the solutions obtained with different instances of the proposed method, trained on case 30, case 57 and case 118 power grids, and each of them tested on all grid sizes. Table 4 is similar, but comparing voltage phase values.

The best results for each test case are marked in bold; as would be expected, most of the best results are obtained from grids tested on grids of the same size as the ones they were trained on. The results of the TGN instances tested on grids of the same size as the ones they are trained on are the same as in Section 4.3. As shown in Table 3, even when tested on grids of different size, the proposed method performs better than the DC approximation method when calculating voltage magnitude, this is expected as the DC approximation method considers all voltage magnitudes constant at 1 PU. Table 4 shows that in most cases, the proposed TGN based method performs better than the DC approximation when calculating voltage phase as well. At times the

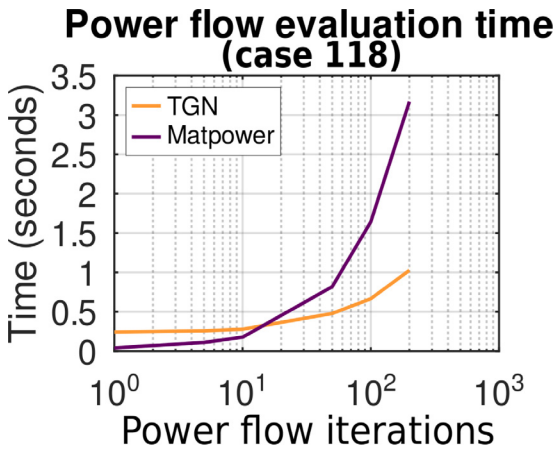

Fig. 11. Time in seconds needed to solve different numbers of power grid scenarios, for the case of 118 buses, using the TGN based solver and the N–R based Matpower approach.

results are very similar, like with the TGN instance trained on case 57 and tested on case 30 grids, and with the TGN instance trained on case 118 but tested on case 57 grids. In the worst case, which is with the TGN trained on case 30 but tested on case 57 grids, the DC approximation obtained a smaller error, however the TGN solution is still quite decent. As shown, the worst results are obtained when testing the case 57 grid, this can be explained by the wide range of values the injection parameters can take for this particular grid case, which presents values very different from the ones seen in the other two cases. Still, the errors in the worse case are considerably small, and it is shown that smaller grids are able to generalize to bigger grids, and vice versa.

4.5. Time considerations

As was mentioned in Section 3.2, the time complexity of the model is linear, and thus the calculation time does not increase as sharply as the N–R method with respect to the size of the electrical grid. To illustrate this, Fig. 11 shows the time in seconds needed to run a different number of scenarios of the 118 bus test case power grid. The number of power flow iterations is shown on a logarithmic scale. In this case, running n scenarios multiplies the number of inputs by n for the proposed solver, and the scenarios are solved in parallel. With the N–R based approach, the n scenarios are processed sequentially. It is shown that although for a small number of inputs the N–R based method is faster, as the number of inputs grows, the time required is substantially shorter with the proposed method. These considerations show an important reduction in the time needed to carry out numerous power flow iterations, which in combination with the robustness to single branch outages and differences in branch characteristics, make it a beneficial tool for power grid planning and risk assessment.

5. Conclusion

The proposed TGN based power flow solver takes advantage of the intuitive connection between the electrical grid data and graph representations to learn the relationships and dynamics between the different types of elements present in electrical grid models to analyze power flow. An important aspect of the presented work is the generalization capability to infer decent results for essentially different grids (varying injection, branch characteristics and topology). As far as the authors know, there is no other work that solves the power flow problem by training neural networks with both different injections and different grid configurations. The proposed method does not imitate any other existing method, but rather is based on minimizing the active and reactive power imbalance at each node of each sample during the training of the parameters.

The proposed method exploits several benefits of GNNs, e.g. they scale linearly with the number of edges and embedding size. Furthermore, since the voltage variables are not directly modified by the proposed method, we completely avoid the computation of Jacobian matrices and their inverse, which is necessary in the N–R method. These two characteristics are key reasons as to why the proposed model computation time scales in a more linear way with respect to the test grid size than the N–R method. It is worth mentioning that the testing of different grid sizes is not possible for conventional MLP methods, and that these methods are inefficient for larger grids as their size depends on the grid size, whereas the presented method does not, due to it being based on local operations and shared modules.

Through the shown numerical tests, it is shown that the proposed TGN based method obtains results very close to those obtained with a conventional Newton–Raphson based method, even when the learning is unsupervised. The tests are carried out in batches, with each sample of the batch representing an independent electrical grid from the rest. However, in future work, steps can be taken to capture sequentiality in time, i.e. instead of the samples being autonomous from each other, if each sample represents the state of the grid over a certain time duration Δt, then H samples would represent the grid state evolution over a total time of $H \cdot \Delta t$ (assuming reliable injection forecast information is available). Additionally, the framework of the proposed model can be improved to continuously learn and adapt to the environment.

The results presented constitute a beneficial step toward a NN based system that can be applied for contingency analysis, real-time dispatch and techno-economic analyses, or as an aid to improve different stages of power system planning, optimization, operation and control of electrical grids.

CRediT authorship contribution statement

Tania B. Lopez-Garcia: Methodology, Software, Writing – original draft. **José A. Domínguez-Navarro:** Conceptualization, Supervision, Critical revision.

Declaration of competing interest

The authors declare that they have no known competing financial interests or personal relationships that could have appeared to influence the work reported in this paper.

Data availability

Data will be made available on request.

Acknowledgments

This paper was supported in part by the National Council of Science and Technology (CONACYT), Mexico, under scholarship 710033.

This paper was supported in part by the Spanish National Plan for Scientific and Technical Research and Innovation, under project PID2019-104711RB-I00.

References

Abadi, M., Agarwal, A., Barham, P., Brevdo, E., Chen, Z., Citro, C., Corrado, G.S., Davis, A., Dean, J., Devin, M., Ghemawat, S., Goodfellow, I., Harp, A., Irving, G., Isard, M., Jia, Y., Jozefowicz, R., Kaiser, L., Kudlur, M., Levenberg, J., Mané, D., Monga, R., Moore, S., Murray, D., Olah, C., Schuster, M., Shlens, J., Steiner, B., Sutskever, I., Talwar, K., Tucker, P., Vanhoucke, V., Vasudevan, V., Viégas, F., Vinyals, O., Warden, P., Wattenberg, M., Wicke, M., Yu, Y., Zheng, X., 2015. TensorFlow: Large-scale machine learning on heterogeneous systems. URL: https://www.tensorflow.org/. Software available from tensorflow.org.

van Amerongen, R.A., 1989. A general-purpose version of the fast decoupled loadflow. IEEE Trans. Power Syst. 4 (2), 760–770. http://dx.doi.org/10.1109/59.193851.

Avelar, P.H.C., Lemos, H., Prates, M.O.R., Gori, M., Lamb, L., 2019. Typed graph networks. ArXiv abs/1901.07984.

Babatunde, O., Munda, J., Hamam, Y., 2020. Power system flexibility: A review. Energy Rep. 6, 101–106. http://dx.doi.org/10.1016/j.egyr.2019.11.048, The 6th International Conference on Power and Energy Systems Engineering.

Battaglia, P.W., Hamrick, J.B., Bapst, V., Sanchez-Gonzalez, A., Zambaldi, V., Malinowski, M., Tacchetti, A., Raposo, D., Santoro, A., Faulkner, R., Gulcehre, C., Song, F., Ballard, A., Gilmer, J., Dahl, G., Vaswani, A., Allen, K., Nash, C., Langston, V., Dyer, C., Heess, N., Wierstra, D., Kohli, P., Botvinick, M., Vinyals, O., Li, Y., Pascanu, R., 2018. Relational inductive biases, deep learning, and graph networks. arXiv.

Donon, B., Clément, R., Donnot, B., Marot, A., Guyon, I., Schoenauer, M., 2020. Neural networks for power flow: Graph neural solver. Electr. Power Syst. Res. 189, http://dx.doi.org/10.1016/j.epsr.2020.106547.

Fikri, M., Cheddadi, B., Sabri, O., Haidi, T., Abdelaziz, B., Majdoub, M., 2018. Power flow analysis by numerical techniques and artificial neural networks. In: 3rd Renewable Energies, Power Systems and Green Inclusive Economy, REPS and GIE 2018. Institute of Electrical and Electronics Engineers Inc., pp. 1–5. http://dx.doi.org/10.1109/REPSGIE.2018.8488870.

Gilmer, J., Schoenholz, S.S., Riley, P.F., Vinyals, O., Dahl, G.E., 2017. Neural Message Passing for Quantum Chemistry. In: JMLR.org (Ed.), International Conference on Machine Learning. Sydney, pp. 1263–1272. http://dx.doi.org/10.5555/3305381.3305512.

Glover, J.D., Sarma, M.S., Overbye, T.J., 2012. Power System Analysis and Design, fifth ed. Cengage Learning.

Hu, X., Hu, H., Verma, S., Zhang, Z.-L., 2021. Physics-Guided Deep Neural Networks for Power Flow Analysis. IEEE Trans. Power Syst. 36 (3), 2082–2092. http://dx.doi.org/10.1109/TPWRS.2020.3029557.

Kipf, T.N., Welling, M., 2017. Semi-supervised classification with graph convolutional networks. In: 5th International Conference on Learning Representations, ICLR 2017, Toulon, France, April 24-26, 2017, Conference Track Proceedings. OpenReview.net.

Lopez-Garcia, T.B., Coronado-Mendoza, A., Domínguez-Navarro, J.A., 2020. Artificial neural networks in microgrids: A review. Eng. Appl. Artif. Intell. 95, http://dx.doi.org/10.1016/j.engappai.2020.103894.

Owerko, D., Gama, F., Ribeiro, A., 2020. Optimal Power Flow Using Graph Neural Networks. In: IEEE International Conference on Acoustics, Speech and Signal Processing. ICASSP, pp. 5930–5934. http://dx.doi.org/10.1109/ICASSP40776.2020.9053140.

Smith, O., Cattell, O., Farcot, E., O'Dea, R.D., Hopcraft, K.I., 2022. The effect of renewable energy incorporation on power grid stability and resilience. Sci. Adv. 9 (8), 760–770. http://dx.doi.org/10.1126/sciadv.abj6734.

Stott, B., 1974. Review of load-flow calculation methods. Proc. IEEE 62 (7), 916–929.

Topping, J., Giovanni, F.D., Chamberlain, B.P., Dong, X., Bronstein, M.M., 2022. Understanding over-squashing and bottlenecks on graphs via curvature. In: International Conference on Learning Representations. URL: https://openreview.net/forum?id=7UmjRGzp-A.

Tovar-Facio, J., Martín, M., Ponce-Ortega, J.M., 2021. Sustainable energy transition: modeling and optimization. Curr. Opin. Chem. Eng. 31, 100661. http://dx.doi.org/10.1016/j.coche.2020.100661.

Van Hertern, D., Verboornen, J., Purchala, K., Belrnans, R., KlingH, W.L., 2006. Usefulness of DC Power Flow for Active Power Flow Analysis with Flow Controlling Devices. In: The 8th IEE International Conference on AC and DC Power Transmission. IET, pp. 58–62. http://dx.doi.org/10.1049/cp:20060013.

Vankayala, V.S.S., Rao, N.D., 1993. Artificial neural networks and their applications to power systems—a bibliographical survey. Electr. Power Syst. Res. 28 (1), 67–79.

Xie, L., Singh, C., Mitter, S.K., Dahleh, M.A., Oren, S.S., 2021. Toward carbon-neutral electricity and mobility: Is the grid infrastructure ready? Joule 5 (8), 1908–1913. http://dx.doi.org/10.1016/J.JOULE.2021.06.011.

Zimmerman, R., Murillo-Sanchez, C., Thomas, R., 2011. MATPOWER: Steady-State Operations, Planning and Analysis Tools for Power Systems Research and Education,. Power Syst. IEEE Trans. 26 (1), 12–19. http://dx.doi.org/10.1109/TPWRS.2010.2051168.

Reliability Engineering and System Safety 215 (2021) 107881

Contents lists available at ScienceDirect

Reliability Engineering and System Safety

journal homepage: www.elsevier.com/locate/ress

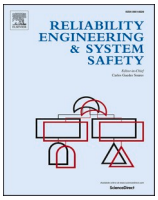

The effects of the high penetration of renewable energies on the reliability and vulnerability of interconnected electric power systems

Jesus Beyza , Jose M. Yusta *

University of Zaragoza, Department of Electrical Engineering, C/ Maria de Luna 3, Zaragoza 50018, Spain

ARTICLE INFO

Keywords:
Critical infrastructures
Interconnections
Power systems
Reliability
Renewable energies
Robustness
Vulnerability

ABSTRACT

Renewable energy sources and cross-border electrical interconnections can significantly impact the security of the supply of power systems. This article jointly analyses the reliability and vulnerability of electrical networks to quantify systems' performance by increasing and decreasing renewable resources and the degree of coupling of electrical infrastructures. This comparison seeks to measure the influence of renewable generation and the impact of interconnection lines on the operational behaviour of systems under different types of contingencies or disturbances. The reliability assessment is performed using PLEXOS, and the vulnerability assessment is carried out with a network disintegration procedure implemented in MATLAB. Here, different statistical indices of the networks are measured. The procedures are applied sequentially in six case studies with different generation mixes and interconnection lines based on the well-known IEEE RTS-96 and IEEE RTS-GMLC test networks. From the analysed cases, the resulting tables and graphs obtained from the simulation are presented, and the joint impact from the two perspectives is compared. The results obtained show that renewable sources have a greater impact on reliability and that electrical interconnections impact both reliability and vulnerability. These conclusions highlight the importance of analysing the operational security of infrastructures taking into account both approaches simultaneously.

1. Introduction

In recent years, electrical power systems have become increasingly interconnected, complex and interdependent. Electrical networks can fail not only because of the complexity of their technical operation but also because of their interdependence with other critical systems. These infrastructures are often interrupted by recurring and nonrecurring disturbances, which significantly impact the services they provide to society. Recurrent disturbances correspond to asset failures or malfunctioning of protective devices while nonrecurring disturbances involve extreme events such as natural disasters or pernicious human actions. Both events degrade system components and interrupt operations in much of the infrastructure [1].

More recently, the increasingly frequent adoption of renewable energy sources within power systems has brought substantial new challenges by integrating them into existing networks [2]. Renewable generators introduce uncertainties and expose systems to unexpected power outages [3]. These new problems, combined with the previous ones, force operators to more closely monitor the security levels of their electrical infrastructure to respond to these undesirable events.

On the other hand, the coupling of two or more electrical systems reduces the uncertainty associated with the new energy vectors and facilitates the optimal management of renewable resources. However, the interconnection of infrastructures with different generation mixes also poses great challenges for independent network managers, since the behaviour of one of the systems could affect the operation of the other joint network, or an inadequate connection could seriously impact the operational security of the system.

Based on the above, transmission system operators (TSO) must ask themselves what concepts can be used to measure the joint performance of electrical networks interconnected with different generation mixes against disturbances and contingencies, how to quantify both concepts in practice, and what are the similarities and differences between the concepts used.

In the field of electrical engineering, reliability studies analyse the continuity of operations in the event of failure of one or two infrastructure assets, while vulnerability and robustness studies assess the network performance against the loss of multiple assets [4,5]. The first

* Corresponding author.
E-mail addresses: jbeyza@unizar.es (J. Beyza), jmyusta@unizar.es (J.M. Yusta).

https://doi.org/10.1016/j.ress.2021.107881
Received 29 January 2021; Received in revised form 28 April 2021; Accepted 17 June 2021
Available online 25 June 2021

type of study is related to the system's ability to meet customer demand, and the second type of study is associated with the ability to maintain, at least partially, the energy supply within the network [6]. Robustness is the inverse of vulnerability. Both are important concepts that can describe in a representative way the performance of the coupled electrical infrastructure during and after a disturbance or contingency.

On the one hand, a reliability study is the most appropriate tool for the operator to evaluate the power system's performance, measure the frequency, duration and cost of interruptions, and compare different levels of coupling and integration of renewable energies in the infrastructure [7,8]. The procedures for evaluating reliability are the Monte Carlo simulation approach and the analytical approach [9]. The first uses statistical information on failures and repairs of components to randomly verify the state of the network assets, and the second uses mathematical formulations to analyse the problems associated with reliability indices.

On the other hand, a vulnerability or robustness study is the most appropriate tool for the operator to measure the infrastructure's capacity to respond to extreme events, quantify the entire network skeleton's structural performance, and identify the weakest buses that require significant reinforcement [10,11]. Similar to the reliability study, vulnerability is classified into functional vulnerability and structural vulnerability [12]. The first type quantifies the system's technical and operational characteristics during critical contingency scenarios, and the second type measures the topological characteristics of the infrastructure throughout the network disintegration process. Unlike the reliability procedure, the vulnerability study does not consider the probabilities of failure of the assets during contingency events but rather considers the iterative removal of all network elements.

TSO face challenges in daily operations of electrical power systems. Power quality, voltage and frequency stability, generation and demand balance, and generation and transmission capacity problems are some of the main targets of network managers and planners [2]. These attributes in the presence of renewable energy sources must be studied to maintain the stability of the entire electrical network. The high penetration of renewable sources, therefore, creates many technical challenges in power systems. The general behaviour of electrical networks with renewable generation differs from that of systems with dispatchable generation. For this reason, TSOs must react instantly to the increasing penetration rates of renewables, modifying system planning and operation.

For example, electrical networks may face failures or contingencies that jeopardise the normal operation of the infrastructure. Failures can be symmetrical and asymmetrical, and short-circuits to ground can occur for both types [13]. In conventional electrical power systems, synchronous generators can remain connected during and after a failure because they have inherent characteristics to provide a stable system operation and participate in generation balance. Conversely, in electrical systems with a high proportion of renewable energies, renewable generators influence the security of supply because they do not exactly replace the functional behaviour of conventional generators. To overcome these challenges, grid codes dictate that renewable sources must contribute to voltage and frequency stability, responding with synthetic inertia, primary frequency control, voltage regulation, and damping of power swings [14]; that is, renewable generators must remain connected during failures, instead of disconnecting, to maintain the balance between active and reactive power.

The effect of the high penetration of renewable energies on the reliability and vulnerability of interconnected electrical systems is a new field of research, which requires proposing integrated methodological frameworks to study different interrelated attributes of both concepts. Renewable resources and interconnections play a key role in the security of supply, which is why their study and analysis is a growing concern [15,16].

Electrical grids with a high proportion of renewable energy sources must adjust their production in a timely and adequate manner according to uncertain changes in these energy sources [17,18]. To mitigate the adverse implications of intermittencies in renewable resources, some studies propose long-term scheduling strategies for generators considering the criticality of the sources and developing contingency tests [19,20]. Other studies list the benefits and challenges of integrating renewable energy resources and present different control strategies responsible for this incorporation [21].

The operation of electrical grids is also affected by the intermittency of renewable resources and the operational status of infrastructure assets and components. Accordingly, some studies propose procedures to analyse potential threats and vulnerabilities, considering changes in operating status and the variability of renewable sources [22,23].

Other researchers indicate that various types of renewable energy could make the system more vulnerable and less reliable due to their uncertainty and availability [24]. In this context, some academics propose models based on linear programming to evaluate and increase the reliability of integrated energy systems [25]. These authors consider that wind and photovoltaic generators could mitigate interruptions caused by possible contingencies. Similarly, other authors propose analytical approaches highlighting the capacity of energy systems to adopt different levels of reliability according to the theoretical output powers of renewable generators [26].

In turn, one of the most important challenges in studying the vulnerability of integrated energy systems is the analysis of cascading events. Blackouts are highly difficult to analyse and mitigate because these events can start for countless reasons and operating conditions. Consequently, studying them all is practically unfeasible. Graph theory could be a viable approach to model dynamic behaviour, to analyse the propagation of these events, and to quantify the structural robustness of an electrical network [27–30]. Some relevant studies in the area identify critical assets [31–33] and possible cascading failure-initiating events [34–36]. Other documents establish vulnerability indices based on short-circuit studies and centrality measures of graph theory [37,38]. These studies seek to identify and classify critical components according to their consequences, determine undesirable events and potential vulnerabilities, and propose countermeasures to reduce the power grid's vulnerability [39,40].

Similarly, other studies consider that power outages caused by adverse weather conditions must be examined in reliability and robustness studies. Some studies analyse this problem in detail and propose new protection metrics and techniques for systems integrated with renewable sources [41,42]. Other scholars propose theoretical frameworks to quantify the performance of a system under different types of events or contingencies [43,44]. Furthermore, some studies analyse the benefits and limitations of using power flow-based approaches to assess the vulnerability and reliability of integrated systems [45,46].

Renewable energy vectors may also decrease the reliability of an electrical system because poor performance could lead to power outages that would inevitably harm a nation's economy and society [47,48]. In this context, some academics propose methodologies based on energy hub-based methods [49], model order reduction [50], metaheuristic searching genetic algorithms [51] and multi-criteria decision analysis [52] for assessing the adequacy of renewable generation. In reference [53], a complete review of the improvements obtained in reliability, thanks to renewable sources, can be consulted.

The concepts of reliability and vulnerability/robustness are discussed from different perspectives in a wide range of studies in the scientific literature. However, few studies have considered the two concepts in an integrated manner and addressed the remaining two questions raised by the system operator in the context of the research problem described at the beginning of this work [54]. Due to the arduous process of decarbonisation of current power systems, this manuscript considers that vulnerability and reliability should be analysed together to assess in more detail the impact of renewable energy sources on interconnected electrical systems. Joint vulnerability and

reliability studies could help to improve the structural performance, planning and energy security of integrated power grids. A contingency or disturbance in a system with a high proportion of renewable energies could slightly impact reliability levels but simultaneously severely impact vulnerability levels. The latter, combined with an increase in the number of interconnections between different power systems, could increase interdependencies and propagate disturbances between different infrastructures. This motivates the specific objective of this study, which is to develop a theoretical and data-driven methodological framework to explore the characteristics and relationships between both concepts in interconnected and integrated power systems with renewable energy sources. This comparison seeks to quantify the degree of influence of renewable sources and couplings on the joint reliability and structural vulnerability assessments.

To achieve this, first, a reliability study is performed by applying the Sequential Monte Carlo method and calculating the indices of expected energy not supplied (EENS), expected demand not supplied (EDNS), expected frequency of load curtailment (EFLC), loss of load expectancy (LOLE), loss of load probability (LOLP) and average duration of load curtailment (ADLC). The variability of the renewable resource is included to more precisely estimate the statistical indices in the integrated system with renewable energies. Then, a structural vulnerability study is carried out by executing a network disintegration procedure, which consists of randomly removing each of the buses of the interconnected infrastructures, running direct current optimal power flows, measuring the disconnected load (DL) index in each disintegration step and quantifying the damage area (DA) index of the total decomposition of the infrastructure [55]. Given the random nature of the results, 1000 independent experiments are performed to obtain an ideal statistical sample [56]. The results obtained are discussed, in the end, both graphically and numerically in an integrated risk assessment framework. This allows transmission system operators to have complete information to make their expansion planning decisions for electrical systems. Renewable sources and interconnections could contribute to improving the operating conditions of the infrastructure but at the same time worsen both the joint reliability and the vulnerability of the entire system. These procedures take into account the basic guidelines found in the scientific literature. Numerical tests to investigate the similarities and differences between the two concepts are carried out in six case studies built with the IEEE RTS-96 and IEEE RTS-GMLC test systems [57, 58]. The latter is an updated version of the first infrastructure that incorporates renewable energy.

Reliability evaluation of electric power systems assumes that failed assets are immediately disconnected and that the electrical infrastructure returns to a steady state with adequate generation for minimal load reductions. Although the study of power flows converges on a feasible solution representing a steady-state operating point, a stable transition to other equilibrium points is not guaranteed after a failure. The evaluation of transitory stability can be a key factor in reliability studies and even in vulnerability studies. However, the evaluation of transient stability is computationally expensive, and therefore system dynamics are often ignored in reliability studies [59]. This study disregards this attribute in the reliability and vulnerability procedures; however, the proposed study framework could be combined with transient stability evaluations and cascading failure simulators for electrical power systems. A probabilistic hybrid model of optimal power flows and transient stability for mitigating cascading failures is already available in the literature [60].

The main contributions of this work are summarised below:

- A combined study of the concepts of vulnerability and reliability is performed to quantify the operational status of coupled and integrated power systems with thermal generation and coupled and integrated power systems with a high penetration of renewables.
- The impact of interconnections on the reliability and vulnerability of power systems with a high share of renewable energy is analysed.
- The interconnections are analysed in order to design reliable and robust systems.

This article is organised as follows: Section 2 details the reliability and robustness approaches used to evaluate the operating status of coupled electrical systems with renewable energy sources in the event of contingencies. Section 3 describes the six case studies created with the IEEE RTS-96 and IEEE RTS-GMLC test networks. Section 4 presents the simulation results obtained after applying the two procedures described in the cases studied. Section 5 discusses the reliability and vulnerability results jointly. Finally, Section 6 draws the main conclusions of this document.

2. Simulation framework for the analysis of reliability and vulnerability of power systems

This section describes the simulation procedure to assess both the reliability and vulnerability of electrical grids integrated with renewable energy sources. The simulation framework uses the elementary patterns found in the scientific literature. The reliability analysis is carried out by applying the sequential Monte Carlo method, and the vulnerability analysis is performed by running a network disintegration procedure, which consists of the random and iterative removal of each of the buses.

2.1. Reliability assessment

The electrical power system, which is the backbone of modern societies, must meet the population's needs with adequate, stable and reliable energy. Statistical reliability indices are the most appropriate tool used by the transmission system operators to measure and quantify the electrical infrastructure's performance. Reliability considers n-1 contingencies, that is, the non-trivial loss of an asset from the power grid. This study aims to prevent emergencies, including the propagation of incidents in the infrastructure. Failures are considered statistically independent because interruptions in elements are not related to other contingencies in the network [61].

The reliability assessment is used to measure the frequency, duration, and annual costs of interruptions as well as system availability to compare different network designs, couplings and generation mixes [2]. The sequential Monte Carlo method is a procedure to realistically simulate the actual chronological process of the network, study the system's random behaviour, and measure different reliability indices of the infrastructure [62,63]. This procedure can be summarised in the ordered and systematic steps shown in Fig. 1 and described below:

Step 1. Establish the operational state of the network assets, that is, normal or failure. At the beginning, all the elements function within their established limits.

Step 1. Model different events that cause interruptions in the electrical infrastructure. Typical disturbances include power line outages, transformer problems and electrical substation failures. These events can be evaluated using two important parameters: the mean time to failure, MTTF, and the mean time to repair, MTTR. These are defined for all network assets and are inversely related to failure and repair rates.

$$\mathrm{MTTF} = \frac{1}{\lambda}; \mathrm{Unit}: [\mathrm{hours}] \tag{1}$$

$$\mathrm{MTTR} = \frac{1}{\mu}; \mathrm{Unit}: [\mathrm{hours}] \tag{2}$$

where λ is the failure rate and μ is the repair rate.

Step 1. Quantify the time spent in normal (up time) and failed (down time) states, that is, the time to repair, TTR, and the time to failure, TTF, calculated as

$$\mathrm{TTR} = -\ln(\mathrm{r}) \times \mathrm{MTTR} \tag{3}$$

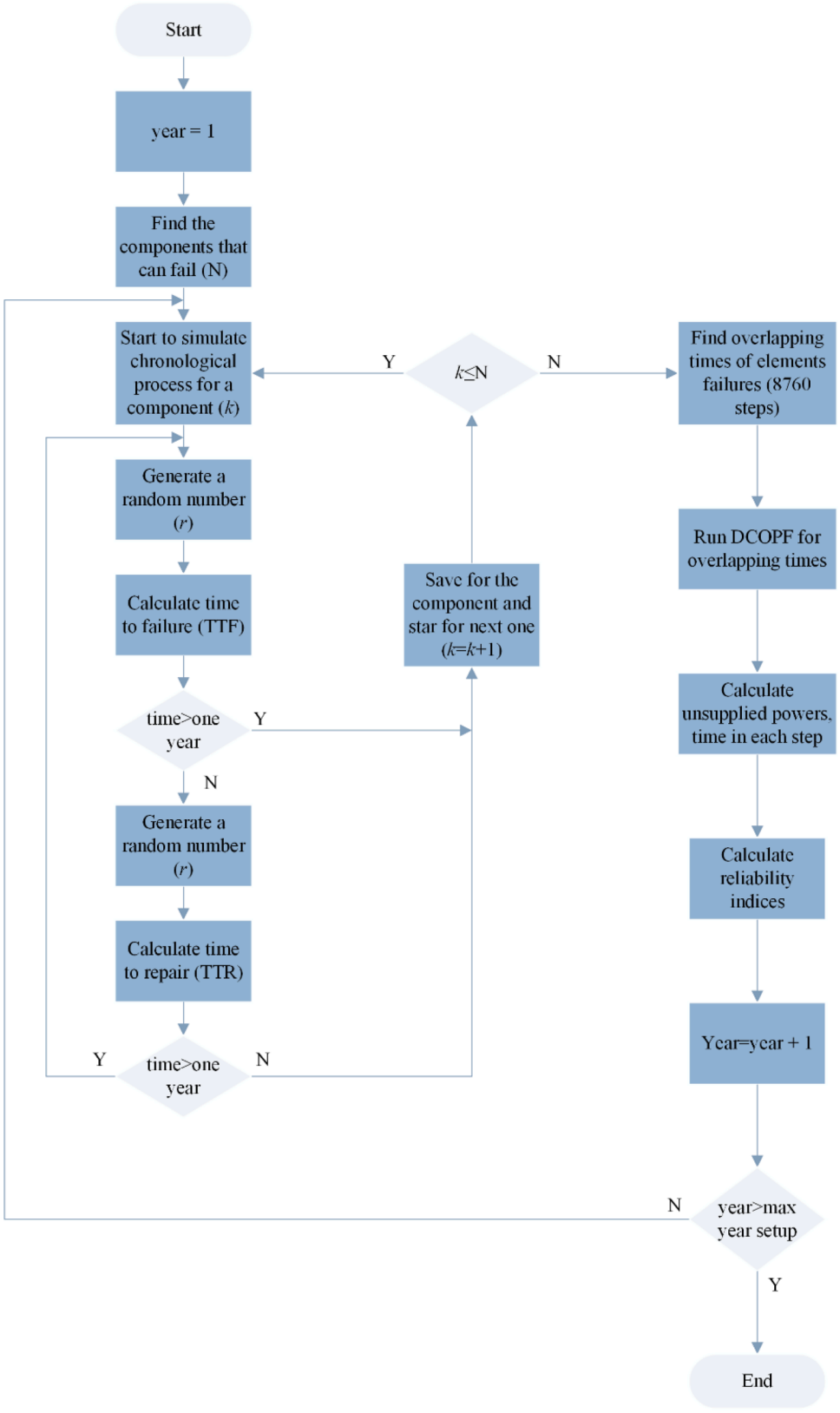

Fig. 1. Procedure to perform the reliability assessment.

$$TTF = -\boldsymbol{ln}(\boldsymbol{r})/\boldsymbol{\lambda} \times \ 8760 \tag{4}$$

where r is a random number uniformly distributed between [0,1] and calculated using congruential generators [4]. This step is repeated for a specific time, usually one year.

Step 2.Computes the overlapping times of elements failures, i.e., when various components are simultaneously out of service, for a temporal resolution of 1 hour in a 1-year horizon, that is, 8760-time steps of

1 hour each.

Step 3.Conducting a power flow study to measure power supply and to specify normal system operations after asset failure. Here, a direct current optimal power flow (DCOPF) is used to consider the operational limits of an infrastructure and stochastic models of wind and solar generation are considered to assess different active power levels.

Step 4.Assess the suitability and security of the electrical system through reliability indices, using the power flow results from the previous step. The measurements used in this study are presented below:

- The EENS index is the sum of the energy not supplied in each of the 8760 1-hr steps.

$$\boldsymbol{EENS} = \frac{\sum_{i=1}^{N_y}\sum_{j=1}^{N_i}\boldsymbol{E}_{j,i}}{\boldsymbol{N_y}}; \boldsymbol{Unit} : [\boldsymbol{MWh} \,/\, \boldsymbol{year}] \tag{5}$$

where $\boldsymbol{E}_{j,i}$ is the energy not supplied in the interruption j of iteration i, $\boldsymbol{N_y}$ is the total number of simulated years and $\boldsymbol{N_i}$ is the total number of interruptions in year i.

- The EDNS index is the average energy not supplied in each of the 8760 1-hr steps.

$$\boldsymbol{EDNS} = \frac{\boldsymbol{EENS}}{8760}; \boldsymbol{Unit} : [\boldsymbol{MW}] \tag{6}$$

- The EFLC index is the frequency of the transitions from zero to zero of power not supplied.

$$\boldsymbol{EFLC} = \frac{\sum_{i=1}^{N_y}\boldsymbol{N_i}}{\boldsymbol{N_y}}; \boldsymbol{Unit} : [\boldsymbol{outages} \,/\, \boldsymbol{year}] \tag{7}$$

- The LOLE index is the expected number of hours in a given period that the energy not supplied is above zero.

$$\boldsymbol{LOLE} = \frac{\sum_{i=1}^{N_y}\sum_{j=1}^{N_i}\boldsymbol{D}_{j,i}}{\boldsymbol{N_y}}; \boldsymbol{Unit} : [\boldsymbol{hours} \,/\, \boldsymbol{year}] \tag{8}$$

where $\boldsymbol{D}_{j,i}$ is the duration of interruption j in iteration i.

- The LOLP index is the expected percentage of hours that the energy not supplied is above zero.

$$\boldsymbol{LOLP} = \frac{\boldsymbol{LOLE}}{8760}; \boldsymbol{Unit} : [\%] \tag{9}$$

- The ADLC index is the average number of hours of load curtailment.

$$\boldsymbol{ADLC} = \frac{\boldsymbol{LOLE}}{\boldsymbol{EFLC}}; \boldsymbol{Unit} : [\boldsymbol{hours} \,/\, \boldsymbol{outage}] \tag{10}$$

Step 1. Repeat the previous steps until reaching a covariance less than 6% in the EENS index [64].

In electrical systems with a high penetration of renewable energy, the role of wind generators and photovoltaic plants can be examined from different perspectives. However, appropriate models must be defined to perform the different analyses. Renewable energy sources can not only improve infrastructure performance but also have negative effects on the entire network [2].

To consider renewable energies in reliability analysis, the random nature of resources is taken into account by calculating the error of power prediction through the statistical metrics Root Mean Squared Error (RMSE), Maximum Absolute Error (MaxAE), Mean Absolute Error (MAE), Mean Bias Error (MBE) and Mean Absolute Percentage Error (MAPE) [65,66]. These measurements are expressed as follows:

- The RMSE index is a measure of the global error over the entire forecast period.

$$\boldsymbol{RMSE} = \sqrt{\frac{1}{\boldsymbol{N}}\sum_{i=1}^{N}(\widehat{\boldsymbol{p}}_i - \boldsymbol{p}_i)^2} \tag{11}$$

- The MaxAE index is an indicator of local deviations of forecast errors.

$$\boldsymbol{MaxAE} = \boldsymbol{max}_{i=1,2,\ldots,N}|\widehat{\boldsymbol{p}}_i - \boldsymbol{p}_i| \tag{12}$$

- The MAE index is a global error metric, which is useful for evaluating forecast performance.

$$\boldsymbol{MAE} = \frac{1}{\boldsymbol{N}}\sum_{i=1}^{N}|\widehat{\boldsymbol{p}}_i - \boldsymbol{p}_i| \tag{13}$$

- The MBE and MAPE indices indicate the mean bias of the forecasts.

$$\boldsymbol{MBE} = \frac{1}{\boldsymbol{N}}\sum_{i=1}^{N}(\widehat{\boldsymbol{p}}_i - \boldsymbol{p}_i) \tag{14}$$

$$\boldsymbol{MAPE} = \frac{1}{\boldsymbol{N}}\sum_{i=1}^{N}\left|\frac{\widehat{\boldsymbol{p}}_i - \boldsymbol{p}_i}{\boldsymbol{Capacity}}\right| \tag{15}$$

In all equations, $\boldsymbol{p}_i$ represents the current power generation of the renewable resource over time i, $\widehat{\boldsymbol{p}}_i$ is the power generation of the renewable resource estimated in the forecasting period and N is the estimated number of points in the forecast period.

The closer the forecast is to the actual value, the smaller the dispersion of the metrics will be. These considerations are examined in step five.

2.2. Vulnerability assessment

Most electrical networks are interconnected for security and reliability reasons. The high demand for electrical energy places the system in a state of operational stress, which could easily cause a drop in network performance. Interconnections play a key role in the robustness of infrastructure but at the same time, affect the propagation of contingencies between different coupled transmission systems [67].

Vulnerability is a concept used to characterise the lack of robustness of a system, that is, the ability to maintain its function intact when subjected to disturbances or threats [68]. Vulnerability is measured as a function of the size of the largest connected infrastructure, both before and after events [69]. Here, a statistical index is required to measure the functionality of the coupled network during such events. In this work, a disconnected load (DL) index is used to measure the system's functionality during contingency events [70].

$$DL = 100 - \left(\frac{L_i}{L_{total}^{BC}} \times \ 100\right); Unit : [\%] \tag{16}$$

where L_{total}^{BC} is the total load of the infrastructure in its base case and L_i is the total remaining load connected to the largest network in iteration i.

The DL index varies between 0 and 100 and is measured as a function

of the fraction of removed buses, f. As the DL index increases, the impact on the loads connected in the interconnected network increases.

Fig. 2 shows the proposed procedure to assess the vulnerability of interconnected power systems through the evolution of the DL index.

The first step consists of collecting technical data on the electrical networks, considering the models shown in Fig. 3 and assuming that coupled systems have generators, buses, loads, transmission lines, switches, and interconnection lines that represent the two-way dependencies between infrastructures. Here, DCOPFs are run to quantify the total base load of the coupled system, L_{total}^{BC}.

The electrical networks are decomposed by randomly and iteratively eliminating the buses, one by one, and by assuming that the buses fail during the iterative process. This random sequence of buses is determined by a uniform, pseudo-random number generator, which contains a permutation of integers without repetitions. The default Mersenne Twister algorithm is used in Matlab [71]. Random events include random hazards, such as natural phenomena, involuntary human failures or technical failures in network equipment and hardware.

The algorithm begins by randomly removing a bus from the coupled network. If it is a slack bus, it reconnects, and the procedure is repeated with another random bus. The slack bus is not eliminated because it balances energy in a power grid. Removing a bus implies eliminating all the power lines connected to it and forming a new topological structure of the coupled system. In this step, the algorithm determines the subnets using a depth-first search algorithm [72] and identifies the island or islands with slack buses to run the DCOPF. Here, the total remaining connected load, L_i, is quantified, and the DL index is measured.

After each successive bus removal, the constant reconfiguration of the electrical network can lead to divergent results when executing a routine of AC power flows. Therefore, this procedure uses DCOPF because it is a convergent and non-iterative method, which generates linear constraints that lead to solutions in a short time. In addition, it is a useful and accurate method to quickly estimate active power flows, considering the operating limits of the electrical network [30]. The latter is important given the various resulting topologies and the number of runs.

Subsequently, another bus is randomly removed from the previous subnet, leaving out all those islands that do not contain the reference generator. The goal is to have a single electrical network during the decay process. The above procedure is repeated iteratively until the system is completely disintegrated and no more buses are left to remove. All of the above is considered a simulation sample. According to the central limit theorem, each experiment must be repeated more than 30 times to obtain an ideal statistical sample [56]. Here, 1000 samples of independent experiments are performed.

Last, once the desired number of experiments is reached, the DL index results are averaged.

Fig. 4 illustrates the process of disintegration of the coupled networks of Fig. 3. Note how, by randomly removing node b_3 at $t = 1$, the coupled system is divided into two independent islands, one of which has no links. The next bus in the group containing the slack bus (island 1) is then randomly removed, that is, node b_6 at $t = 2$. The procedure is repeated identically both at $t = 3$ and at $t = 4$, eliminating nodes b_4 and b_7, respectively. Last, node b_2 is eliminated at $t = 5$, ending the iterative process. In each iteration, DCOPFs are run to measure the DL indicator. All the above process is repeated up to 1000 times, albeit changing the order in which the buses are removed, to obtain a statistical sample.

The proposed vulnerability procedure assumes that an electrical network integrated with renewable energies operates with the programmed wind and photovoltaic resources; that is, it considers an operating condition of a full day and a forecast interval of 3 h [73]. However, given the dynamics of the network decomposition process, the disintegration time is of seconds or minutes; thus, the variability of renewable resources is not a determining factor in the vulnerability study.

3. Test systems used

This section presents the IEEE RTS-96 and IEEE RTS-GMLC test networks used to construct the six case studies analysed in this work [57, 58]. The first network represents an electrical system with coal-fired power plants, while the second network is based on the same infrastructure but with greater renewable generation. The objective is to use the two infrastructures with different percentages of renewables but interconnect them with different coupling degrees.

3.1. Description of the case studies

The IEEE RTS-96 test system corresponds to a power system composed of three equal power grids merged. In this work, only one (hereafter Network 1) of the three electrical networks is used. This electrical infrastructure is composed of 24 buses, 33 generators and 38 power lines and transformers. The peak load for a one-year period is 2850 MW. The fundamental data of the system under study, including the parameters of the lines, the general characteristics of the load and the input data for the stochastic failure model for buses, transformers and lines, can be found in [57]. Fig. 5a) shows the topological configuration of this test network. This system is chosen because it is well documented and analysed in the scientific literature [54].

The IEEE RTS-GMLC test system is an updated version of the IEEE RTS-96 test system but with renewable energy sources. This network is identically formed by three equal power systems with different degrees of renewable penetration. Here, one (hereafter Network 2) of the three electrical networks is also used to maintain accuracy in the models. The new network contains large-scale photovoltaic (PV) generators at buses 1–4, 13 and 19, low-power rooftop PV (RTPV) generators at bus 18 and wind generation (WIND) at bus 22. Generator capacities for these sources are 404, 94 and 713.5 MW, respectively. Fig. 5b) shows the topology of the system under study. The system data, such as the length of the lines, the load characteristics and the updated parameters of the generators, are given in [58]. The failure rates and repair times of renewable generators are considered similar to those used in hydroelectric plants. This network is located in the southwestern United States, which is an area with good solar and wind resources. The demand profiles and the data for photovoltaic and wind generation are obtained from the Low Carbon Study [74] and the Western Wind and Solar Integration Study Phase 2 [75], respectively. The wind turbines were assumed to be 80 m high. Fig. 6 shows the monthly demand in two time zones, and Fig. 7 shows the estimated production of wind generation at bus 22. On the one hand, it can be observed that the demand remains stable most of the time, presenting slight increases in the summer months; in contrast, the wind resource is the inverse, presenting production losses in the same period.

To analyse the effect of connecting power systems with different generation mixes and different degrees of coupling on reliability and vulnerability, six different case studies are proposed using the previous test networks. The cases are as follows:

- Case one. IEEE RTS system coupled to the IEEE RTS-GMLC system through interconnection links 23-17, 13-15 and 7-3.
- Case two. IEEE RTS system coupled to the IEEE RTS-GMLC system through interconnection links 23-17 and 7-3.
- Case three. IEEE RTS system coupled to the IEEE RTS-GMLC system through interconnection links 23-17.
- Case four. Two IEEE RTS-GMLC systems coupled through interconnection links 23-17, 13-15 and 7-3.
- Case five. Two IEEE RTS-GMLC systems coupled through interconnection links 23-17 and 7-3.
- Case six. Two IEEE RTS-GMLC systems coupled through interconnection links 23-17.

The 23-17, 13-15 and 7-3 power lines are rated at 608, 608 and 208

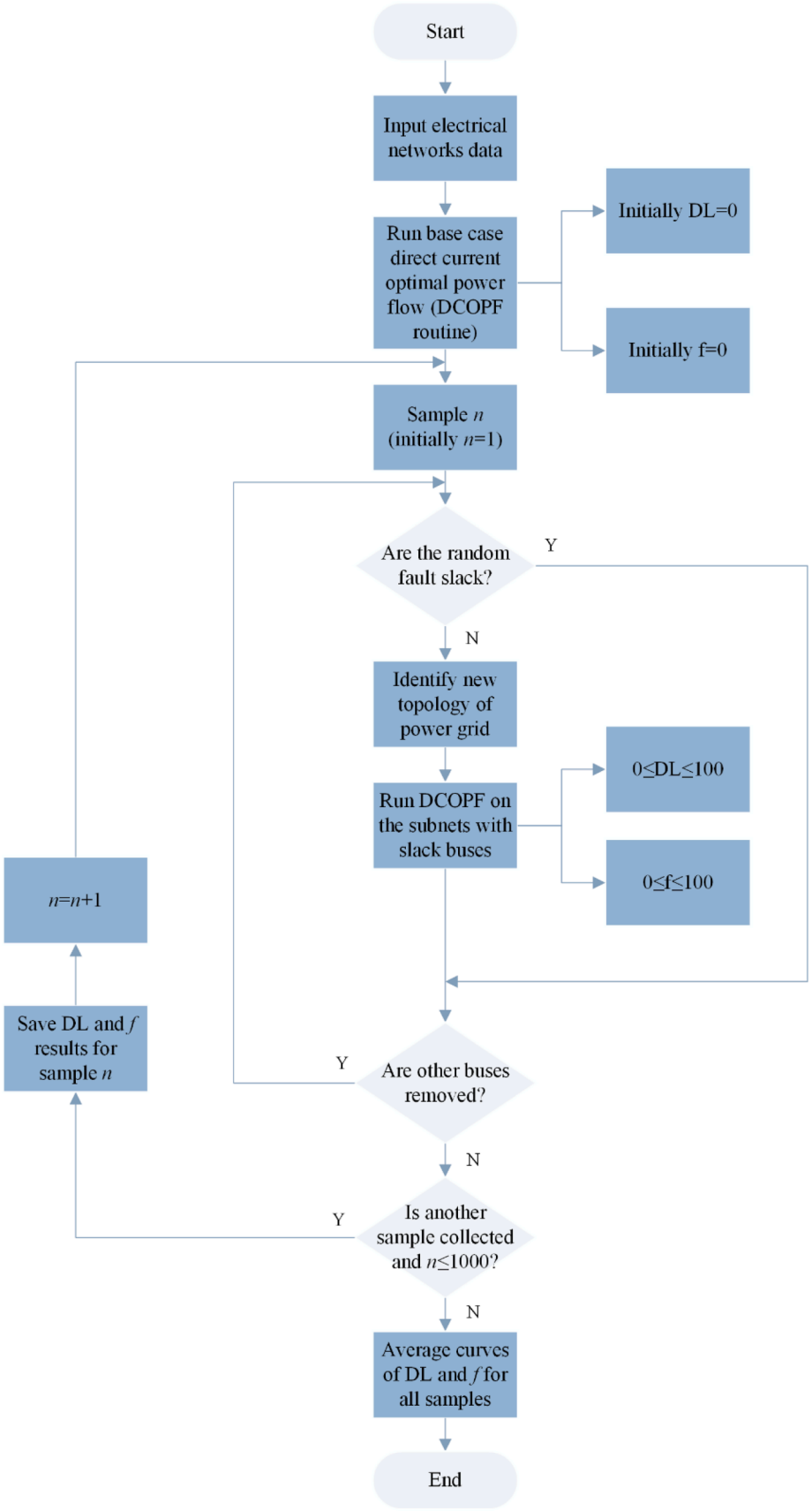

Fig. 2. Procedure to perform the vulnerability assessment.

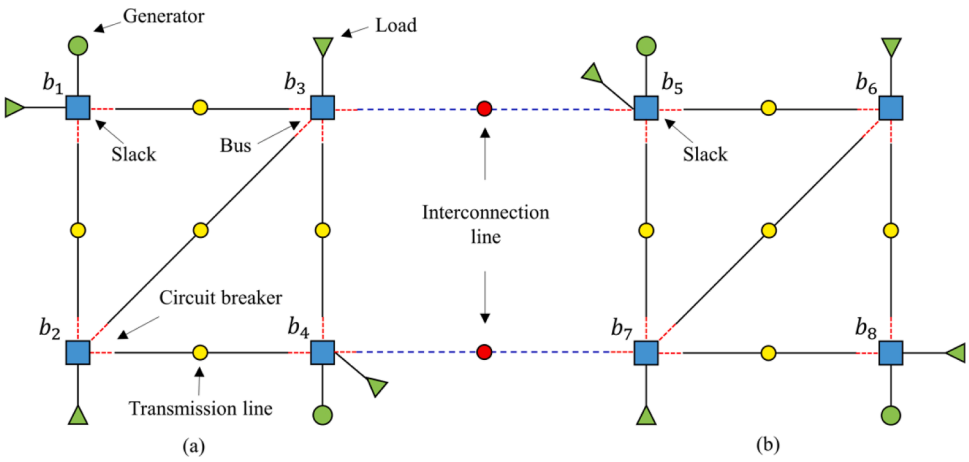

Fig. 3. Interconnected power system. (a) Power grid one and (b) power grid two.

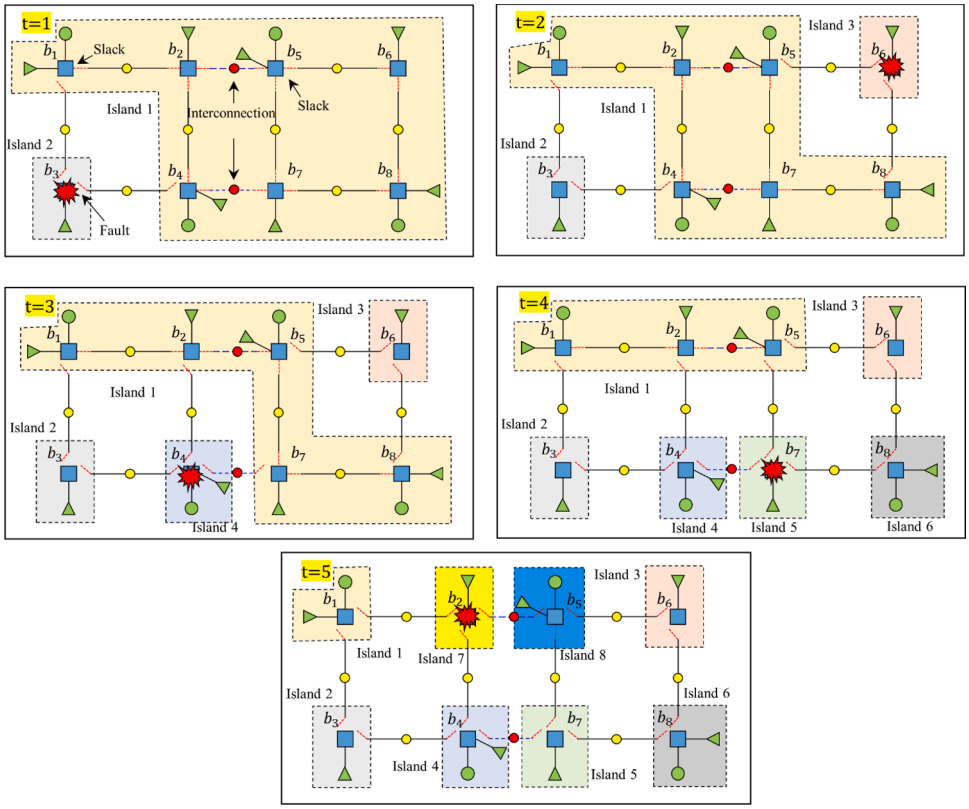

Fig. 4. Disintegration process of an interconnected power system.

MW, respectively.

The first three cases correspond to the coupling of an entirely thermal system with an integrated system with renewable resources, while the remaining three cases are purely renewable networks but with different degrees of coupling between them. The aim is to quantify the total effect of renewable sources during the proposed evaluations. Fig. 8 depicts the coupling of case one.

4. Simulation results of the case studies

In this section, the simulation results obtained after applying the reliability and vulnerability procedures in the six case studies described above are presented. The reliability indices EENS, EDNS, EFLC, LOLE, LOLP and ADLC are calculated using PLEXOS, while the DL index is measured through the disintegration algorithm implemented using MATLAB. The two proposed simulation frameworks run in parallel on a personal computer with a 3.40 GHz Intel® Core™ i7 CPU and 16 GB of RAM.

4.1. Effect of renewable sources and interconnections on the reliability of power systems

The reliability assessment can be performed after applying the procedural steps described in the previous sections to all the components of the networks studied. Here, it was considered that the renewable sources PV and WIND regulated their generation according to the maximum capacity of the resource available at a given time, while the RTPV sources fed into the system all the available energy according to the

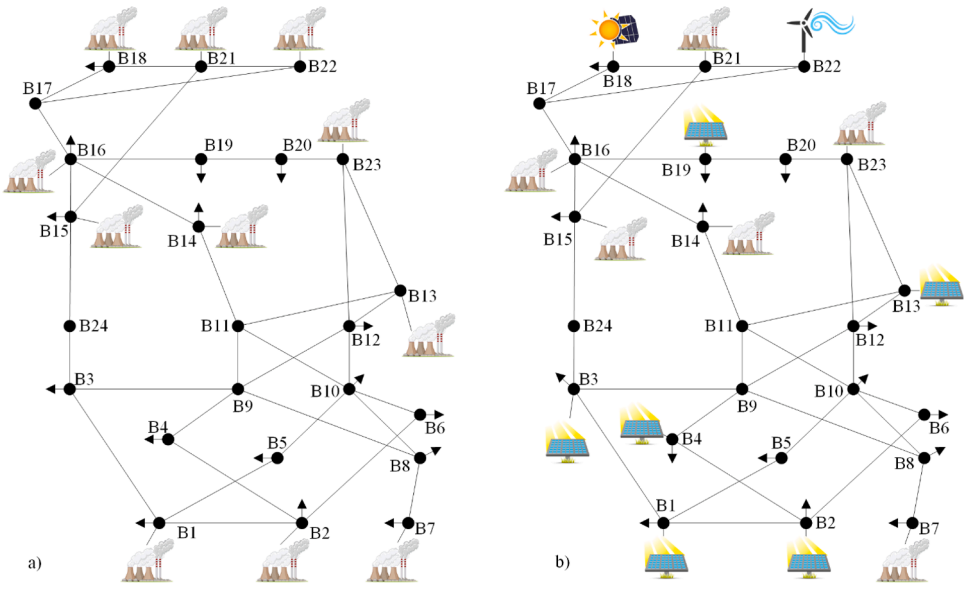

Fig. 5. Test systems under study. (a) IEEE RTS network (Network 1) and (b) IEEE RTS-GMLC network (Network 2).

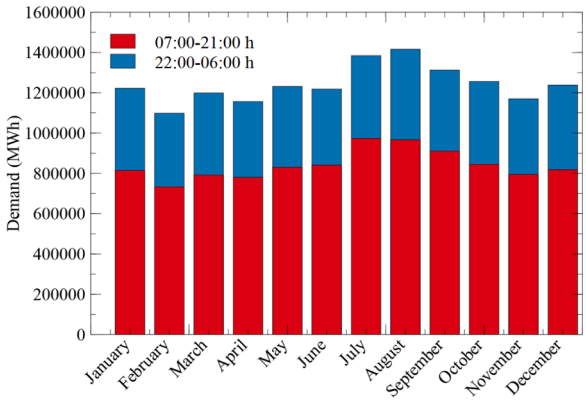

Fig. 6. Monthly demand in two-hourly intervals of the IEEE RTS-GMLC network.

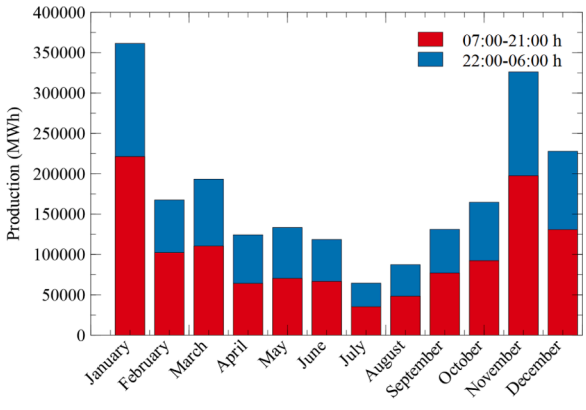

Fig. 7. Production of wind energy at bus 22 of the IEEE RTS-GMLC network.

resource. Additionally, to make the model more realistic, some variability was given to the historical generation included in the IEEE RTS-GMLC system, calculating the error in the forecasting of the renewable resource through the statistical metrics of RMSE, MaxAE, MAE, MBE and MAPE [65,66].

Table 1 shows that the prediction of solar technologies is more accurate than that of wind technologies and that the larger the plant is, the lower the dispersion of the values. Thus, the generation value available for each photovoltaic plant or wind farm was the average value, and the MAPE index calculated for each technology was the standard deviation. This allowed the resulting values to oscillate according to their forecast error.

Table 2 shows the simulation results of the reliability indices for the six case studies. Five hundred iterations of one year were run in each network, obtaining covariance values (COV) less than 6% in all cases [64].

For the simulations performed here, the findings showed that systems with higher thermal generation (cases 1 to 3) are more reliable than systems with higher renewable generation (cases 4 to 6) and that the EENS index increased as the degree of interconnection between infrastructures decreased. In cases 1 to 3, generation in area 2 did not depend on the availability of wind and solar resources, so area 1 was better supported in times of stress. However, the decrease in the level of interconnection translated into more non-supplied energy, going from 3984.86 to 4468.60 MWh/year due to the lack of power-sharing between the two infrastructures. In cases 4 to 6, the EENS index was almost identical between the two areas, and the remaining reliability indices also increased as the interconnection links between the infrastructures were reduced. These three cases, being systems with high integration of renewable resources, maintain the lowest reliability levels compared to the first three cases that incorporate thermal resources.

On the other hand, the EENS index increased only 2.9% for area 1 when comparing cases 1 and 3; however, this same index increased by 26.70% for area 2 when the same cases were considered. This indicates that although the integrated system with renewables is less reliable overall, the interconnections with the thermal system improved its reliability due to the surplus energy of the attached infrastructure. This behaviour was not observed in cases 4 and 6 since there was not the same availability of energy resources in the coupled network to be exported through interconnection links. For greater detail, Table 3 shows the energy exchanged through interconnection lines 23-17, 13-15 and 7-3. Here, the indices of net transfer capacity (NTC), exchanged energy (EE), maximum line capacity (MLC), maximum percentage of line capacity (MPLC) and percentage of exchange energy (PEE) were calculated, according to the definitions found in [76]. These indices are presented below:

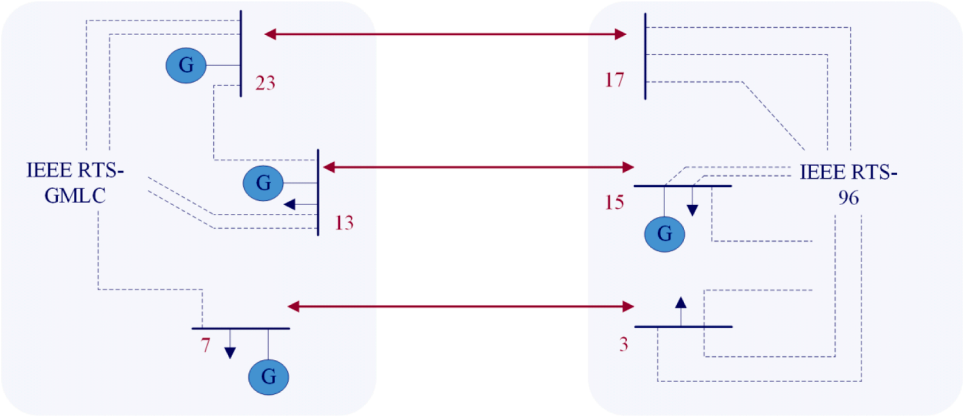

Fig. 8. Schematic representation of case one.

Table 1
Deviation in the prediction of renewable resources in the IEEE RTS-GMLC system.

	Wind	PV	RTPV
RMSE (MW)	181.43	10.72	2.71
MaxAE (MW)	710.73	76.02	20.00
MAE (MW)	113.57	5.06	0.31
MBE (MW)	12.53	0.35	9.40
MAPE (%)	15.92	5.40	6.91

- The NTC index is the maximum exchange capacity between areas in MW; that is, the sum of the individual capacities of each interconnection line.
- The EE index is the total energy exchanges from one area to another during a year.

$$\mathrm{EE} = \frac{\sum_{i=1}^{N_y}\sum_{j=1}^{L}\sum_{k=1}^{8760} F}{N_y}; \text{Unit} : [\mathrm{MWh} / \mathrm{year}] \tag{17}$$

where N_y is the total number of simulated years, L is the total number of interconnecting power lines, and F is the active power.

- The MLC index is the maximum exchange capacity of an interconnection line in MW. This measure is related to the NTC indicator and measures the congestion of the links.
- The MPLC is the percentage of congestion of the interconnection links.

$$MPLC = \frac{MLC}{NTC} \times 100; \text{Unit} : [\%] \tag{18}$$

Table 2
Results of the reliability indices for the case studies.

	Case 1	Case 2	Case 3	Case 4	Case 5	Case 6
EENS (MWh/year)	3984.86	4170.12	4468.60	6204.61	7375.17	7759.00
EENS-Area 1 (MWh/year)	2439.92	2478.80	2510.70	3179.16	3765.11	3954.30
EENS-Area 2 (MWh/year)	1544.95	1691.32	1957.90	3025.45	3610.07	3798.52
EDNS (MW)	0.45	0.48	0.51	0.71	0.84	0.89
EFLC (occurrences/year)	8.01	7.53	7.06	11.74	12.15	13.38
LOLE (h/year)	51.52	51.59	55.37	70.28	76.54	84.45
LOLP (%)	0.59	0.59	0.63	0.80	0.87	0.96
ADLC (h/year)	6.44	6.85	7.85	5.99	6.30	6.31
COV EENS (%)	1.49	3.42	2.86	2.62	2.64	2.48
Computation time (h)	20.31	22.66	18.30	22.08	22.75	20.61

Table 3
Use of interconnection lines in the case studies.

		NTC(MW)	EE 1→2 (MWh/year)	EE 2→1 (MWh/year)	MLC (MW)	MPLC (%)	PEE (%)
Case 1	Total exchange	1424	367,935.12	−1,404,490.21	517.05	36.31	11.89
	23-17	608	300,782.93	−232,210.49	212.07	34.88	3.58
	13-15	608	56,130.02	−813,704.71	238.56	39.24	5.84
	7-3	208	11,022.17	−358,575.01	97.01	46.64	2.48
Case 2	Total exchange	816	311,833.57	−1,454,868.98	521.86	63.95	11.85
	23-17	608	286,185.26	−880,640.19	424.38	69.80	7.83
	7-3	208	25,648.32	574,228.79	144.95	69.69	4.02
Case 3	23-17	608	231,384.52	−1,417,972.08	414.61	68.19	11.06
Case 4	Total exchange	1424	534,093.19	−537,023.36	329.74	23.16	7.19
	23-17	608	516,090.32	−10,154.14	139.81	23.00	3.53
	13-15	608	1748.42	−374,736.66	168.59	27.73	2.53
	7-3	208	16,254.45	−152,132.55	71.57	34.41	1.13
Case 5	Total exchange	816	273,040.77	−330,817.11	412.19	50.51	4.05
	23-17	608	266,691.14	−78,868.83	306.92	50.48	2.32
	7-3	208	6349.63	−251,948.28	116.40	55.96	1.73
Case 6	23-17	608	102,980.38	−196,491.69	398.12	65.48	2.01

- The PEE index is the ratio of energy exchanged between areas during a year.

$$\text{PEE} = \frac{\text{EE}}{\text{Annual demand}} \times 100; \text{Unit} : [\%] \tag{19}$$

In cases 1 to 3, it was observed that the PEE index was higher than in cases 4 to 6 and that the three infrastructures with coupled thermal and renewable generation were less sensitive to the removal of interconnection lines, as evidenced by the EE index. On the other hand, in cases 4 to 6, there was a significant decrease in the energy exchanged as the degree of coupling of the networks decreased. This behaviour was due to both the high capacity of the interconnection links and the large generating capacity. In other words, the power system with thermal generation had sufficient generating capacity to support the integrated system with renewable sources. In contrast, the EE index decreased significantly when connecting integrated networks with renewable sources through a single link. This was due to the lower reliability of the systems, caused by the variability or outage of the renewable resource.

Fig. 9 more graphically shows the flows in the interconnection lines for case 1. It was observed that the power system with thermal generation directly supported the system with a high proportion of renewables. The flows of lines 23-17 were distributed equally in both directions, although area 1 supported more than area 2. The non-renewable generator at bus 23 was rated at 670 MW, so it was able to support area 2 through bus 17. This bus depended on the availability of the hydroelectric plants at bus 22. Flows from the lines 13-15 and 7-3 were distributed from area 2 to area 1. Bus 13, depending on the 93 MW of photovoltaic energy, required the contribution of the thermal generator connected to bus 15. Bus 7, due to the topological configuration, turned out to import energy at bus 3 in all the case studies.

Identically, Fig. 10 shows the results for case 4. In general, areas one and two exchanged the same amount of energy, with the EENS index being almost the same in all cases. Lines 23-17 distributed the energy from area 1 to area 2. Bus 17, despite not having its generation, was connected to buses 18 and 22, which had 94 MW of unmanageable rooftop photovoltaic production and 713 MW of wind production, respectively. This made it sensitive to variations in renewable resources and random failures of infrastructure elements. Lines 13-15 and 7-3 had similar behaviour to case 1, although the amount of exchanged energy was lower.

4.2. Effect of renewable sources and interconnections on the vulnerability of power systems

The decomposition curves in Fig. 11 correspond to the six case studies analysed, obtained by averaging a total set of 1000 samples from independent experiments. The DL index had a value of 0 when the networks were initially connected; then, the DL index progressively increased until reaching a value close to 100 as the systems disintegrated. This indicated that the loads were disconnecting. The computation times for the six case studies were 9.47, 7.23, 6.64, 9.41, 8.65 and 7.02 min, respectively.

In general terms, the curves for the most connected coupled systems, cases 1 and 4, showed that the two infrastructures disintegrated with the removal of approximately 75% of the buses. In the rest of the cases analysed with interconnected topologies, the networks disintegrated with removing 65% of the buses during the disintegration events. It was also observed that the cases presented a worse structural performance as the degree of coupling between the infrastructures decreased since the curves were always above those of the most coupled networks in their respective comparisons. In other words, the systems with combined thermal and renewable generation and the systems with greater shares of renewable generation interconnected with three lines had a more robust structural performance when analysed compared to the other networks or cases.

Given that the vulnerability assessment included multiple measurements in each stage of infrastructure decomposition and not a single index, it was also proposed to measure the vulnerability index called the damage area index, DA, to accurately assess each vulnerability index's behaviour curves of Fig. 11. The damage area index is defined as the region under the disintegration curves [55]. It is calculated by evaluating the integrals of the curve functions from the minimum and maximum limits of the fraction of removed buses. Note that a high DA represents a greater disconnected load in the network and implies greater damage to the interconnected infrastructure.

Table 4 shows some results corresponding to the removal of a given number of elements (f), their impact on the disconnected load (DL) of the network, and the damage area (DA) index for each of the six case studies.

On the one hand, DL was slightly lower in case 4 than in case 1 for both $f = 12.50\%$ and $f = 25.00\%$; however, this behaviour changed in the rest of the fractions considered, making this network slightly more vulnerable than its counterpart, as evidenced by the DA index. This showed that the system with the highest share of renewable generation, case 4, was less robust than the system with higher thermal generation, case 1.

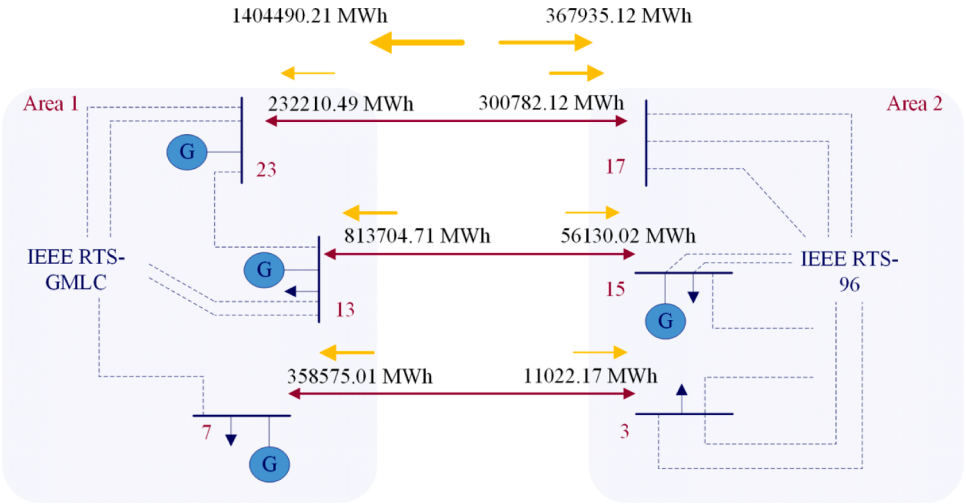

Fig. 9. Diagram of the flows in the interconnection lines of case one.

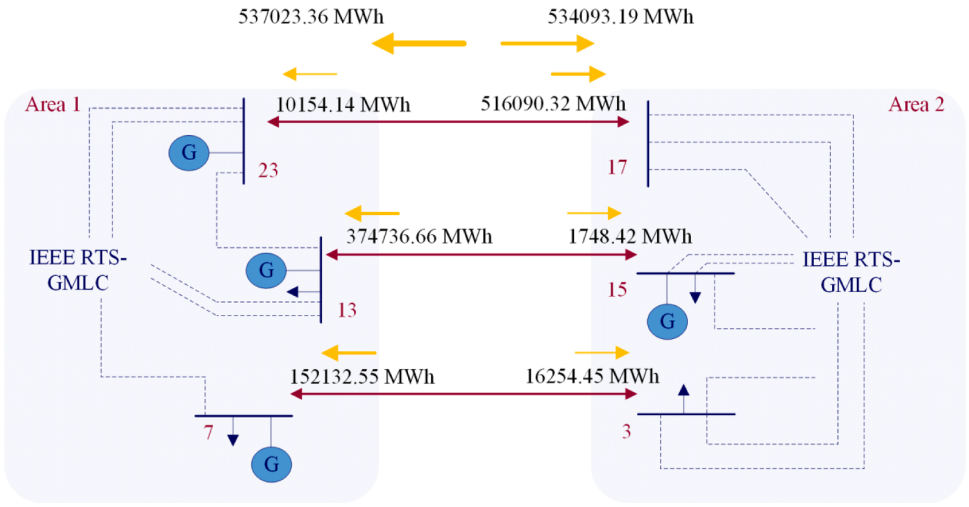

Fig. 10. Diagram of the flows in the interconnection lines of case four.

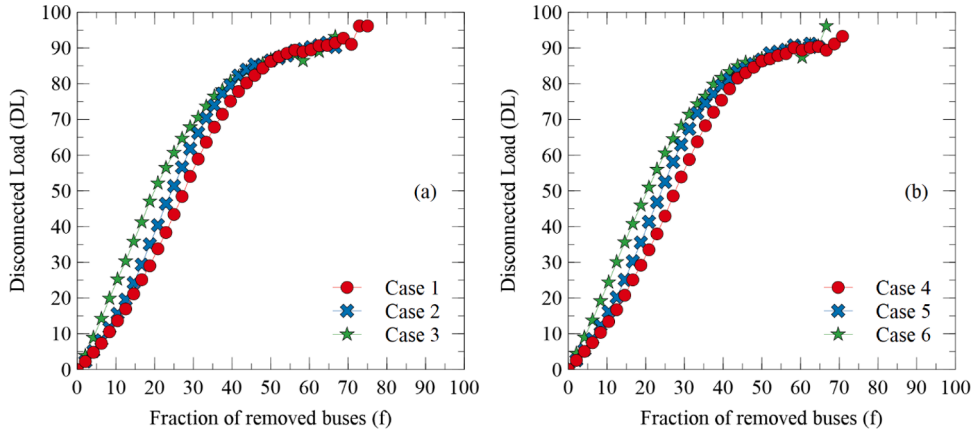

Fig. 11. Disintegration curves for the six case studies.

Table 4
Impact of bus removal on disconnected load (DL) for the case studies.

	$f =$ 12.50%	$f =$ 25.00%	$f =$ 37.50%	$f =$ 50.00%	$f =$ 62.50%	Vulnerability (DA)
Case 1	16.94	43.38	71.40	86.21	90.61	3491.72
Case 2	19.52	51.33	77.21	86.49	90.73	3703.92
Case 3	30.31	60.66	78.20	86.74	89.01	3965.88
Case 4	16.72	42.92	71.99	86.32	90.07	3494.66
Case 5	20.16	52.47	77.10	86.72	91.17	3735.42
Case 6	30.10	60.55	79.80	86.98	90.87	3982.91

Likewise, the other topological configurations showed very similar results during the network disintegration processes. When comparing cases 2 and 5, corresponding to systems with the same degree of coupling but with a different percentage of generation mix, it was observed that the infrastructure with the highest thermal generation, case 2, was less vulnerable than the system with the highest renewable generation. In contrast, the infrastructure integrated with renewables in case 6 was more robust than the infrastructure with higher thermal generation in case 3 up to $f = 25.00\%$; however, it suffered a drop at the end of the disintegration process, which increased the vulnerability of this system. These results were also observed in the DA measure, since the systems with higher thermal generation, cases 2 and 3, presented less damage than those obtained in cases 5 and 6.

On the other hand, the findings showed that highly interconnected systems were more robust than less connected systems and that different topological configurations played a key role in the operational security of networks. In the latter, the systems coupled with two lines showed variations throughout the study, but in any case, the vulnerability was always better than the networks coupled with a single power line. Systems with three interconnection links improved their vulnerability results. Although electrical interconnections improve the networks' operational and economic aspects, they are elements that can propagate disturbances and affect any coupled infrastructure, regardless of the existing generation mixes in the systems. Similarly, the infrastructures with the highest thermal generation were more robust than the infrastructures with the highest renewable generation in global terms, since the decomposition curves and the damage areas of cases 1 to 3 were always slightly above or below the decomposition curves and damage areas for cases 4 to 6, respectively. This was due to the generating capacity of renewable sources, which influenced the load they could maintain during disintegration events.

5. Joint discussion of the results

This section comprehensively analyses the results of reliability and vulnerability. Here, the effect of renewable sources and the impact of

cross-border interconnection lines on interconnected electrical systems are studied.

5.1. Integration of reliability and vulnerability

During the last two decades, the use of renewable energy sources and cross-border interconnections has increased in electric power systems due to environmental and energy security risk concerns [2]. Renewable energy sources are sustainable energy resources with environmental benefits, and interconnections are critical assets for the mutual sharing of energy and have operational benefits. However, there are substantial challenges both for integrating and evaluating them in existing power grids. Reliability and vulnerability assessments have been the slogans of electric utilities to address the above problems. This study considers that both concepts should be taken into account within a joint-decision framework to compensate for the limitations of some of the approaches used in studying the effect of renewable sources and the impact of cross-border interconnection lines. These evaluations should also be complemented to improve long-term planning, analyse structural performance, and evaluate the security conditions of these critical infrastructure systems, amongst many other things.

Previously, reliability and vulnerability were assessed separately in Sections 4.1 and 4.2, measuring statistical indices that quantified the network's operational conditions after an n-1 contingency and plotting disintegration curves obtained from measuring disconnected load in the network as a result of n-k contingencies, respectively. The EENS reliability index found in Table 2 and the DA vulnerability index found in Table 4 were used here to compare both concepts effectively.

On the one hand, Table 5 compares the impact of the interconnections on the reliability and vulnerability of power systems with thermal and renewable generation (cases 1 to 3) and purely renewable generation (cases 4 to 6). Here, the EENS reliability index and the DA vulnerability index were used, and the percentage increase in both indices was quantified with respect to the most connected case for its generation type. That is, cases 2 and 3 versus case 1 and cases 5 and 6 versus case 4. The objective was to determine the impact of the degree of interconnectedness between the systems from both perspectives.

In general terms, fewer interconnections significantly impacted both the reliability and vulnerability of the integrated systems studied. In infrastructures with thermal and renewable generation, cases 1 to 3, the increase in the EENS reliability index was 5 and 12% and for the DA vulnerability index 6 and 14%. In infrastructures with a higher share of renewables, cases 4 to 6, the increases were 19 and 25% in the reliability index and 7 and 14% in the vulnerability index. That is, the fewer the interconnection lines there are, the greater the impact on the reliability and vulnerability of the interconnected electrical systems. Likewise, when comparing the increases of both concepts together, cases 1 to 3 versus cases 4 to 6, it was seen that interconnections had a greater impact on the reliability of renewable generation systems than in the systems with thermal generation since the change in vulnerability remained at 6 and 14% regardless of the type of generation. In particular, there was a greater impact in cases 4 and 5 and a smaller impact in cases 1 and 2.

On the other hand, Table 6 shows a composite analysis of the effect of renewable sources on the reliability and vulnerability of integrated power grids with different types of generation. The EENS and DA measures were used, and the increase in reliability and vulnerability of the systems with the same number of interconnections was quantified but with different energy vectors, that is, cases 1 and 4, 2 and 5, and 3 and 6.

Here, it was observed that renewable sources severely affected reliability and did not greatly influence the vulnerability of interconnected power systems. For example, in cases 1 and 4, there was an impact of 55.70% on the reliability index versus 0.08% on vulnerability. The two remaining sets presented very similar results of 76.86 and 73.63% reliability and 0.85 and 0.43% vulnerability. The interconnected electrical networks with the greatest share of renewables, cases 4, 5 and 6, were between two and three times less reliable than the power networks with the highest thermal generation; however, they did not show considerable vulnerability variations. In other words, the presence of renewable resources in the generation mix was only a determining factor in the reliability assessment of the studied systems. These changes were due to the inability of the generators to satisfy load conditions, since the thermal power plants of cases 1 to 3 had a greater generating capacity than the renewable sources of cases 4 to 6, so they could withstand abrupt variations in the network operating conditions.

In conclusion, the previous results show, on the one hand, that cross-border interconnections in power systems with a high degree of coupling, regardless of the energy vector, always have positive impacts on the operational conditions of the infrastructures because they allow neighbours to import the necessary electricity and to face undesirable events such as weather events, failures or blackouts. It also reduces the need to build new power plants and facilitates optimal resource management, amongst other factors. Given that cross-border interconnections are essential for supply security, the findings show that these assets affect both the reliability and vulnerability of power networks.

On the other hand, renewable sources are so essential in the global climate context that their incorporation into power systems is undeniable. However, these energy vectors are sometimes less capable of responding to certain stress situations, affecting the security of supply in certain operating states. The results obtained showed that renewable sources impact reliability more than vulnerability. For this reason, backup mechanisms such as energy storage systems with rapid response times could be included to ensure highly reliable and highly robust systems.

6. Conclusions

This article has highlighted the possible effect of greater penetration of renewable resources and the possible impact of cross-border interconnections on the reliability and vulnerability of electric power systems. Increasing the share of renewables can potentially present important challenges that must be addressed together to comply with existing security standards. Reliability analyses the system's capacity to meet demand with continuity and with an acceptable level of quality in the event of failure of one or two assets, and vulnerability quantifies the structural performance of the network under the non-trivial loss of multiple assets. In such situations, transmission system operators must simultaneously consider both concepts to quantify the performance of interconnected and integrated electrical infrastructures with different

Table 5
Impact of interconnections on the reliability and vulnerability of interconnected electrical systems.

	Coupled systems	Total links	Reliability (EENS)	Increase (%)	Vulnerability (DA)	Increase (%)
Case 1	RTS -GMLC	3	3984.86		3491.72	
Case 2	RTS -GMLC	2	4170.12	5	3703.92	6
Case 3	RTS -GMLC	1	4468.60	12	3965.88	14
Case 4	GMLC-GMLC	3	6204.61		3494.66	
Case 5	GMLC-GMLC	2	7375.17	19	3735.42	7
Case 6	GMLC-GMLC	1	7759.00	25	3982.91	14

Table 6
Effect of renewable sources on the reliability and vulnerability of interconnected electrical systems.

	Coupled systems	Total links	Reliability (EENS)	Increase (%)	Vulnerability (DA)	Increase (%)
Case 1	RTS -GMLC	3	3984.86		3491.72	
Case 4	GMLC-GMLC	3	6204.61	55.70	3494.66	0.08
Case 2	RTS -GMLC	2	4170.12		3703.92	
Case 5	GMLC-GMLC	2	7375.17	76.86	3735.42	0.85
Case 3	RTS -GMLC	1	4468.60		3965.88	
Case 6	GMLC-GMLC	1	7759.00	73.63	3982.91	0.43

shares of renewable energies against disturbances and contingencies. These concepts can be quantified in practice using the definitions found in their respective fields of research.

The results showed that the interconnections simultaneously impacted both the reliability and vulnerability of the different interconnected networks. The loss of a single interconnection link worsened reliability by more than 5% in the case of interconnected power systems with thermal generators and by 19% in the case of systems with higher shares of renewables, while vulnerability worsened between 6 and 7%.

On the other hand, the results showed that a greater proportion of renewable energy sources worsened the reliability of the different integrated systems with the same number of interconnections by more than 50%; however, the vulnerability was barely affected. In other words, higher penetration of renewable energies has more influence on reliability indices than on vulnerability indices of power systems. Therefore, mechanisms must be implemented to increase the response capacity of infrastructures with a high proportion of renewable energies against n-1 or n-2 contingencies.

In short, this work concludes that interconnection lines improve power-sharing between the coupled networks, but at the same time, they are critical assets prone to propagating disturbances from one system to another. A greater interconnection capacity is the best solution to design reliable and robust systems and to respond to n-1 and n- k contingencies, respectively.

CRediT authorship contribution statement

Jesus Beyza: Conceptualization, Methodology, Software, Validation, Formal analysis, Investigation, Visualization, Writing – original draft, Writing – review & editing. **Jose M. Yusta:** Conceptualization, Methodology, Validation, Formal analysis, Investigation, Writing – original draft, Writing – review & editing, Funding acquisition.

Declaration of Competing Interest

None

Acknowledgement

This work was supported by the Ministry of Science and Innovation of Spain under project PID2019-104711RB-100: Smart-grid design and operation under the threat of interrupted supply from electric power transmission systems with a high penetration of renewable energies.

References

[1] Li B, Ofori-Boateng D, Gel YR, Zhang J. A hybrid approach for transmission grid resilience assessment using reliability metrics and power system local network topology. Sustain Resilient Infrastruct 2020;6(1–2):1–16.
[2] Zare Oskouei M, Mohammadi-Ivatloo B. Integration of renewable energy sources into the power grid through powerfactory. Cham: Springer International Publishing; 2020.
[3] Sder L, Hofmann L, Orths A, Holttinen H, Wan Y, Tuohy A. Experience from wind integration in some high penetration areas. IEEE Trans Energy Convers 2007;22(1):4–12.
[4] Billinton R, Li W. Reliability assessment of electric power systems using Monte Carlo methods. Boston, MA: Springer US; 1994.
[5] Chen Q, McCalley JD. Identifying high risk N-k contingencies for online security assessment. IEEE Trans Power Syst 2005;20(2):823–34.
[6] Cuadra L, Salcedo-Sanz S, Del Ser J, Jiménez-Fernández S, Geem ZW. A critical review of robustness in power grids using complex networks concepts. Energies 2015;8(9):9211–65.
[7] Urgun D, Singh C. A hybrid Monte Carlo simulation and multi label classification method for composite system reliability evaluation. IEEE Trans Power Syst 2019;34(2):908–17.
[8] Heylen E, Deconinck G, Van Hertem D. Review and classification of reliability indicators for power systems with a high share of renewable energy sources. Renew Sustain Energy Rev 2018;97:554–68. January2018.
[9] Gbadamosi SL, Nwulu NI. Reliability assessment of composite generation and transmission expansion planning incorporating renewable energy sources. J Renew Sustain Energy 2020;12(2):1–14.
[10] Sabouhi H, Doroudi A, Fotuhi-Firuzabad M, Bashiri M. A novel matrix based systematic approach for vulnerability assessment. COMPEL - Int J Comput Math Electr Electron Eng 2020;40(1):1–17.
[11] Kröger W, Zio E. Vulnerable systems. London: Springer London; 2011.
[12] Wolf S, et al. Clarifying vulnerability definitions and assessments using formalisation. Int J Clim Change Strat Manage 2013;5(1):1756–8692.
[13] Grainger JJ, Stevenson WDJ. Power system analysis. McGraw-Hill, Inc.; 1994.
[14] ENTSO-E, "ENTSO-E network code for requirements for grid connection applicable to all generators," 2013.
[15] Abedi A, Romerio F. Multi-period vulnerability analysis of power grids under multiple outages: an AC-based bilevel optimization approach. Int J Crit Infrastruct Prot 2020;30:100365.
[16] Tabar VS, Ghassemzadeh S, Tohidi S. Increasing resiliency against information vulnerability of renewable resources in the operation of smart multi-area microgrid. Energy 2021;220:119776.
[17] Fan M, Sun K, Lane D, Gu W, Li Z, Zhang F. A novel generation rescheduling algorithm to improve power system reliability with high renewable energy penetration. IEEE Trans Power Syst 2018;33(3):3349–57.
[18] Sivasankari S, Chidambararaj N. Generation rescheduling based congestion management in restructured power system. Middle-East J Sci Res 2017;25(4):859–63.
[19] Kumar DS, Sharma A, Srinivasan D, Reindl T. Impact analysis of large power networks with high share of renewables in transient conditions. IET Renew Power Gener 2020;14(8):1349–58.
[20] Jiang Y, Wang G, Roy S, Liu CC. Power system severe contingency screening considering renewable energy. IEEE Power Energy Soc Gen Meet 2016;2016:1–5. -Novem.
[21] Ayadi F, Colak I, Garip I, Bulbul HI. Impacts of renewable energy resources in smart grid. In: 8th Int Conf Smart Grid icSmartGrid. 2020. IEEE; 2020. p. 183–8. icSmartGrid.
[22] Zhang L, et al. A data-driven approach to anomaly detection and vulnerability dynamic analysis for large-scale integrated energy systems. Energy Convers Manage 2021;234:113926. no. February.
[23] Eryilmaz S, Kan C. Reliability based modeling and analysis for a wind power system integrated by two wind farms considering wind speed dependence. Reliab Eng Syst Saf 2020;203:107077. no. January.
[24] Capitanescu F. Evaluating reactive power reserves scarcity during the energy transition toward 100% renewable supply. Electr Power Syst Res 2021;190:106672. no. January2021.
[25] Akhtar I, Kirmani S. Reliability assessment of power systems considering renewable energy sources. In: Mater. Today Proc.; 2021.
[26] Eryilmaz S, Bulanık İ, Devrim Y. Reliability based modeling of hybrid solar/wind power system for long term performance assessment. Reliab Eng Syst Saf 2021;209:107478. May2021.
[27] Yang S, Chen W, Zhang X, Yang W. A graph-based method for vulnerability analysis of renewable energy integrated power systems to cascading failures. Reliab Eng Syst Saf 2021;207:107354. March2021.
[28] Zhou D, Hu F, Wang S, Chen J. Power network robustness analysis based on electrical engineering and complex network theory. Phys A Stat Mech Appl 2021;564:125540.
[29] Li K, Liu K, Wang M. Robustness of the Chinese power grid to cascading failures under attack and defence strategies. Int J Crit Infrastruct Prot 2021;33(June 21):100432. Apr.
[30] Beyza J, Yusta JM. Integrated risk assessment for robustness evaluation and resilience optimisation of power systems after cascading failures. Energies Apr. 2021;14(7):2028.

[31] Zhu W, Milanović JV. Assessment of the robustness of cyber-physical systems using small-worldness of weighted complex networks. Int J Electr Power Energy Syst 2021;125:106486. no. February2021.
[32] Zhu D, Wang R, Duan J, Cheng W. Comprehensive weight method based on game theory for identify critical transmission lines in power system. Int J Electr Power Energy Syst 2021;124:106362. no. January2021.
[33] Wang S, Lv W, Zhang J, Luan S, Chen C, Gu X. Method of power network critical nodes identification and robustness enhancement based on a cooperative framework. Reliab Eng Syst Saf 2021;207:107313. no. March2021.
[34] Sperstad IB, Solvang EH, Jakobsen SH. A graph-based modelling framework for vulnerability analysis of critical sequences of events in power systems. Int J Electr Power Energy Syst 2021;125:106408. February2021.
[35] Liu Y, Zhang N, Wu D, Botterud A, Yao R, Kang C. Searching for critical power system cascading failures with graph convolutional network. IEEE Trans Control Netw Syst 2021:1–10.
[36] Nguyen T, Liu BH, Nguyen N, Dumba B, Chou JT. Smart grid vulnerability and defense analysis under cascading failure attacks. IEEE Trans Power Deliv 2021:1–9.
[37] Zhao Y, Liu S, Lin Z, Yang L, Gao Q, Chen Y. Identification of critical lines for enhancing disaster resilience of power systems with renewables based on complex network theory. IET Gener Transm Distrib 2020;14(20):4459–67.
[38] Athari MH, Wang Z. Impacts of wind power uncertainty on grid vulnerability to cascading overload failures. IEEE Trans Sustain Energy 2018;9(1):128–37.
[39] Zio E. Challenges in the vulnerability and risk analysis of critical infrastructures. Reliab Eng Syst Saf 2016;152:137–50.
[40] Athari MH, Wang Z. Modeling the uncertainties in renewable generation and smart grid loads for the study of the grid vulnerability. In: 2016 IEEE Power Energy Soc Innov Smart Grid Technol Conf ISGT. IEEE; 2016. p. 1–5. 2016.
[41] Hossain E, Roy S, Mohammad N, Nawar N, Dipta DR. Metrics and enhancement strategies for grid resilience and reliability during natural disasters. Appl Energy 2021;290:116709. no. January.
[42] Zhou D, Hu F, WANG S, Chen J. Robustness analysis of power system dynamic process and repair strategy. Electr Power Syst Res 2021;194:107046. May2021.
[43] Sperstad IB, Kjølle GH, Gjerde O. A comprehensive framework for vulnerability analysis of extraordinary events in power systems. Reliab Eng Syst Saf 2020;196:106788. no. April2020.
[44] Cicilio P, et al. Resilience in an evolving electrical grid. Energies 2021;14(3):694.
[45] Abedi A, Gaudard L, Romerio F. Power flow-based approaches to assess vulnerability, reliability, and contingency of the power systems: the benefits and limitations. Reliab Eng Syst Saf 2020;201:106961. no. September2020.
[46] Abedi A, Hesamzadeh MR, Romerio F. An ACOPF-based bilevel optimization approach for vulnerability assessment of a power system. Int J Electr Power Energy Syst 2021;125:106455. no. February2021.
[47] Salim NA, Jasni J, Othman MM. Reliability assessment by sensitivity analysis due to electrical power sequential tripping for energy sustainability. Int J Electr Power Energy Syst 2021;126:106582. no. March2021.
[48] Liang C, Guo L, Zocca A, Yu S, Low SH, Wierman A. An integrated approach for failure mitigation & localization in power systems. Electr Power Syst Res 2021;190:106613. no. January2021.
[49] Huang W, et al. Reliability and vulnerability assessment of multi-energy systems: an energy hub based method. IEEE Trans Power Syst 2021;8950:1–12. no. February2021.
[50] Ndawula MB, Hernando-Gil I, Li R, Gu C, De Paola A. Model order reduction for reliability assessment of flexible power networks. Int J Electr Power Energy Syst 2021;127:106623. no. May2021.
[51] Abdalla AN, et al. Metaheuristic searching genetic algorithm based reliability assessment of hybrid power generation system. Energy Explor Exploit 2021;39(1):488–501.
[52] Ezbakhe F, Pérez-Foguet A. Decision analysis for sustainable development: the case of renewable energy planning under uncertainty. Eur J Oper Res 2021;291(2):601–13.
[53] Kumar S, Saket RK, Dheer DK, Holm-Nielsen JB, Sanjeevikumar P. Reliability enhancement of electrical power system including impacts of renewable energy sources: a comprehensive review. IET Gener Transm Distrib 2020;14(10):1799–815.
[54] Johansson J, Hassel H, Zio E. Reliability and vulnerability analyses of critical infrastructures: comparing two approaches in the context of power systems. Reliab Eng Syst Saf 2013;120:27–38.
[55] Beyza J, Garcia-Paricio E, Yusta JM. Ranking critical assets in interdependent energy transmission networks. Electr Power Syst Res Jul. 2019;172:242–52.
[56] Anderson DR, Sweeney DJ, Williams TA. Essentials of statistics for business and economics. South-Western; 2011.
[57] Reliability Test System Task. The IEEE reliability test system -1996 a report prepared by the reliability test system task force of the application of probability methods subcommittee. IEEE Trans Power Syst 1999;14(3):1010–20.
[58] NREL, "Reliability test system grid modernization lab consortium (RTS-GMLC)," 2016. [Online]. Available: https://github.com/GridMod/RTS-GMLC.
[59] Benidris M, Mitra J, Singh C. Integrated evaluation of reliability and stability of power systems. IEEE Trans Power Syst 2017;32(5):4131–9.
[60] Adnan M, Tariq M. Cascading overload failure analysis in renewable integrated power grids. Reliab Eng Syst Saf 2020;198:106887. no. February.
[61] Billinton R, Jonnavithula A. Application of sequential Monte Carlo simulation to evaluation of distributions of composite system indices. IEE Proc Gener Transm Distrib 1997;144(2):87–90.
[62] Ali Kadhem A, Abdul Wahab NI, Aris I, Jasni J, Abdalla AN. Computational techniques for assessing the reliability and sustainability of electrical power systems: a review. Renew Sustain Energy Rev 2017;80:1175–86.
[63] Zhou P, Jin RY, Fan LW. Reliability and economic evaluation of power system with renewables: a review. Renew Sustain Energy Rev 2016;58:537–47.
[64] W. Wangdee, "Bulk electric system reliability simulation and application," no. December 2005.
[65] Zhang J, Hodge B-M, Florita A, Lu S, Hamann HF, Banunarayanan V. Metrics for evaluating the accuracy of solar power forecasting. In: 3rd Int Work Integr Sol Power Power Syst. 17436. Energynautics GmbH; 2013. p. 1–10.
[66] J. Zhang et al., "Wind power forecasting." pp. 1–16, 2013.
[67] ENTSOE, "Final report system disturbance on 4 November 2006," Nov-. [Online]. Available: https://www.entsoe.eu/fileadmin/user_upload/_library/publications/ce/otherreports/Final-Report-20070130.pdf.
[68] Holmgren ÅJ. Using graph models to analyze the vulnerability of electric power networks. Risk Anal 2006;26(4):955–69.
[69] Albert R, Barabási A-L. Statistical mechanics of complex networks. Rev Mod Phys. 2002;74(1):47–97.
[70] Beyza J, Ruiz-Paredes HF, Garcia-Paricio E, Yusta JM. Assessing the criticality of interdependent power and gas systems using complex networks and load flow techniques. Phys A Stat Mech Appl 2020;540:123169.
[71] "Create Arrays of Random Numbers, MATLAB & simulink." [Online]. Available: https://www.mathworks.com/help/matlab/math/create-arrays-of-random-numbers.html. [Accessed: 07-Apr-2021].
[72] Even S. Depth-first search," Graph algorithms. Cambridge University Press; 2011. p. 46–64.
[73] REE, "Previsión intradiaria H+3 eólica más fotovoltaica." [Online]. Available: https://www.esios.ree.es/es/analisis/10359?vis=1&start_date=11-04-2021T00%3A00&end_date=11-04-2021T23%3A00&compare_start_date=10-04-2021T00%3A00&groupby=hour. [Accessed: 11-Apr-2021].
[74] G. Brinkman, J. Jorgenson, A. Ehlen, and J.H. Caldwell, "Low carbon grid study: analysis of a 50% emission reduction in California," pp. 1–54, 2016.
[75] D. Lew et al., "The western wind and solar integration study phase 2," 2013.
[76] Beyza J, Gil P, Masera M, Yusta JM. Security assessment of cross-border electricity interconnections. Reliab Eng Syst Saf 2020;201:106950. no. February.

Assessment of cross-border electricity interconnection projects using MCDA methods

Natalia Naval, Jose M. Yusta

University of Zaragoza, Department of Electrical Engineering, C/Maria de Luna 3, 50018, Zaragoza, Spain

E-mail address: naval@unizar.es, jmyusta@unizar.es

Abstract

European Union (EU)-funded Projects of Common Interest (PCIs) are key to promoting the development of interconnection infrastructures of the power grids of member countries. In addition, these foster the integration of renewable energy sources and improve both electricity market competition and electricity supply security. However, selecting these projects is a complex task given the high number of factors involved in this type of analysis. This paper aims to develop a multi-criteria decision analysis (MCDA) method for appropriately assessing and prioritizing cross-border electricity interconnection projects considering technical, economic, environmental and social criteria. Additionally, this work analyzes interconnection effects on the resilience of interconnected power systems. To verify its validity, this method is applied to a case study to prioritize new Spain-France interconnection infrastructure projects. From the results obtained, it is concluded that the methodology proposed enhances decision-making and reliably helps transmission system operators to assess the effect of each criterion when planning electricity infrastructures and to adequately study projects.

Keywords: Multi-Criteria Decision Analysis; cross-border electricity interconnection; resilience; Analytical Hierarchy Process.

1. Introduction

The European Union (EU) aims at balancing sustainable development with competence and electricity supply security. In the context of an increasingly complex geopolitical environment and the fight against climate change, in recent years, the EU has promoted an ambitious energy policy based on the following three main objectives: promoting energy efficiency, applying measures for reducing greenhouse gas emissions and developing renewable energy sources ("Energy | European Commission," n.d.).

Since the EU strongly depends on external gas and oil for its energy supply security, electricity interconnections play a key role in ensuring the functioning of a fully integrated internal energy market that guarantees affordable energy prices. Electricity interconnections also contribute to electricity supply security, facilitating support functions between neighboring systems and reducing dependence on gas from third countries. Another advantage of cross-border interconnections is to improve the use of

renewable energy by enabling countries with excess renewable capacity to export this energy, thereby avoiding the need to restrict renewable sources that cannot be used locally and reducing the reserve generation capacity (Barrie, 2019; Pollitt, 2019).

Despite the numerous benefits of cross-border interconnections, the development of new interconnections is slow for political (interests of different agents involved in electricity systems, such as operators, regulators, and producers) and financial reasons, among others (Battaglini et al., 2012; Dutton and Lockwood, 2017; Puka and Szulecki, 2014). Accordingly, the EU has introduced Projects of Common Interest (PCIs), which are crucial for developing its transport, storage and smart grid infrastructure and achieving its energy goals to become climate neutral by 2050 (Commission, 2020). These projects have a significant impact on energy markets in improving their competence and common energy security through the diversification of sources and the integration of renewable energy.

Traditionally, Cost-Benefit Analysis (CBA) tools have been used to find strategic solutions in the electricity sector. This analysis focuses on the economic justification of investments. Everything that can be translated into monetary units is tallied. However, some impacts of the projects are difficult to assess, such as environmental impact, electricity system security, and social impact, among others. In recent years, Multi-Criteria Decision Analysis (MCDA) methods have been chosen to structure and analyze more complex problems and conflicting contexts. These planning techniques may help decision makers assess and prioritize projects under various criteria without having to express them as monetary units. In other words, these criteria can be expressed in quantitative or qualitative values using various scales. In addition, all interested parties of a project can participate in MCDA, leading to a reliable and realistic assessment. Another advantage is the possibility to perform a sensitivity analysis of the most influential factors in decision making (Ahmad et al., 2017; Cavallaro, 2009; Mouter et al., 2020).

Some studies review multi-criteria decision-making (MCDM) methods used in previous papers on energy resource planning to identify the basic concepts of these methods and understand their advantages and limitations, criteria assessment, and applications (Ilbahar et al., 2019; Kumar et al., 2017; Rojas-Zerpa and Yusta, 2014). Focusing on the application of these decision-making techniques, (Kabak and Dağdeviren, 2014) propose a hybrid MCDM method, simultaneously combining two techniques, Analytic Network Process (ANP) and Benefits, Opportunities, Costs and Risks (BOCR), to assess and prioritize energy strategies in Turkey. (Ren and Dong, 2018) combine the technique Fuzzy Analytic Hierarchy Process with Grey Relational Analysis to study the electricity supply sustainability and security in different countries (Brazil, Russia, India, China and South Africa). (Abedi et al., 2019) apply the Technique for Order Preferences by Similarity to an Ideal Solution (TOPSIS) to compare different Institute of Electrical and Electronics Engineers - Reliability Test System 96 (IEEE-RTS-96) topologies based on reliability and vulnerability criteria. (Siksnelyte and Zavadskas, 2019) also use this technique to study the sustainability of the electricity sector in European Union countries in 2017.

Selecting the most appropriate MCDM method for solving the problem of interest requires identifying the necessary stages of application of these methods, such as criteria selection, criteria weighting and assessment, among others. (Wang et al., 2009) review the main stages of MCDM for sustainable energy supply. These stages include criteria selection and MCDA for problem-solving.

The criteria are generally associated with numerical indicators. Thus, in the field of cross-border electricity interconnections, different technical indicators are available to analyze electricity supply security depending on whether they focus on system reliability, robustness against cascading failures, or optimal service restoration. (Heylen et al., 2018) present a review and classification of reliability indicators into four groups, namely adequacy, security, socioeconomic and reliability indicators. (Brancucci Martínez-Anido et al., 2012) analyze in depth three reliability indicators (energy not supplied, total loss of power and restoration time) by power grid typology.

The economic impact analysis of new cross-border interconnections and the increasing integration of renewable energy sources has been the object of research in some studies, such as those on Spain-France (Abadie and Chamorro, 2021) and Korea-Japan (Kanagawa and Nakata, 2006) cross-border electricity interconnection and on West Africa's interconnected electricity network (Adeoye and Spataru, 2020). (Abadie and Chamorro, 2021) quantify the potential revenue to a cross-border interconnector using a stochastic model of domestic spot prices. (Kanagawa and Nakata, 2006) propose an energy-economic model to assess the impact of interconnections on CO_2, NOx and SOx emissions and on electricity cost, whereas (Adeoye and Spataru, 2020) also study the impact on electricity generation cost, rapidly growing demand and cross-border electricity trade.

Based on literature review, hardly any multi-criteria method has been proposed to assess this type of project. MCDA and the use of multiple factors help to understand large and complex projects such as the construction of new cross-border electricity interconnections, which affect a large part of society. The lack of studies assessing the impact of cross-border interconnections on the reliability, robustness and restoration of interconnected power systems has also been detected in the literature.

The first aim of this article is to develop and apply a MCDA method to study the security of cross-border interconnections in the European electricity transmission network. Therefore, a methodology for selecting projects through a multidimensional treatment of the problem under technical, economic, environmental and social criteria is proposed in this study.

The second aim is to identify and analyze the indicators included in cross-border electricity interconnection projects that are related to the resilience of interconnected power systems.

As a case study, the method is applied to assess new Spain-France electricity interconnection projects funded by the European Union under the program of key cross border infrastructure projects, also known as PCIs. As a result, the authors provide a tool to help network managers better understand the behavior and limitations of infrastructures and hence adequately prioritize projects selected under given criteria.

The remainder of this paper is organized as follows: Section 2 presents the selected multi-criteria method and the proposed methodology. Subsequently, Section 3 explains the indicators selected to apply the MCDA technique. Section 4 applies the methodology to a case study. Section 5 discusses in depth the relationship of specific indicators with the reliability, robustness and restoration of power systems. Lastly, Section 6 summarizes the major conclusions drawn from this article.

2. Methodology

Among the MCDM techniques, the Analytical Hierarchy Process (AHP) is the most widely used method for solving power grid planning and operation problems (Rietz and Suryanarayanan, 2008; Su et al., 2013; Xiao et al., 2008). This method is simple and flexible and does not incorporate complex mathematics. Its hierarchical structure makes it possible to efficiently organize data on a problem, decomposing and analyzing them by parts, providing an objective and reliable result (Saaty, 1987).

Its main stages are:

1. Objective
2. Criteria and sub-criteria
3. Comparison of alternatives

Figure 1 shows the algorithm of the proposed decision-making methodology using a multi-criteria tool to prioritize cross-border electricity interconnection projects.

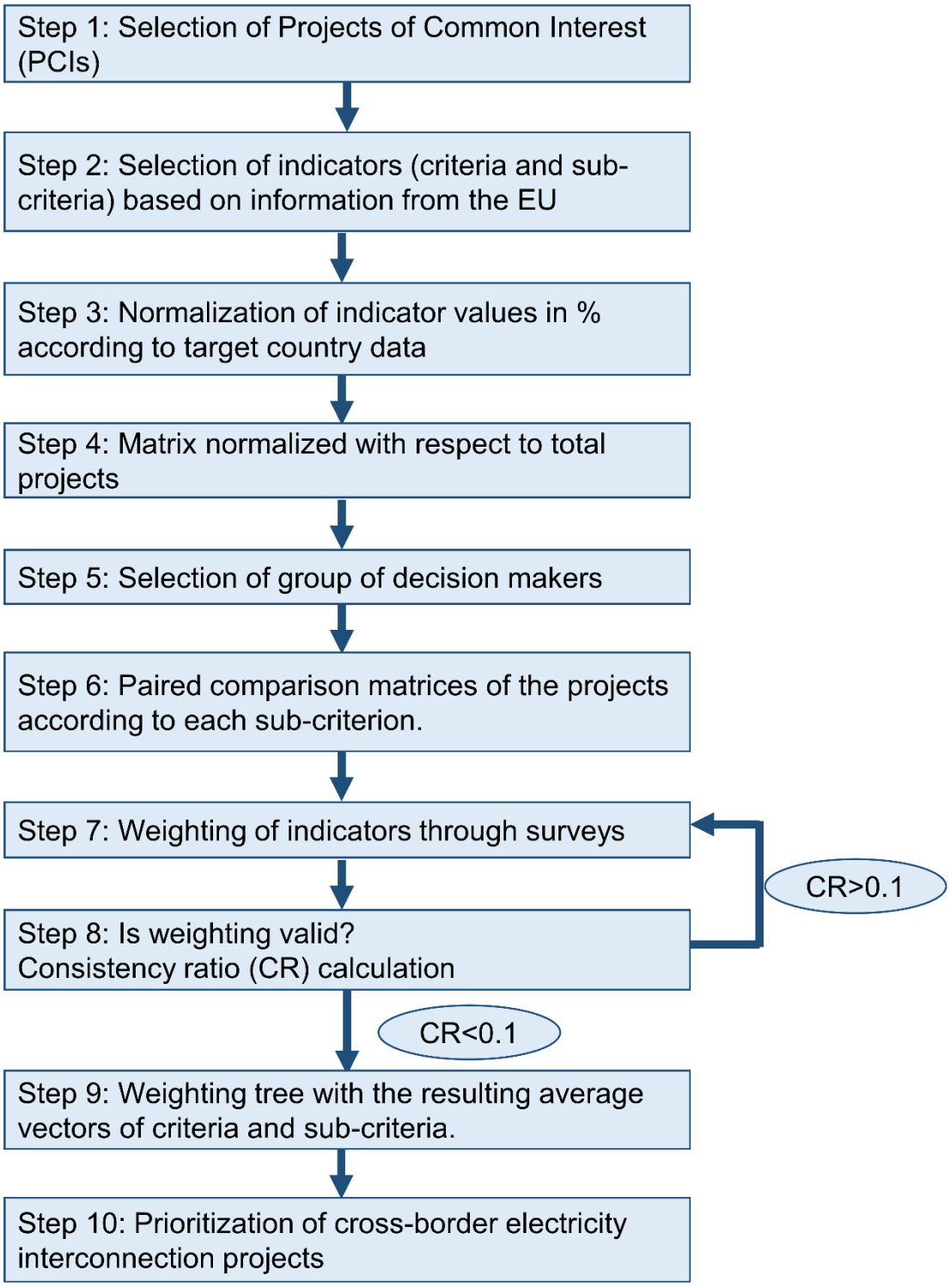

Figure 1. Methodology proposed in this article

Step 1:

The projects on which the multi-criteria technique is applied are selected.

Step 2:

Indicators that directly affect project selection should be chosen based on available data. First, four criteria are established to provide an overview of the problem, subsequently setting different sub-criteria within the four selected criteria. In this way, transmission and storage projects are assessed for compliance with European policies on electricity market integration, supply security and sustainability.

Step 3:

The previous data are then normalized according to the target country data. This normalization makes it possible to construct a matrix of normalized values, in percentage, with the group of selected projects, thus obtaining uniform results. For this purpose, the values of the electricity situation of the country and year of study are assessed, including renewable electricity generation, electricity demand, and emissions of CO_2 and other pollutants, among others. In addition, the total cost of each project is calculated assuming a lifespan of 40 years (Silva Montes et al., 2017).

Step 4:

From this matrix, another matrix is constructed with normalized values to the total number of projects under analysis. There are two possibilities:

- If the increase in the indicator has a positive impact, 100% is assigned to the project with the highest value, and the values of the other projects are calculated proportionally.
- If the increase in the indicator has a negative impact, 100% is assigned to the project with the lowest value, and the values of the other projects are obtained proportionally.

The AHP method is applied based on this last matrix.

Step 5:

The most appropriate group of decision-makers must be selected to reliably and realistically analyze the transmission projects according to the proposed criteria. Several groups of decision makers must be considered because the experience of each decision maker will help to the enrich the solution. The strengths of some decision makers in specific fields will compensate for the weaknesses of other decision makers in those fields.

The following groups of decision makers are proposed in this article:

- Social sub-criteria: the potential adverse social impacts of the project must be identified and managed. Therefore, local and regional public agencies and citizen associations, among others, must be considered.
- Economic sub-criteria: specialists in financial planning and budget control, such as financial advisors, must be consulted.
- Environmental sub-criteria: in studying these actions, experts in managing projects with an environmental impact should be included. These professionals are specialized in reducing the environmental impact of projects by appropriately selecting technologies, routes, and work techniques, among others. For this reason, environmental management institutes must be consulted.

- Technical sub-criteria: the assessments of distribution network operators, electricity industry experts, and energy regulatory agencies, among others, are crucial in this step since they are well aware of the characteristics and technical limitations of the projects.

Step 6:

Pairwise comparisons are a fundamental element of this method. For this purpose, the selected (social, technical, economic and environmental) criteria and compared, and this procedure is then repeated again to compare the sub-criteria. Therefore, in this case, this process must be performed 5 times to construct the pairwise comparison matrices of the technical, economic, social and environmental sub-criteria, and the pairwise comparison matrix of the criteria, subsequently calculating the average vector of each criterion and sub-criterion.

Step 7:

The different indicators are subjectively weighted through surveys sent to groups of experts. Based on their preference, experts score the criteria using the Saaty scale.

The opinions of different groups of decision makers may have different weights, so they must judge the order of importance of the groups of decision makers.

The collective preference is determined using the geometric mean method because this method complies with the principle of reciprocity (Aczél and Saaty, 1983).

Step 8:

The next step consists of calculating the consistency ratio to validate the judgments obtained in the surveys. For the results to be considered adequate, the consistency ratio must be lower than 0.1. If this condition is not met, the decision makers must repeat their assessments until satisfying this constraint.

Step 9:

Subsequently, with the weights resulting from the criteria and sub-criteria, a weighted tree is constructed with all the data obtained in the previous steps.

Step 10:

Finally, the projects are prioritized. For this purpose, the decision matrix is constructed from the normalized matrix (step 4) and from the weighted tree of criteria and sub-criteria (step 9). To calculate the AHP weight of each project, first, the weight eigenvector of each sub-criterion and corresponding criterion, obtained through expert surveys (steps 6 and 7), is multiplied by the value of the normalized matrix of each indicator (step 4). Lastly, the elements resulting from the previous multiplication are added to calculate the final AHP weight of each project. The project with the highest value will provide the best benefits under the assessed criteria.

3. Indicator selection

Electricity interconnection projects are decisive for the energy transition, so interconnection reinforcement is a priority in the development of the European electricity transmission network in the coming years. Cross-border interconnections have numerous technical and economic benefits in the interconnected countries:

- Increased integration and exchange of renewable energy
- Reduced dependence on imported fossil fuels and, therefore, decreased carbon dioxide emissions
- Improved electricity system security and reliability
- Decreased need for power plants to supply peak demand
- Increased number of possibilities of sharing regulation reserves
- Increased price competition between neighboring electric power systems

The indicators used in MCDA to select transmission and storage projects are chosen based on the 3rd European Network of Transmission System Operators for Electricity (ENTSO-E) guideline for CBA of these projects (Commission, 2021). These benefits derive from the energy targets set by the EU to ensure an internal energy market, energy supply security and energy sector sustainability. They express the economic viability of the projects and are divided into benefit, cost and residual impact indicators.

However, this article proposes a reclassification to implement technical, economic, environmental and social criteria necessary for a complete and coherent energy planning. Therefore, here, each indicator is associated with a sub-criterion, which in turn is grouped into (social, economic, environmental and technical) criteria.

3.1.Social criteria

3.1.1. Socioeconomic welfare (S1)

Socioeconomic welfare is an indicator related to the reduction of congestion in power grids. This indicator is assessed as the reduction in variable generation costs in the transmission network provided by a project. By increasing the exchange capacity between two areas, generators in the lower-priced area can export energy to the higher-priced area. This indicator is measured in euros/year.

3.1.2. Residual social impact (S2)

Impact of the project on the population. This indicator is expressed as the number of km that the interconnection crosses in socially sensitive areas.

3.2. Economic criteria

3.2.1. Investment costs (EC1)

Investment costs are the expenses in licenses, feasibility studies, design, land acquisition, execution, among others, required to start a project. These costs are expressed as euros.

3.2.2. Operation and maintenance costs (EC2)

Operation costs include both direct and indirect labor for infrastructure exploitation. Conversely, maintenance costs cover all expenses needed to ensure the lifespan of the equipment and systems. These costs are expressed as euros.

3.3. Environmental criteria

3.3.1. Variation in CO_2 emissions (EN1)

EN1 quantifies the change in the volume of CO_2 emissions in the electricity system resulting from the benefits of the project under analysis. This indicator is expressed as tons of CO_2/year.

3.3.2. (Non-CO_2) emissions reduction (EN2)

This indicator represents the benefit associated with the reduction of emissions of air pollutants other than CO_2 (NOx, SOx, and non-methane volatile organic compounds (NMVOC)). This indicator is expressed as tons/year.

EN2.1: NOx emissions reduction indicator

EN2.2: SOx emissions reduction indicator

EN2.3: NMVOC emissions reduction indicator

3.3.3. Residual environmental impact (EN3)

Impact of the project associated with nature and biodiversity. This indicator is measured in the number of km that the interconnection crosses in sensitive environmental areas.

3.4. Technical criteria

3.4.1. Integration of renewable energy (T1)

This indicator represents the value of the avoided curtailment of renewable energy (MWh/year) because the project reduces or avoids the need to apply the mechanism of technical constraints due to distribution network overloads or voltage control and the replacement of renewables by conventional electricity generation.

3.4.2. Variation in distribution network losses (T2)

T2 measures the energy efficiency of a project. Generally, transmission projects arise from the need to transport electricity over long distances, which implies an increase in global system losses. This indicator is expressed as MWh/year and €/year.

In network studies, grid losses with and without the project are calculated by following the steps indicate below:

- Use of a network model representative of the area
- Adequate period (in general, 1 year, in 1-hour intervals)
- Market results/generation pattern with and without the project or under grid stress
- Monetization of losses

3.4.3. Electricity supply security: Expected energy not supplied (EENS) (T3)

EENS is the indicator that measures the power cut to the electricity system due to outages resulting from incidents in the transmission network of the electricity system. EENS is expressed as MWh/year.

The project for a new cross-border interconnection line may facilitate the adaptation of the electricity system by increasing the generation capacity when facing lost load.

This indicator is calculated using Monte Carlo simulations with several climatic datasets and plant (and, if possible, network) disruption patterns.

3.4.4. Electricity supply security: Additional coverage margin (T4)

Additional coverage margin is the electricity generation capacity (MW) that would not be necessary to install after implementing the project under assessment while maintaining the same level of energy not supplied.

Transmission capacity increases the adequacy margin by enabling the use of surplus generation located elsewhere. T4 replaces the construction of additional electricity generation capacity in a specific area. This indicator is calculated through market simulations for each hour of the year, obtaining the level of electricity generation capacity required in the different areas with and without a project.

3.4.5. Electricity supply security: System flexibility (T5)

This indicator measures the impact of the project on increasing the capacity of the electricity system to adapt to rapid and profound changes in net demand under high levels of renewable energy generation due to the intermittency and variability of these sources.

This indicator is measured using the value of the net demand corresponding to the difference between electricity demand and renewable energy generation (Blanco et al., 2016).

The values of the following parameters must be calculated step by step (see Figure 2):

- Hourly ramp of net demand (Ro), measured in MW
- Existing grid transfer capacity (GTC) without a new interconnection
- Remaining hourly ramp of net demand (Rr), calculated as the difference between Ro and GTC.
- Increased GTC, ΔGTC, with the new cross-border interconnection project
- Indicator, expressed as percentage of the quotient between ΔGTC and Rr.

    - If Rr is negative, the flexibility percentage will be 0% because the existing transfer capacity is greater than the hourly ramp, and the new project will not improve this indicator at all.
    - If Rr is equal to ΔGTC, the flexibility percentage will be 100%; therefore, the increased transfer capacity added by the new project will suffice to completely cover the ramp throughout the year.

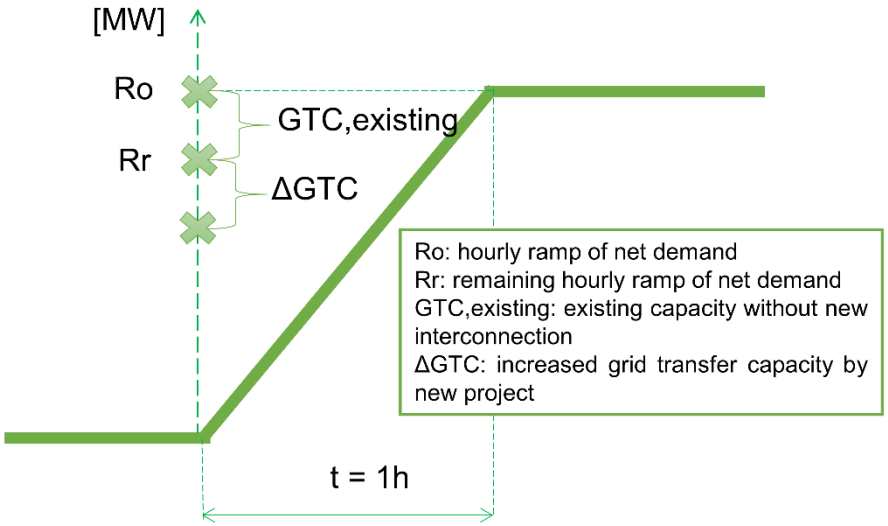

Figure 2. Concept of electricity system flexibility

3.4.6. Electricity supply security: system stability (T6)

This indicator qualitatively measures the impact of the project on the electricity supply stability (transient (T6.1), voltage (T6.2) and frequency (T6.3) stability). Therefore, a value of 0 means that the project does not provide any improvement; +, provides a small improvement; and ++, provides a significant improvement.

4. Case study

4.1. Case study definition

The European Union is promoting new cross-border electricity interconnection projects for two key reasons:

- On the one hand, to guarantee that the internal electricity market in Europe favors the most economical energy exchange and strengthens electricity supply security, both through cooperation among member states and diversification of the construction of new electricity generation systems with renewable sources.
- On the other hand, to accelerate the energy transition, facilitating the exchange of electricity from renewable sources. The EU has prioritized interconnections between Spain and France to improve the cross-border interconnection ratio of Spain, which is still much lower than that of the other member countries. The goal is to solve the problem of the electrical isolation of Spain, which is considered an energy island due to its low capacity to exchange electricity with Europe. Increasing cross-border interconnections may improve the electricity supply security and continuity and the integration of renewable energy sources.

Therefore, to validate the proposed methodology, three Spanish interconnection infrastructures proposed in EU PCIs have been chosen as a case study (see Figure 3).

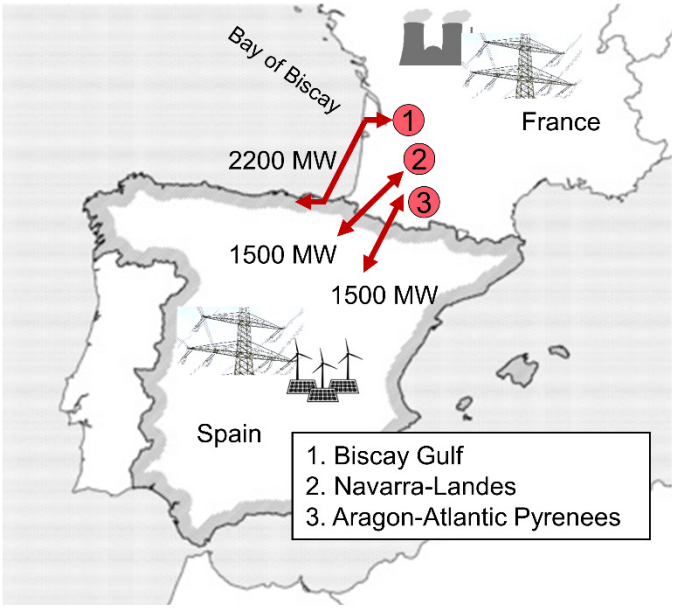

Figure 3. Spain-France electricity interconnection projects of common interest

Table 1 summarizes the main characteristics of the three Spain-France interconnection projects. For more detailed information, see reference ("TYNDP 2020 Project Collection," n.d.). In particular, project 1 is already in the administrative authorization phase, whereas projects 2 and 3 remain in the phase of technical and environmental impact studies to define the best possible route and hence have a very low degree of maturation.

Table 1. Characteristics of Spain-France interconnection projects

Project	Type of elements	Total length (km)	Type of technology	Increase in capacity in Spain (MW)
1. Bay of Biscay	Submarine power cable	370	DC	2200
2. Navarra-Landes	Underground cable, overhead lines, substations	375	DC+AC	1500
3. Aragon-Atlantic Pyrenees	Underground cable, overhead lines, substations	340	DC+AC	1500

4.2. Results

The results from the step-by-step application of the methodology proposed in Section 2 are explained in this section.

Step 1:

The three Spain-France interconnection infrastructure proposals of PCIs are selected to apply the methodology.

Step 2:

Coherent energy planning requires implementing economic, technical, social and environmental criteria, as well as some sub-criteria linked to each decision-making criteria. These sub-criteria are based on EU data and aim to provide a common and uniform basis for analyzing projects regarding their value for European society (Commission, 2021).

Step 3:

The indicators selected in step 2 are normalized to 2020 data of the Spanish electricity system (see Table 2) (REE, 2021; Spanish Ministry for Ecological Transition and the Demographic Challenge, 2022).

Table 2. Data of the Spanish electricity system

CO_2 emissions (kton)	36,130.85
NO_x emissions (kton)	702.7
SO_x emissions (kton)	126.9
NMVOC emissions (kton)	563.1
Electricity demand (GWh)	249,991
Renewable electricity generation (GWh)	110,566

The total cost of each project, considering a lifespan of 40 years, is calculated using the following equation:

$$\text{Total cost of the project} = \text{Capital Expenses (CAPEX)} + 40 \cdot \text{Operating Expenses (OPEX)}$$

Step 4:

From the matrix obtained in step 3, another matrix is constructed with values normalized to the total number of projects under assessment. Table 3 presents the normalized matrix.

Table 3. Matrix normalized to the total number of projects

	Projects		
Indicators	**1**	**2**	**3**
S1	100%	49.12%	64.35%
S2	100%	55%	18.03%
EC1	66.86%	79.59%	100%
EC2	59.12%	63.47%	100%
EN1	100%	42.77%	42.77%
EN2.1	27.83%	100%	100%
EN2.2	100%	74.50%	74.50%
EN2.3	100%	54.43%	54.43%
EN3	100%	13.45%	2.24%
T1	100%	48.81%	48.81%
T2	65.34%	100%	76.33%
T3	100%	48.49%	48.49%
T4	100%	47.71%	43.92%
T5	100%	68.57%	68.57%
T6.1	++	++	++

T6.2	++	++	++
T6.3	+	+	+

Regarding the economic indicators, project 1 has a higher investment cost since it mainly uses a submarine cable, which is very expensive and longer than the other infrastructures. Such a facility there requires great coordination between experts in electric power systems, structures, geologists and mariners. The route must be well analyzed to minimize environmental impact and maximize electrical protection.

From the environmental and social indicators, projects 2 and 3 have a greater environmental and social impact because these interconnections cross highly sensitive areas, such as the Pyrenees mountains, with great natural and heritage value. Furthermore, the economy of the populations living in this area depends to a large extent on sustainable and responsible tourism, based on its rich natural heritage and landscape. Therefore, project promoters must avoid any environmental impact as much as possible, as well as the evolution of the corresponding environmental impact.

Concerning the technical indicators, project 1 provides better results given its higher increase in interconnection capacity (2200 MW versus 1500 MW of the other two projects). This increased interconnection capacity makes it possible to expand renewable energy exports, to increase integration in the European market and to use the most economical power plants to meet the electricity demand at all times. In addition, project 1 strengthens the electricity supply security of both countries, by increasing their energy support, thus reducing the electricity generation capacity in reserve.

Step 5:

Adequately applying the multi-criteria method requires defining the group of decision-makers. This group consists of specialists and professionals from different areas related to electricity infrastructure planning, environmental impact of energy systems, land planning and management, and cost and budget management, among others.

Steps 6 and 7:

In these two steps of the methodology, through surveys, the groups of experts must select the most important criterion and sub-criterion by pairwise comparison, scoring the degree of preference from 1 to 9 using the Saaty scale. Additionally, the eigenvector that determines the final weight attributed by the decision-making groups to each criterion and sub-criterion is obtained.

In this study, all opinions of the decision-making groups are considered equally important. In addition, as previously mentioned, the weighted geometric mean is used to determine the collective preference.

Table 4 presents the results from the criteria comparison surveys, following the methodology proposed in Section 2.

Table 4. Criteria weighting through surveys

	Social	**Technical**	**Environmental**	**Economic**	**Weighted eigenvector**
Social	1	0.41	0.51	1.16	16.22%

Technical	2.43	1	1	2.28	35.50%
Environmental	1.97	1	1	2.24	33.46%
Economic	0.86	0.44	0.45	1	14.82%

As shown above, the technical criterion is the most important criterion (35.50%), closely followed by the environmental criterion (33.46%). The main objective of these projects is to move towards a reliable, robust and flexible electricity system with a high penetration of renewable energy sources. In addition, the experts have also considered environmental criteria important because large electricity infrastructure projects have multiple effects on the landscape and the environment.

The same process is followed for each sub-criterion of three criteria.

For the social criterion, a 2x2 social sub-criteria matrix is obtained (see Table 5).

Table 5. Weighting of the social sub-criteria

	S1	**S2**	**Weighted eigenvector**
S1	1	1.19	54.32%
S2	0.84	1	45.68%

The indicator S1, corresponding to the increase in socioeconomic welfare, obtains a higher weight than S2 because reducing distribution network congestion is considered more important in this type of project than crossing socially sensitive areas. Implementing new interconnections reduces power generation constraints and increases market competition since energy exchanges become more efficient and less expensive.

Regarding the technical criterion, a 5x5 matrix of technical sub-criteria is obtained (see Table 6). The integration of renewables has a higher weighting (38.87%) because electricity interconnection infrastructures maximize the volume of renewable energy production that a system can integrate under secure conditions since surpluses can be sent to other neighboring systems instead of being wasted. Furthermore, in the absence of renewable energy generation or in the presence of grid problems, interconnections make it possible to receive energy from other countries.

Table 6. Weighting of the technical sub-criteria

	T1	**T2**	**T3**	**T4**	**T5**	**Weighted eigenvector**
T1	1	3.2	2.43	2.43	2.43	38.87%
T2	0.31	1	0.58	0.58	0.58	10.30%
T3	0.41	1.73	1	1	1.41	18.05%
T4	0.41	1.73	1	1	1.41	18.05%
T5	0.41	1.73	0.71	0.71	1	14.73%

For the economic criterion, a 2x2 matrix of economic sub-criteria is obtained (see Table 7). The experts deem investment costs and operation and maintenance costs equally important.

Table 7. Weighting of the economic sub-criteria

	EC1	EC2	Weighted eigenvector
EC1	1	1	50%
EC2	1	1	50%

In relation to the environmental criterion, a 5x5 matrix of environmental sub-criteria is obtained (see Table 8).

Table 8. Weighting of the environmental sub-criteria

	EN1	EN2.1	EN2.2	EN2.3	EN3	Weighted eigenvector
EN1	1	1.73	1.73	1.73	1.32	28.68%
EN2.1	0.58	1	1	1	0.8	16.71%
EN2.2	0.58	1	1	1	0.8	16.71%
EN2.3	0.58	1	1	1	0.8	16.71%
EN3	0.76	1.26	1.26	1.26	1	21.20%

According to the decision-making groups, CO_2 emissions reduction is the most important indicator (EN1, 28.68%), followed by environmental impact (EN3, 21.20%). The projects under study will reduce these emissions by increasing the integration of renewable energy sources into the electricity system, in line with the EU goal of a climate-neutral system by 2050. The environmental impact is also considered essential. In this regard, a complete environmental study will allow to assess the magnitude of the impact of each project on the areas involved and to take measures to minimize the impact on the landscape, fauna and habitats of community interest.

Step 8:

In this step, the consistency ratio is calculated to validate the judgments assessed in the surveys. To this end, first, the maximum eigenvalue, the consistency index and the random consistency index are calculated using formulas indicated in reference (Rietz and Suryanarayanan, 2008) (see results outlined in Table 9). The maximum eigenvalue is obtained using the matrix product of the pairwise comparison matrix of criteria and sub-criteria and the comparison eigenvector (outlined in the Tables of steps 6 and 7) and the corresponding sum of the elements of the matrix product. The consistency index depends on the maximum eigenvalue and the number of compared criteria. The random consistency index depends on the number of compared criteria. Lastly, the consistency ratio is calculated as the quotient between the consistency index and the random index. As shown below, the consistency ratio is lower than 0.1 in all cases, which means that the obtained matrices are consistent and that the judgments made by the decision-making groups are valid.

Table 9. Calculation of the consistency ratio

	Maximum eigenvalue	Consistency index	Random consistency index	Number of alternatives	Consistency ratio
Comparison matrix of criteria	4.004	0.0033	0.99	4	0.0033

Comparison matrix of social sub-criteria	2.00	0	0	2	0
Comparison matrix of technical sub-criteria	5.028	0.007	1.188	5	0.0059
Comparison matrix of economic sub-criteria	2	0	0	2	0
Comparison matrix of environmental sub-criteria	5.001	0.00025	1.188	5	0.00021

Step 9:

From the weights of the criteria and sub-criteria, a weighted tree is constructed, thus obtaining the final weighting of each sub-criterion (see Figure 4).

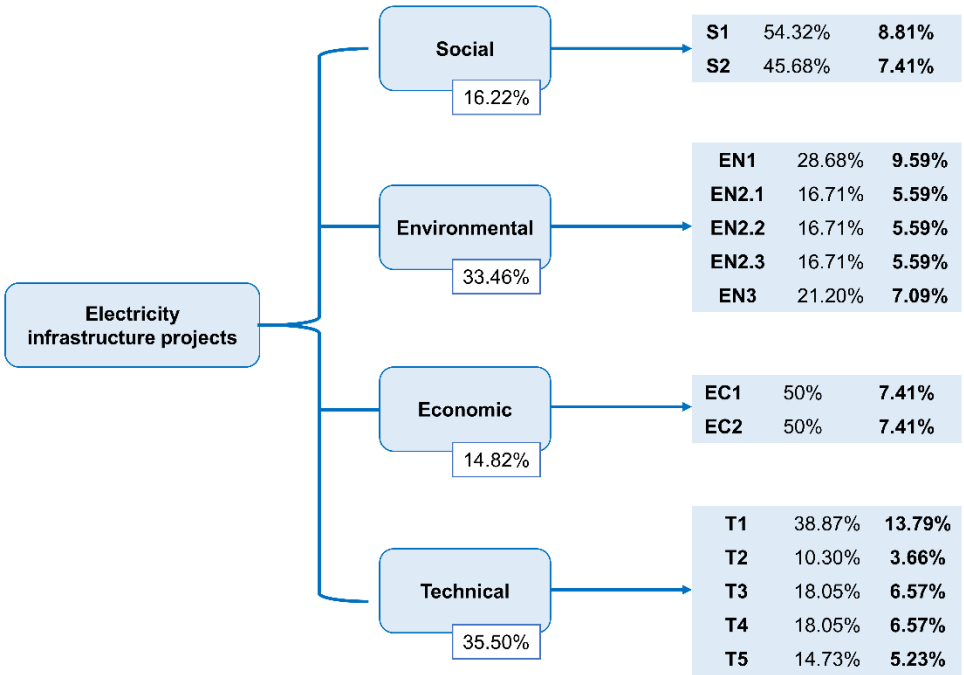

Figure 4. Weighted tree

Step 10:

Finally, the weights obtained in the previous step are applied to the normalized matrix of projects (step 4), thereby prioritizing the projects (see Table 10).

Table 10. Prioritization of the projects

	Projects		
Indicators	**1**	**2**	**3**
S1	0.0881	0.0433	0.0567
S2	0.0741	0.0099	0.0016

EC1	0.0495	0.0589	0.0741
EC2	0.0438	0.0470	0.0741
EN1	0.0959	0.0410	0.0410
EN2.1	0.0155	0.0559	0.0559
EN2.2	0.0559	0.0416	0.0416
EN2.3	0.0559	0.0304	0.0304
EN3	0.0709	0.0389	0.0127
T1	0.1379	0.0673	0.0673
T2	0.0238	0.0365	0.0278
T3	0.0641	0.0311	0.0311
T4	0.0641	0.0305	0.0281
T5	0.0523	0.0358	0.0358
AHP score	**0.8937**	**0.5648**	**0.5815**

After applying the multi-criteria method, the most beneficial project in the decision-making process is project 1 (0.8937), followed by project 3 (0.5815) and, lastly, project 2 (0.5648). Project 1 is technically better because this approach enables a greater integration and exchange of renewable energy while improving electricity supply security by helping to balance power generation and demand in any situation of renewable energy availability and supporting interconnected systems when facing electrical disturbances.

Project 1 also has the lowest environmental impact because the high-voltage direct current (HVDC) submarine power cable interconnection through the Bay of Biscay avoids the Pyrenees mountains, a region that is characterized by its considerable landscape relevance and cultural heritage. This justification is mainly based on the result from the indicator EN3. In addition, the route is parallel to the coast, thus avoiding fishing areas, ports, and areas of special importance for endangered fauna, as well as an unnecessary increase in the length of the power line. Additionally, this project integrates and exchanges a greater amount of renewable power generation (T1), which translates into a greater reduction of CO_2 emissions (EN1). However, the use of a long submarine power cable requires a higher investment and operational cost (EC1, EC2) than conventional options, such as airlines presents but is nevertheless preferred for minimizing the environmental impact.

Regarding the social indicators, project 1 further reduces the expected congestion at the border by increasing the energy exchange capacity (2200MW). In addition, the increased flow in both directions enables the use of less expensive energy at all times, providing a greater socio-economic benefit (S1) across Europe. Furthermore, the route avoids urban centers and highways at all times, taking advantage of forest roads and tracks. Simultaneously, the location of the power conversion station minimizes the visual and sound impact, ensuring a greater distance from population centers. For this reason, the S2 indicator of project 1 is better than that of the other two projects.

Project 1 is already in the administrative authorization phase, whereas the other two projects remain in the planning phase. Therefore, in the following years, the initial route could be modified to minimize the environmental impact and improve technical aspects.

In short, the methodology proposed in this article helps the decision maker to transparently assess several projects from social, technical, economic, and environmental

points of view and to select the alternative that achieves the best balance of all criteria under consideration.

5. Discussion of security indicators

Electric power systems are key for the daily functioning of any country. These systems are complex and susceptible to failures and threats, which may cause serious outages, affecting services provided to society (economic activities, and public health, among others). For this reason, all countries aim to develop a reliable and secure system that guarantees electricity supply in any situation.

Resilience is an intrinsic property of a system defined as its ability to quickly absorb and/or restore from external disturbances by continuing to supply energy. The concept of resilience integrates four fundamental characteristics that reflect the level of resilience of electricity systems: capacity of resistance to the event, speed of restoration, preparedness for high-impact, unlikely future events and adaptability to a major contingency (Hossain et al., 2019).

The three basic levels that determine the resilience of an electricity system are defined below.

- Reliability: is the capacity of the electricity system to continuously meet the demand with an acceptable level of quality and to maintain the exploitation indices under specific environmental and operational conditions during a determined period (Beyza et al., 2020).
- Robustness: is the capacity of the electricity system to absorb the effects of an ongoing disruptive event. This property is essential since an attack may cause a component to fail, which, in turn, may affect other components as well. This phenomenon is termed a cascading failure (Rehak et al., 2022).
- Restoration: is the ability of a component to restore its activity to its initial operating level once the disturbance has ended (Rehak et al., 2022).

5.1. Discussion of reliability indicators

Reliability is the capacity of an electricity system to meet the electricity demand, comply with the operating restrictions of the system, and respond to changes in the system due to variations in demand or generation, and failures in power lines and equipment, among others.

The main index that evaluates the reliability of an electricity system is EENS (MWh/year). This indicator (T3) is related to the penetration of renewable energy sources into the electricity system. Because they are intermittent generation sources, there is a higher likelihood of loss of load and failure to supply power. Therefore, increasing renewable energy production increases the impact on this indicator. This indicator provides information on the number of outages and on their magnitude and reflects the improvement in the reliability of electric power systems since adding a new cross-border interconnection improves energy exchange between different areas in facing the risk of loss of load at peak hours (Beyza et al., 2021; Brancucci Martínez-Anido et al., 2012).

The EENS indicator is measured using models which simulate the electricity dispatch for one year using probabilistic Monte Carlo techniques. This approach is used over analytical methods for its practicality given the complexity, non-linearity and involvement of many components in the electricity system. The process considers the effect of weather conditions on the likelihood of power line failures, the heuristic representation of generator instability, the redistribution of resources after a contingency, and the time required for system restoration, among others. Therefore, the value of this indicator is a realistic estimate and is used to assess the reliability of electricity systems.

The EENS results (indicator T3) indicate a double increase in project 1 when compared with the other two projects, which translates into a double improvement in the reliability of the current Spanish electricity system. This indicator provides useful information to study the behavior of the distribution network when facing contingencies and helps decision-making in planning improvements to existing electricity systems. The cross-border electricity interconnection proposed in project 1 increases the power transfer capacity between the countries (Spain-France) by 46%, thus having a positive impact on the operating conditions of the Spanish system and further reducing the congestion of power lines. As such, the cross-border electricity interconnection increases reliability since interconnection lines improve energy exchange between different areas of the interconnected infrastructure.

5.2. Discussion of robustness and restoration indicators

Robustness is the internal capacity of the electricity system to continue to function under the effects of unforeseen failures. The outage of one transmission line may cause the overload of other lines, which increases the likelihood that other assets will fail and cause a failure of the entire system. This indicator is related to the effect of cascading failures.

Restoration is the capacity of the network to quickly reestablish itself after a high-impact external event or a failure of a system component and to restore the operating conditions of the electricity distribution network.

A parameter linked to the robustness and restoration of a system is the additional installed generation capacity to meet the expected demand in the event of maintenance, plant breakdowns, demand peaks due to extreme weather conditions or interruptions in the transmission line (T4). Cross-border interconnections make it possible to use the excess electricity generation capacity of an area to cover deficits in other areas of the system under these conditions. Therefore, this capacity will be smaller than the sum of the needs of the individual networks without interconnection (Blanco et al., 2016; Zhang, 2010), thereby reducing the need to build new power plants and facilitating the optimal management of available resources.

Another indicator associated with grid robustness and restoration is the system flexibility (T5), that is, the ability of the grid to adapt to changing, diverse and dynamic conditions, from the point of view of renewable energy sources, and to external factors which increase the vulnerability of the system. Flexibility is an important property of electric power systems with high renewable penetration for smoothing out system disturbances in extreme cases or expected deviations from renewable electricity generation and electricity

demand, in addition to avoiding grid saturations or surges and problems with power supply quality.

Cross-border interconnections play a key role in achieving a robust and flexible power system by enabling backup functions between neighboring systems in the face of power failures or outages. The improvement in flexibility depends on the net transfer capacity; therefore, energy can only be imported/exported within the limits imposed by the fixed transfer capacities of power lines between different network areas. The integration of the electricity markets makes it possible to add a slack bus to maintain the maximum balance between what is injected into and exported from the grid and to moderate the energy flow problems of individual grid areas by taking advantage of the flexibility potential of other areas of the grid (Ulbig and Andersson, 2015).

The indicators T4 and T5 enable operators of energy control centers to better analyze in real time the operation of the electricity system and its operational limits in the event of a series of simultaneous contingencies, and the available sources to balance and restore the system as quickly as possible.

Project 1 has the best value of the T4 indicator, which is related to the robustness of the electricity system. Cross-border electricity interconnection is the most significant instant backup for electricity supply security. Increasing the exchange capacity between different countries decreases the reserve margin necessary in a country to meet the demand in a short period in the face of power outages because reserve plants can be shared to enable a system to continuously operate in the event of a failure, thus reducing the need for investment in long-term generation.

The flexibility indicator (T5) is associated with the response capacity of the electricity system when facing expected or unforeseen variations, either in demand and/or generation. This value is essential to achieve a robust electricity system with high levels of renewable energy penetration since a small mismatch between demand and generation may lead to variation in system frequency and affect the operational reliability.

Project 1 has a greater interchangeability and, therefore, a higher capacity to share resources and optimize their use in case of imbalances, thus reducing the use of fossil fuels and foreign energy dependence. Furthermore, interconnections generally decrease production ramps in manageable power plants and help export/import between both countries, in case of energy excess or deficit, respectively.

In addition, these last indicators also show a direct relationship with improvements in the resilience of electric power systems because increasing cross-border interconnection provides more energy resources to restore the electricity supply when facing a major contingency, which may cause the loss of much of the electricity infrastructure after the event. Thus, project 1 may further reduce the time need to restore electricity service by increasing the transfer capacity between countries.

In short, achieving a secure, reliable and robust system requires preparing response plans for any event that may compromise the normal operation of the electricity system. By increasing cross-border interconnection, electricity supply security becomes an international rather than a national problem. Therefore, good coordination between countries, a robust network, and sufficient resources are essential to tackle critical

problems. Increasing electricity interconnection capacity is the best compromise solution in the design of transmission network topologies based on reliability and robustness criteria.

6. Conclusions

The goal of this paper is to propose a MCDA methodology for selecting and ranking cross-border electricity interconnection projects based on data available from the EU. This tool maximizes the amount of information, synthesized and organized, available at all times to decision-makers, enabling them to assess and select the most beneficial project, considering technical, economic, environmental and social criteria.

The following statements are the main conclusions drawn from this article:

- MCDA and the use of a wide variety of criteria, objectives and participants help to understand large and complex projects, which affect a large part of society.
- Unlike the CBA method, MCDA makes it possible to assess the environmental and social impact and security of an electrical system, among other factors, for a complete and realistic analysis of electricity interconnection projects.
- EU data normalization using the methodology proposed in this study and the subsequent application of the AHP method enable a prioritization of the project portfolio with a clear and explicit approach.
- This tool provides a complete view of the real impact of cross-border electricity infrastructure projects, helping to prioritize projects according to technical, social, economic and environmental criteria.
- This research also makes it possible to analyze and relate some indicators with the reliability, robustness and restoration of power grids to improve the understanding of the behavior of interconnected power systems.
- Selecting experts in all areas involved in planning electricity infrastructure projects for weighting different criteria and sub-criteria improves the project selection process. Thus, the proposed methodology is based on objective indicators and quantitative techniques, which will strengthen the defense of the best option.

In short, the MCDA methodology proposed in this article may considerably facilitate a comprehensive analysis of all aspects involved in the assessment of electricity infrastructure projects and help operators understand the behavior and infrastructure limitations of transmission power grids. Using this approach, projects may be adequately prioritized while shortening the time needed to achieve a reliable, robust and flexible European electricity system.

Acknowledgments

This work was funded by the Spanish Ministry of Science and Innovation MCIN/AEI/10.13039/501100011033 under the project PID2019-104711RB-100: Smart-grid design and operation under the threat of interrupted supply from electric power transmission systems with a high penetration of renewable energies.

References

Abadie, L.M., Chamorro, J.M., 2021. Evaluation of a cross-border electricity interconnection: The case of Spain-France. Energy 233. https://doi.org/10.1016/j.energy.2021.121177

Abedi, A., Beyza, J., Romerio, F., Dominguez-Navarro, J.A., Yusta, J.M., 2019. MCDM approach for the integrated assessment of vulnerability and reliability of power systems. IET Gener. Transm. Distrib. 13, 4741–4746. https://doi.org/10.1049/iet-gtd.2018.6693

Aczél, J., Saaty, T.L., 1983. Procedures for synthesizing ratio judgements. J. Math. Psychol. 27, 93–102. https://doi.org/10.1016/0022-2496(83)90028-7

Adeoye, O., Spataru, C., 2020. Quantifying the integration of renewable energy sources in West Africa's interconnected electricity network. Renew. Sustain. Energy Rev. 120. https://doi.org/10.1016/j.rser.2019.109647

Ahmad, S., Nadeem, A., Akhanova, G., Houghton, T., Muhammad-Sukki, F., 2017. Multi-criteria evaluation of renewable and nuclear resources for electricity generation in Kazakhstan. Energy 141, 1880–1891. https://doi.org/10.1016/j.energy.2017.11.102

Barrie, B.M., 2019. The Development of cross border interconnection and trading. Glob. Energy Interconnect. 2, 254–263. https://doi.org/10.1016/j.gloei.2019.07.018

Battaglini, A., Komendantova, N., Brtnik, P., Patt, A., 2012. Perception of barriers for expansion of electricity grids in the European Union. Energy Policy 47, 254–259. https://doi.org/10.1016/j.enpol.2012.04.065

Beyza, J., Gil, P., Masera, M., Yusta, J.M., 2020. Security assessment of cross-border electricity interconnections. Reliab. Eng. Syst. Saf. 201. https://doi.org/10.1016/j.ress.2020.106950

Beyza, J., Yusta, J.M., Evangelista, M.A., Artal-Sevil, J.S., Rendon, J.A., 2021. Evaluation of Reliability and Robustness of Electric Power Systems with Renewable Energies. 2021 23rd IEEE Int. Autumn Meet. Power, Electron. Comput. ROPEC 2021. https://doi.org/10.1109/ROPEC53248.2021.9668112

Blanco, M.P., Spisto, A., Hrelja, N., Fulli, G., 2016. Generation Adequacy Methodologies Review. JRC Sci. fo Policy Rep. 106.

Brancucci Martínez-Anido, C., Bolado, R., De Vries, L., Fulli, G., Vandenbergh, M., Masera, M., 2012. European power grid reliability indicators, what do they really tell? Electr. Power Syst. Res. 90, 79–84. https://doi.org/10.1016/j.epsr.2012.04.007

Cavallaro, F., 2009. Multi-criteria decision aid to assess concentrated solar thermal technologies. Renew. Energy 34, 1678–1685. https://doi.org/10.1016/j.renene.2008.12.034

Commission, E., 2021. 3rd ENTSO-E Guideline for Cost Benefit Analysis of grid.

Commission, E., 2020. Regulation (EU) No 347/2013 of the European Parliament and of the Council as regards the Union list of projects of common interest 1–19.

Dutton, J., Lockwood, M., 2017. Ideas, institutions and interests in the politics of cross-border electricity interconnection: Greenlink, Britain and Ireland. Energy Policy

105, 375–385. https://doi.org/10.1016/j.enpol.2017.03.001

Energy | European Commission [WWW Document], n.d. URL https://ec.europa.eu/info/policies/energy_en (accessed 5.9.22).

Heylen, E., Deconinck, G., Van Hertem, D., 2018. Review and classification of reliability indicators for power systems with a high share of renewable energy sources. Renew. Sustain. Energy Rev. 97, 554–568. https://doi.org/10.1016/j.rser.2018.08.032

Hossain, N.U.I., Jaradat, R., Hosseini, S., Marufuzzaman, M., Buchanan, R.K., 2019. A framework for modeling and assessing system resilience using a Bayesian network: A case study of an interdependent electrical infrastructure system. Int. J. Crit. Infrastruct. Prot. 25, 62–83. https://doi.org/10.1016/j.ijcip.2019.02.002

Ilbahar, E., Cebi, S., Kahraman, C., 2019. A state-of-the-art review on multi-attribute renewable energy decision making. Energy Strateg. Rev. 25, 18–33. https://doi.org/10.1016/j.esr.2019.04.014

Kabak, M., Dağdeviren, M., 2014. Prioritization of renewable energy sources for Turkey by using a hybrid MCDM methodology. Energy Convers. Manag. 79, 25–33. https://doi.org/10.1016/j.enconman.2013.11.036

Kanagawa, M., Nakata, T., 2006. Analysis of the impact of electricity grid interconnection between Korea and Japan - Feasibility study for energy network in Northeast Asia. Energy Policy 34, 1015–1025. https://doi.org/10.1016/j.enpol.2004.10.003

Kumar, A., Sah, B., Singh, A.R., Deng, Y., He, X., Kumar, P., Bansal, R.C., 2017. A review of multi criteria decision making (MCDM) towards sustainable renewable energy development. Renew. Sustain. Energy Rev. 69, 596–609. https://doi.org/10.1016/j.rser.2016.11.191

Mouter, N., Dean, M., Koopmans, C., Vasallo, J.M., 2020. Comparing cost-benefit analysis and multi-criteria analysis. Adv. Transp. Policy Planning, Acad. Press 6, 225–254. https://doi.org/10.1016/bs.atpp.2020.07.009

Pollitt, M.G., 2019. The European Single Market in Electricity: An Economic Assessment. Rev. Ind. Organ. 55, 63–87. https://doi.org/10.1007/S11151-019-09682-W/FIGURES/3

Puka, L., Szulecki, K., 2014. The politics and economics of cross-border electricity infrastructure: A framework for analysis. Energy Res. Soc. Sci. 4, 124–134. https://doi.org/10.1016/j.erss.2014.10.003

REE, 2021. The Spanish Electricity System 2020.

Rehak, D., Hromada, M., Onderkova, V., Walker, N., Fuggini, C., 2022. Dynamic robustness modelling of electricity critical infrastructure elements as a part of energy security. Int. J. Electr. Power Energy Syst. 136, 107700. https://doi.org/10.1016/j.ijepes.2021.107700

Ren, J., Dong, L., 2018. Evaluation of electricity supply sustainability and security: Multi-criteria decision analysis approach. J. Clean. Prod. 172, 438–453. https://doi.org/10.1016/j.jclepro.2017.10.167

Rietz, R.K., Suryanarayanan, S., 2008. A review of the application of analytic hierarchy process to the planning and operation of electric power microgrids. 40th North Am. Power Symp. NAPS2008 1–6. https://doi.org/10.1109/NAPS.2008.5307403

Rojas-Zerpa, J.C., Yusta, J.M., 2014. Methodologies, technologies and applications for electric supply planning in rural remote areas. Energy Sustain. Dev. 20, 66–76. https://doi.org/10.1016/j.esd.2014.03.003

Saaty, R.W., 1987. The analytic hierarchy process-what it is and how it is used. Math. Model. 9, 161–176. https://doi.org/10.1016/0270-0255(87)90473-8

Siksnelyte, I., Zavadskas, E.K., 2019. Achievements of the European Union countries in seeking a sustainable electricity sector. Energies 12, 1–16. https://doi.org/10.3390/en12122254

Silva Montes, C., Silva Castro, I., Martinez, O., 2017. Vida Útil De Elementos De Transmisión 1–102.

Spanish Ministry for Ecological Transition and the Demographic Challenge, 2022. National Greenhouse Gas Inventory Report. 2022 Edition. (1990-2020) 1–982.

Su, S., Xiong, W., Ren, Q., Li, B., Sun, W., 2013. The Application of Analytic Hierarchy Process (AHP) in the Power Grid Planning. Adv. Mater. Res. 860–863, 2540–2543.

TYNDP 2020 Project Collection [WWW Document], n.d. URL https://tyndp2020-project-platform.azurewebsites.net/projectsheets (accessed 5.13.22).

Ulbig, A., Andersson, G., 2015. Analyzing operational flexibility of electric power systems. Int. J. Electr. Power Energy Syst. 72, 155–164. https://doi.org/10.1016/j.ijepes.2015.02.028

Wang, J.J., Jing, Y.Y., Zhang, C.F., Zhao, J.H., 2009. Review on multi-criteria decision analysis aid in sustainable energy decision-making. Renew. Sustain. Energy Rev. 13, 2263–2278. https://doi.org/10.1016/j.rser.2009.06.021

Xiao, J., Cui, Y., Luo, F., Liu, M., Wang, J., Li, Y., Gao, Y., Wang, S., 2008. Comprehensive method on evaluation of distribution network planning. 3rd Int. Conf. Deregul. Restruct. Power Technol. DRPT 2008 1249–1254. https://doi.org/10.1109/DRPT.2008.4523598

Zhang, X.-P., 2010. Fundamentals of electric power systems, in: Restructured Electric Power Systems: Analysis of Electricity Markets with Equilibrium Models. Institute of Electrical and Electronics Engineers (IEEE), pp. 1–51.